Jurassic active continental margin deep-water basin and carbonate platform formation in the north-western Tethyan realm (Austria, Germany)

By

HANS-JÜRGEN GAWLICK, SIGRID MISSONI, FELIX SCHLAGINTWEIT & HISASHI SUZUKI

With 100 figures

Field Trip Guide

29th IAS Meeting of Sedimentology
Schladming, Austria

Addresses of the authors:
HANS-JÜRGEN GAWLICK, SIGRID MISSONI
University of Leoben
Department of Applied Geosciences and Geophysics, Petroleum Geology
Peter-Tunner-Strasse 5
8700 Leoben, Austria
E-Mail: hans-juergen.gawlick@unileoben.ac.at, s.missoni@daad-alumni.de

FELIX SCHLAGINTWEIT
Lerchenauer Strasse 167
80935 München, Germany
E-Mail: ef.schlagintweit@t-online.de

HISASHI SUZUKI
Otani University
Koyama-Kamifusa-cho, Kita-ku
Kyoto 603-8143, Japan
E-mail: hsuzuki@res.otani.ac.jp

Journal of Alpine Geology	54	S. 189-291	Wien 2012

Content

Abstract

The topic of this field trip is to get to know and understand the sedimentation of Austria's Northern Calcareous Alps and its tectonic circumstances from Triassic rifting/drifting to Jurassic collision/accretion. The Northern Calcareous Alps as part of the Eastern Alps is one of the most prominent Alpine areas. Together with the Carpathians, the Southern Alps and the Dinarides, they constituted an up to 700 km wide and approximately 2000

km long shelf strip of the northwestern Tethys margin.

The Jurassic sedimentation in this realm was controlled by its palaeogeographic position between two oceans and their evolution, respectively: the Neotethys Ocean to the east/southeast and the Alpine Atlantic to the west/ northwest. The opening of the Central Atlantic Ocean with its continuation into the Alpine Atlantic (= Ligurian-Penninic Ocean) resulted in a new Mediterranean plate configuration. The "Apulian" plate was formed. Successive spreading of the Alpine Atlantic led to closure of parts of the Neotethys and deformation of the Triassic carbonate shelf since late Early Jurassic time.

Deformation and accretion started in the Neotethys Ocean with intra-oceanic thrusting in the late Early Jurassic. This thrusting process resulted in the obduction of the accreted ophiolites onto the outer shelf in Middle Jurassic time. The former Triassic to Early Jurassic passive continental margin with its huge Triassic carbonate platforms took a lower plate position in this developing thin-skinned orogen. Thrusting started in the outer shelf region and successively propagated towards the inner shelf. In the late Middle Jurassic contractional tectonics reached the inner parts of the shelf and affected the Triassic carbonate platforms. Deep-water trench-like basins formed in sequence in front of advancing nappes: Thus the initial trench-like basins formed in the south. Later, in the early Late Jurassic, further trench-like basins formed farer to the north. The trench-like basins accumulated thick successions of gravitatively redeposited sediments deriving from the accreted older sedimentary sequences. Some slides and blocks experienced low temperature - high pressure metamorphism before redeposition, indicating deep burial in the framework of subduction processes in Jurassic times. Uplift of the accreted nappes led to the formation of shallow-water carbonate platforms on top of the nappe stack. The build-up, progradation and degradation of carbonate platforms in Late Jurassic to Early Cretaceous times progressively sealed the trenches and rises morphology by the deposition of hemipelagic and shallow-water carbonates.

This Jurassic evolution of the Northern Calcareous Alps is best preserved in their central region. During the fieldtrip we will visit some of the finest outcrops documenting this earliest phase of Alpine mountain building and degradation.

What you will see:

A complete, very complex active continental margin evolution from Middle Jurassic to Early Cretaceous with the interplay of thrusting, trench formation, mass movements, onset of carbonate platforms, and formation and preservation parameters of organic content. This includes:

- Condensed carbonates (pelagic platform; "Ammonitico Rosso" and grey cherty limestones) of Early to early Middle Jurassic age. These follow on top of the huge Late Triassic Hauptdolomit/Dachstein Limestone carbonate platform and underly the sedimentary sequences deposited during the complex late Middle to Late Jurassic evolution.
- Late Middle to early Late Jurassic deep-water radiolaritic trench-like basins related to thrusting and accretion, which were characterized by fine-grained organic-rich (siliceous) sedimentation with intercalations of olistostromes and huge slides.
- Large scale mass movements from an accretionary wedge into adjacent trench-like basins; each basin fill is characterized by a coarsening-upward cycle.
- Carbonate-clastic radiolaritic deep-water blocks in matrix structure (radiolaritic "wildflysch") as sedimentary basin fill and mélange formation due to contemporaneous contractional tectonic movements.
- Radiolaritic/argillaceous trench-like basin fills with potential source rocks and intercalated potential reservoir rocks.
- Onset of different shallow-water carbonate platforms on an uplifted nappe stack in a contractional margin setting (lower plate position) and progradation of shallow-water carbonates over older deep-water basins.
- Carbonate production and platform configuration in a contractional margin setting with the carbonate factories still working during orogenic uplift and extensional collapse.
- Formation of starved basins between these carbonate platforms as the result of the interplay of tectonics and carbonate production.
- The carbonate platform collapse due to mountain uplift associated with extensional tectonics.
- Early Cretaceous drowning of carbonate platforms due to siliciclastic input
- Siliceous and carbonate sedimentology and sequence stratigraphy in outcrop analogs to reservoirs.

During this field trip in one of the geologically most classical areas of the world, the central Northern Calcareous Alps (Salzkammergut region, Salzburg and Berchtesgaden Calcareous Alps), we will visit locations documenting the whole early convergence story.

1. Introduction

As introduction a short outline of the whole Permian/ Triassic to Early Cretaceous sedimentary and geodynamic evolution of the northwestern Neotethys realm (e.g., Eastern and Southern Alps, Western Carpathians, Pannonian realm, Dinarides) is provided in order to better understand the topics of the field trip (Fig. 1). We will see Late Permian to Middle Jurassic rocks from different provenance areas as reworked, differently sized (millimetre to square kilometre) components in the late Middle to early Late Jurassic deep-water basin successions. Beside age dating of the matrix sediments, unravelling the derivation of these components is of great importance for the reconstruction of basin formation during that time span. The overall geodynamic evolution is crucial for the initiation of the large-scaled mass movements into these deep-water basins and the time-equivalent to subsequent formation of carbonate platforms. The Eastern Alps, especially the Northern Calcareous Alps (Fig. 2) as part of this northwestern Neotethyan realm, provide an excellent opportunity to study this story. More than 150 years of

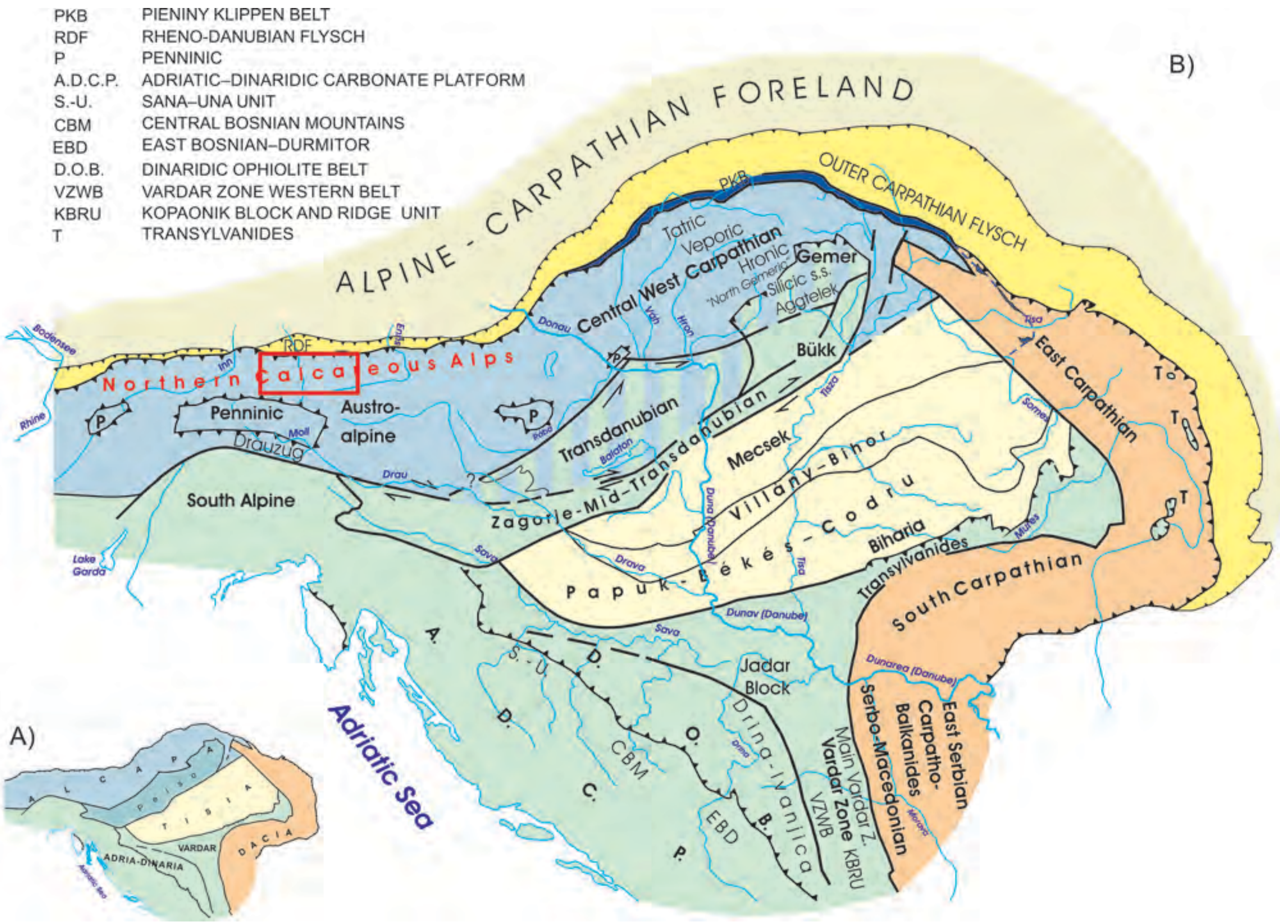

Fig. 1: **A**) Mega-units and mountain belts in the Alpine-Carpathian-Dinaride-Pannonian realm. **B**) Most important tectonic mega-units/nappe systems in the Alpine-Carpathian-Dinaride-Pannonian realm with more detailed names of the different units and the area of the field trip indicated (after Kovacs et al. 2010, 2011).
For the Austroalpine mega-unit and the exact geographic position of the Northern Calcareous Alps see Fig. 2.

geological investigations form a solid data base with many topics still controversially discussed and remaining open questions. Not only the geodynamic models are controversial but there is also still no consensus on the palaeogeographic configuration of today's mountain puzzle in this region (details in Missoni & Gawlick 2011a).

There is a large number of contrasting palaeogeographic reconstructions of the Alpine Belt and adjacent regions for the Late Triassic to Jurassic period (e.g., Frisch 1979, Haas et al. 1995, Gawlick et al. 1999a, 2008, Stampfli & Borel 2002, Schmid et al. 2004, 2008, Stampfli & Kozur 2006, and many others; compare Zacher & Lupu 1999). Our reconstruction of the Austroalpine domain´s tectonostratigraphic evolution follows a causal approach. It is based on the tectonic events steering the depositional areas´ development and the deposition of the different sedimentary successions (= formations and lithostratigraphic names), respectively. The formations are classified in respect of their event-related deposition within a palaeogeographic domain. The subordinate control of the history of the Austroalpine domain was the situation of the latter as part of a continent between two oceanic domains: the Alpine Atlantic Ocean (= South Penninic/Piemont/Ligurian Ocean) to the west/northwest related to the Central Atlantic Ocean (e.g., Frisch 1979, Lemoine & Trümpy 1987 - the term "Alpine Tethys" should not be used in order to avoid confusion: e.g., Dal Piaz 1999, Stampfli & Borel 2002, Schmid et al. 2004, 2008, Stampfli & Kozur 2006) and the Neotethys Ocean to the south/southeast (not Meliata Ocean - compare Krystyn et al. 2008) (Fig. 3, Fig. 6).

In Triassic to Early Cretaceous times the Northern Calcareous Alps, together with the Western Carpathians, the Dinarides, the Albanides, the Hellenides and other regions, formed a continuous NNE-SSW trending belt facing the north-western margin of the Neotethys Ocean (Fig. 3) and undergoing the same history: Formation of oceanic crust since Late Anisian, onset of inneroceanic thrusting in late Early Jurassic, ophiolite obduction in Middle-Late Jurassic, followed by the formation of shallow-water platforms, extensional collapse due to tectonic thickening and mountain uplift before the Jurassic/Cretaceous boundary, and infilling of the foreland basins with the erosional products of this orogen in the Early Cretaceous. The detailed documentation of the geodynamic evolution as synthesized in Missoni & Gawlick (2011a, b) clearly demonstrates that a prominent orogenic event with

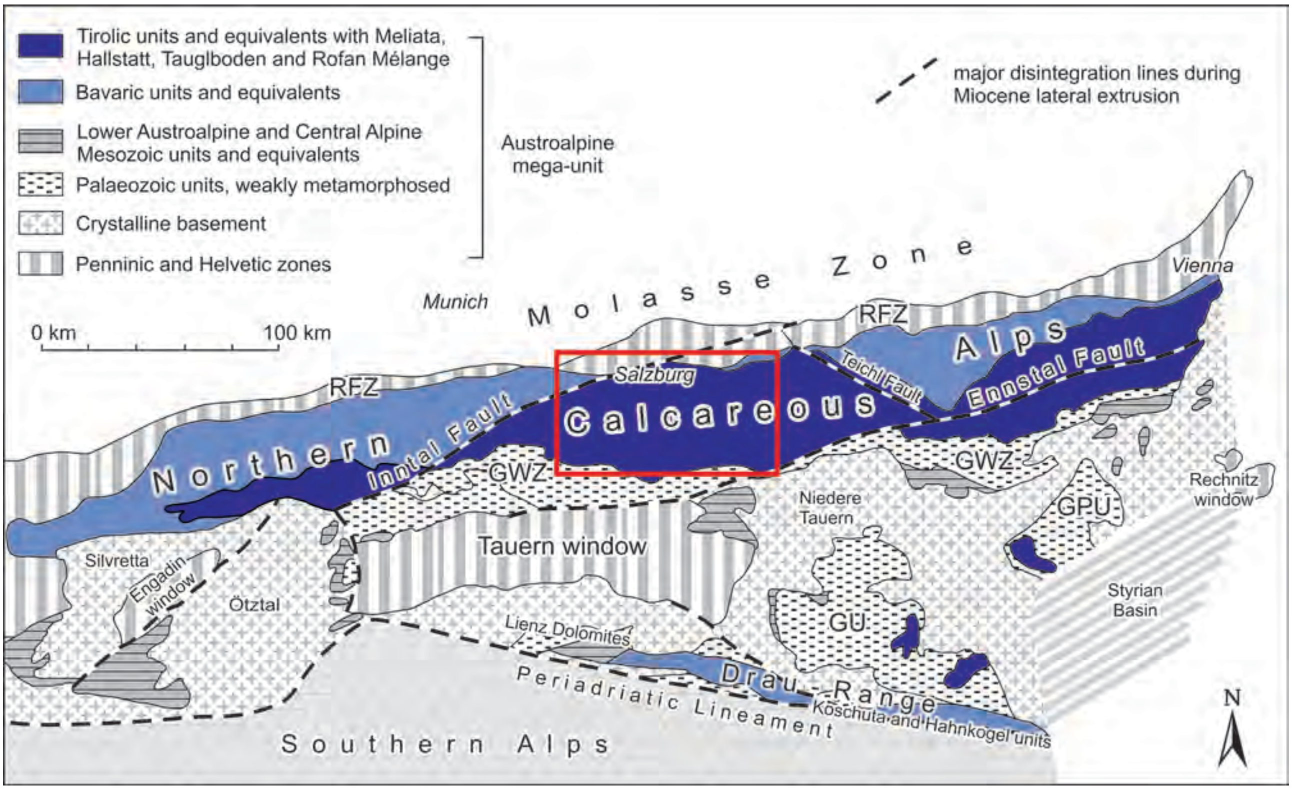

Fig. 2: Tectonic sketch map of the Eastern Alps and field trip area (compare Fig. 8; after TOLLMANN 1977, FRISCH & GAWLICK 2003). *GPU* Graz Palaeozoic Unit; *GU* Gurktal Unit; *GWZ* Greywacke Zone; *RFZ* Rhenodanubian Flysch Zone.

oceanic accretion, fold thrust belt formation and foreland basin creation has taken place in that period. The regional importance of this event affected the complete western margin of the Neotethys margin; therefore the name Neotethyan Belt for this Jurassic orogen was introduced by MISSONI & GAWLICK (2011b).

Overall geodynamic and sedimentary evolution:
Following a major post-Variscan regression and Permian crustal extension (e.g., SCHUSTER & STÜWE 2008), sedimentation in the northwestern Tethyan realm started in the Middle/Late Permian with coarse-grained siliciclastic sediments in the northwest (Alpine Verrucano - compare TOLLMANN 1976a, 1985) and evaporites to the southeast (Alpine Haselgebirge: TOLLMANN 1976a, 1985) due to early Neotethyan crustal extension (SCHUSTER et al. 2001). In the Early Triassic, siliciclastic sedimentation continued with the deposition of the Alpine Buntsandstein in the northwest and with deposition of the marine Werfen Beds in the southeast (Fig. 4). Around the Early/Middle Triassic boundary, carbonate production started with the build-up of carbonate ramps (top Werfen Formation, Gutenstein and Steinalm Formations: Fig. 4). The opening event with open marine influence is manifested below the Middle Anisian Steinalm Formation (LEIN et al. 2010). Shallow-water carbonate sedimentation with overlying hemipelagic carbonates (GALLET et al. 1998) as the result of a partial drowning event due to the final break-up of the Neotethys Ocean in the late Pelsonian (LEIN & GAWLICK 2008) dominated in the entire Eastern Alps in the Middle Triassic.

In late Middle to early Late Triassic times, the Wetterstein Carbonate Platform was formed (Fig. 4). This platform was overlain by siliciclastic sediments of the Lunz and Northalpine Raibl Formations or by the Reingraben Formation (*Halobia* Beds) in the Hallstatt realm (HORNUNG et al. 2007, KRYSTYN 2008). After this siliciclastic event a new carbonate ramp built up in Tuvalian time (Opponitz and Waxeneck Formations). On top, the classic Late Triassic Hauptdolomit/Dachstein Carbonate Platform was formed during optimum climatic and geodynamic conditions in the Norian and Rhaetian.

At the Triassic/Jurassic boundary, the carbonate production rate significantly decreased. This occurred in connection with an environmental crisis that led to mass extinction and was accompanied by a sea-level drop (compare SEPKOSKI 1996). This mass extinction coincided with an environmental change: a global cooling and sea-level fall (e.g., OGG 2004a, b) around the Triassic/Jurassic-boundary (e.g., HUBBARD & BOUTLER 2000, GUEX et al. 2004), followed by a warming event and long-term sea-level rise in the Hettangian (MCELWAIN et al. 1999, GUEX et al. 2004, OGG 2004b). Also a perturbation of the global carbon cycle (e.g., PÁLFY et al. 2001, HESSELBO et al. 2002, WARD et al. 2004) as well as significant sea-level changes can be recognized (e.g., HALLAM 1997). Regardless of the causes of this mass extinction (e.g., MARZOLI et al. 2004, LUCAS & TANNER 2007), which are intensively debated (summarized e.g., in PÁLFY 2008), these environmental events left a signature in the Austroalpine domain (e.g., HILLEBRANDT & KRYSTYN 2009).

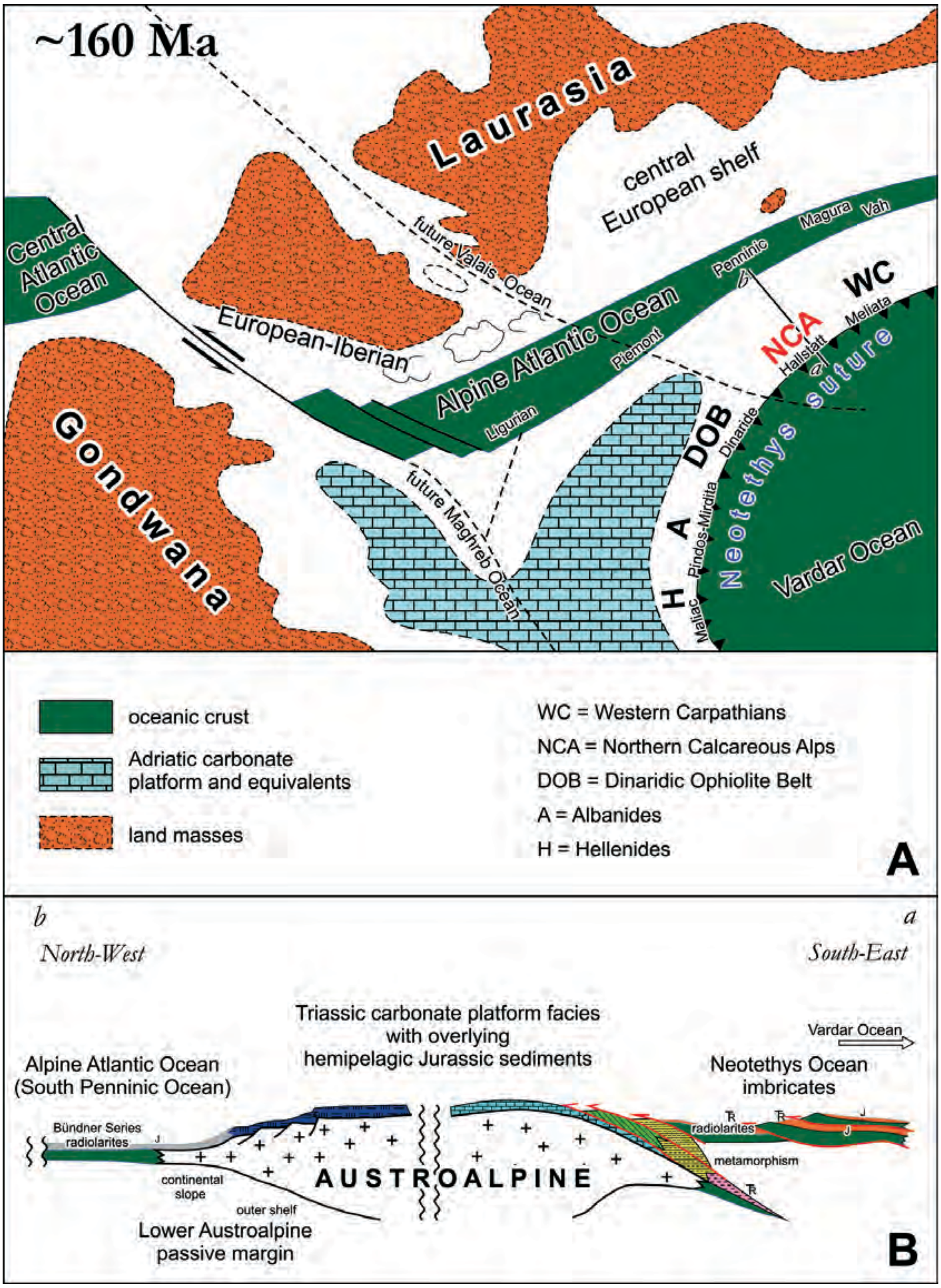

Fig. 3: **A**) Palaeogeographic position of the Northern Calcareous Alps as part of the Austroalpine domain in Late Jurassic time (after FRISCH 1979, GAWLICK et al. 2008). In this reconstruction the Northern Calcareous Alps are part of the Jurassic Neotethyan Belt (orogen) striking from the Carpathians to the Hellenides. The Neotethys suture is equivalent to the obducted West-Vardar ophiolite complex (e.g., Dinaridic Ophiolite Belt) in the sense of SCHMID et al. (2008) = far-travelled ophiolite nappes of the western Neotethys Ocean in the sense of GAWLICK et al. (2008) (see ROBERTSON 2012 for discussion). The eastern part of the Neotethys Ocean remained open = Vardar Ocean (compare Figs. 73-100). Toarcian to Early Cretaceous Adria-Apulia carbonate platform and equivalents according to GOLONKA (2002), VLAHOVIC et al. (2005), and BERNOULLI & JENKYNS (2009). **B**) Schematic cross section reconstructed for Middle to Late Jurassic times. It shows the passive continental margin of the Lower Austroalpine domain facing the Penninic Ocean to the northwest (e.g., TOLLMANN 1985, FAUPL & WAGREICH 2000) and the lower plate position and imbrication of the Austroalpine domain in relation to the obducted Neotethys oceanic crust (after GAWLICK et al. 2008). Compare FRISCH (1979, 1980a, b).

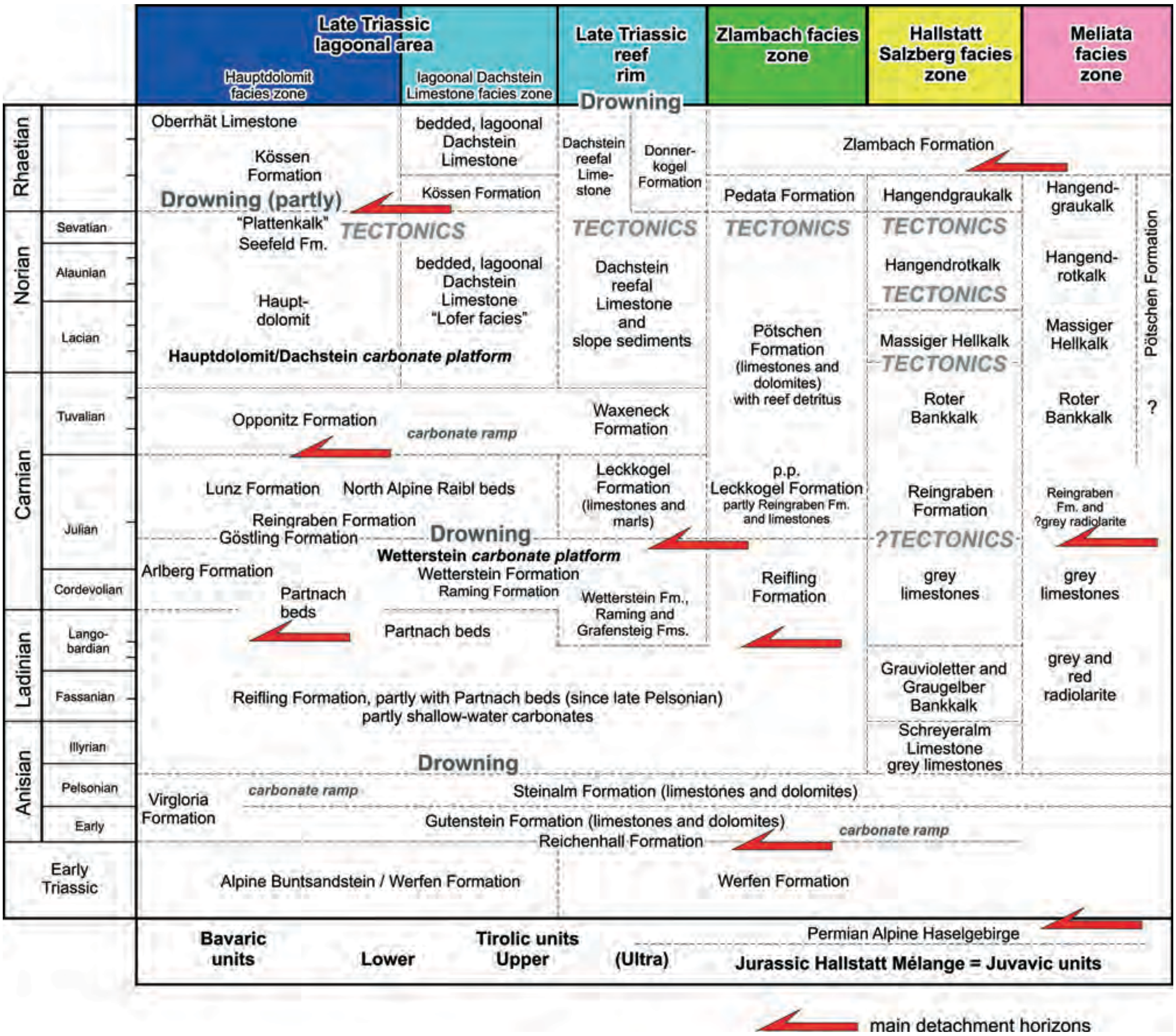

Fig. 4: Lithostratigraphic table of Triassic formations and tectonic events in the Northern Calcareous Alps (modified after Tollmann 1985, Gawlick & Frisch 2003, Piller et al. 2004). The main detachment horizons are indicated because of their importance during Jurassic nappe stacking and disintegration of the sequence in the course of mélange formation. The colours of the different facies belts in this figure correspond to the colours in the other figures, clarifying the provenance of the different clasts and slides in the Jurassic basin successions (after Missoni & Gawlick 2011a). Compare also Fig. 6.

Earliest Jurassic sediments are missing on top of the morphologic highs (former Hauptdolomit/Dachstein Carbonate Platform). Only in basinal areas sedimentation was continuous (Hillebrandt & Krystyn 2009). Lack of sufficient sediment supply led to drowning of the Hauptdolomit/Dachstein Carbonate Platform in Late Hettangian times due to a sea-level rise. The spread and morphology of the facies zones in the Early to early Middle Jurassic followed in general the Triassic inventory (Figs. 5) except in the lower Austroalpine units and equivalents.

Later on, a horst and graben morphology developed (Bernoulli & Jenkyns 1974, Eberli 1988, Krainer et al. 1994) and triggered breccia formation along submarine slopes and escarpments, mainly in Late Pliensbachian to Early Toarcian times (Böhm et al. 1995). An increasing pelagic influence was manifested in the Early to Middle Jurassic sediments (Garrison & Fischer 1969, Böhm 1992). Breccia formation in late Early Jurassic time is mostly interpreted as a result of the opening of the Ligurian/Penninic (= Alpine Atlantic) Ocean (e.g., Bernoulli & Jenkyns 1974, Eberli 1988, Krainer et al. 1994), named Penninic Ocean in the Eastern Alpine realm (compare Fig. 3). Whereas the older part of the Early Jurassic sequences near to the Penninic realm (Lower Austroalpine passive continental margin) shows the typical features of a rifted margin (e.g., Eberli 1988), the other areas of the Austroalpine were only slightly influenced by these rifting processes. In contrast, late Early Jurassic (Late Pliensbachian to Early Toarcian) tectonics affected mainly the Dachstein Limestone facies belt (Fig. 5) and resulted

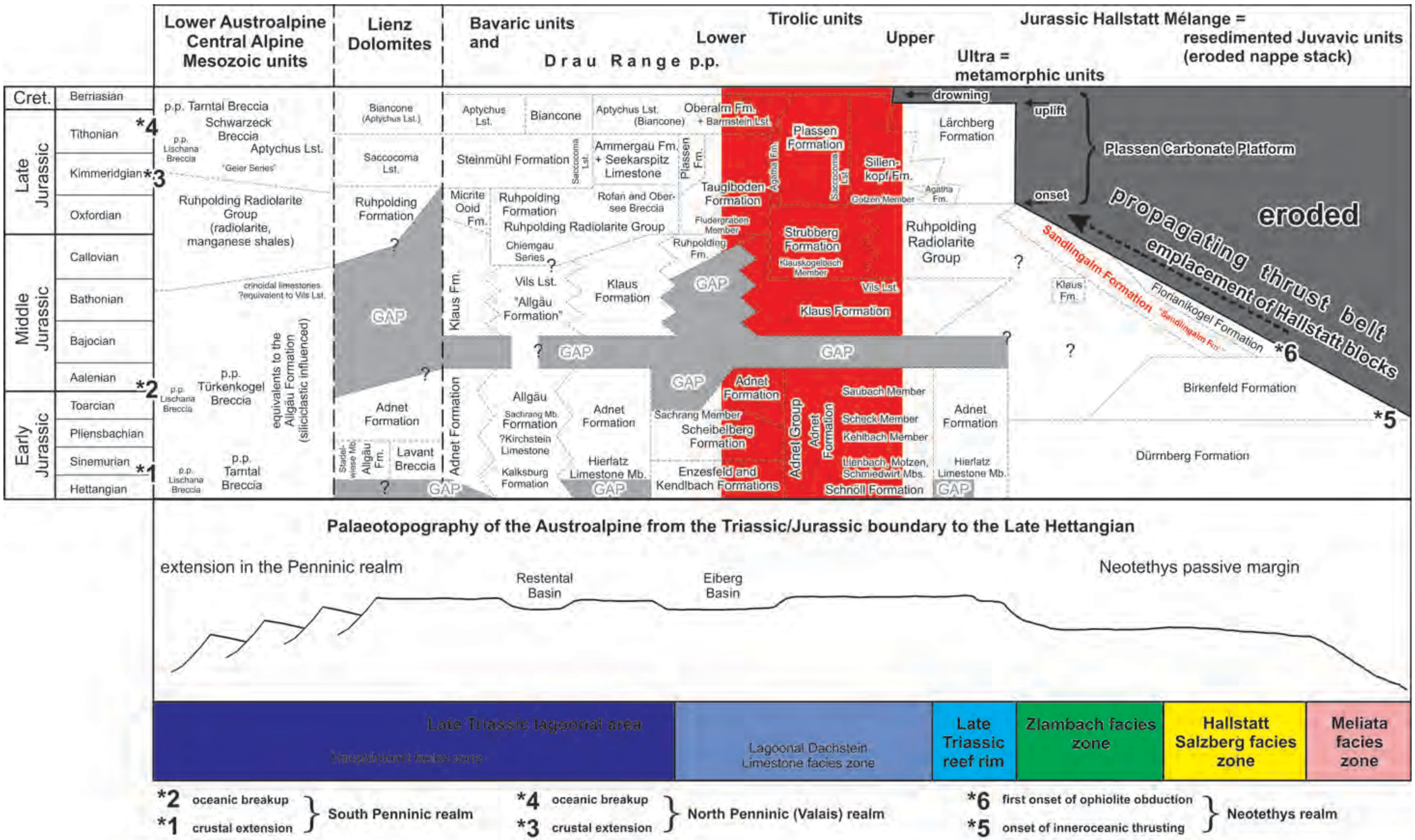

Fig. 5: Stratigraphic table with lithostratigraphic names and main tectonic events of the Jurassic in the Austroalpine realm with their variations depending on the palaeogeographic position (after GAWLICK et al. 2009a; compare Fig. 4, Fig. 6). In red the sedimentary succession which will be visited during the field trip. Bavaric units, Tirolic units, Hallstatt Mélange = Northern Calcareous Alps.

in a completely new palaeogeographic setting. Meanwhile the Lower Austroalpine passive margin was not or only mildly influenced by these tectonic processes.
Many authors interpreted the above described change in the late Early Jurassic as a result of the opening of the Penninic Ocean (e.g., Eberli 1988, Krainer et al. 1994). In contrast, Frisch & Gawlick (2003), Gawlick et al. (2009a) and Missoni & Gawlick (2011a, b) attributed this "event" to the onset of subduction in the Neotethys Ocean realm.
In late Early to Middle Jurassic times the situation generally changed also in the former (Triassic) carbonate platform area due to the partial closure of the Neotethys Ocean (Fig. 3). Concerning the active margin, the Austroalpine domain attained the lower plate position (Gawlick et al. 1999a). The tectonics of this time span were characterized by a propagating thrust belt in front of the overriding ophiolite nappe stack, as proven in the Albanides and Dinarides (Gawlick et al. 2008, 2009b). In the Eastern Alps and the Northern Calcareous Alps, respectively, the obducted ophiolite nappe stack is not preserved. Here, only pebbles in the Late Jurassic to Early Cretaceous deep-water sedimentary successions prove this ophiolite obduction stage (summarized in Gawlick et al. 2009a). The same story is visible in the southern Western Carpathians (Froitzheim et al. 2008, Kovacs et al. 2011, Haas et al. 2011).
Middle Jurassic northwest-directed thrusting caused the formation of deep-water trench-like basins in front of the propagating nappes which obliquely cut through former facies belts. Tectonic shortening decreased in Late Jurassic time. In contrast to the Triassic evolution, shallow-water carbonates are generally missing in the Austroalpine domain during most time of the Jurassic until the Late Oxfordian, when new shallow-water carbonate ramps and platforms established (Fig. 3) and sealed the main tectonic shortening structures. They existed until the Early Cretaceous. Siliciclastic influenced sediments occurred in the southern Northern Calcareous Alps in the Kimmeridgian and in the more northward parts in the Early Cretaceous (Fig. 3).

NW-SE directions refer to Triassic-Jurassic palaeogeographic reconstructions. North-South geographic directions refer to the Present as a result of a complex rotation history of the Eastern Alps since Late Cretaceous (e.g., Haubold et al. 1999, Csontos & Vörös 2004, Thöny et al. 2006, Pueyo et al. 2007).

1.1. Triassic-Jurassic palaeogeography, sedimentary successions and stratigraphy

The reconstruction of the Triassic palaeogeography, i.e., the facies zones of the shallow-water Hauptdolomit/Dachstein Carbonate Platform and its gradual transition to the hemipelagic Hallstatt Zone, has been arranged in a characteristic shore parallel fashion (Fig. 6) (Lein 1985, Krystyn & Lein 1995 in Haas et al. 1995, Gawlick et al. 1999a). Their Late Anisian to Early Jurassic sedimentary succession represented an open marine, distal periplatform setting on the Triassic European continental margin facing the Neotethys Ocean (= Meliata Ocean or Meliata-Hallstatt Ocean according to, e.g., Kozur 1991, Schweigl & Neubauer 1997, Neubauer et al. 2000, Stampfli et al. 2001, Stampfli & Kozur 2006).
The variegated Hallstatt Salzberg facies represents the oceanward belt on this margin, giving way to siliceous limestones and radiolarites towards the Neotethys Ocean (= Meliata facies; Fig. 6). In the sedimentary environment of the Hallstatt Salzberg facies with relatively stable hemipelagic conditions for at least 40 Ma, the existence of large intermediate shallow-water carbonate platforms is quite unrealistic (Gawlick & Böhm 2000). Only the Zlambach facies zone received shallow-water debris from the large, flat-topped Triassic carbonate platforms.

1.1.1. Hauptdolomit facies zone

Triassic

The Hauptdolomit facies zone is preserved only in the lower structural units of the Northern Calcareous Alps (Bavaric and in parts Tirolic nappes: see chapter geological overview). Permian and Early Triassic sediments are mostly missing in these profiles as a result of the usage of shallower detachment levels during younger tectonic movements (Tollmann 1985). The thickness of the Middle and Late Triassic formations (Fig. 4) can only be roughly estimated due to the polyphase tectonic history, but could be around 4-5 km (Brandner 1984).
Carbonate production started around the Early/Middle Triassic-boundary with carbonate ramp sediments above the Alpine Buntsandstein (Stingl 1989) and the evaporitic Reichenhall Formation. The lower Gutenstein Formation was formed in a restricted, periodically hypersaline lagoonal area. The overlying Steinalm Formation represent sediments of more open marine conditions, partly forming small build-ups and reefal structures created particularly by calcareous algae and microbial mats. The Gutenstein and Steinalm Formations are named Virgloria Formation in the western Northern Calcareous Alps (Piller et al. 2004). In Late Anisian time a large part of this (Steinalm) carbonate ramp was drowned and widespread basinal carbonate sedimentation took place (grey, cherty limestones of the Reifling Formation) (Bechstädt & Mostler 1974, 1976, Krystyn 1991, Krystyn & Lein 1996). According to Gawlick (2000a) and Missoni & Gawlick (2011a) the hemipelagic carbonatic basins were separated from the open shelf area by the growing Wetterstein carbonate platforms to the southeast in the Late Ladinian (Langobardian) (compare Krystyn & Lein 1996). The Reifling sedimentation was replaced by fine-grained siliciclastic deposition of the Partnach Beds. During Early Carnian, after a regressive/transgressive cycle the Wetterstein Carbonate Platform (Arlberg and Wetterstein Formations) started to prograde into this facies belt (Brandner & Resch 1981, Krystyn & Lein 1996). South of the rapidly southeastward (towards the Dachstein Limestone facies zone) prograding platform (Raming Formation as slope deposits: Lein 1989), a basinal area prevailed in Early Carnian (Cordevolian) time. The youngest sediments in

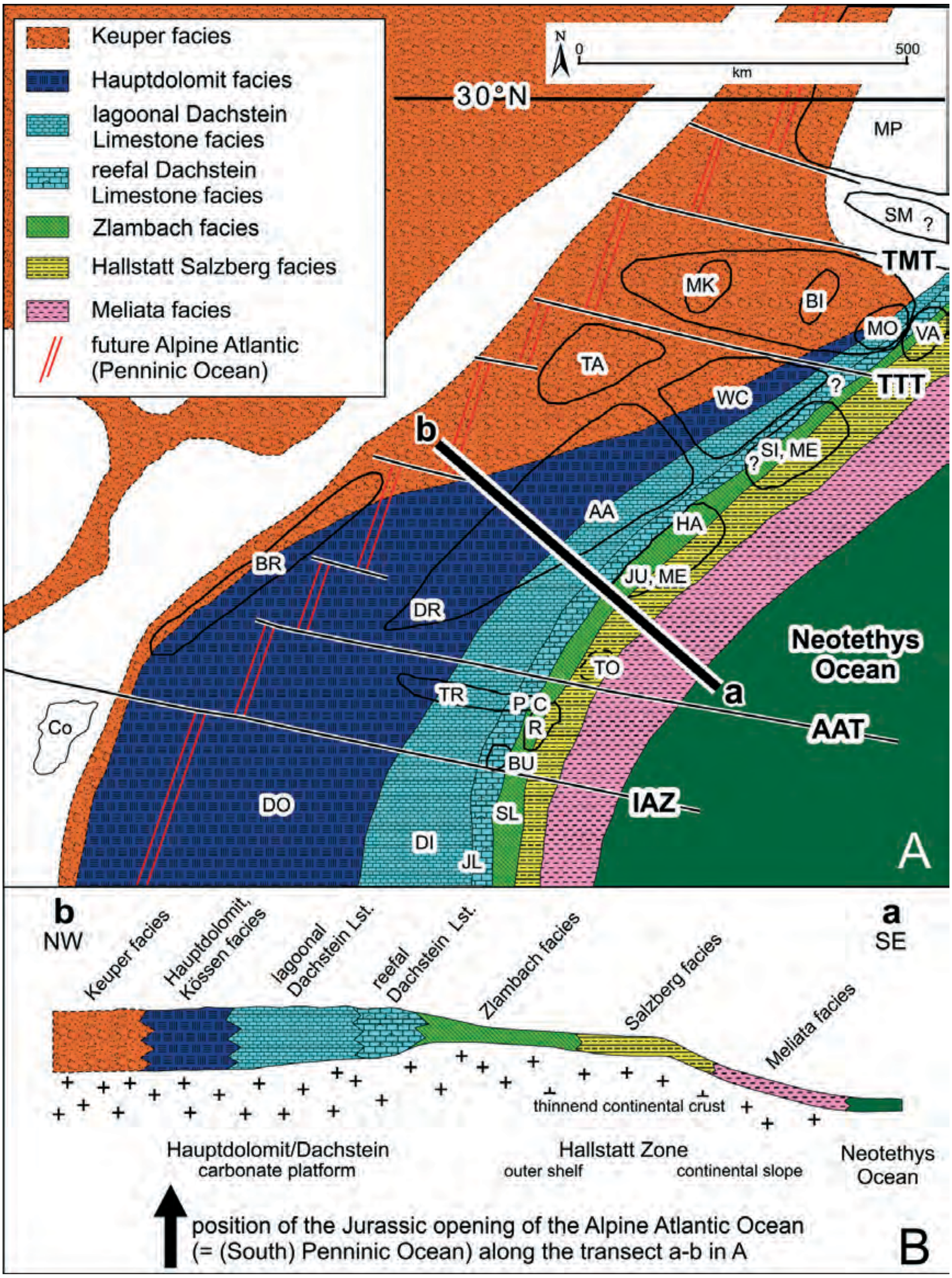

Fig. 6: **A**) Late Triassic palaeogeographic position and facies zones of the Austroalpine domain as part of the northwestern Neotethys passive margin, modified after KRYSTYN & LEIN in HAAS et al. (1995) and GAWLICK et al. (1999a, 2008). **B**) Schematic cross section (for position, see line a-b in A) showing the typical passive continental margin facies distribution across the Austroalpine domain in Late Triassic time (after GAWLICK & FRISCH 2003). Compare Fig. 3.
IAZ = Iberia-Adria Zone transform fault, AAT = future Austroalpine-Adria transform fault, TTT = future Tisza-Tatra transform fault, TMT = future Tisza-Moesia transform fault, AA = Austroalpine, BI = Bihor, BR = Briançonnais, BU = Bükk, C = Csovar, Co = Corsica, DI = Dinarids, DO = Dolomites, DR = Drau Range, HA = Hallstatt Zone, JU = Juvavicum, JL = Julian Alps, ME = Meliaticum, MK = Mecsek, MO = Moma unit, MP = Moesian platform, P = Pilis-Buda, R = Rudabanyaicum, SI = Silicicum, SL = Slovenian trough, SM = Serbo-Macedonian unit, TA = Tatricum, TO = Tornaicum, TR = Transdanubian Range, VA = Vascau unit, WC = central West Carpathians. For other reconstructions of the western Tethyan realm see, e.g., SENGÖR (1985a, b), CHANNELL et al. (1990, 1992), DERCOURT et al. (1986, 1993), MARCOUX & BAUD (1996), CHANNELL & KOZUR (1997), STAMPFLI & BOREL (2002), STAMPFLI & KOZUR (2006).

these basinal areas were the organic-rich grey, cherty limestones of the Göstling Formation. As consequence of the Lunz/Reingraben event (SCHLAGER & SCHÖLLNBERGER 1974, LEIN et al. 1997), the Wetterstein Carbonate Platform drowned nearly in the whole area in Julian time and deposition of siliciclastic sediments (Lunz and Northalpine Raibl Formations) took over (TOLLMANN 1976a, 1985, KRAINER 1985). These siliciclastic deposits filled the basinal areas between the Wetterstein Carbonate Platforms, with the result of a uniform topography at the end of this siliciclastic event. In the Late Carnian, the siliciclastic input decreased rapidly and a new carbonate ramp was established (Opponitz-Waxeneck carbonate ramp). The transition between the early Late Carnian "Northalpine Raibl Formation" and the more carbonatic sedimentation farer to the south is gradual. Around the Carnian/Norian-boundary this carbonate ramp passed in the Late Triassic Hauptdolomit/Dachstein Carbonate Platform (for details see TOLLMANN 1976a, 1985, GAWLICK & BÖHM 2000). The Hauptdolomit ranges from?latest Carnian/earliest Norian to the Middle/Late Norian, with newly formed intraplatform basins in Middle to Late Norian times (Seefeld Formation) (TOLLMANN 1976a, DONOFRIO et al. 2003, compare BECHTEL et al. 2007). In the Late Norian, opening of the restricted Hauptdolomit lagoon resulted in deposition of the "Plattenkalk". In Early Rhaetian the lagoon deepened and renewed siliciclastic input led to deposition of the mixed terrigenous-carbonatic Kössen Formation (stratigraphic details in GOLEBIOWSKI 1990, 1991). In Late Rhaetian, the Kössen Formation was in many places overlain by shallow-water carbonates including reefal build-ups in some areas (Oberrhät Limestone: FLÜGEL 1981). Within the Hauptdolomit facies zone, these shallow-water carbonates prograded from north towards south.

Jurassic

In the earlier Early Jurassic, the sedimentation was mainly controlled by the Late Triassic topography (Fig. 5; BÖHM 2003, GAWLICK & FRISCH 2003, GAWLICK et al. 2009a). Only in the westernmost part of the Austroalpine domain extensional tectonics led to the formation of the southeastern (Lower Austroalpine and equivalents) passive continental margin of the (South) Penninic Ocean (FRISCH 1979, EBERLI 1988, HÄUSLER 1988) as part of the Central Atlantic system (Fig. 3, details of the whole evolution in GAWLICK et al. 2009a). Near to the future oceanic realm (start of sea-floor spreading in Late Toarcian: RATSCHBACHER et al. 2004) asymmetric, breccia-filled basins are common features (e.g., EBERLI 1988). The influence of this extensional process decreased in eastern direction towards the Dachstein Limestone facies zone. Therefore, in most areas block tilting was relatively mild in the Hauptdolomit facies zone in direction towards the Dachstein Limestone facies belt.
The Rhaetian shallow-water carbonates were overlain by red and grey crinoidal limestones in the Hettangian and Sinemurian, partly with a gap in the depositional record (EBLI 1997). On top of the Rhaetian Kössen Formation cherty and marly bedded limestones were deposited (Kalksburg Formation and Kirchstein Limestone). These sediments progressed gradually into the hemipelagic Allgäu Formation (Sinemurian to ?Bathonian). In the depositional areas of the Adnet and Enzesfeld Formations, condensed sedimentation prevailed partly until the late Middle Jurassic. Red limestone deposition resumed in the form of the Steinmühl or Klaus Limestones (Bajocian to Tithonian; KRYSTYN 1971, 1972). In the Callovian to Oxfordian there was a widespread deepening of the depositional environment, which resulted in the sedimentation of cherty limestones, cherty marls, and radiolarites. In basinal areas on top of the Allgäu Formation, dark grey cherty marls and cherty limestones were deposited. These were formerly interpreted as early to late Middle Jurassic Allgäu Formation (EBLI 1997, PILLER et al. 2004), but are in fact time equivalents of the Ruhpolding Radiolarite Group (Chiemgau series) in the sense of GAWLICK & FRISCH (2003), followed by *Saccocoma* Limestone. On the Early to Middle Jurassic topographic highs, red condensed limestones or condensed radiolarites were deposited (Callovian to Kimmeridgian). In the Kimmeridgian the siliceous sedimentation passed gradually to a marlier and then limier one, which is characteristic for the Tithonian to Early Berriasian (Ammergau Formation, Aptychus beds, Biancone). Typical Aptychus beds beside Biancone were deposited in the Late Tithonian.

1.1.2. Dachstein Limestone facies zone

Triassic

In the Dachstein Limestone facies zone (mainly preserved in the Tirolic unit: see chapter geological overview) the stratigraphic and facial evolution reflects the intermediate passive margin setting between the Hauptdolomit facies zone and the Hallstatt facies belt (Fig. 6). The thickness of the Middle and Late Triassic formations is slightly higher compared to that in the Hauptdolomit facies zone.
Carbonate production began in the Late Olenekian, slightly earlier than in the Hauptdolomit facies zone (MOSTLER & ROSSNER 1984), followed by the evaporitic Reichenhall Formation around the Olenekian/Anisian-boundary. Increased carbonate productivity started also around the Early/Middle Triassic-boundary with carbonate ramp sediments (Gutenstein and Steinalm Formations) above the Alpine Buntsandstein/Werfen Formation and the evaporitic Reichenhall Formation. In Late Anisian time, large part of this carbonate ramp drowned and widespread basinal sedimentation took place, with dolomites predominating, (Reifling Formation) (e.g., MISSONI & GAWLICK. 2011a). The siliciclastic influenced Partnach Formation was deposited in the northern part of this facies belt, whereas in the more southeastern part of this facies belt the Wetterstein Carbonate Platform was formed since the Late Ladinian (KRYSTYN & LEIN 1996). Transitional to the hemipelagic open shelf areas, the Raming and Grafensteig Formations (HOHENEGGER & LEIN 1977) were formed. This platform drowned in Julian time nearly in the whole facies belt in the wake of the Lunz/Reingraben event (SCHLAGER & SCHÖLLNBERGER 1974). Siliciclastic (e.g., Lunz/Raibl Formation, Reingraben Formation) and carbonatic sediments (Cidaris Limestone) were deposited. As in the

Hauptdolomit facies belt, these siliciclastic rocks filled the basinal areas between the Wetterstein Carbonate Platforms, leading to a nearly uniform topography at the end of the siliciclastic event. In the Late Carnian the siliciclastic input decreased rapidly and a new carbonate ramp was established. The Opponitz Formation was deposited under shallow-water, partly evaporitic conditions in the northern part of the Dachstein facies belt. Towards south, the environment passed gradually to a more open marine one, however, with the shallow-water Waxeneck Formation in the southern part of the Dachstein Limestone facies zone (KRYSTYN et al. 1990). Around the Carnian/Norian-boundary, this carbonate ramp passed into the lagoonal to reefal Dachstein Limestone platform. The Dachstein Limestone ranged from the lowermost Norian to the Late Norian, without recognised intraplatform basins in the Middle or Late Norian. In Early Rhaetian, the northern part of the Dachstein Limestone lagoon deepened by siliciclastic input and changed to the mixed terrigenous-carbonatic sedimentation of the Kössen Formation, intercalated by the *Lithodendron* reef limestone (GOLEBIOWSKI 1990, 1991). In the Late Rhaetian, the Kössen Formation was occasionally overlain by shallow-water, partly reefal carbonates (Oberrhät Limestone or Rhaetian Dachstein Limestone). The Rhaetian Dachstein Carbonate Platform (FLÜGEL 1981, SCHÄFER & SENOWBARI-DARYAN 1981) prograded from south towards north.

The southern part of the Dachstein Limestone facies zone, i.e., the reef rim (Upper Tirolic nappe), represented the transitional area from the lagoonal area to the open marine shelf (reef rim and transitional zone to the Hallstatt facies zone). The early Middle Triassic sedimentary succession of this transitional area is similar to those of the other parts of this facies belt. An Early Ladinian transition of the Reifling Formation into the Hallstatt Limestone is partly preserved. The formation of the Wetterstein Carbonate Platform started in the Late Ladinian. It rapidly prograded towards southeast (Raming Formation: LEIN 1989). The Lunz/Reingraben event affected these areas only peripheral with thin, fine-grained siliciclastic sediments (Reingraben Beds). In some areas, shallow-water organisms survived the event as recorded in the Julian Leckkogel Formation (DULLO & LEIN 1982). The Leckkogel Formation passed gradually into the Late Carnian Waxeneck Formation (LEIN in KRYSTYN et al. 1990) and later into “Hallstatt Limestones“ or the Norian to earliest Rhaetian reefal Dachstein Limestone (ZANKL 1969, FLÜGEL 1981, KRYSTYN et al. 2009) which drowned in Early Rhaetian time (KRYSTYN et al. 2009: newly introduced Donnerkogel Formation). In fact, in this palaeogeographic area a vertical mixture of basinal sediments, fore reef to back reef sediments, and partly lagoonal sediments occurred, reflecting sea-level fluctuations and possibly ?extensional tectonic movements (LEIN 1985, GAWLICK 1998, 2000a, GAWLICK & BÖHM 2000, compare MISSONI et al. 2008). In Late Norian time, in some areas of this facies belt hemipelagic sequences were deposited in newly formed basins (Mürztal facies, Aflenz facies: LEIN 1982, 1985, 2000, TOLLMANN 1985).

Jurassic

In the Early Liassic, the sedimentation was controlled by the topography of the Late Triassic Hauptdolomit/Dachstein Carbonate Platform (Fig. 5, BÖHM 2003, GAWLICK & FRISCH 2003). On top of the Rhaetian shallow-water carbonates red condensed limestones of the Adnet Group (Hettangian to Toarcian: BÖHM 1992, 2003) were sedimented, partly above a depositional gap. On top of the Rhaetian Kössen Formation cherty and marly bedded limestones (Scheibelberg Formation: Hettangian to Toarcian; Kendlbach Formation: Hettangian: BÖHM 1992, 2003, EBLI 1997, KRAINER & MOSTLER 1997) were deposited in the transitional areas to the Rhaetian Kössen Basin crinoidal or sponge spicula rich limestones of the Enzesfeld Formation (Hettangian to Sinemurian: BÖHM 1992). In the Late Pliensbachian and Early Toarcian, a horst and graben morphology developed (BERNOULLI & JENKYNS 1974, KRAINER et al. 1994) and triggered breccia formation along submarine slopes and escarpments (BÖHM et al. 1995). On the horsts, the Toarcian and most of the Middle Jurassic (if deposited) are either characterized by starved sedimentation and ferro-manganese crusts or by a hiatus. In contrast, the grabens were filled with deep-water carbonates and breccias shed along fault scarps. Neptunian dykes developed in various places. In these newly formed basinal areas grey bedded limestones were deposited, whereas the topographic highs were covered by condensed red limestones of the Klaus Formation (e.g., KRYSTYN 1972).

This sedimentation pattern diachronously changed dramatically in the late Middle Jurassic (GAWLICK & FRISCH 2003) when deposition of radiolarian cherts, radiolarian-rich marls and limestones of the Ruhpolding Radiolarite Group commenced (DIERSCHE 1980). For details see chapter 2.

1.1.3. Hallstatt facies zone (preserved in the reworked Jurassic Hallstatt Mélange)

The mostly condensed Triassic to Early Jurassic hemipelagic succession was deposited in an outer shelf depositional setting (Fig. 4, Fig. 6).

The Hallstatt facies zone (i.e., Hallstatt Zone) is subdivided into three facies zones:

a) Zlambach/Pötschen facies zone (grey Hallstatt facies, Zlambach/Pötschen facies with shallow-water allodapic limestone intercalations from the Dachstein reef rim).
b) Hallstatt Limestone facies zone (red or variously coloured Hallstatt facies or Hallstatt Salzberg facies) (for newest review see KRYSTYN 2008).
c) Meliata facies zone (LEIN 1987a, GAWLICK et al. 1999a); including the Pötschen Limestone *sensu stricto* (compare MOSTLER 1978). Recently the depositional area of the Pötschen Limestone without shallow-water influx (Pötschen Formation *sensu stricto*) has been interpreted as transitional facies from the Meliata facies belt (continental slope) to the oceanic realm (MISSONI & GAWLICK 2011a, b, compare GAWLICK et al. 2008).

Remnants of this facies belt are only present in the Middle to Late Jurassic radiolaritic trenches and on top of them, where all sedimentary rock types of the Hallstatt facies belt from the Triassic platform transitional area to the Meliata facies zone occur (for details: GAWLICK & FRISCH 2003, GAWLICK et al. 2009a, MISSONI & GAWLICK 2011a).

Zlambach/Pötschen facies zone

Early Triassic as well as Early and Middle Anisian sediments of this facies belt are not preserved within continuous sections. Fine-grained siliciclastic sediments of the Werfen Formation only occur as components together with components of the Gutenstein and Steinalm Formations and the complete reconstructable hemipelagic Late Anisian to Early Jurassic succession of this facies belt (GAWLICK 1996). Late Anisian to Ladinian Reifling Limestone is also proven in the form of small components within late Middle Jurassic mass-flow deposits (GAWLICK 1996, 2000b). The oldest continuously preserved sections start with well bedded, chert-rich limestone or hemipelagic dolomite of earliest Carnian age (GAWLICK 1998). The Julian *Halobia* Beds did not form a uniform, laterally persistent sedimentary layer in this facies belt but are partly preserved in some sections (MANDL 1984). In Late Carnian to Middle Norian times, mostly well-bedded cherty hemipelagic limestones of the Pötschen Formation with shallow-water allodapic limestone intercalations were deposited in more distal shelf areas (LEIN 1985, GAWLICK 1998, MISSONI & GAWLICK 2011a), probably transitional to the red or variously coloured Hallstatt facies zone (LEIN 1981, LEIN & GAWLICK 1999). Hemipelagic dolomites (Pötschen Dolomite similar to the Baca Dolomite of the Slovenian Trough and equivalents in the Cukali area of Albania) and bedded cherty limestones occurred in more proximal position near to the transitional area of the carbonate platforms and ramps. Here the carbonate platform facies and evolution is reflected in the carbonate basinal facies (REIJMER & EVERAAS 1991). Due to sea-level fluctuations occasionally shallow-water carbonates were deposited also (GAWLICK 1998). Terrigenous input and synsedimentary tectonics (strike-slip related movements according to MISSONI et al. 2008), led to more complex sedimentary facies patterns in Late Norian to Early Rhaetian times. This is expressed in different lithologies of the Pedata Formation: e.g., Pedata Plattenkalk, Pedata Dolomite, Pedata Limestone (MANDL 1984, GAWLICK 1998, 2000a). Also the basinal areas of the Mürzalpen facies and Aflenz facies were deepened during this time interval (LOBITZER 1974, LEIN 1982). Since Middle Rhaetian times (KRYSTYN 1987, 2008) the marly Zlambach Formation was deposited, which passed gradually into the Early Jurassic Dürrnberg Formation (GAWLICK et al. 2001, 2009a). The youngest known sediments in the Hallstatt facies zone are thick cherty to marly successions of the Toarcian to Aalenian Birkenfeld Formation (GAWLICK et al. 2009a, Missoni & GAWLICK 2011a, b).

Hallstatt Limestone facies zone

As distal continuation of the Zlambach/Pötschen facies zone (grey Hallstatt facies), the red or variously coloured Hallstatt facies (LEIN 1987a, KRYSTYN 2008) sedimentation started with the drowning of the Steinalm carbonate ramp in Anisian (Late Pelsonian) time. Early Triassic Werfen Formation is only proven as components in Late Triassic Hallstatt Limestone (LEIN 1981). The Steinalm Formation followed stratigraphically the lower Anisian Gutenstein Formation. Hemipelagic sedimention started in late Middle Anisian with the condensed red Schreyeralm Limestone (e.g., KRYSTYN et al. 1971, TOLLMANN 1985), followed by the Grauvioletter-Graugelber Bankkalk (Ladinian), the Hellkalk (Late Ladinian to Early Carnian), *Halobia* Beds (Julian), the Roter Bankkalk (Tuvalian), the Massiger Hellkalk (Lacian), the Hangendrotkalk (Alaunian to Sevatian), the Hangendgraukalk (Early Rhaetian) (KRYSTYN 1980, 2008) and the Zlambach Marls (Middle to Late Rhaetian: KRYSTYN 1987, 2008). These passed gradually into the Early Jurassic Dürrnberg Formation which is overlain by the Birkenfeld Formation (see above).

Meliata facies zone

The Meliata facies zone represents the most distal part of the Triassic shelf area, the continental slope and the transition to the Neotethys Ocean. Rare remnants of this facies belt are described from the eastern (MANDL & ONDREJICKOVÁ 1991, 1993, KOZUR & MOSTLER 1992) and from the central Northern Calcareous Alps (GAWLICK 1993). These remnants occur partly as metamorphosed isolated slides (Florianikogel area) or as breccia components. A general stratigraphic reconstruction shows Middle Triassic radiolarites and partly cherty marls followed by Early Carnian *Halobia* Beds and Late Carnian to Early Rhaetian Hallstatt Limestone (red and grey). Younger sediments are so far not proven, but a similar sedimentary succession like in the Hallstatt Limestone facies zone can be expected. The Meliata facies zone is thought to have been the most basinward facies belt underlain by continental crust, incorporated in the evolving imbricate wedge during the closure of the western part of the Neotethys Ocean (late Early Jurassic as mentioned by GAWLICK & FRISCH 2003, GAWLICK et al. 2009a, MISSONI & GAWLICK 2011a, b). Recently also sequences of the Pötschen Limestone *sensu stricto* have been interpreted to derive from the transitional area of the Meliata facies zone to the Neotethys Ocean (MISSONI & GAWLICK 2011a, b; compare GAWLICK et al. 2008, 2009b).

1.2. Geological overview

Classical concept and historical alternatives

The classic tectonic subdivision of the Northern Calcareous Alps (compare Fig. 2) (in its fundamentals established by HAUG 1906, later modifications by, e.g., HAHN 1913, KOBER 1923, SPENGLER 1951, PLÖCHINGER 1980, TOLLMANN 1985) defined three nappe groups. These are, from bottom to top: Bavaric, Tirolic, and Juvavic nappe group (today only preserved in the Hallstatt Mélange). This tectonic concept, established in the Berchtesgaden Alps and in the

Salzkammergut area, was widely accepted. Later, a subdivision into three tectonic units ("Stockwerke" *sensu* LEBLING et al. 1935) was proposed: the Tirolic unit ("Tirolische Einheit" *sensu* HAHN 1913) at the base, overlain by the Lower Juvavic unit ("Tiefjuvavische Einheit": Hallstatt nappes), and the Upper Juvavic unit ("Hochjuvavische Einheit": Berchtesgaden and Dachstein nappes). Subsequently, in the salt-mine of Hallein MEDWENITSCH (1962) subdivided the Lower Juvavic nappe into a Lower ("Untere Hallstätter Decke": Zlambach nappe - grey Hallstatt facies rocks) and an Upper Hallstatt nappe ("Obere Hallstätter Decke": Sandling nappe - variously coloured Hallstatt Limestone nappe). In this concept fragmentary blocks of Lower Juvavic Hallstatt Limestones (TOLLMANN 1976b) framed the Upper Juvavic nappes (TOLLMANN 1985 for details and figures).

In an alternative concept, evaporites, subsumed as Alpine Haselgebirge (Permian salt-claystone succession; Haselgebirge Mélange according to SPÖTL et al. 1998), acted as a ductile paste and motor of gravitational tectonics. Gravitational tectonics in the Juvavic units should have started in the Oxfordian (e.g., TOLLMANN 1981, 1987, MANDL 1982, LEIN 1985, 1987a) or Late Tithonian (PLÖCHINGER 1974, 1976, 1984), leading to Late Jurassic to Early Cretaceous sliding of Alpine Haselgebirge and Hallstatt Limestone successions towards the north. According to these models (summarized in, e.g., TOLLMANN 1987, LEIN 1987b), sliding began in a phase of enhanced radiolarite sedimentation when troughs with marine sedimentation were arranged along the median longitudinal axis of the Northern Calcareous Alps (DIERSCHE 1980). Mainly based on ammonite stratigraphy (summarized in DIERSCHE 1980), the onset of radiolarite sedimentation was estimated as Oxfordian. Hence, the radiolarite basins were filled up by deep-water cherty limestones to radiolarites with intercalated breccias and turbidites. Slump folds are characteristic features in these sediments (e.g., GARRISON & FISCHER 1969, SCHLAGER & SCHLAGER 1973, DIERSCHE 1980, TOLLMANN 1987).

The formation of the generally asymmetric radiolarite basins was attributed to extensional tectonics (e.g., SCHLAGER & SCHLAGER 1973, DIERSCHE 1980, VECSEI et al. 1989). Another group of authors attributed basin formation and breccia mobilization to strike-slip tectonics (e.g., FISCHER 1965, WÄCHTER 1987, FRANK & SCHLAGER 2006, ORTNER et al. 2008).

Current concept

In the current concept, based on new results, we follow:

1) The tectonic subdivision of the Eastern Alps of TOLLMANN (1977) with some modern modifications (FRISCH & GAWLICK 2003, compare SCHMID et al. 2004) (Fig. 2),
2) The palaeogeographic reconstructions of KRYSTYN & LEIN in HAAS et al. (1995) with some modifications (Fig. 6), and
3) The concept that the Jurassic geodynamic history of the Austroalpine domain mirrors its palaeogeographic position between two oceanic domains (Fig. 3):
   A) To the west (northwest) the newly formed Penninic Ocean as part of the Alpine Atlantic, where continental extension started around the Triassic/Jurassic boundary or in the Hettangian, with the first oceanic crust formed in the late Early Jurassic (Toarcian), and
   B) to the east (southeast) the Neotethys Ocean, in which closure started before the Early/Middle Jurassic boundary.

The Juvavic nappe stack represented the Jurassic accreted wedge of the Northern Calcareous Alps (FRISCH & GAWLICK 2003). It became completely eroded with remnants of this nappe complex only preserved in the Middle to Late Jurassic radiolaritic trench-like (wildflysch) basin fills (GAWLICK & FRISCH 2003). These basins were situated in front of the propagating thrust belt or on top of them and were later overthrusted. In these radiolaritic basins all sedimentary rocks of the Meliata facies zone, the Hallstatt facies belt and from the reefal belt of the Triassic carbonate platform occur as redeposits. Some blocks show the effect of transported metamorphism (GAWLICK & HÖPFER 1999, MISSONI & GAWLICK 2011a, compare FRANK & SCHLAGER 2006).

In the Bajocian the sedimentary evolution in the southern (palaeogeographically southeastern - Fig. 3) part of the Tirolic realm as well as in the Hallstatt realm differed from that in the northern (palaeogeographically northwestern - Fig. 2) part. Deep-water trench-like basins formed in front of advancing nappes (Fig. 7). The first basin group in the southern parts of the Northern Calcareous Alps received mass-flow deposits and large, up to nappe sized slides which derived from the Hallstatt Zone (= Hallstatt Mélange). The thickness of the basin fills may reach up to 2.000 metres. The nappe stack carrying the Hallstatt Mélange is defined as Upper Tirolic nappe (group) (Fig. 7).

The second basin group, the Tauglboden and the Rofan trench-like basins in the north were subjected to high subsidence and sedimentation rates in the Oxfordian to earliest Kimmeridgian. The Trattberg Rise was eroded and supplied the Tauglboden Basin to its north with mass-flow deposits and slides. The nappe carrying the Tauglboden Mélange is defined as lower Tirolic nappe. On the other hand, the Rofan Basin was carried by lowermost Tirolic nappe. It formed later than the Tauglboden Basin and received the material from the Hauptdolomit facies zone.

2. The Field Trip

In the Alpine-Carpathian domain the sedimentation pattern diachronously changed from carbonate to siliceous deposition in the Middle Jurassic (SCHLAGER & SCHÖLLNBERGER 1974). Also the tectonic regime changed. A characteristic new feature was the formation of trench-like radiolaritic basins with up to 2.000 metres of sediment infill (GAWLICK 1996) in their south-eastern, oceanward parts. This region was characterized by rapid subsidence due to tectonic load. In contrast, the northwestern, continentward edges of the Alpine-Carpathian domain were characterized by uplift and condensed sedimentation or erosion. The derivation of the resedimented components differs. In the southeastern basin group the material was

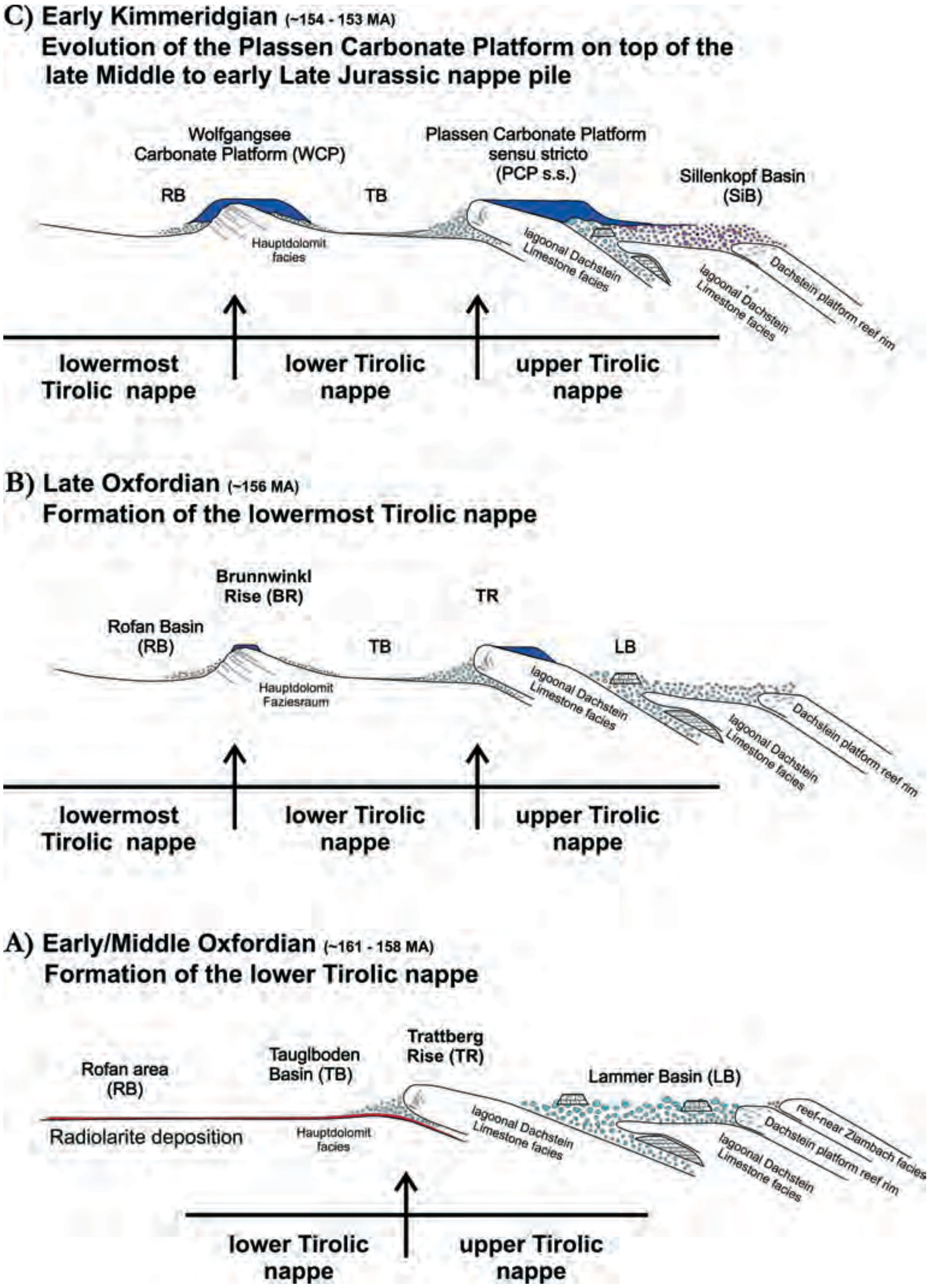

Fig 7: Oxfordian to Kimmeridgian tectonic and sedimentary evolution of the southern Northern Calcareous Alps and nappe subdivision. **A**) After the Middle Jurassic imbrication of the Middle Triassic to Early Jurassic Hallstatt facies belt, a new nappe front was formed in the lagoonal Dachstein Limestone facies zone (= Trattberg Rise). North of this nappe front a new deep-water basin was formed (= Tauglboden Basin). In contrast to the more northern regions (Rofan Basin area), where thin radiolarite sequences were deposited, the sedimentation in the Tauglboden Basin was characterized by an up to 800 m thick succession, consisting of radiolarites, slump deposits and different types of mass flows and slides. The Trattberg Rise separated the upper Tirolic nappe from the lower Tirolic nappe. **B**) Due to further tectonic shortening in the younger Middle or Late Oxfordian, a new nappe front established further north (= Brunnwinkl Rise). This uplifted nappe front domain supplied the newly created Rofan Basin to its north with eroded material (mass flows and slides). The lower Tirolic nappe was subdivided in a lowermost and a lower Tirolic nappe. In the Late Oxfordian first shallow-water carbonates were deposited, initially only in the area of the Trattberg Rise and later, from the Oxfordian/ Kimmeridgian boundary onwards, also in the area of the Brunnwinkl Rise (compare Fig. 78). The Plassen Carbonate Platform started sealing the older nappe structures. **C**) In the Early Kimmeridgian the Plassen Carbonate Platform rapidly prograded over the adjacent basins. The Plassen Carbonate Platform *s. str.* prograded unidirectionally towards south: The Trattberg Rise was uplifted and shielded the Tauglboden Basin to its north. In contrast the Wolfgangsee Platform prograded both in southern and northern directions (Fig. 78).

shed either from the Triassic to Early Jurassic distal, hemipelagic to pelagic continental margin (Hallstatt and Meliata Zones) or from the Zlambach facies and the Dachstein reef rim zone. In contrast in the northwestern basin group, the material derived from the Triassic to Middle Jurassic lagoonal area (Dachstein and Hauptdolomit facies zones) (Fig. 6).

Each reconstruction of the Jurassic tectonic movements depends on detailed studies on the components and the stratigraphy of the siliceous matrix sediments. The following different carbonate-clastic, radiolaritic sequences with characteristic Middle to Late Jurassic sedimentation in the Northern Calcareous Alps can be distinguished (from south to north, except the Sillenkopf Basin which represents a remnant radiolaritic basin between the Lärchberg and the Plassen Carbonate Platform):

A. Florianikogel Basin with the Florianikogel Formation (Fig. 5): Its ?Bajocian to Callovian sediments contain material from the Hallstatt Limestone and Meliata facies zones (Mandl & Odreijicová 1991, 1993, Kozur & Mostler 1992, Gawlick et al. 2009a) (Fig. 4, Fig. 6) and also include volcanogenic greywacke layers with erosional products derived from the Neotethys oceanic crust (Neubauer et al. 2007). This basin fill is similar to the Meliata Formation in the sense of Kozur & Mock (1985) in the Western Carpathians (Kozur & Mock 1997, Mock et al. 1998).

B. Sandlingalm Basin group with the Sandlingalm Formation (Fig. 5): These ?Bajocian/Bathonian to Late Oxfordian basins contain only material from the Hallstatt Limestone facies zone and limestones of the Meliata Zone (Pötschen Formation without shallow-water material; Fig. 4).

C. Lammer Basin with the Strubberg Formation (Fig. 5, Fig. 7): This Early Callovian to Middle Oxfordian basin contains mainly material from the Zlambach facies zone and the Dachstein Limestone reefs (Gawlick 1996, Gawlick & Frisch 2003, Missoni & Gawlick 2011a) (Fig. 5).

D. Tauglboden Basin with the Tauglboden Formation (Fig. 5, Fig. 7): In this Early Oxfordian to Tithonian basin

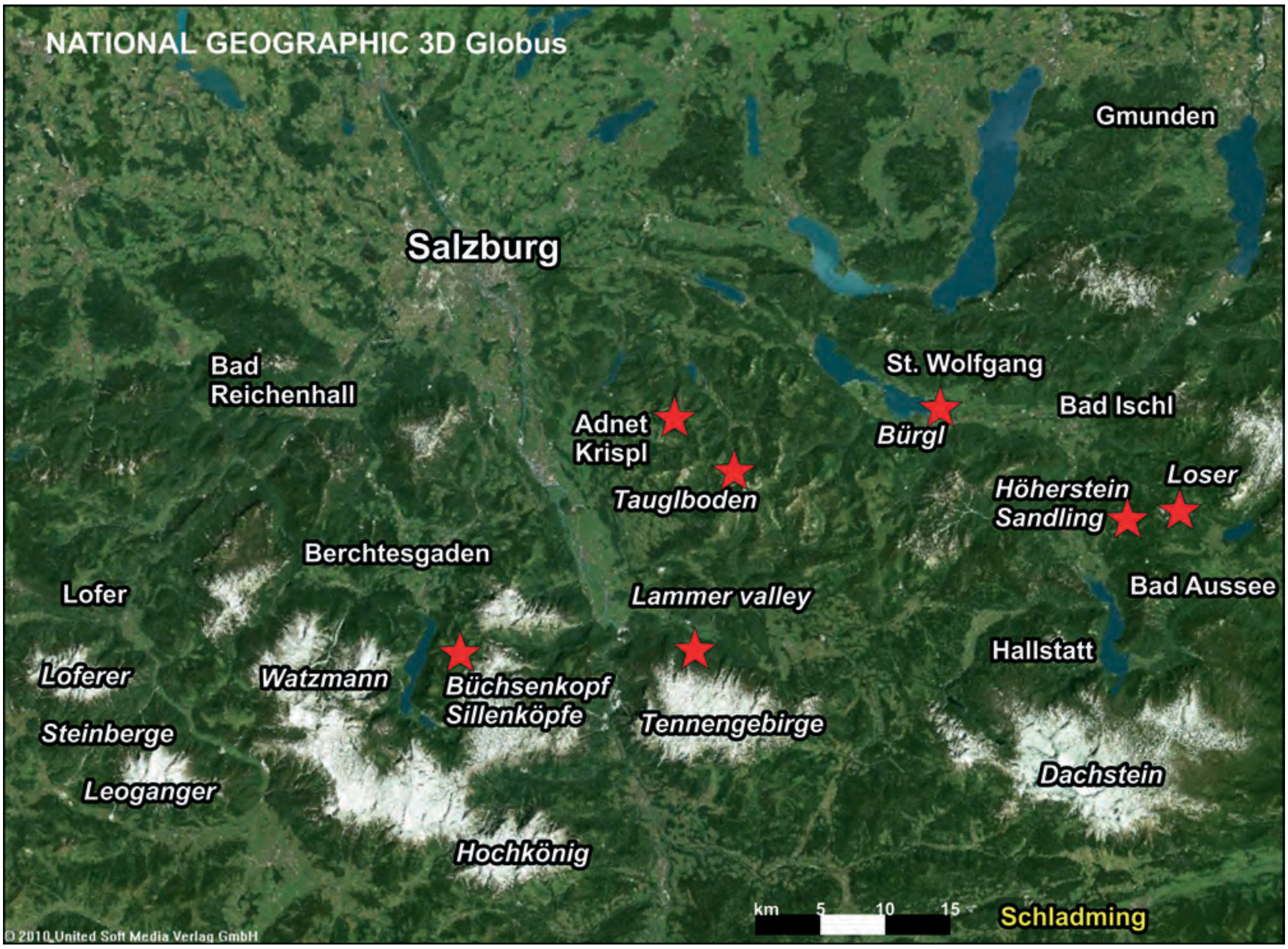

Fig. 8: Satellite image of the central Northern Calcareous Alps (Salzkammergut area, Salzburg and Berchtesgaden Calcareous Alps), showing the localities which will be visited during this field trip (red stars). In the Mount Sandling area we will study the Sandlingalm Basin fill, the proximal Tauglboden Basin fill and the overlying resediments of the Plassen Carbonate Platform *s. str*. South of St. Wolfgang on the southeastern end of the Wolfgangsee (lake) we will have a look at the northern part of the Plassen Carbonate Platform and its drowning sequence. Near the village Adnet we will study the succession of the northern Tauglboden Basin and in the Tauglboden area the basin fill of the central Tauglboden Basin. In the Lammer valley and south of Berchtesgaden we will see the Lammer Basin fill and the Sillenkopf Basin fill (optional).

(Huckriede 1971, Gawlick et al. 2009a), the first phase of resedimentation started in the Early Oxfordian (Gawlick et al. 2007a) with material derived from the lagoonal Dachstein Limestone facies zone and ended around the Middle/ Late Oxfordian boundary. After a period of tectonic quiescence and low sediment supply in latest Oxfordian to Early Tithonian, the second phase of intense resedimentation had its climax in Late Tithonian, when an overall extensional regime prevailed (Missoni & Gawlick 2011a, b). The change from older, Triassic to Middle Jurassic clasts in the first phase to predominantly Late Jurassic reefal sediment clasts in the second phase is characteristic (Steiger 1981, Gawlick et al. 2005).

E. Rofan Basin with the Rofan Breccia (Fig. 5, Fig. 7): Resedimentation started in the Late Oxfordian (Gawlick et al. 2009a) with material derived from the Hauptdolomit facies zone (Fig. 5, Fig. 6; Wächter 1987) and prevailed until the Oxfordian/Kimmeridgian boundary or Early Kimmeridgian. By that time the sedimentation changed to mostly carbonate detritus, derived from a Late Jurassic carbonate platform to the south (Wolfgangsee Carbonate Platform - Gawlick et al. 2007b, 2009a).

F. Sillenkopf Basin (Fig. 5, Fig. 7): The Kimmeridgian to ?Tithonian Sillenkopf Basin represents another type of basin. Its Sillenkopf Formation basin fill contains components of mixed palaeogeographic origin (Missoni et al. 2001a). The spectra of clasts in the Sillenkopf Formation prove the following provenance areas: A) The accreted Hallstatt units and an overlying Late Jurassic shallow-water carbonate platform, B) a deeply eroded hinterland further south (probably a part of the crystalline basement of the Northern Calcareous Alps), and C) an ophiolite nappe pile probably carrying an island arc (Missoni & Kuhlemann 2001), similar to the obducted ophiolites which acted as source for radiolaritic-ophiolitic mélanges in the Dinaridic/ Albanide realm.

The radiolarite basins A to E were formed in sequence, propagating from southeast to northwest (= from the Meliata to the Hauptdolomit facies zone) in the time span from the Bajocian to the Oxfordian/Kimmeridgian boundary. Basins A and C were accreted and overthrusted, basin B only partly. Basins D, E, F, and partly B existed in Kimmeridgian to early Early Tithonian times as remnant basins in between newly formed shallow-water carbonate platform areas of the Plassen Carbonate Platform *sensu lato*, the evolution of which commenced in the Late Oxfordian (Auer et al. 2009).

The main aim of this field trip through the central Northern Calcareous Alps (Fig. 8) is the study of the following deep-water basin fills with their underlying and overlying sedimentary successions:

- Sandlingalm Basin fill,
- Lammer Basin fill,
- Tauglboden Basin fill,
- Sillenkopf Basin fill (optional).

The onset and drowning/demise of carbonate platforms (Plassen Carbonate Platform *sensu lato*) on top of the nappe stack and their progradation over the radiolarite basins and the remaining starved deep-water basins between the platforms is the second main topic of this field trip. We will have a look at the following parts and phenomena of the Plassen Carbonate Platform *sensu lato*:

- The Wolfgangsee Carbonate Platform as the northernmost representative of the Plassen Carbonate Platform *sensu lato*,
- the fore-slope shedding of the Plassen Carbonate Platform sensu stricto (central platform),
- resediments from the Lärchberg Carbonate Platform (southern platform, optional).

On some days of the field trip, we will cross different basin fills and parts of the Plassen Carbonate Platform, respectively. To avoid confusion, the stop discriptions were sorted according to the different topics and not in strict chronological order according to the way of walking or driving. This particularly applies for our hiking trip in the central Salzkammergut area, where two basin fills, the Haselgebirge Mélange and the overlying sedimentary rocks of the Plassen Carbonate Platform, will be visited.

Radiolarian biostratigraphy

Radiolarian dating is essential to unravel the stratigraphic and chronological evolution of the individual basin fills. Only this allows to show the in sequence formation of these different deep-water trench-like basins. Obviously all reworked clasts and slides occur in a radiolaritic/ argillaceous matrix. The chaotic basin fills themselves overly a sequence of radiolarites. Thus radiolarians occur across the complete succession of interest whilst there is a lack of other microfossils allowing age dating. This makes radiolarian biostratigraphy extremely useful and important for the analysis of the Jurassic basin evolution. A short summary of the currently used radiolarian stratigraphy of the Northern Calcareous Alps is given in the following (details in Gawlick et al. 2009a).

The age and genesis of the Jurassic radiolarites in the Tethyan realm was described in detail, e.g., by Bosellini & Winterer (1975), Jenkyns & Winterer (1982), Baumgartner (1987) and Bernoulli & Jenkyns (2009). Radiolarian zonations for Jurassic Tethyan radiolarites of Baumgartner (1984, 1987), Baumgartner et al. (1995a, b), and De Wever et al. (2001) were the base for the first radiolarian zonation of the Austroalpine domain and the Northern Calcareous Alps, respectively (Suzuki & Gawlick 2003). Since the year 2003 many new studies on the stratigraphic ranges resulted in the revised radiolarian zonation (e.g., Beccaro 2004, 2006).

The radiolarian zonation for the Jurassic of the Northern Calcareous Alps consists of the eight zones (Fig. 9, compare Steiger 1992, Suzuki & Gawlick 2003), i.e., *Trexus dodgensis* zone (Hettangian to Sinemurian), *Hsuum exiguum* zone (Toarcian to Aalenian), *Eucyrtidiellum unumaense* zone (Bajocian to Bathonian), *Zhamoidellum ovum* zone (Callovian to Oxfordian), *Podocapsa amphitreptera* zone (Kimmeridgian), *Cinguloturris cylindra* zone (Early Tithonian), *Triactoma blakei* zone ("Middle" Tithonian), and *Syringocapsa lucifer* zone (Late Tithonian). The uppermost two zones were documented

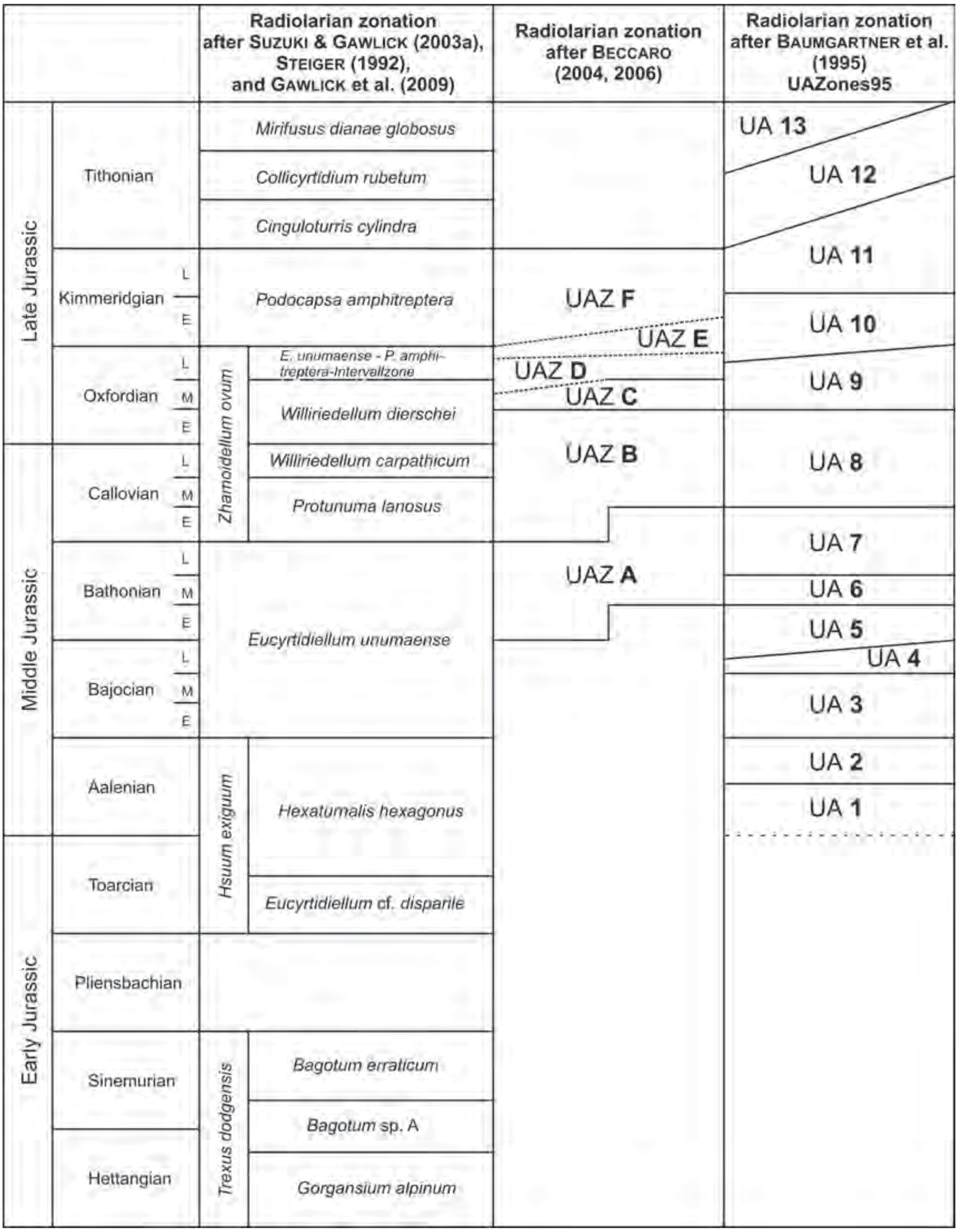

Fig. 9: Modified zonation for the radiolarians of the Northern Calcareous Alps according to SUZUKI & GAWLICK (2003), STEIGER (1992) and GAWLICK et al. (2009a). The shift of the upper limit of the *Williriedellum dierschei* subzone/the lower limit of the *Eucyrtidiellum unumaense - Podocapsa amphitreptera* interval zone at least up to the boundary Middle/Late Oxfordian or even higher is according to AUER et al. (2009). For comparison see the radiolarian zonations of BECCARO (2004, 2006) and BAUMGARTNER et al. (1995a).

in detail by STEIGER (1992). In this paper, the *Triactoma blakei* zone (Middle Tithonian) corresponds to the *Collicyrtidium rubetum* zone and the *Syringocapsa lucifer* zone corresponds to the *Mirifusus dianae globosus* zone. The *Trexus dodgensis* zone is subdivided into three subzones: *Gorgansium alpinum* subzone (Hettangian), *Bagotum* sp. A subzone (Hettangian/Sinemurian boundary) and *Bagotum erraticum* subzone (Sinemurian).
The *Hsuum exiguum* zone is further subdivided into two subzones: *Eucyrtidiellum* cf. *disparile* subzone (Early Toarcian) and *Hexasaturnalis hexagonus* subzone (Late Toarcium to Aalenium).
The *Zhamoidellum ovum* zone is subdivided into four subzones or interval zones: *Protunuma lanosus* subzone

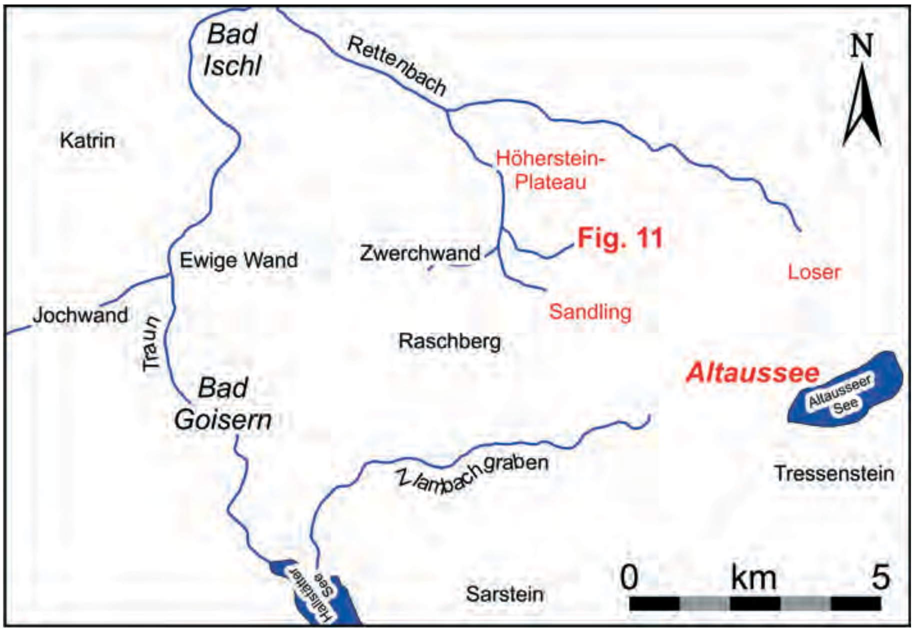

Fig. 10: Field trip area in the central Salzkammergut area. For details of our hiking trip in the area of Mt. Sandling and the Höherstein plateau see Fig. 11.

(Early to Middle Callovian), *Williriedellum carpathicum* subzone (Late Callovian), *Williriedellum dierschei* subzone (Early to Middle Oxfordian), and *Eucyrtidiellum unumaense-Podocapsa amphitreptera* interval zone (Late Oxfordian).

Thus in total, the Jurassic of the Northern Calcareous Alps can be subdivided into fourteen radiolarian zones. For this field trip is the time span Bathonian to Tithonian of special interest.

2.1. Sandlingalm Basin: material from the Hallstatt Limestone facies zone

This basin fill contains blocks up to kilometre-size, which derived exclusively from the Hallstatt Limestone facies and the Meliata facies zones (including cherty Pötschen Limestone without reefal detritus) in a radiolaritic matrix. The sedimentary succession of the Sandlingalm Basin (Figs. 13) is composed of various slide masses in a Callovian-

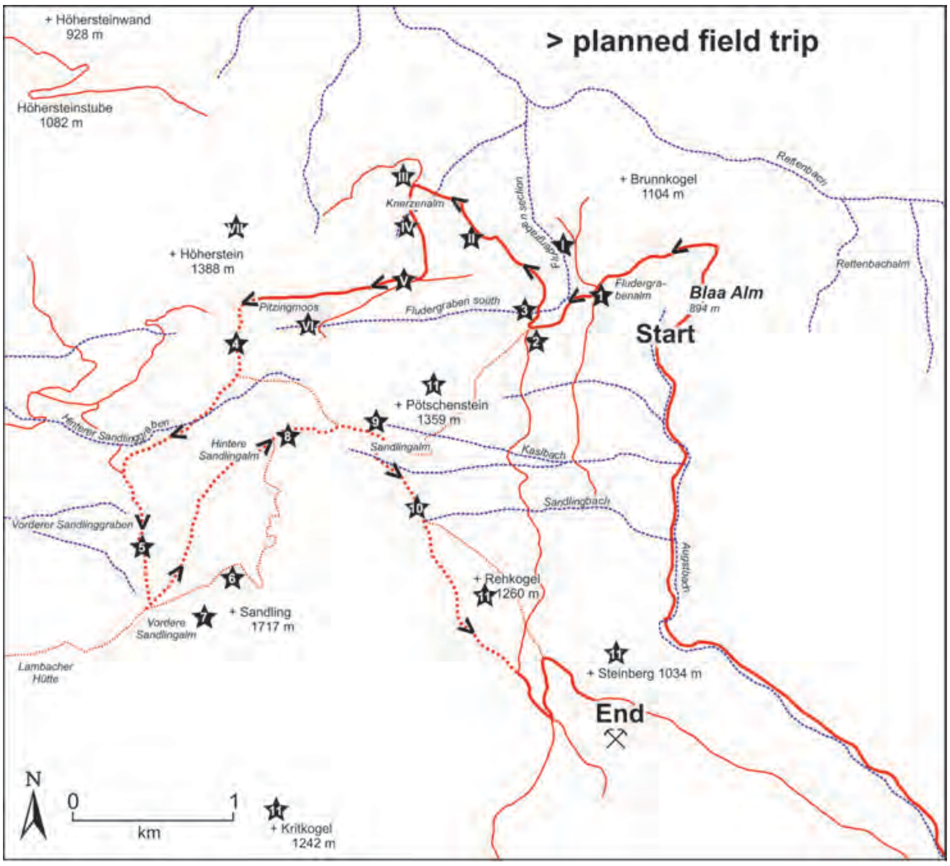

Fig. 11: Map with the field trip stops in the area Fludergraben - Mt. Sandling - Höherstein plateau/Knerzenalm area. The Arabic numbers define the stops in the depositional area of the Sandlingalm Basin with the overlying sediments of the Plassen Carbonate Platform. The Roman numbers describe the stops in the depositional area of the Tauglboden Basin (see chapter 2.3).

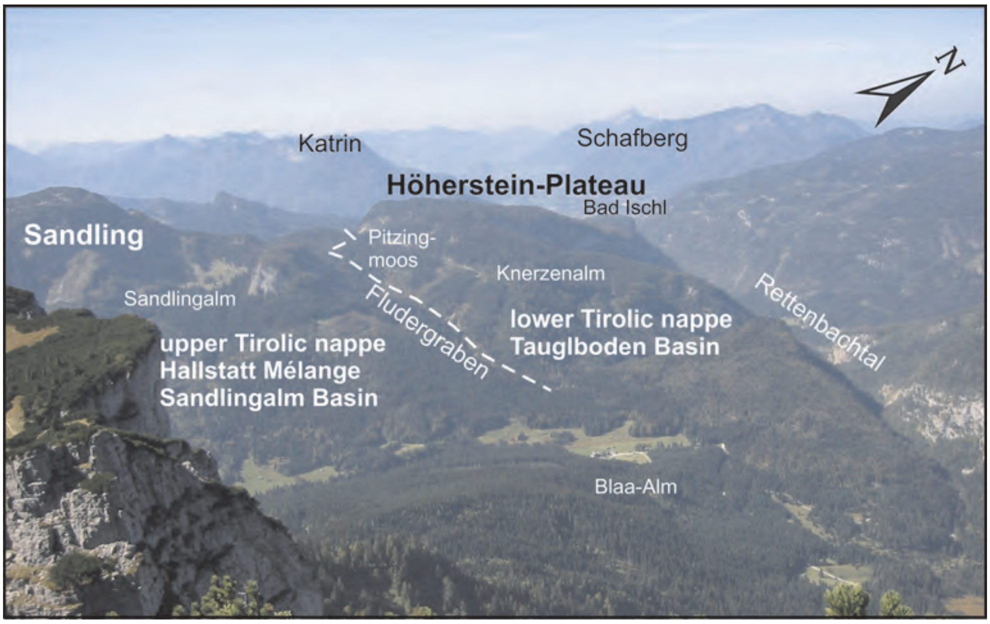

Fig. 12: View from the east on parts of the field trip area. For definition of the upper and lower Tirolic nappes see Fig. 7 and FRISCH & GAWLICK (2003).

Oxfordian radiolaritic matrix. Resedimentation of Hallstatt blocks in this basin started in the Early Callovian and ended around the Oxfordian/Kimmeridgian boundary with the emplacement of the Haselgebirge Mélange (MISSONI & GAWLICK 2011a) and the subsequent sedimentation of grey siliceous deep-water limestones started (compare GAWLICK et al. 2010 for the field trip area). These limestones belong to the basinal sequence aside the early Plassen Carbonate Platform *sensu lato* and were deposited on top of slide masses sealing the chaotic basin fill (compare Figs. 97-100).
We will study in detail the type-area of this basin in the central Salzkammergut area north of the township Altaussee (GAWLICK et al. 2007a; Fig. 10). For details see Fig. 11, Fig. 12.

Stop 1 in Fig. 11: Fludergrabenalm
Early to Middle Jurassic red nodular limestones

In the lowermost part of the Sandlingalm Basin succession, red nodular limestones are preserved. They form the stratigraphic substratum of the younger radiolaritic basin fill. These red nodular limestones belong to the Early and Middle Jurassic Adnet and Klaus Formations. In the uppermost part of the succession *Bositra* Limestones occur (Fig. 14). These are in parts siliceous and are rich in radiolarians. In the uppermost part of the Fludergrabenalm succession fine-grained turbiditic layers occur. They contain components deriving from the Hallstatt Limestone facies belt as documented by the microfacies characteristics. These components yielded small, broken remnants of conodonts. Radiolarians from these radiolaria-rich wackestones belong to the *Protunuma lanosus* subzone of the *Zhamoidellum ovum* Zone (Early to Middle Callovian) (SUZUKI & GAWLICK 2003). Most probably the age of the topmost part of this succession is Early Callovian.
Characteristic for the Early Callovian radiolarite succession of the Sandlingalm Basin is the occurrence of reworked material from the Hallstatt Limestone facies zone. The fast deepening of the depositional area is indicated by the rapid facies change from red nodular limestones to radiolarites. The lowermost radiolarites are red. Upsection they change quickly over violet-pinkish and dark grey to black colours and massive appearance. These dark radiolarites crop out along the way to stop 2.

Stop 2 in Fig. 11: Radiolarite quarry west of the Fludergrabenalm
Late Middle Jurassic (Callovian) radiolarites

Few tens of metres upsection, well preserved dark-grey to black radiolarites with several slump deposits of violet-pinkish radiolarites can be studied in the radiolarite quarry west of the Fludergrabenalm, near to the southern Fludergraben valley (Fig. 15). Whereas the dark radiolarites represent a more or less parallel bedded, only slightly deformed sequence, the violet-pinkish radiolarites show typical slump structures and represent sediment slides. Well preserved radiolaria from both sequences proof an identical gross age of both types of radiolarites (Early to Middle Callovian: GAWLICK et al. 2010). Also the microfacies characteristics of both radiolarite types are similar: radiolarian wackestones to packstones. There are differences in the preservation of the original sedimentary structures though: in the dark radiolarites fine lamination is often preserved; in contrast the violet-pinkish radiolarites are massive and in parts bioturbated. Turbidite layers occur only in the dark radiolarites in the form of channelized, up to 5 centimetres thick layers. The components in these turbidites can be identified as various Hallstatt Limestones derived from the Hallstatt Limestone facies zone (Fig. 6, 22). Also Rhaetian to Early Jurassic components from the same provenance area occur.
This outcrop proves the rapid deepening of the depositional area and the creation of relief. Radiolarite deposition occurred both in the deeper basin areas and on the flanks

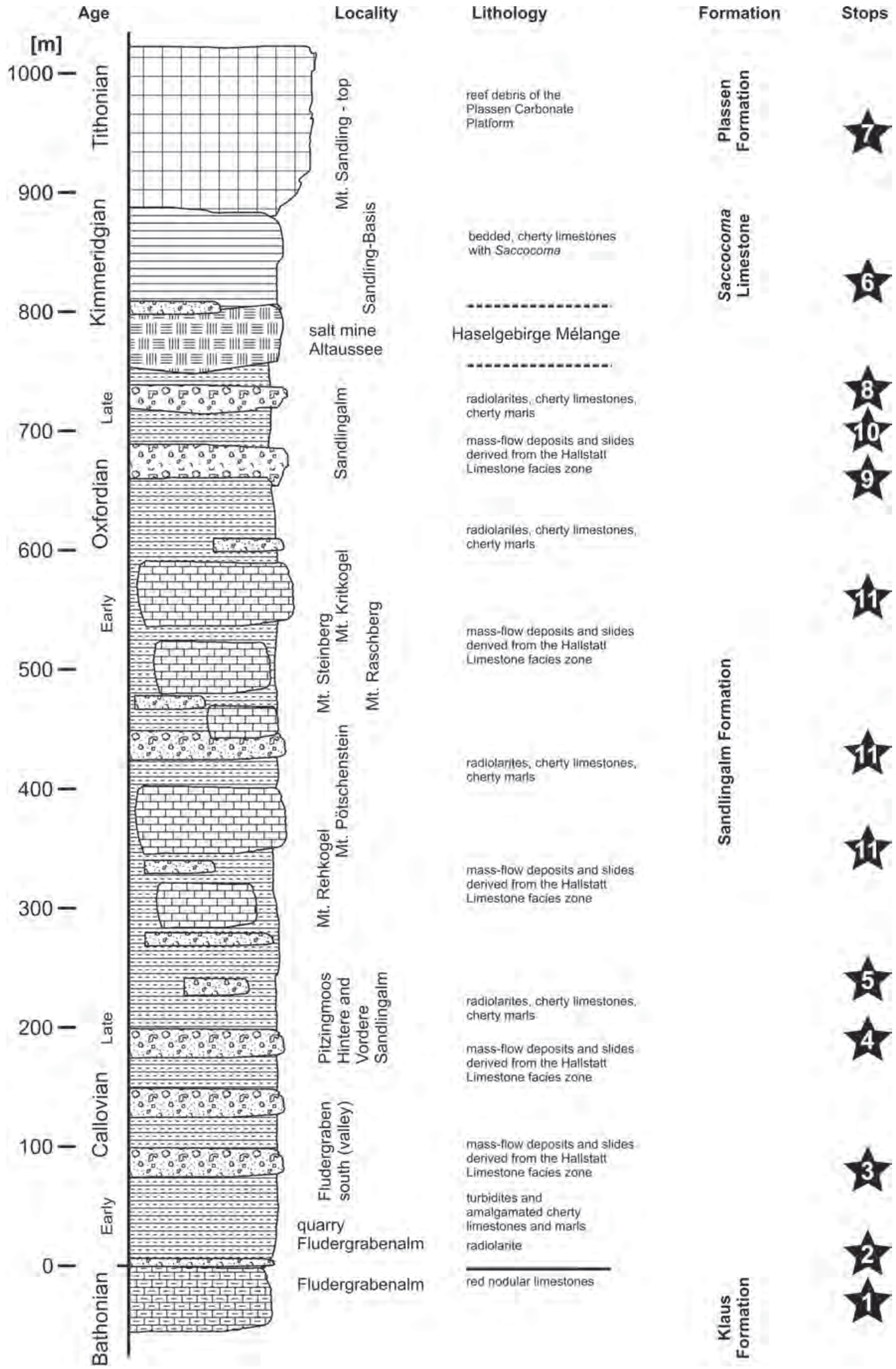

Fig. 13: Schematic lithostratigraphic column of the Sandlingalm Basin fill (Sandlingalm Formation) in the type region (Mount Sandling) with reference to the respective localities visited during this field trip (based on GAWLICK et al. 2007a, 2010). For the geographic locations of the stops see Fig. 11.

of the basin. Due to continuing tectonic movements, the flanks of the basin obviously became unstable and the cherty sediments slid (?crept) downslope forming typical slump deposits. Contemporaneously, exotic material was shed into the basin, indicating that older sequences were eroded and transported northwards. This is proven by the occurrence of the Early to Middle Jurassic red nodular limestones underlying the radiolarites. Such red nodular limestones were originally deposited on morphological highs of the Late Triassic palaeotopography (Fig. 5) in the shallow-water lagoonal or reefal Dachstein Limestone facies belts. In the Hallstatt Limestone facies belt, grey cherty limestones and marls are characteristic deposits in the Early to Middle Jurassic. They occur reworked as components in the turbidites and microbreccias.

Stop. 3 in Fig. 11: Southern Fludergraben valley
Late Middle Jurassic (Callovian) mass-flow deposits in a radiolaritic matrix

Upsection of the radiolarite sequence of the quarry, in the adjacent valley several mass-flow deposits are intercalated in cherty marls, cherty limestones and radiolarites (Fig. 17, Fig. 23). In some cases erosive basal contacts are visible. Moreover carbonate turbidites intercalations occur within a marly sequence (Fig. 18).
The components are of different size and range between several centimetres to some tens of centimetres; sometimes up to several metres sized slides occur (Figs. 19-21). All components derive from the Hallstatt Limestone facies zone transitional to the Meliata facies zone (Figs. 6, 19, 22, 24). By conodont and ammonite dating (MANDL 1982, WEGERER et al. 2001, GAWLICK et al. 2010) a reworked sequence from the Ladinian/Carnian to the Toarcian was proven in the southern Fludergraben valley succession. In other outcrops nearby, also Anisian components were dated by means of conodonts (GAWLICK et al. 2007a) (Fig. 22).

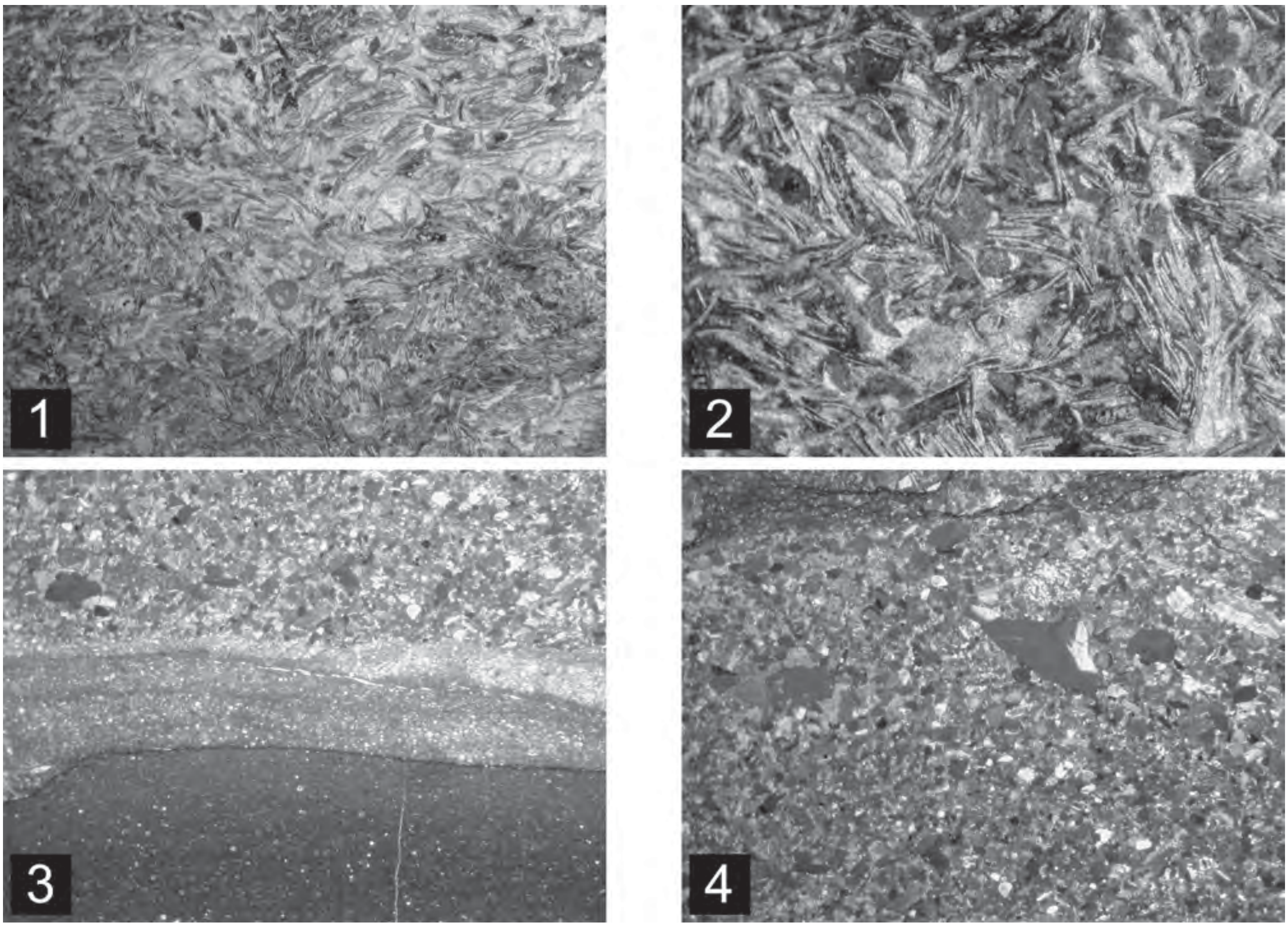

Fig. 14: Microfacies of the condensed red limestones (Klaus Formation) below the red cherty limestones with intercalated fine-grained turbidites. The components of the turbidites derive from the Hallstatt Limestone facies zone.
1. *Bositra* Limestone with some crinoids and rare foraminifera. Sample D 617. Width of photo: 1.4 cm. **2**. Magnification of 1. Strong recrystallization of the *Bositra* shells is visible; nearly all crinoids are broken. Width of photo: 0.5 cm. **3**. Microbreccia consisting of Hallstatt Limestone components, intercalated in radiolarian wackestones. The radiolarian wackestones occur as laminated layers originating from low-density and low-velocity turbidites. The contact to the turbiditic microbreccia is erosive. Sample Blaa 1. Width of photo: 1.4 cm. **4**. Sample Blaa 1, other view of the microbreccia. Caused by the size of the components, they cannot be assigned to a distinct member of the Hallstatt Limestone Formation. Clearly to determine are components of the Early Norian Massiger Hellkalk and the Middle Norian Hangendrotkalk. Late Norian to Early Rhaetian Hangendgraukalk components are probable. Width of photo: 1.4 cm.

Fig. 15: Radiolarite quarry west of the Fludergrabenalm. Slumps of reddish radiolarites occur in laminated, dark-grey to black bedded radiolarites. In addition, there are some fine-grained turbidite intercalations with material derived from the Hallstatt Limestone facies zone.

Fig. 17: Fludergraben south: different mass-flow deposits intercalated in dark-grey pelagic sediments consisting of radiolarites, cherty limestones and argillaceous marls. The components in these mass-flow deposits derive from the Hallstatt Limestone facies zone.

Beside the different Hallstatt Limestone and Lower Jurassic clasts, pelagic Pötschen Limestone components (grey cherty limestones) of Middle Norian age (Krystyn oral. comm.) occur. These clasts derive from the Meliata facies zone according to Missoni & Gawlick (2011a). The mixture of material from two different facies zones of the distal continental margin is only visible here in the lower part of the Sandlingalm Basin fill. Higher in the section, exclusively material from the Hallstatt Limestone facies zone prevails. This clearly shows that a nappe stack consisting of imbricated Meliata and Hallstatt nappes was eroded during that time.

The age of the matrix was dated Early Callovian by means of radiolarians (Gawlick et al. 2007a). Lithologically, these background sediments consist of radiolarites, cherty limestones and argillaceous material. Several turbidite layers are intercalated in the fine-grained deep-water sedimentary rocks. They are made up of crinoids- and filament- (*Bositra* shells) rich reddish limestones and occur in channels. The lower part of the succession with these mass-low deposits is partly sheared with the components being broken and tectonized (Fig. 21).

The lower part of the basin fill with the described component spectrum in its mass flows is about 200 m thick. Upwards in the section, the quantity of the Early Jurassic components in the different mass-flow deposits decreases.

Fig. 16: Microfacies of the radiolarites and the turbiditic intercalations in the radiolarite quarry west of the Fludergrabenalm; forest road to the Knerzenalm. Page 212.

1. Greyish-reddish radiolarite; radiolaria wackestone to packstone. Most radiolarians are well preserved. Sample EW 241. Width of photo: 1.4 cm. **2**. Microbreccia with different components derived from the Hallstatt Zone. Most components can be determined as Lower Jurassic (Dürrnberg and Birkenfeld Formations); the grey biomicrites are Hallstatt Limestone components (Massiger Hellkalk or Hangendgraukalk); Crinoids are common. Sample D 594. Width of photo: 1.4 cm. **3**. Sample D 594, different view. Beside crinoids and completely chertified components, some Triassic grey Hallstatt Limestones and, in the centre of the photo, a spicula-rich packstone of the Dürrnberg Formation are visible. Width of photo: 0.5 cm. **4**. Sample D 594, other view. Note the component of the Birkenfeld Formation in the centre. Width of photo: 0.5 cm. **5**. Laminated grey radiolaria wackestone, in parts completely chertified. Most radiolaria are recrystallized. Only few radiolaria are well preserved and are filled with fine-grained sediment. Sample D 595. Width of photo: 1.4 cm. **6**. Contact radiolarite-microbreccia. The mostly angular clasts of the microbreccia are pressed into the underlying radiolaria wackestone. Sample D 595. Width of photo: 0.5 cm. **7**. Crinoids and grey biomicrites are the dominating components of this turbiditic microbreccia, intercalated in radiolaria wackestones. Sample D 595. Width of photo: 0.5 cm. **8**. Several fine-grained turbiditic layers intercalated in radiolaria wackestones. Most components are grey Hallstatt Limestones beside several Early Jurassic components (Dürrnberg and Birkenfeld Formations). Characteristic for the late Middle Jurassic matrix is also the occurrence of filaments. Sample D 596. Width of photo: 1.4 cm.

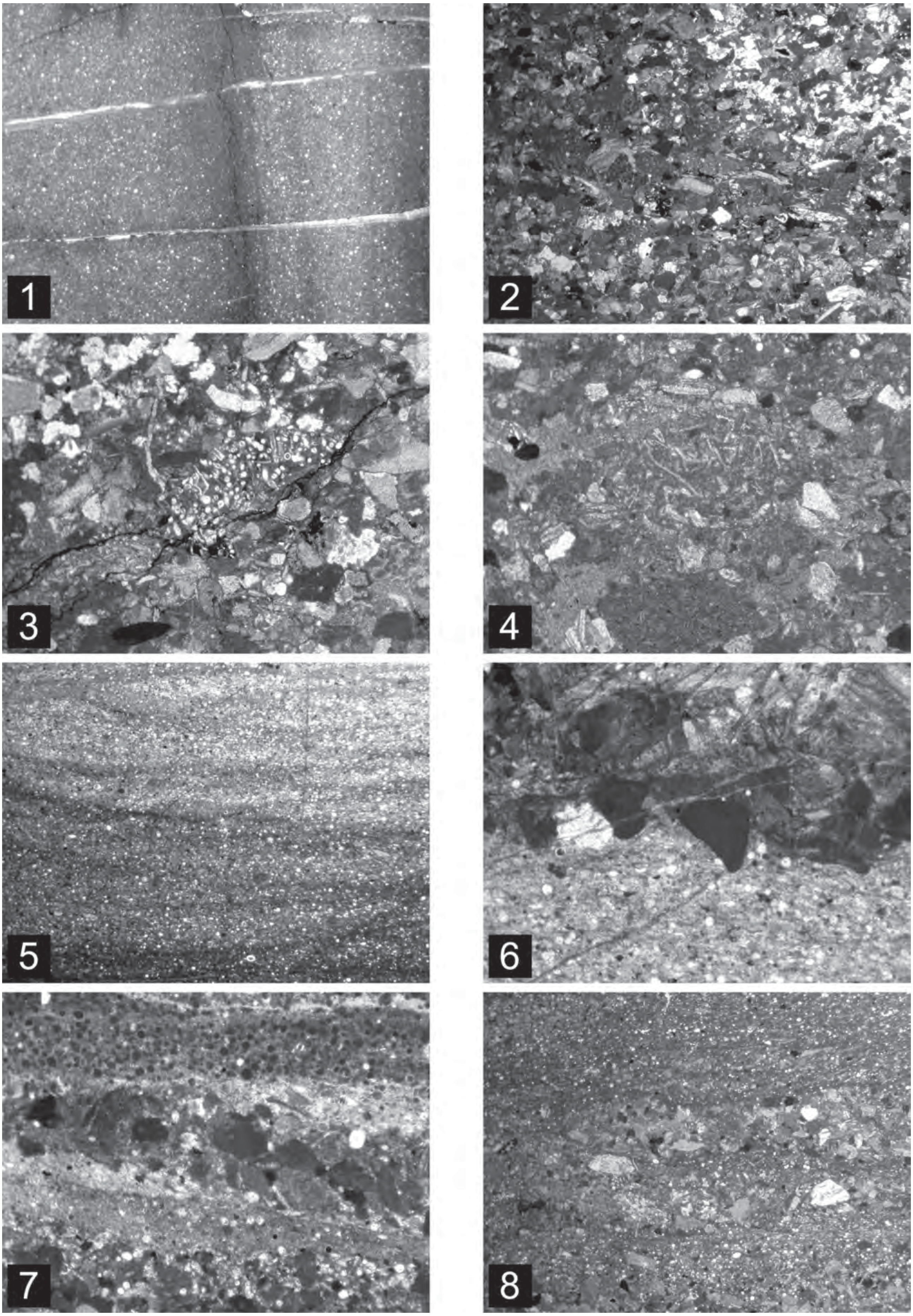
1
2
3
4
5
6
7
8

Fig. 18: Fludergraben south: several carbonate turbidite layers in a marly sequence. Typically, bioturbation is weak to not existent in this kind of fine-laminated succession.

Fig. 19: Disorganized gravelly mud with different grey and reddish subangular Hallstatt Limestone clasts of mainly Late Triassic age. Middle Triassic clasts are rare. Fludergraben south.

The age of the matrix of this part of the sequence is dated by means of radiolarians as Late Callovian (*Williriedellum carpathicum* subzone of the *Zhamoidellum ovum* zone) (WEGERER et al. 2001, GAWLICK et al. 2007a, 2010). The higher part of the basin succession is characterized by abundant mass-flow deposits and up to hundreds of metres sized slides consisting of Late Triassic Hallstatt Limestones.

Stops 4 and 5 in Fig. 11: Outcrops along the path
Late Middle Jurassic (Callovian) mass-flow deposits in a radiolaritic matrix

On the way from Pitzingmoos to the Hintere Sandlingalm (west of Mt. Sandling), after a wet area we will see several mass-flow deposits consisting of Hallstatt Limestone clasts (Fig. 25). The components vary in size, with blocks larger than 10 cm often occurring. The composition of the various mass-flow deposits differ slightly. Sometimes red Hallstatt Limestone components dominate, whilst in general a predominance of grey Hallstatt Limestone is more common. All components are of Late Triassic age (Carnian to Early Rhaetian), dated by means of conodonts (GAWLICK et al.

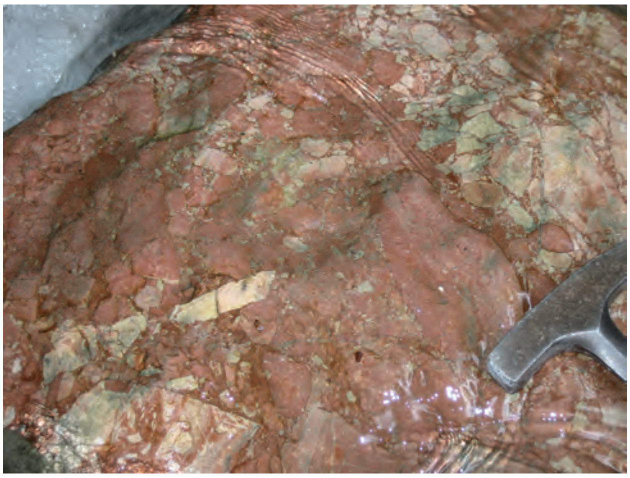

Fig. 20a and b: Different massive and matrix free mass-flow deposits which consist of red and grey Hallstatt Limestone clasts of Middle to Late Triassic age. Fludergraben south.

Fig. 21a and b: Deformed and slightly broken exotic clasts in a cherty argillaceous matrix. Fludergraben south. Width of photo A: 1 m. Width of photo B: 60 cm.

2010). These mass-flow deposits underlie up to km²-sized slides (e.g., Mt. Raschberg to the west). Several slides many hundreds of metres large occur in this stratigraphic position all around Mt. Sandling (compare Points/Stops 11 in Fig. 11: Mt. Pötschenstein, Mt. Rehkogel, Mt. Kritkogel beside others).

The stops 6 and 7 are described in the chapter 2.5 (stop 1: Mt. Sandling - Late Jurassic Plassen Carbonate Platform).

Stops 8, 9 and 10 in Fig. 11: Northern and eastern side of Mount Sandling

Early Late Jurassic (Oxfordian) mass-flow deposits in a radiolaritic matrix

North of Mt. Sandling on the way from the Hintere

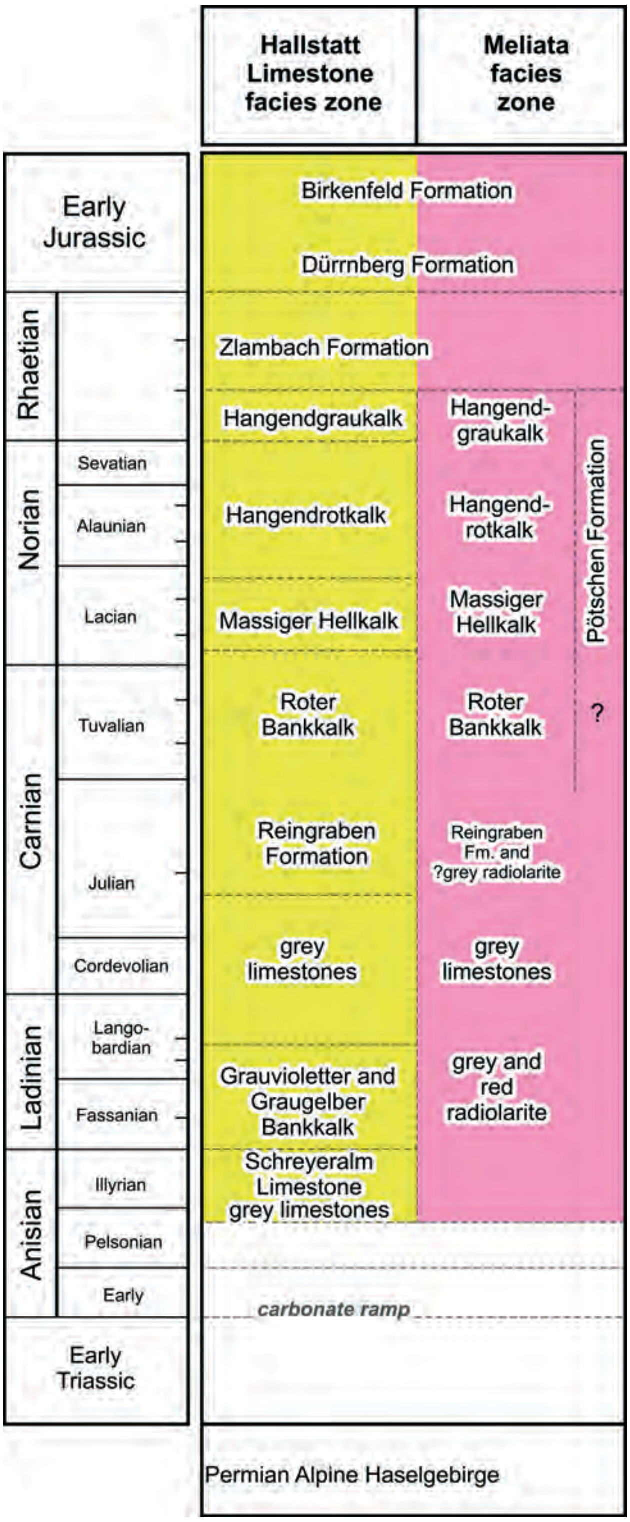

Fig. 22: Derivation of the clasts in the lowermost part of the Sandlingalm Basin fill. Components from the Hallstatt Limestone facies zone and the Meliata facies zone are mixed in the occurring mass flows. Compare Fig. 4, Fig. 6.

Sandlingalm to the Sandlingalm, there are several mass-flow deposits intercalated in a radiolaritic matrix. The age of the radiolarites is dated by means of radiolarians as Oxfordian, probably reaching up to the Late Oxfordian (GAWLICK et al. 2007a). The Hallstatt Limestone clasts are exclusively of late Middle to Late Triassic age as proven by conodonts (GAWLICK et al. 2007a). These mass-flow deposits represent the topmost part of the basin fill and

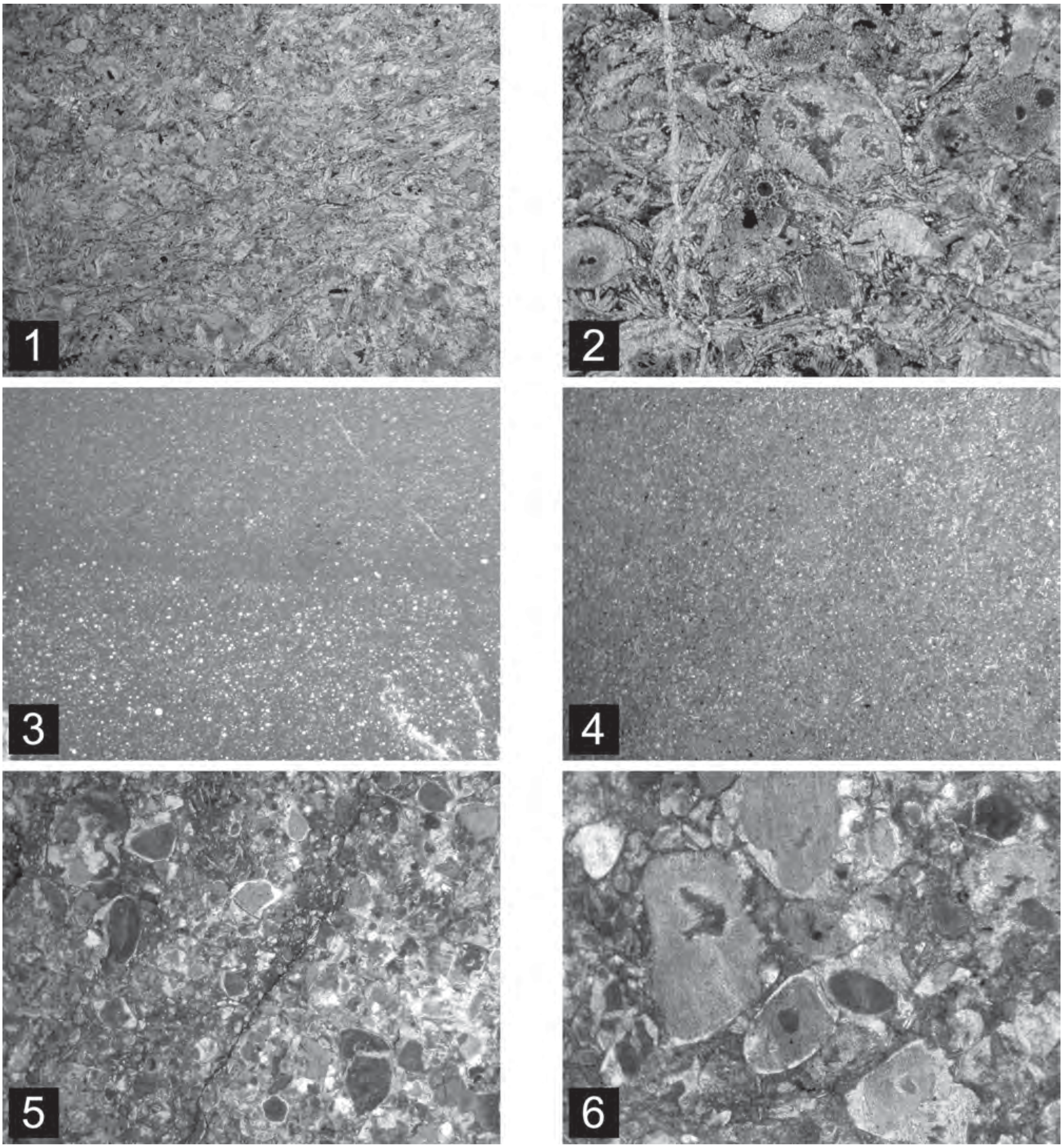

Fig. 23: Microfacies of the radiolaritic matrix between polymictic mass-flow deposits in the southern Fludergraben (valley).
1. Filament- and radiolaria-rich limestone turbidite intercalated within cherty limestones and radiolarites. The microfacies characteristics describe the limestones as transitional between the Klaus Formation and the Vils Limestone. Sample D 597. Width of photo: 1.4 cm. **2**. Magnification of 1. Width of photo: 0.5 cm. **3**. Laminated cherty limestone consisting of radiolaria wackestone to packstone. Sample D 598. Width of photo: 1.4 cm. **4**. Grey cherty marl with recrystallized radiolaria and filaments. The black minerals are pyrite. Sample D 599. Width of photo: 1.4 cm. **5**. Poorly sorted crinoidal grainstone from a channel fill intercalated in cherty sediments. This turbidite represents a layer of Vils Limestone, deposited in a distal basin position. Sample D 599. Width of photo: 1.4 cm. **6**. Magnification of 5. Width of photo: 0.5 cm.

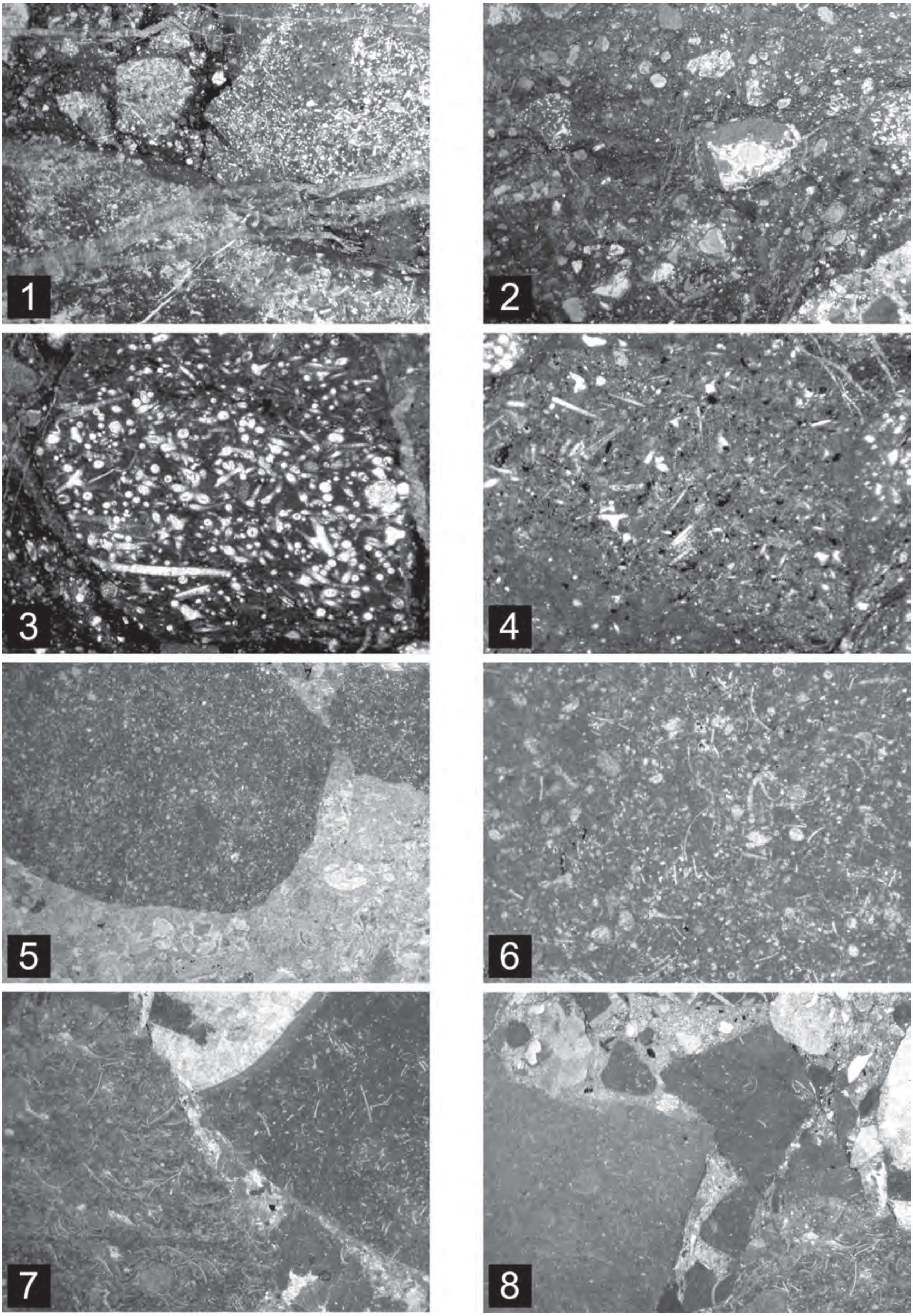
1
2
3
4
5
6
7
8

Fig. 24: Microfacies of clasts in the mass-flow deposit in the southern Fludergraben valley. These clasts occur in the polymictic microbreccias intercalated in Early Callovian radiolaritic matrix rocks. Page 216.
1. Several angular clasts of the spicula- and radiolaria-rich Dürrnberg Formation. Sample D 601. Width of photo: 1.4 cm. **2**. Microbreccia which consists mainly of Early Jurassic clasts; most clasts are angular. The matrix is cherty marl. Sample D 602. Width of photo: 1.4 cm. **3**. Sample D 602: other view, other component. Spicula-rich packstone of the higher part of the Dürrnberg Formation. Width of photo: 0.5 cm. **4**. Sample D 602: other view, other component. Spicula-rich wackestone with some filaments und small benthic foraminifera. Lower part of the Birkenfeld Formation. Width of photo: 0.5 cm. **5**. Several radiolaria- and filament-rich clasts of the Birkenfeld Formation. The matrix is rich in crinoids. Sample D 610. Width of photo: 1.4 cm. **6**. Magnification from 5. Beside filaments some fine-grained remnants of crinoids are common as well as recrystallized radiolaria. Width of photo: 0.5 cm. **7**. Polymictic mass-flow deposit consisting of different filament-rich Hallstatt Limestone clasts of Late Triassic age. All clasts are angular. Sample D 615. Width of photo: 1.4 cm. **8**. Sample D 615, other view. Poorly sorted part of the mass-flow deposit. The matrix consists of fine-grained Hallstatt Limestone components and crinoids. Width of photo: 1.4 cm.

Fig. 25a and b: Different mass-flow deposits consisting of red and grey Hallstatt Limestone clasts exclusively of Late Ladinian to Early Rhaetian age. Younger clasts are missing here in contrast to the component spectrum in the lower part of the Sandlingalm Basin succession. These mass-flow deposits are matrix-free. Width of photo A: 80 cm. Width of photo B: 30 cm.

were deposited on top of the up to km^2-sized slides.
In contrast to the Late Callovian radiolarites below this mega-slide level, the matrix age of these mass-flow deposits is Oxfordian. Therefore the emplacement of the km^2-sized slides can be roughly dated as Callovian/Oxfordian boundary to Early Oxfordian.
The topmost mass-flow deposits of the basin fill below the Haselgebirge Mélange (Point 10 in Fig. 11) contain not only Late Triassic Hallstatt Limestone clasts but also Middle Triassic (Late Anisian) clasts, dated by means of conodonts (Gawlick et al. 2007a). This proves that erosion cut deeper and deeper into the original Hallstatt Limestone succession. Whereas the mass flows in the lower part of the basin fill contain a lot of Jurassic clasts, these clasts decrease in quantity upsection. In the middle part of the basin fill, mass flows with exclusively Late Triassic Hallstatt Limestone components were deposited. In the upper part of the basin fill, Middle Triassic clasts occurred, with the topmost mass flows containing the oldest clasts.
The Alpine Haselgebirge Mélange is situated directly on top of this part of the basin fill. It was thrusted over this basin fill around the Oxfordian/Kimmeridgian boundary. Here in the Mt. Sandling area, the time of emplacement is proven by age dating of the underlying and overlying sedimentary rocks (Gawlick et al. 2010). The same conclusions concerning the timing were drawn at other locations, too: around Mt. Plassen (west of the township Hallstatt) (Wegerer et al. 2001, Suzuki & Gawlick 2009), in the area of the salt mine Bad Dürrnberg (Missoni & Gawlick 2011a), and in the Berchtesgaden area (Missoni et al. 2001b). The salt mine Altaussee, the biggest salt mine in the Northern Calcareous Alps, is situated directly below the Kimmeridgian to Tithonian succession of Mt. Sandling.

Salzburg and Berchtesgaden Calcareous Alps
In the Salzburg Calcareous Alps we will also cross several localities within the Sandlingalm Basin fill, e.g., in the area of Hallein - Bad Dürrnberg south of Salzburg. In this area only the middle and the upper part of the basin fill are exposed. The matrix is rarely visible in the grassland area. Due to mining activities for more than 2500 years in the Bad Dürrnberg area, the anthropogenic overprint in this area is much higher than in the area around Mount Sandling. Therefore, and since the main focus is not the study of the Middle and Late Triassic sedimentary

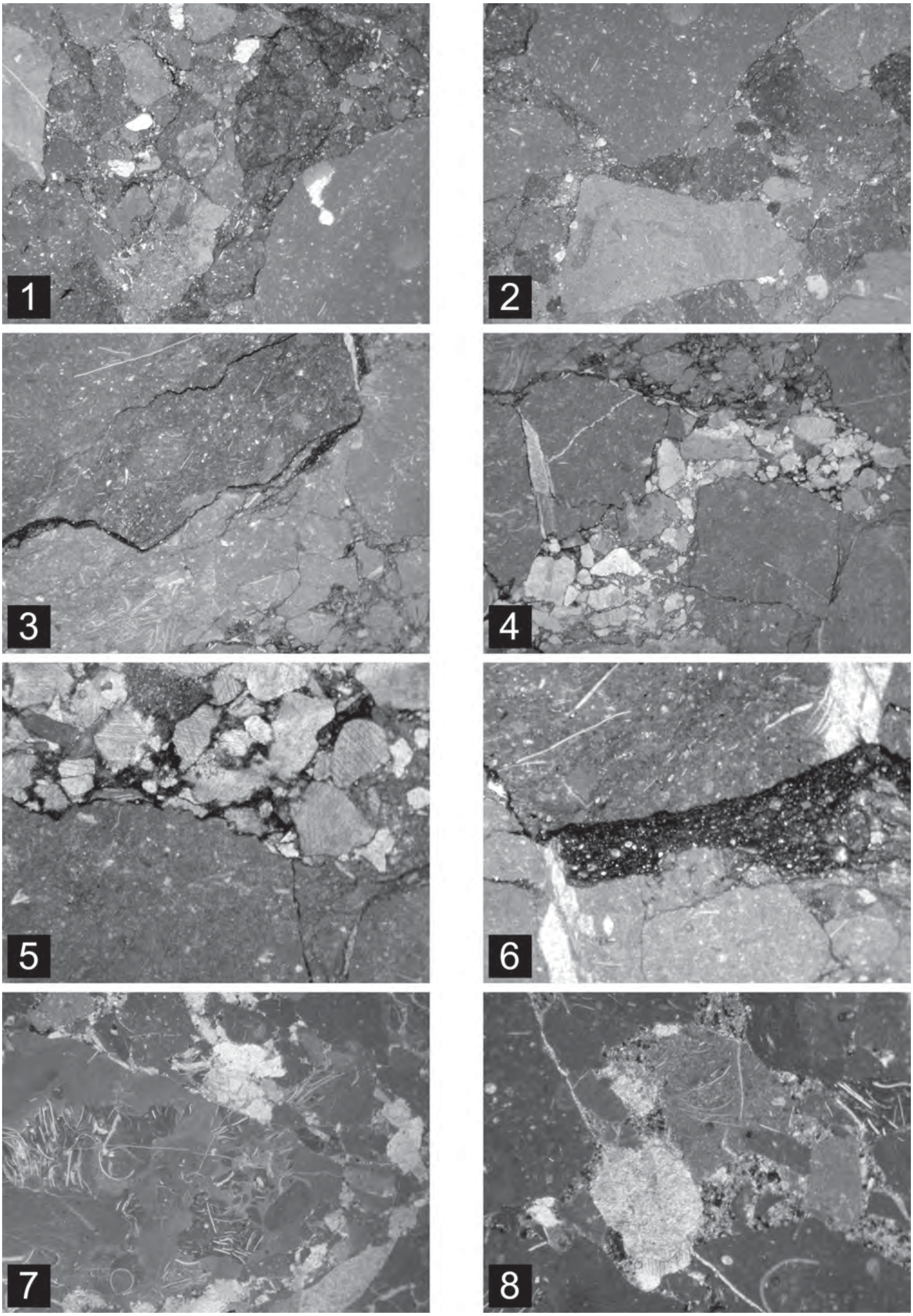
1
2
3
4
5
6
7
8

Fig. 26: Microfacies of the polymictic mass-flow deposits north of Mount Sandling, which consist exclusively of Late Triassic Hallstatt Limestone components. Page 218.
1. Polymictic mass-flow deposit with different components of the Late Triassic Hallstatt Limestone Formation. Sample D 211. Width of photo: 1.4 cm. **2**. Sample D 211, other view. This mass-flow deposit is practically free of matrix. Width of photo: 1.4 cm. **3**. Polymictic mass-flow deposit which consists of different Late Triassic clasts of the Hallstatt Limestone Formation. In contrast to the other mass flow, dark-grey matrix fills the space between the components. Sample D 213. Width of photo: 1.4 cm. **4**. Sample D 213, other view. Crinoids occur in the dark-grey cherty marls as part of the matrix between the different Late Triassic Hallstatt Limestone clasts. Width of photo: 1.4 cm. **5**. Sample D 213, other view. In addition to crinoids, partly also some recrystallized radiolaria occur in the matrix. Width of photo: 0.5 cm. **6**. Sample D 213, other view. Typical for the matrix is the existence of fine-grained components. Width of photo: 0.5 cm. **7**. Polymictic mass-flow deposit which consists of different Late Triassic clasts of the Hallstatt Limestone Formation. Sample D 214. Width of photo: 1.4 cm. **8**. Sample D 214, other view. The matrix between the components is strongly recrystallized and partly completely dissolved. Later the empty room was filled by clayey material. This feature is typical for different carbonate rocks in contact with the evaporites of the Alpine Haselgebirge. In this region the upper part of the Sandlingalm Formation was originally topped by today dissolved or eroded Alpine Haselgebirge Mélange.

successions of the Hallstatt Limestone, during this field trip we will neither visit the Sandlingalm Basin fill in the Salzburg Calcareous Alps nor that of the Berchtesgaden Calcareous Alps, where the Sandlingalm Basin fill is widespread preserved as well (for details Missoni & Gawlick 2011a).

2.2. Lammer Basin: material from the Zlambach facies and Dachstein reef zones

The type area Lammer Basin is located in the Salzburg Calcareous Alps between the Osterhorn Mountains (incl. the Trattberg Rise) in the north and the Tennengebirge in the south (Fig. 28). The Lammer Basin formed as an elongate trough in the former area of the Late Triassic lagoonal carbonate platform (today the lower Tirolic nappe of the Northern Calcareous Alps - Fig. 7). It contains a more than 1.5 km thick series of deep-water radiolarites, cherty limestones, cherty shales and marls, intercalated with breccias, mega-olistoliths and slides (Strubberg Formation). Redeposition started sometime in the Late Callovian to around the Callovian/Oxfordian boundary and therefore later than in the Sandlingalm Basin.
The components in the mass-flow deposits and blocks derive mainly from the Zlambach and Dachstein reef facies zones. In general, the sedimentary record of the Lammer Basin fill in the Salzburg and Berchtesgaden Alps documents a shift of depocentres within the basin (Missoni & Gawlick 2011a): in an early stage of sedimentation the original depocentre of the basin was filled by slide blocks which derived from the accreted proximal Zlambach facies zone. The northern depocentre, after a shift of the basin axis, received material from the reefal part of the Late Triassic carbonate platform. This is shown in two independent sedimentary successions, in which both the component size of the matrix- to grain-supported mass-flow deposits and the olistoliths show a general coarsening-upward trend. The older, southern depocentre is visible in the type-area of this basin, the Lammer valley in the Salzburg Calcareous Alps. The shift of the basin axis to the north is documented in the Berchtesgaden Calcareous Alps west of the Lammer valley. Up to kilometre sized Dachstein reef blocks terminated the carbonate-clastic, radiolaritic basin fill and can be interpreted as nappe relics. The Lammer Basin succession started in the Early Callovian with cherty limestones, radiolarites and marlstones. Upsection thin turbidites and, later, different types of internally chaotic debris-flow deposits with variable matrix portion are intercalated. The overlying, typically radiolarian-rich parts contain disorganized deposits with various clasts from the proximal Hallstatt

Fig. 27: Microfacies of mass-flow components northwest of Mount Rehkogel. Beside the dominating Late Triassic Hallstatt Limestone clasts, rare clasts of late Middle to Late Anisian Schreyeralm Limestone occur. Page 220.
1. Different filament-rich grey Hallstatt Limestone clasts with typical microfacies characteristics of the Late Norian Hangendgraukalk. Sample D 627. Width of photo: 1.4 cm. **2**. Different Late Triassic Hallstatt Limestone clasts (mostly components of the Roter Bankkalk and the Massiger Hellkalk). Sample D 628. Width of photo: 1.4 cm. **3**. Sample D 628, other view. Sparitic calcite cement filling the space between the red Hallstatt Limestone clasts (Roter Bankkalk) This indicates rock-fall transport. Also components of the Massiger Hellkalk are identifiable. Width of photo: 1.4 cm. **4**. Different filament-rich reddish Hallstatt Limestone clasts (mostly Roter Bankkalk and Hangendrotkalk). Most clasts are angular. The matrix between the components is marly and contains recrystallized radiolaria. Sample D 629. Width of photo: 1.4 cm. **5**. Different Hallstatt Limestone clasts. The matrix between the components consists of fine-grained clasts of the same origin. Sample D 630. Width of photo: 1.4 cm. **6**. Various strongly recrystallized and pervasively broken Hallstatt Limestone clasts mostly of Early Carnian age; partly with remnants of a dark-grey clay-rich matrix. Sample D 631. Width of photo: 1.4 cm. **7**. Filament-rich Late Anisian Schreyeralm Limestone. Sample EW 4. Width of photo: 1.4 cm. **8**. Sample EW 4, other component. Beside the filaments some benthic foraminifera and recrystallized radiolaria occur. This microfacies characteristic is typical for the lower part of the Late Anisian Schreyeralm Limestone directly on top of the Steinalm Formation, soon after the drowning event. Width of photo: 0.5 cm.

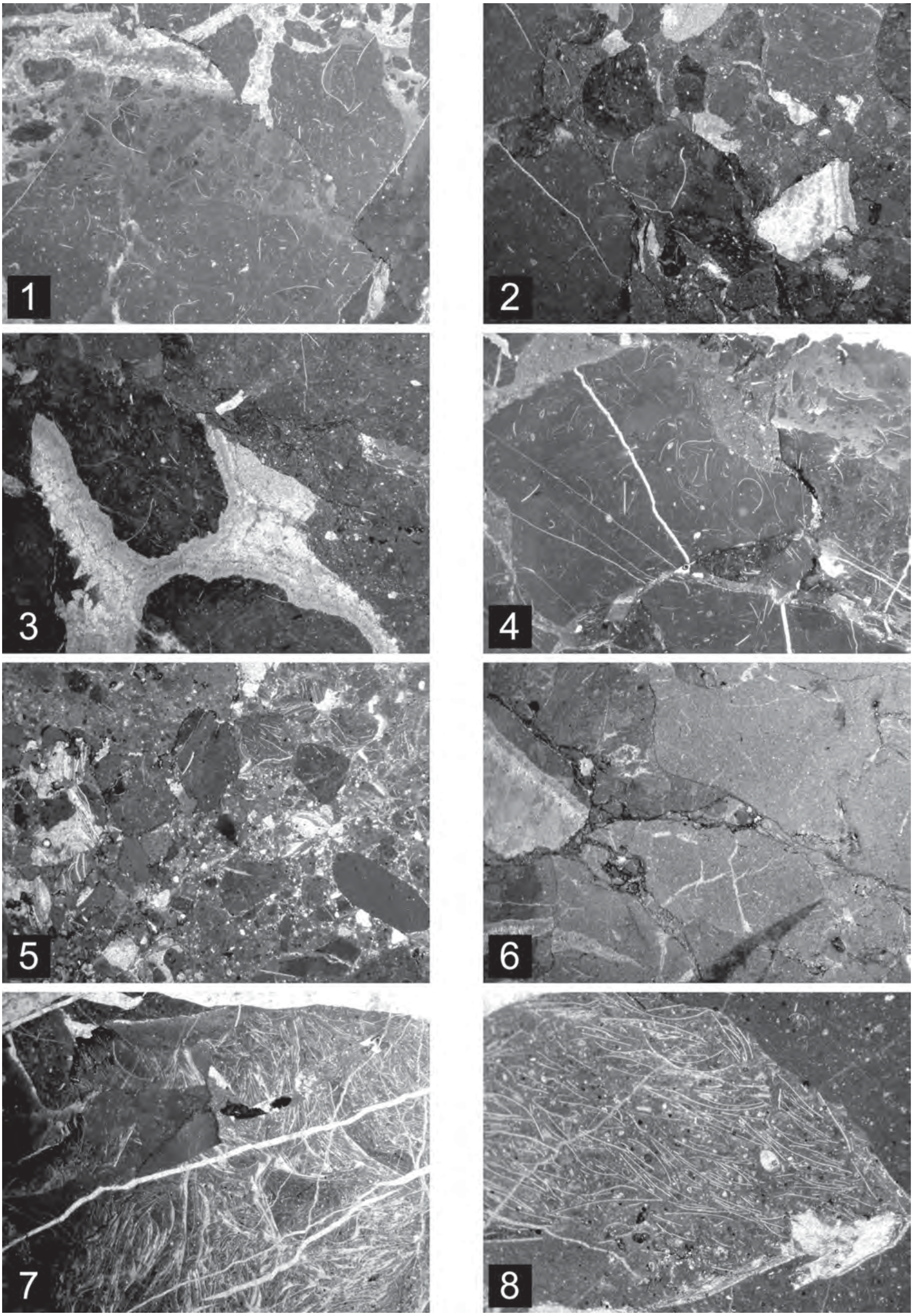
1
2
3
4
5
6
7
8

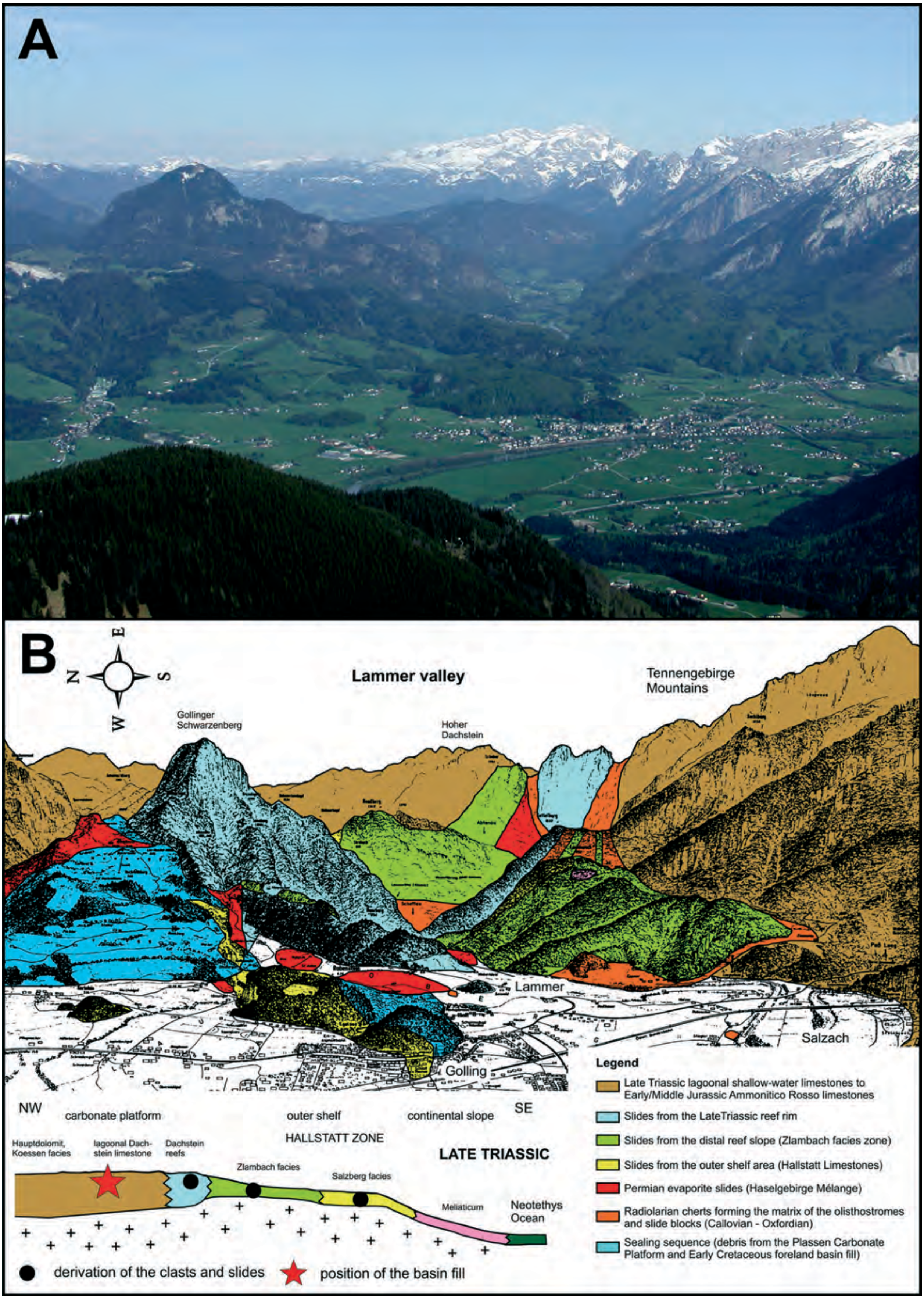

Fig. 28: **A**) View from the west showing the type area of the Lammer Basin fill. **B**) Geological interpretation of the landscape picture. The basin fill consists of allochthonous material of different age and facies provenance, which generally derives from the outer shelf area transitional to the Neotethys Ocean. This view point is optional.

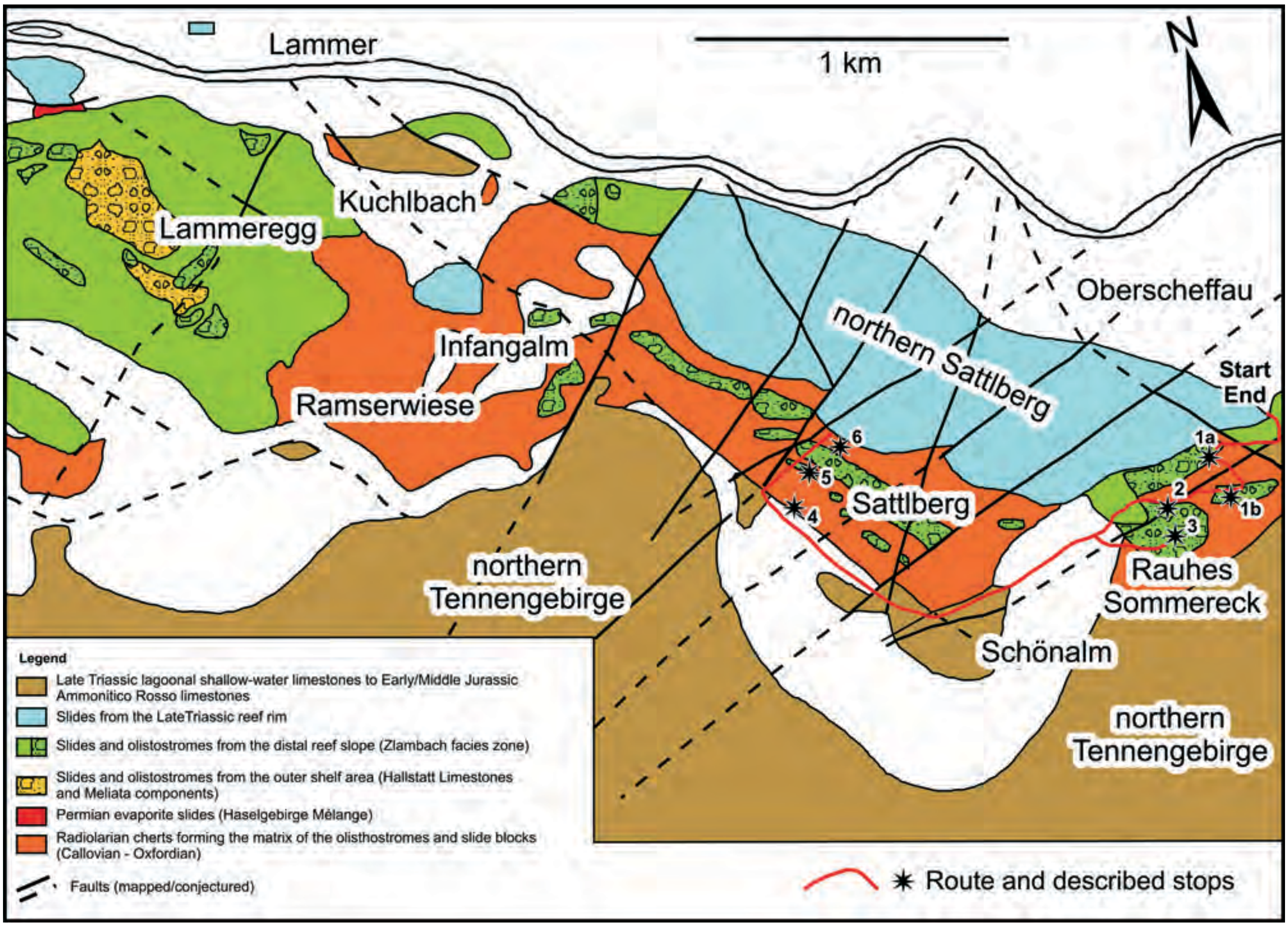

Fig. 29: Geological map of the western Lammer basin fill and field trip stops (after GAWLICK 1996, 2000b).

Zone (Pötschen Formation of the Zlambach facies zone; Carnian to Norian). Even higher in the section, mass-flow deposits with small resedimented clasts of Late Triassic condensed cephalopod limestones (Hallstatt Limestone) occasionally occur together with large slides of similarly aged Pötschen Formation. A younger generation of mass-flow deposits also contains Pötschen Formation material but shows a wider component spectrum ranging in age from the Anisian to the Early Jurassic. The middle part of the Strubberg Formation is characterized by large resedimented blocks and slide sheets of the siliciclastic Werfen Formation (Early Triassic). These are overlain by 2-3 km sized slides of the Pötschen Formation, again composed of various dolomites and limestones (Carnian to Early Jurassic). Mass-flow deposits on top of these large slides contain clasts and hectometre-sized blocks of the Hallstatt cephalopod limestones (Carnian to Norian) and small clasts of Middle Triassic radiolarites and cherty limestones (Meliata facies zone). These mass-flow deposits were transported in a piggy-back manner. The piggy-back transportation of Hallstatt Limestone and Meliata facies zone components in slide masses derived from the Zlambach facies area show that Callovian to Oxfordian resedimentation was a multiple process. These slides are overlain by mass-flow deposits (~Middle Oxfordian) with clasts from the Pötschen Formation (Carnian to Norian). The upper part of the Strubberg Formation (?Middle to Late Oxfordian) is characterized by mass flows and slides with Hallstatt Limestone (Carnian to Norian) clasts. In other mass-flow deposits, components from the Dachstein reefal limestone facies occur. The sequence is terminated by large slides of the reefal Dachstein limestone facies zone (Early Triassic to Early Jurassic). Contemporaneous with the emplacement of the latter, slides with high-pressure metamorphic rocks from the Hallstatt Limestone facies zone appeared (GAWLICK & HÖPFER 1999, compare FRANK & SCHLAGER 2006). Sediment redeposition ended in the Lammer Basin in the ?Late Oxfordian, contemporaneous with the formation of the Trattberg Rise and the Tauglboden Basin to the north. On top of the youngest generation of slides, resediments from the Plassen Carbonate Platform (Kimmeridgian to Tithonian) sealed the thick, mass-flow and slide dominated Lammer Basin succession.

We will study the Lammer Basin fill in the Lammer valley type area of the southern Salzburg Calcareous Alps and in the southeastern Berchtesgaden Calcareous Alps (optional).

2.2.1. Lammer Basin in the Salzburg Calcareous Alps

The type area of the Lammer Basin fill is situated in the Lammer valley, Salzburg Calcareous Alps, between the townships Golling in the west and Abtenau in the east (Fig. 29, Fig. 30). We will visit locations in the central

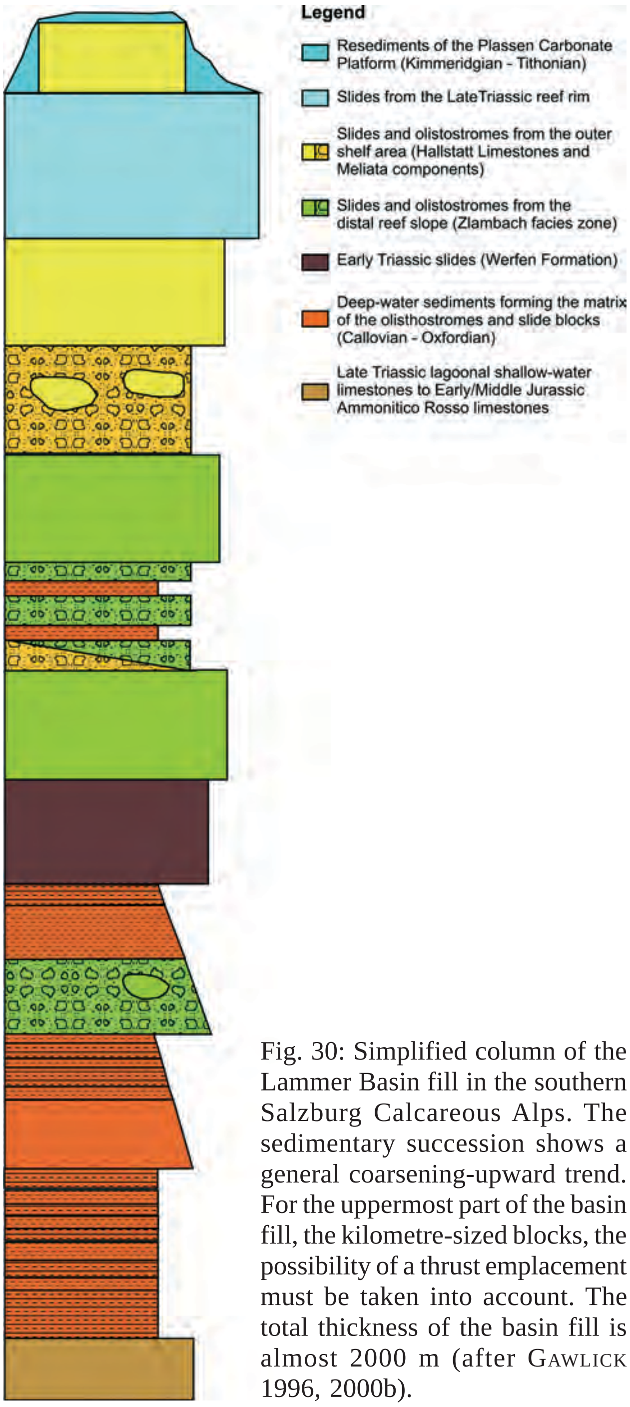

Fig. 30: Simplified column of the Lammer Basin fill in the southern Salzburg Calcareous Alps. The sedimentary succession shows a general coarsening-upward trend. For the uppermost part of the basin fill, the kilometre-sized blocks, the possibility of a thrust emplacement must be taken into account. The total thickness of the basin fill is almost 2000 m (after GAWLICK 1996, 2000b).

Lammer valley (Fig. 29) along the northern edge of the Tennengebirge Mountain that expose the basal part of the basin fill. We will study, how the Lammer Basin evolved in the former open lagoon area of the Late Triassic Hauptdolomit/Dachstein Limestone carbonate platform (compare Fig. 7, Fig. 95) and examine the whole Late Triassic to early Late Jurassic sedimentary succession.

Stops 1 and 2: Forest road to the Schönalm area and Mt. Rauhes Sommereck

Late Middle Jurassic to early Late Jurassic olistostromes and slides

Along the forest road from Oberscheffau to the Schönalm area (Fig. 29) several outcrops will be studied. The field trip starts with an outcrop of dolomitized Middle Triassic basinal sediments (dated by means of conodonts). These belong to a large slide deriving from the Dachstein Limestone reef rim zone. Beside the waterfall, several metres along the forest road, cherty dolomites of Early Norian age occur, also dated by means of conodonts. These cherty dolomites (Pötschen Dolomite) derive from the Zlambach facies zone (compare Fig. 95). Several tens of metres further on, dark-grey radiolarian-rich cherty marls of Oxfordian age occur. These cherty deep-water marls represent the matrix of the large slide blocks.

In the second curve of the forest road the first Late Callovian to Early Oxfordian olistostromes are met. The matrix of these olistostromes is represented by dark-grey to black cherty marls and cherty limestones. The components of the olistostromes derive exclusively from the Zlambach facies zone and are all of Late Triassic age (Stop 1a - for the reconstructed sequence see Fig. 33). Similar outcrops are found along the forest road a little higher up (Stop 1b). Here, several olistostromes are intercalated in dark-grey cherty limestones, radiolarites and argillaceous marls. Component analysis of these olistostromes in the lower Lammer Basin succession allowed the reconstruction of a more or less complete Late Carnian to Rhaetian Pötschen sequence. The olistostrome matrix consists of dark grey to black, partly radiolarian-rich cherty marls. The radiolarians are completely recrystallized.

Near the Schönalm area, at the base of Mt. Rauhes Sommereck (Stop 2), several olistostromes intercalated in a dark-grey argillaceous and radiolaritic matrix of Oxfordian age can be observed. The component spectrum is similar to Stops 1a and 1b - the reconstructed source

Fig. 31: Polymictic breccia along the forest road from the village Oberscheffau to the Schönalm area. The breccia consists exclusively of components deriving from the Zlambach facies zone. Different grey deep-water limestones predominate. Moreover there are dolomitic limestone and some cherty dolomite clasts. Conodont dating of the components allowed the reconstruction of a Late Triassic sedimentary succession (Fig. 34; details in GAWLICK 1996, 2000b).

Fig. 32: Polymictic breccia at the base of the early Late Jurassic sedimentary succession of Mt. Rauhes Sommereck. Only Late Triassic components can be recognized. These derive exclusively from the Zlambach facies zone (Fig. 34; details in GAWLICK 1996, 2000b). Size of the photo: 75 cm.

region sedimentary succession differs only marginally (Fig. 34). These olistostromes are situated higher within the preserved sequence. As expected, erosion in the hinterland cut deeper into the original succession - a complete Late Ladinian to Early Jurassic sedimentary succession can be reconstructed from the components. Interestingly in these mass-flow deposits also some Early Jurassic clasts and dark grey marls of Rhaetian age occur. The matrix is made up of dark grey to black, partly radiolarian-rich cherty marls. The radiolarians of this level are completely recrystallized and thus cannot yield depositional ages for these lower olistostromes.

Stop 3: Mt. Rauhes Sommereck
Oxfordian mass-flow deposits and slides

From the Schönalm area (800 m a.s.l.) we have a panoramic view on the whole Late Triassic to early Late Jurassic sedimentary succession. The northern Tennengebirge consists exclusively of Late Triassic lagoonal Dachstein Limestone in Lofer facies, dipping northward. The Schön-

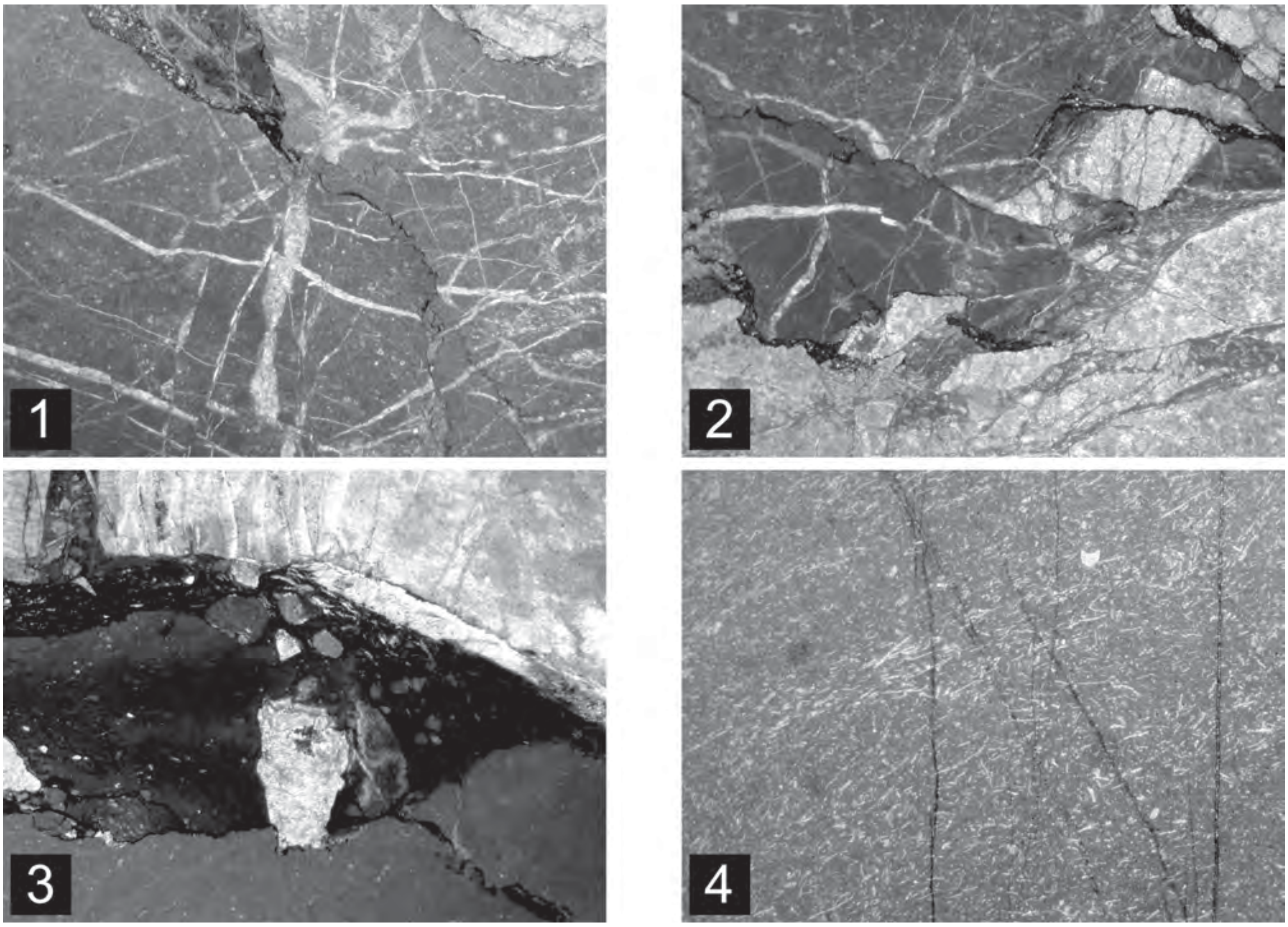

Fig. 33: Microfacies of the different carbonate clasts in the olistostromes along the forest road to the Schönalm at the base of Mt. Rauhes Sommereck. The clasts derive from the Zlambach facies belt (compare Fig. 95) and are predominantly of Late Triassic age.
1. Two radiolarian- and filament-bearing wackestone clasts of Norian age (Pötschen Limestone) practically without matrix. Sample BS 11. Width of photo: 1.4 cm. **2**. Slightly sheared clasts. Recrystallized dolomite clasts (Pötschen Dolomite) beside Pötschen Limestone clasts. Sample BS 11-2. Width of photo: 1.4 cm. **3**. Smaller clasts and dark grey clay matrix between a Pötschen Limestone clast and a recrystallized Pötschen Dolomite clast. Sample 30-89. Width of photo: 1.4 cm. **4**. Filament and radiolarian bearing marly limestone clast of probably Early Jurassic age. Sample BRS 1. Width of photo: 1.4 cm.

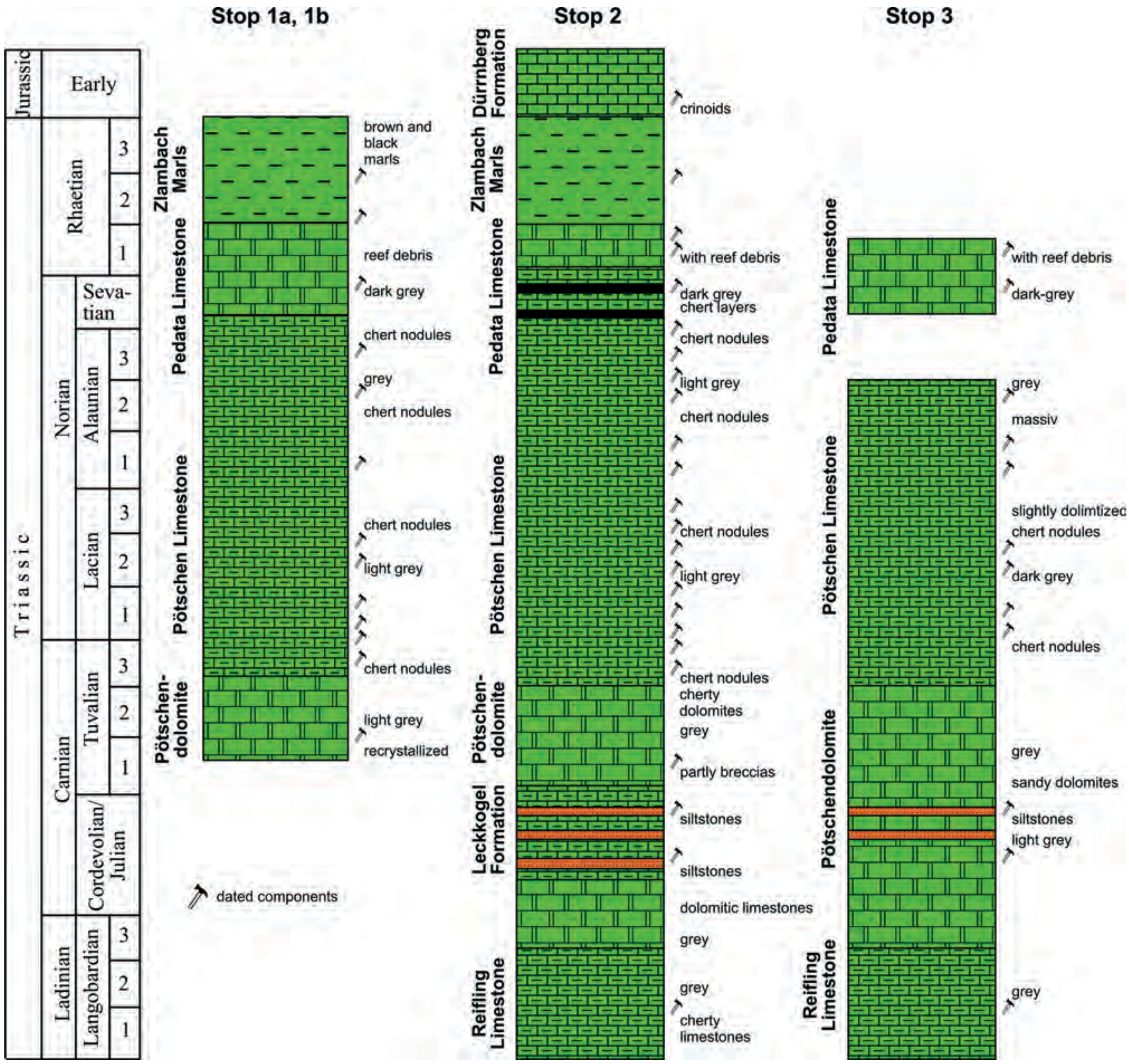

Fig. 34: Correlation of the reconstructed original sedimentary sequences which occur as resedimented components in the early Late Jurassic deep-water cherty sediments of the Lammer Basin fill in the section Rauhes Sommereck. The components derive from virtually identical original sedimentary successions of the Zlambach facies zone (compare Fig. 95). Dating of the components mainly based on conodonts, partly on ammonites, holothurians, foraminifera, and others (details in GAWLICK 1996).

alm area itself, today with glacier morphology, represents a past level of the old Lammer River valley. The Lammer River cut into the softer parts of the Late Triassic succession, the Kössen Formation on top of the Norian lagoonal Dachstein Limestone and below the Rhaetian lagoonal Dachstein Limestone. This is best visible in the southern part of Mt. Sattlberg.

By climbing Mt. Rauhes Sommereck we will study several olistostromes intercalated in the dark grey cherty matrix of Oxfordian age. Along the section both the component sizes and the thicknesses of the individual mass-flows increase. At the same time the matrix becomes more and more marly and is partly enriched in manganese. Near the top of Mt. Rauhes Sommereck (890 m a.s.l.) a several tens of metres large slide is incorporated in an olistostrome (HÖCK & SCHLAGER 1964). This huge slide consists of Middle Norian Pötschen Limestone with some reef debris (GAWLICK 2000b).

The contact to the basal part of the Late Triassic to Middle Jurassic series is poorly exposed in the area of Mt. Rauhes Sommereck.

Stops 4-6: Forest road on the west side of Mt. Sattlberg

Callovian to Oxfordian deep-water sequence with olistostromes and slides

On the way to the best preserved section of the area, the

Fig. 35: A and B) Polymictic breccia near the top of Mt. Rauhes Sommereck. Only Late Triassic components, exclusively deriving from the Zlambach facies zone, can be recognized (Fig. 34; details in GAWLICK 1996, 2000b). Size of the photo A: 60 cm. Size of the photo A: 100 cm.

section Sattlberg west, we will cross the Schönalm area. Near the southern Schönalm area we meet Rhaetian lagoonal Dachstein Limestone, overlain by a condensed Early to Middle Jurassic sedimentary sequence. The grey cherty limestones deposited directly on top of the Dachstein Limestone will not be visited because of their occurrence in steep morphology. These cherty limestones range in age from Late Hettangian to Pliensbachian. They are overlain by red nodular limestones forming mass-flow deposits and slumps. The time span of these mass movements is dated by means of ammonites as Late Pliensbachian to Early Toarcian. Upsection follow mass-flow deposits of grey nodular limestone of Toarcian age. The Middle Jurassic is characterized by extreme condensed red nodular *Bositra* Limestones (Klaus Formation), followed by a black radiolarite of Callovian age. This contact is not visible along the forest road but only higher in the mountains. Along the forest road the first outcrops are within black radiolarites to cherty limestones of Early Callovian age (GAWLICK & SUZUKI 1999) (Fig. 37). Upsection follow black, manganese-rich marls, cherty marls and limestones and radiolarites (Stop 4).

In the middle part of the section there are marly sequences, partly with graded turbiditic beds. Higher in the section, the first breccia layers (Late Callovian) occur (Stop 5). The components in these breccia layers derive exclusively from the Zlambach facies zone. Upsection follows a more than 10 metres thick horizon rich in manganese, which shows a high organic carbon content (up to 5%) also. On top of these manganese deposits the first thicker olistostromes occur. In this higher part of the section a coarsening-upward sequence can clearly be recognized.

The highest part of the succession is characterized by the deposition of black cherty marls, black cherty limestones and on top black radiolarites. This series is of Middle to ?Late Oxfordian age (GAWLICK & SUZUKI 1999). On top of the black radiolarites rests a huge, square kilometre sized slide deriving from the Triassic Dachstein reef rim belt. Here, the sedimentary contact of a late Middle Triassic cherty limestone (Langobardian), resting on the Oxfordian radiolarite can be observed. These slides from the reef rim constitute the youngest part of the Lammer Basin fill (Fig. 30).

More to the west, on top of Mt. Lammeregg, different mass-flow deposits occur. They consist of components of Late Triassic Hallstatt Limestones and Middle Triassic radiolarites. These components originate from the Meliata facies zone and are the result of the earliest stages of resedimentation. These mass flows were deposited during early basin formation in the Zlambach facies zone. Later

Fig. 36: Microfacies of the different carbonate clasts in the olistostromes near the top of the sequence of Mt. Rauhes Sommereck. The clasts derive from the Zlambach facies belt (compare Fig. 95). Late Triassic clasts dominate the clast spectrum, complemented by rare Early Jurassic clasts. Page 227.

1. Different filament- and radiolarian-bearing wackestone clasts (Late Triassic Pötschen Limestone) beside dolomite clasts (Pötschen dolomite) and incorporated black material from the underlying sequence. Several clasts show transported tectonics. Sample BRS 10. Width of photo: 1.4 cm. **2**. Poorly sorted breccia. Pötschen Limestone and Pötschen dolomite components. Black cherty clays occur as matrix. Sample BRS 10-2. Width of photo: 1.4 cm. **3**. Filament-rich Pötschen Limestone clast of Middle Norian age beside marl clasts (Rhaetian Zlambach Formation) and recrystallized limestone clasts. Sample BRS 10-3. Width of photo: 1.4 cm. **4**. Radiolarian-rich matrix between the different clasts. Sample BRS 10-4. Width of photo: 0.5 cm. **5**. Early Jurassic limestone clasts with crinoids, recrystallized radiolarians and spicula. Sample BRS 6. Width of photo: 1.4 cm. **6**. Magnification of 5. Width of photo: 0.5 cm. **7**. Bioturbated Pötschen Limestone clast with recrystallized radiolarians, few filaments and an ammonite remnant. Sample BRS 5. Width of photo: 1.4 cm. **8**. Polymictic breccia with calcite cement between the components (Pötschen Limestone). Sample BRS 2. Width of photo: 1.4 cm.

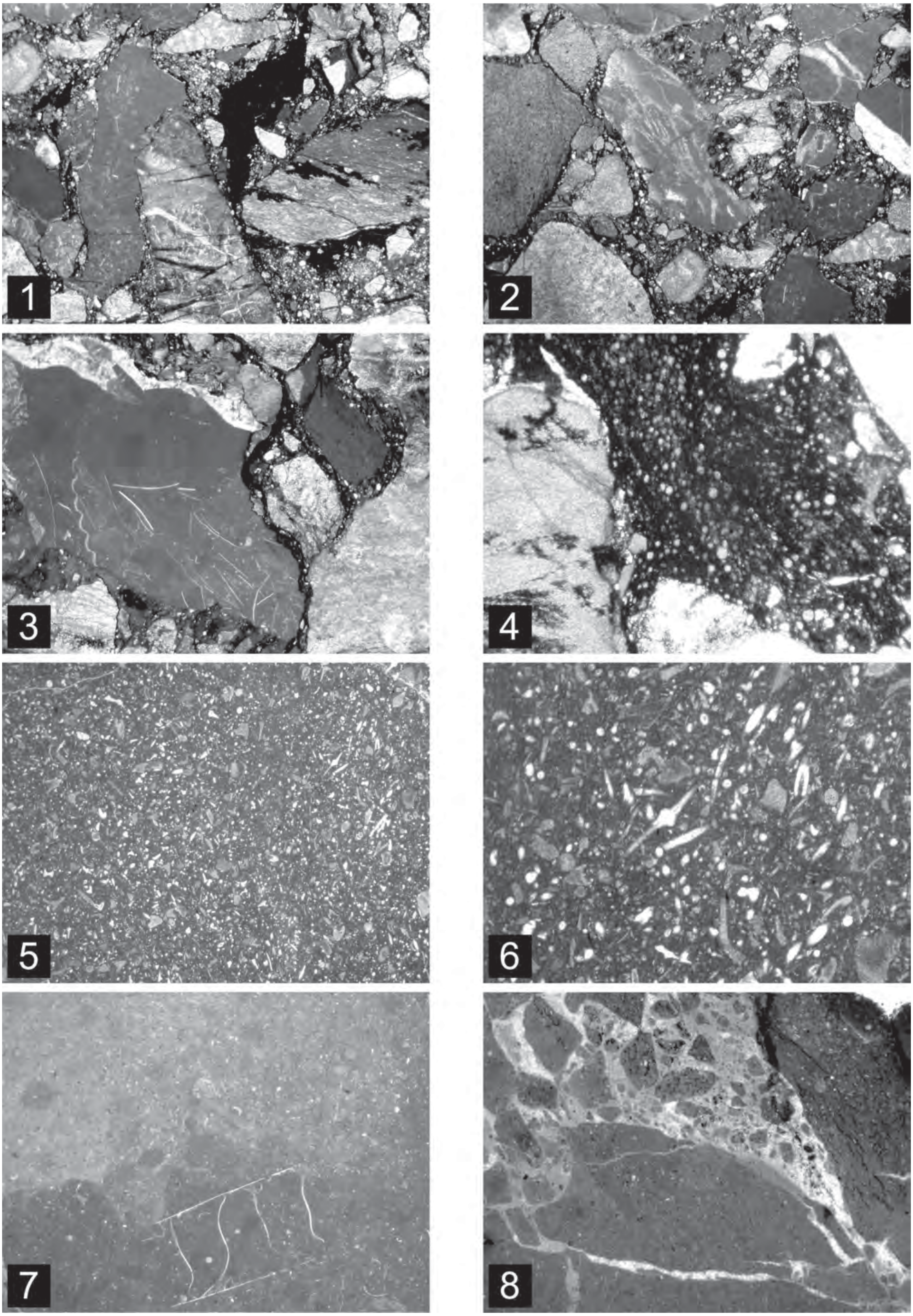
1
2
3
4
5
6
7
8

they were transported in a piggy-back manner to their final, secondary position within the Lammer Basin succession. There, they were sealed by mass-flow deposits of the Lammer Basin fill, similar to the mass-flow deposits we have visited in the Mt. Rauhes Sommereck section. Since these mass flows are in too far distance to the actual excursion route, they will most probably not be visited during the field trip.

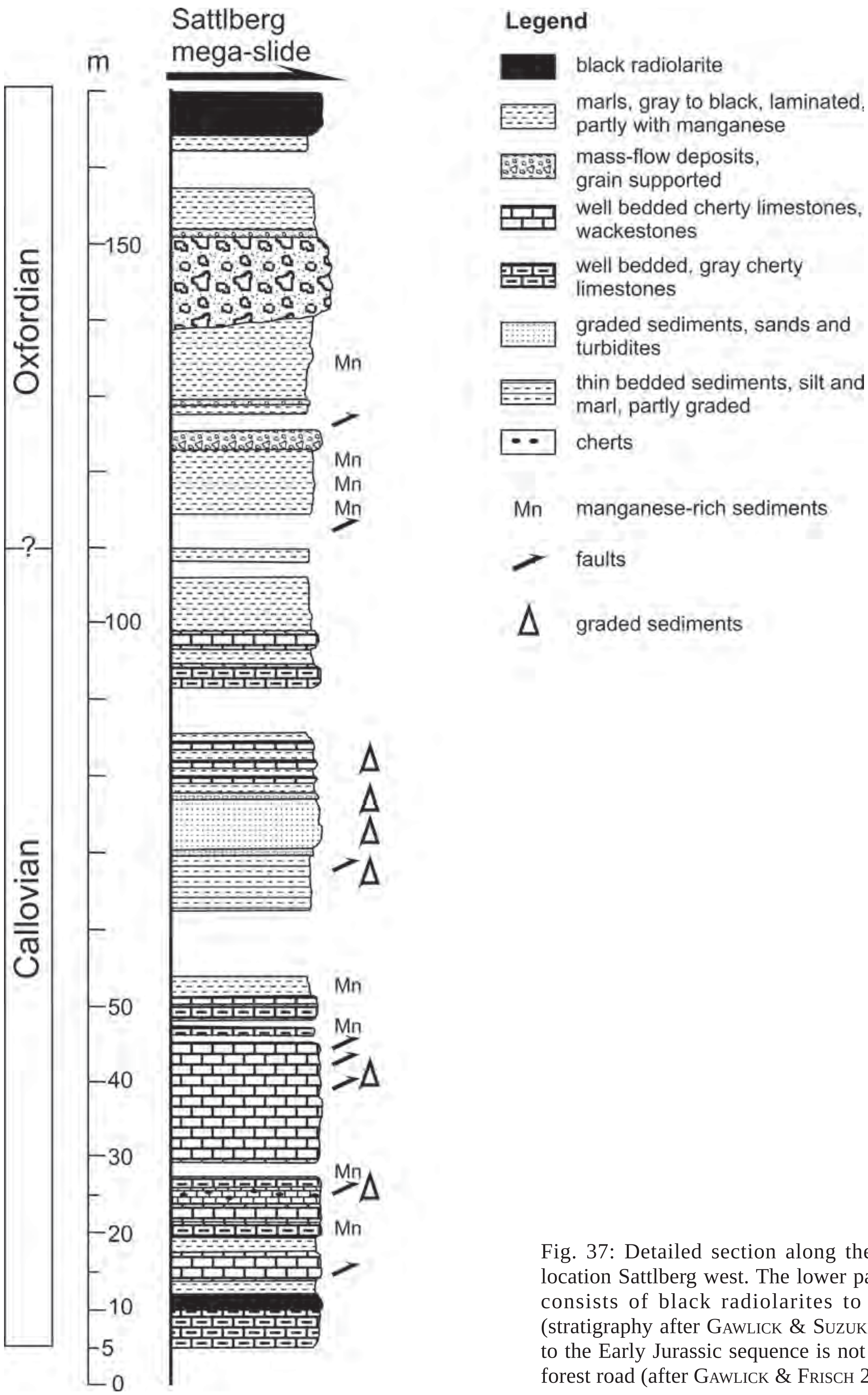

Fig. 37: Detailed section along the forest road at the location Sattlberg west. The lower part of the succession consists of black radiolarites to cherty limestones (stratigraphy after GAWLICK & SUZUKI 1999). The contact to the Early Jurassic sequence is not preserved along the forest road (after GAWLICK & FRISCH 2003).

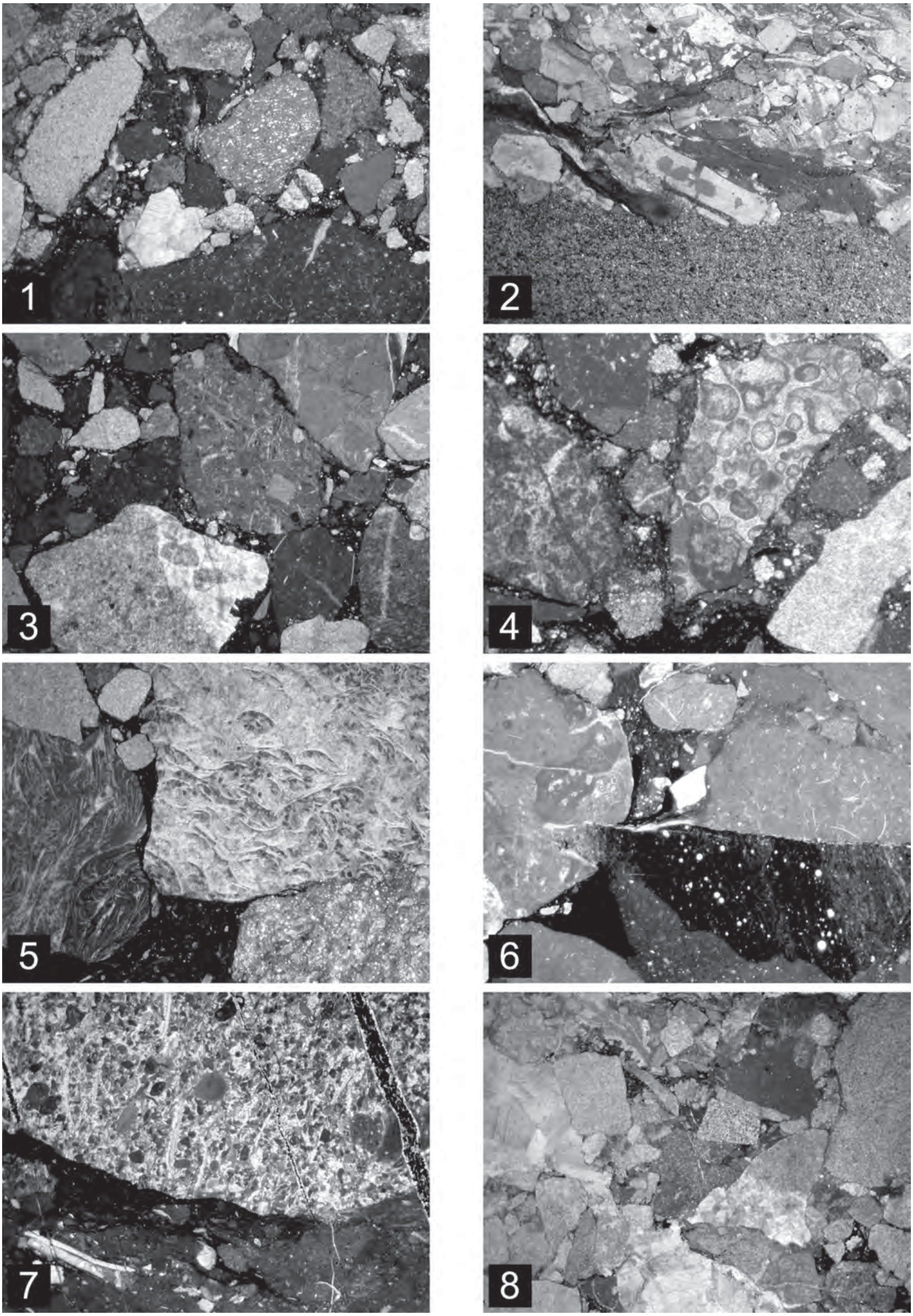
1
2
3
4
5
6
7
8

Fig. 38: Manganese horizon along the forest road to Kuchlbach in the strike of the section Sattlberg west. According to radiolarian dating, the black manganese horizon was deposited around the Callovian/Oxfordian boundary (GAWLICK & SUZUKI 1999).

Fig. 39: Polymictic breccia from the olistostromes of the upper part of the section Sattlberg west. A complete Middle Triassic to Early Jurassic sequence can be reconstructed from the components. (Fig. 41; details in GAWLICK 1996, 2000b). Size of the photo A: 50 cm.

2.2.2. Lammer Basin in the Berchtesgaden Calcareous Alps (optional)

The Lammer Basin strikes from the Salzburg Calcareous Alps in the east to the Berchtesgaden Calcareous Alps to the west. The basin fill in the southwestern Berchtesgaden Calcareous Alps differs slightly from the type area (see explanation above). The visit of this area depends on both the available time and the weather conditions.

Stop 1: Büchsenkopf area
Oxfordian mass-flow deposits and slides

The Büchsenkopf area (Fig. 44) comprises a complete Late Triassic to Late Jurassic sequence. The oldest sedimentary rock in the area is the Rhaetian lagoonal Dachstein Limestone which is overlain by Early Jurassic red nodular limestones (BRAUN 1998). Middle Jurassic red nodular *Bositra* Limestones are missing. The black radiolarite (Callovian: GAWLICK et al. 2003, MISSONI 2003) directly overlies the red nodular limestones (Adnet Formation) with a depositional gap in between. Resedimentation in the area started around the Callovian/Oxfordian boundary but more likely in the Early Oxfordian. Several polymictic olistostromes occur intercalated in black radiolarites to cherty limestones and, more seldom, argillaceous marls. Tens of metres sized slides make up the top of the preserved

Fig. 40: Microfacies of the different carbonate clasts in the olistostromes of the upper part of the section Sattlberg west. The clasts derive from the Zlambach facies belt (compare Fig. 4, Fig. 6). Late Triassic clasts are dominating. Page 229. **1**. Beside several dolomite clasts (Pötschen Dolomite), radiolarian- and filament-rich wacke- to packstones are the dominant components (Pötschen Limestone). Seldom clasts with reef debris occur (Pedata Limestone). Sample 1/89. Width of photo: 1.4 cm. **2**. Contact between the cherty marls of the matrix and a finer-grained turbiditic polymictic breccia intercalation. The elongated clasts are imbricated. Beside the dolomite and limestone clasts some crinoids occur. Sample 14/89. Width of photo: 1.4 cm. **3**. Dark grey filament and radiolarian-bearing wackestone clasts (Pötschen Formation), coarse-grained and fine-grained dolomite clasts (Pötschen Dolomite). The matrix between the components consists of dark siliceous clay. Sample BS 3. Width of photo: 1.4 cm. **4**. Sample BS 3, other view. Grainstone clast with shallow-water components, indicating the reef-near depositional setting of the reworked Triassic sequence. Width of photo: 0.5 cm. **5**. Norian filament limestones. Sample BS 8. Width of photo: 1.4 cm. **6**. Clast with reef-builders, clasts with filaments and a large clast of reworked black Jurassic radiolarite. Sample BS 9. Width of photo: 1.4 cm. **7**. Large grainstone clasts with brachiopods, crinoids and some foraminifera (= Pedata Limestone). Sample O 7. Width of photo: 1.4 cm. **8**. Breccia layer with a component spectrum dominated by different dolomite clasts (Pötschen Dolomite) beside Pedata Limestone clasts and filament-bearing Pötschen Limestone clasts. All these dolomites are deeper-water sediments with conodonts. Sample BS 16. Width of photo: 1.4 cm.

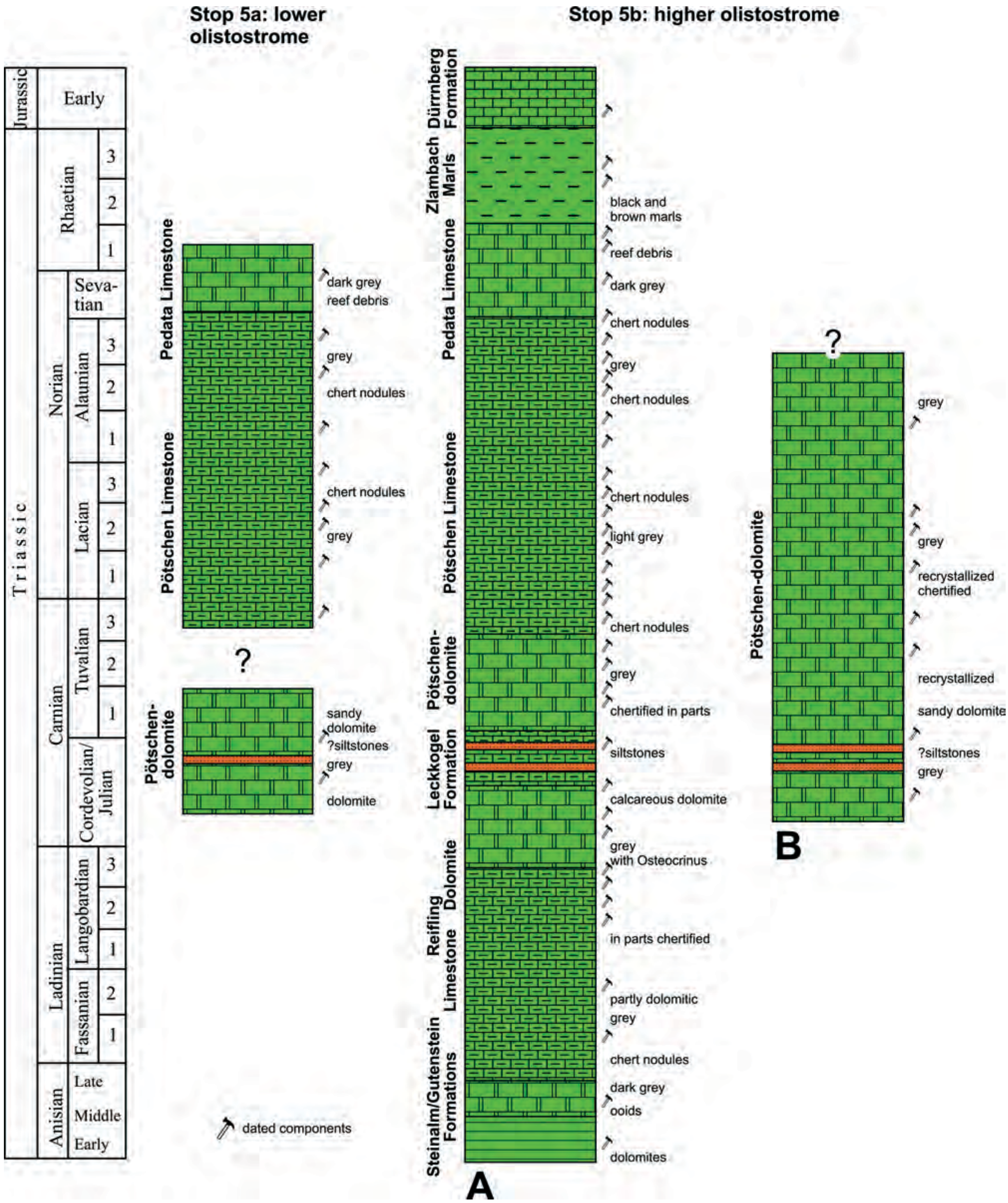

Fig. 41: Correlation of the reconstructed original sedimentary sequences which occur as resedimented components in the early Late Jurassic deep-water cherty sediments of the Lammer Basin fill of the section Sattlberg west. In all cases, the components derive from a more or less identical original sedimentary succession of the Zlambach facies zone (compare Fig. 95. Only the uppermost olistostrome of the section contains material from two provenance areas (Stop 5 in Fig. 11 - two olistostromes 5a and 5b). In addition to the Zlambach facies zone clasts, this olistostrome comprises true Hallstatt Limestone and rare Late Triassic reef rim belt components.

Dating of the components is mainly based on conodonts, less frequent on ammonites, holothurians, foraminifera, and others (details in Gawlick 1996).

Fig. 42: Polymictic breccia on top of Mt. Lammeregg, consisting of different Late Triassic Hallstatt Limestones and Middle Triassic radiolarites from the Meliata facies zone (Fig. 4, Fig. 6; details in Gawlick 1993, 1996). The components derive from the Meliata facies zone. Scale: end of the hammer = 3 cm.

Büchsenkopf area sequence (Fig. 45).
The components of the different mass-flow deposits derive exclusively from the reef slope to reef area of the Late Triassic Dachstein Limestone carbonate platform (Fig. 46, Fig. 47). The material is not of mixed palaeogeographic origin, as know from the Lammer valley type area to the east. The material in the olistostromes and of the large slides, however, is comparable with the youngest slide generation of Lammer Basin fill in the Lammer valley.

In contrast to the Lammer valley type area to the east, the components in the Büchsenkopf area derive from the reef rim facies zone of the Late Triassic carbonate platform. In the Lammer valley these components occur only in the topmost part of the basin fill. In the Büchsenkopf area we face a more northern, younger part of the Lammer Basin fill deposited in the framework of a successive northward shift of the basin axis.

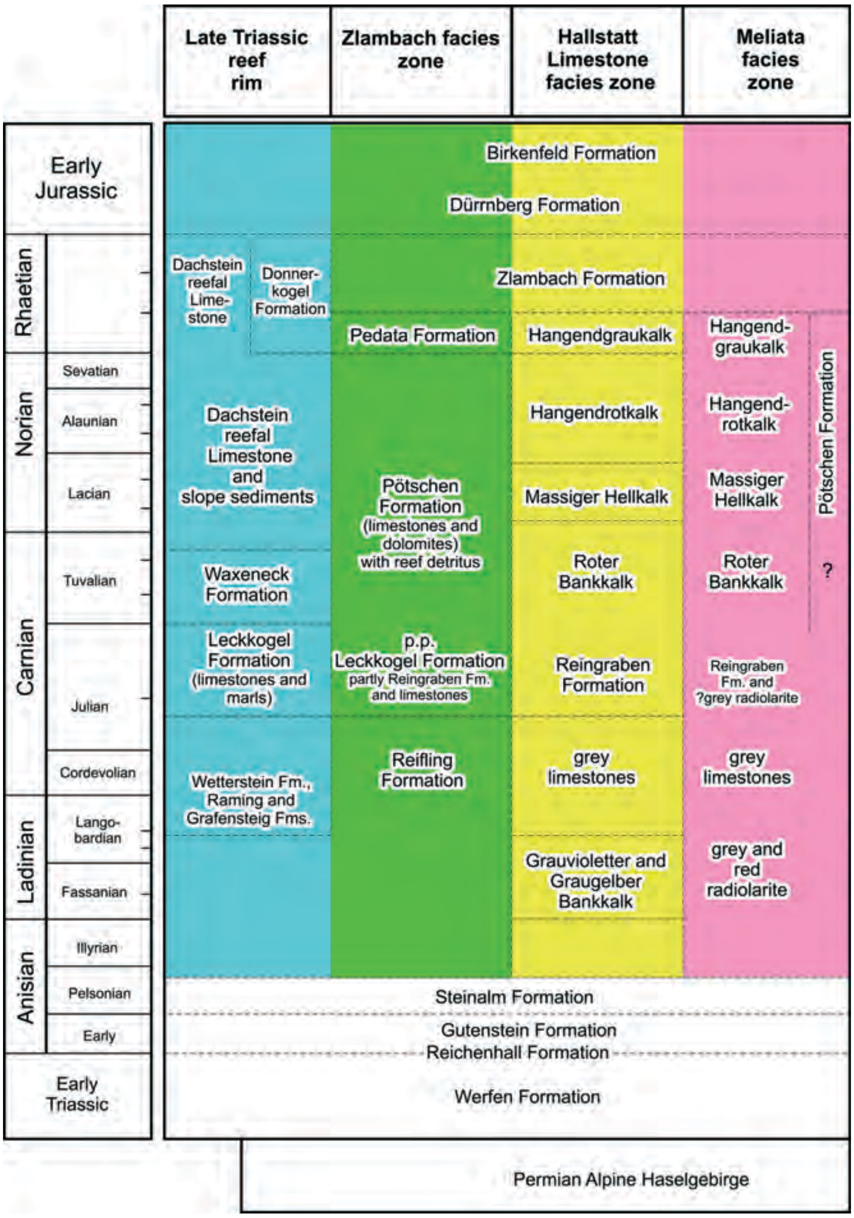

Fig. 43: Palaeogeographic provenance of the clasts in the Lammer Basin fill (compare Fig. 4, Fig. 6). The palaeogeographic origin of clasts and slides older than Middle Anisian cannot be determined as the facies differentiation as consequence of the opening of the Neotethys Ocean started no earlier than Late Anisian. For details see text.

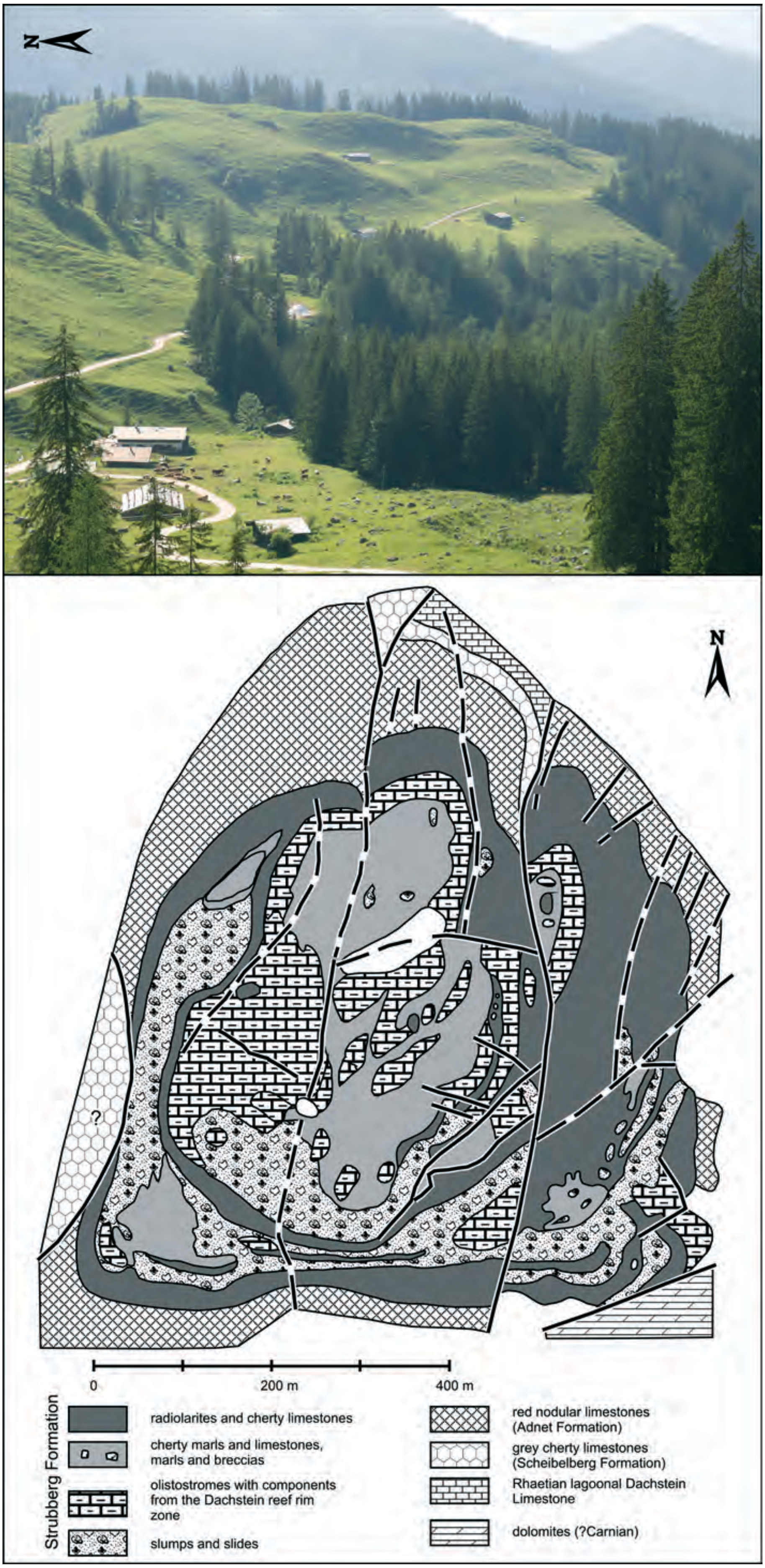

Fig. 44: Photo and geological map of the Büchsenkopf area in the southern Berchtesgaden Calcareous Alps (based on DIERSCHE 1978, after GAWLICK et al. 2003 and MISSONI 2003).

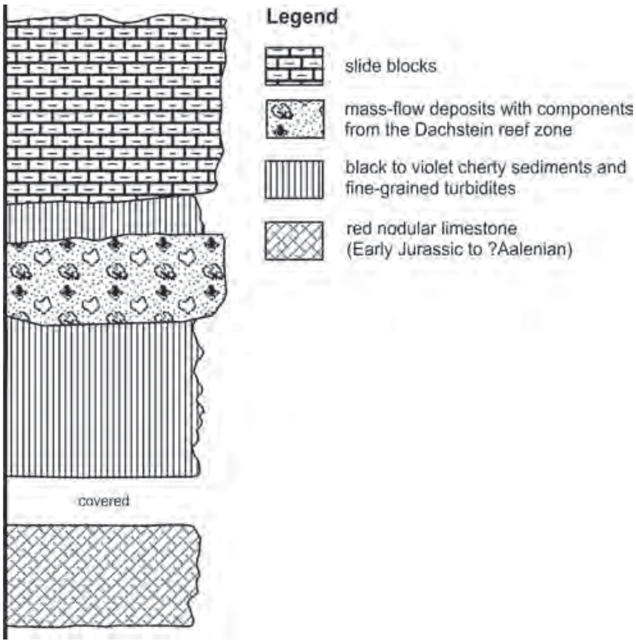

Fig. 45: Generalized sedimentary succession of the Büchsenkopf area. The contact between the Early to Middle Jurassic red nodular limestones is not exposed. The black radiolarites below the first mass-flow deposits are dated as Callovian by means of radiolarians. The first resediments occurred in the Oxfordian according to GAWLICK et al. (2003) and MISSONI (2003). The thickness of the whole preserved succession does not exceed 150 metres. The section is not to scale.

Fig. 46: Polymictic mass flow in the eastern Büchsenkopf area. The grey components derive exclusively from the Late Triassic reef rim. The components were dated by means of conodonts, foraminifera and algae. Size of the photo around 100 cm.

Stop 2: Panoramic view on the basin fill
Oxfordian mass-flow deposits and slides

Upsection, on top of the Büchsenkopf sequence, larger slides of several hundred metres thickness (Fig. 48) occur. Fig. 48 shows the whole Late Triassic to early Late Jurassic sedimentary succession. The base of the succession is represented by Rhaetian lagoonal Dachstein Limestone. It is overlain by red nodular limestones of Early to Middle Jurassic age. Upsection follows a some hundred metres thick succession of radiolaritic sediments with intercalations of mass-flow deposits (= Büchsenkopf series). The sequence is topped by a several hundred metres thick slide from the Dachstein reef slope area (Mt. Jenner). The panoramic view along the way shows dark grey cherty limestones and cherty marls to radiolaritic sediments deposited on top of red nodular limestones. Upsection follow the first mass-flow deposits. The succession is topped by a more than 1000 m thick and several km^2 large slide of Dachstein reef limestones (Mt. Hohes Brett - Fig. 49).

The radiolarians from the cherty limestones and radiolarites directly below the contact yielded a Callovian to Early/Middle Oxfordian age (MISSONI 2003). The upper part of the sequence might have been eroded during the emplacement of the huge slide (compare MISSONI & GAWLICK 2011a).

The matrix of these huge slides consists of dark grey to black cherty marls, cherty limestones and radiolarites, dated by means of radiolarians as Oxfordian (MISSONI 2003). In the Berchtesgaden Calcareous Alps the deposition of the radiolarites of the Lammer Basin fill started in the Callovian and ended in the Oxfordian (MISSONI 2003, MISSONI et al. 2005, MISSONI & GAWLICK 2011a), similar as in the type region to the east.

On the way to the next outcrop (Sillenkopf Basin: chapter

Fig. 47: Microfacies of the matrix, the breccia components and slides of the mass-flow deposits in the Büchsenkopf area (after GAWLICK et al. 2003 and MISSONI 2003). Page 235.
1. Laminated cherty sediments (Callovian to early Oxfordian). Size in width 1.4 cm. Sample Ber 33/2. **2**. Magnification from 1. The radiolarians occur as calcite pseudomorphs. Size in width 0.5 cm. Sample Ber 33/2. **3**. Mass-flow deposits with components of the Gosausee limestone (Late Triassic), non-erosively overlying cherty sediments of the Strubberg Formation,. Size in width 1.4 cm. Sample Bü 14c1. **4**. Matrix supported mass-flow deposits with well-sorted allodapic limestones of the Gosausee limestone. Size in width 1.4 cm. Sample Bü 14c-e. **5**. Synsedimentary parauthochthonous cherty marl slide underlying the mass-flow deposits. Size in width 0.5 cm. Sample Bü 37c. **6**. Mass-flow deposits with biomicritic and biosparitic clasts of the Gosausee limestone. Centre: Manganese-rich sediment of the Strubberg Formation. Large component on the right: spicula-rich biomicrite of the Dürrnberg Formation (Liassic). Size in width 1.4 cm. Sample Bü 22. **7**. Flamestructures at the base of the mass-flow deposits (Büchsenkopf west), matrix supported. Size in width 1.4 cm. Sample Bü 37d. **8**. Matrix supported mass-flow deposits. Right: Late Triassic reefal limestone (Norian to ?Rhaetian). Size in width 1.4 cm. Sample Bü 38e.

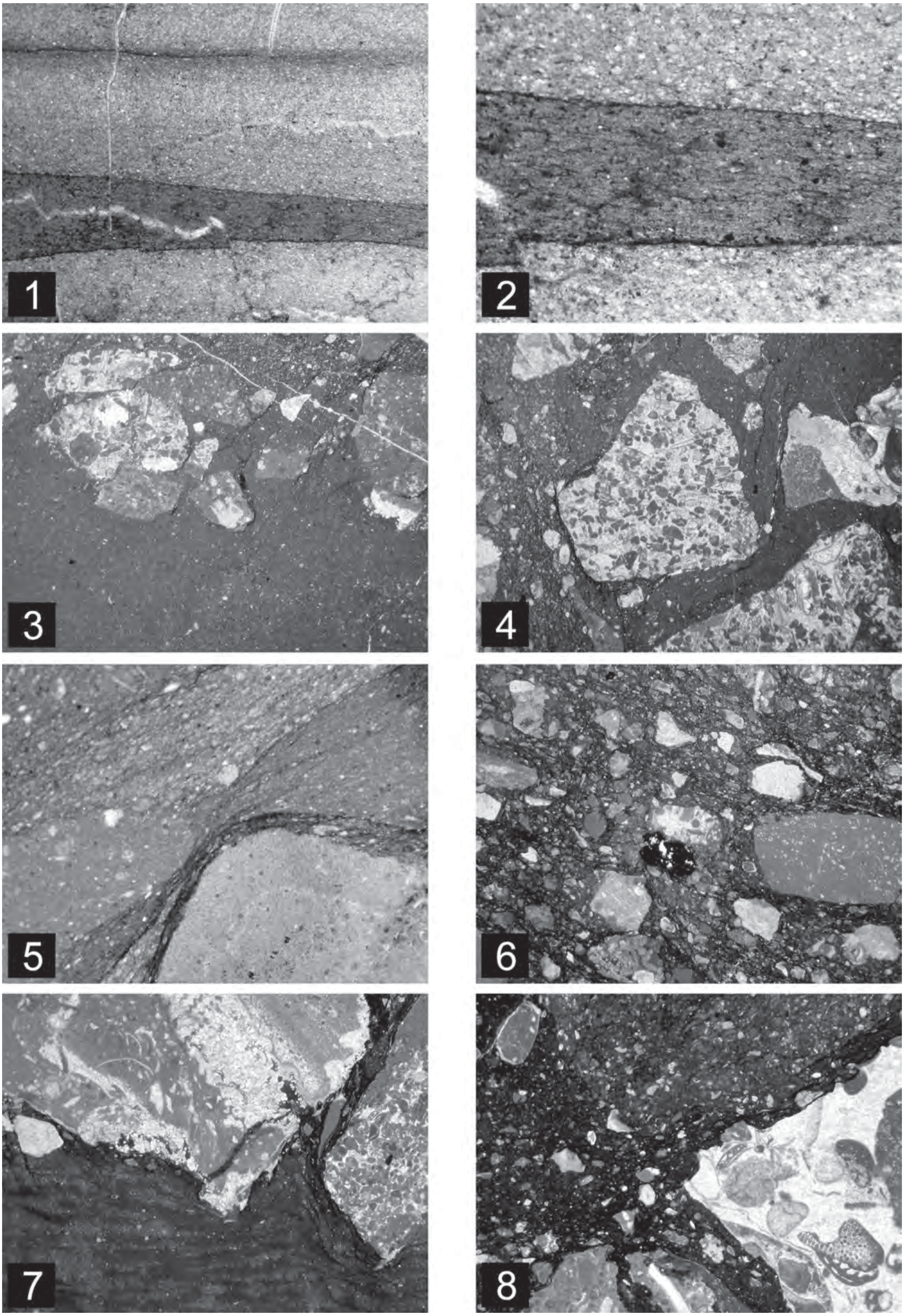
1
2
3
4
5
6
7
8

Fig. 48: Late Triassic to early Late Jurassic sedimentary sequence in the southern Berchtesgaden Calcareous Alps topped by a huge slide of Dachstein reef slope origin. See text for explanations. After MISSONI & GAWLICK (2011a). View from the west (Büchsenkopf area).

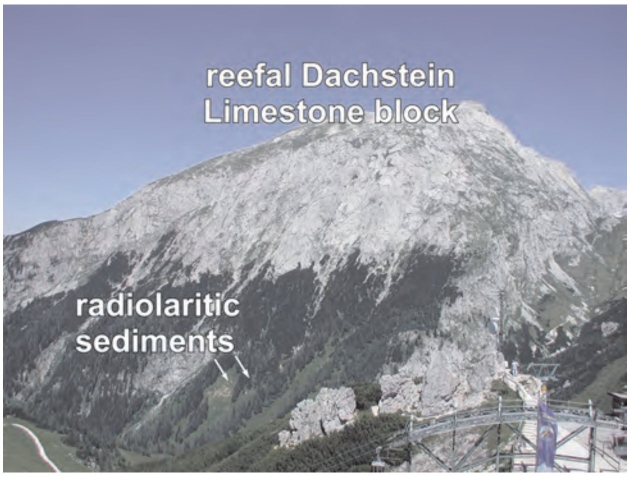

Fig. 49: View from Mt. Jenner to the west on a huge slide block (Dachstein reef limestone) resting on the late Middle to early Late Jurassic cherty matrix. See text for explanations. After MISSONI & GAWLICK (2011a).

2.4.) we cross an important Miocene strike-slip fault (DECKER et al. 1994). The sequences preserved south of this strike slip fault belong also to the lagoonal Dachstein Limestone facies zone. Kössen beds are missing in this area though. That means, we are now palaeogeographically farer to the south, in the southernmost part of the main depositional area of the Lammer Basin.

The Early and Middle Jurassic sequence above the Norian to Rhaetian lagoonal Dachstein Limestone is similar to the successions we have earlier seen below the Lammer Basin fill and what we will see as substratum of the Tauglboden Basin fill (chapter 2.3). In contrast, the late Middle Jurassic to Late Jurassic sequence is either missing or of different composition. Probably it was sheared off by Late Oxfordian to Early Kimmeridgian thrusting processes (compare Fig. 97).

2.3. Tauglboden Basin and Trattberg Rise: material from the lagoonal Dachstein Limestone facies zone

The Tauglboden Basin is the best preserved Late Jurassic basin in the central Northern Calcareous Alps. However, it is not possible to get a comprehensive insight into the basin built by means of one north-south transect. Younger tectonic motions, e.g. around the Early/Late Cretaceous boundary - strike-slip movements (e.g., WAGREICH & DECKER 2001), Oligocene thrusting (e.g., FRISCH & GAWLICK 2003) and Miocene to recent strike-slip movements (e.g., RATSCHBACHER et al. 1991) accompanied by block rotations (PUEYO et al. 2007) strongly modified and obscured the original basin geometry.

We will visit the proximal, southernmost part of this basin in the central Salzkammergut area (north of the township Altaussee) and the central and northern part of the basin in the Salzburg Calcareous Alps. The thickness of the Oxfordian sedimentary succession reaches up to 800 m in the southern part of the basin (Knerzenalm area), about 200 metres in the central (Tauglboden area), and only some tens of metres in the northern part of the basin.

The Trattberg Rise in the inner Northern Calcareous Alps separated the Lammer Basin (= upper Tirolic nappe group; compare Fig. 28) in the south from the Tauglboden Basin in the north (= lower Tirolic nappe group) (FRISCH & GAWLICK 2003) (Fig. 7). The Tauglboden Formation is composed of Oxfordian to Early Tithonian cherty matrix sediments with intercalated polymictic breccias and mass-flow deposits derived from the Trattberg Rise to the south (GARRISON & FISCHER 1969, SCHLAGER & SCHLAGER 1973, DIERSCHE 1980), i.e., the lagoonal Dachstein Limestone facies zone.

Concerning this basin, the differentiation of several sedimentary cycles is of great importance:

1. The first cycle of deposition was characterized by redeposition of older clasts exhibiting a coarsening upward trend. This cycle is restricted to the Oxfordian.
2. The second cycle of deposition was characterized by the deposition of a condensed radiolarite succession. This cycle occurred in the time span latest Oxfordian to Early Tithonian.
3. The third cycle was again characterized by redeposition. It shows an overall fining-upward trend: in a first stage, redeposition of older clasts took place. Later, the deposits were typically made up of a mixture of older clasts and contemporaneously formed reef debris. In the latest stage, the redeposits exclusively consisted of shallow-water carbonates of the Plassen Carbonate Platform.

2.3.1. Proximal Tauglboden Basin - Salzkammergut area

In the central Salzkammergut area northwest of the township Altaussee and southeast of the township Bad Ischl (Fig. 8, Fig. 10, Fig. 11) the proximal part of the Tauglboden Basin is well preserved. In this area, the Tauglboden Basin succession reaches thicknesses of about

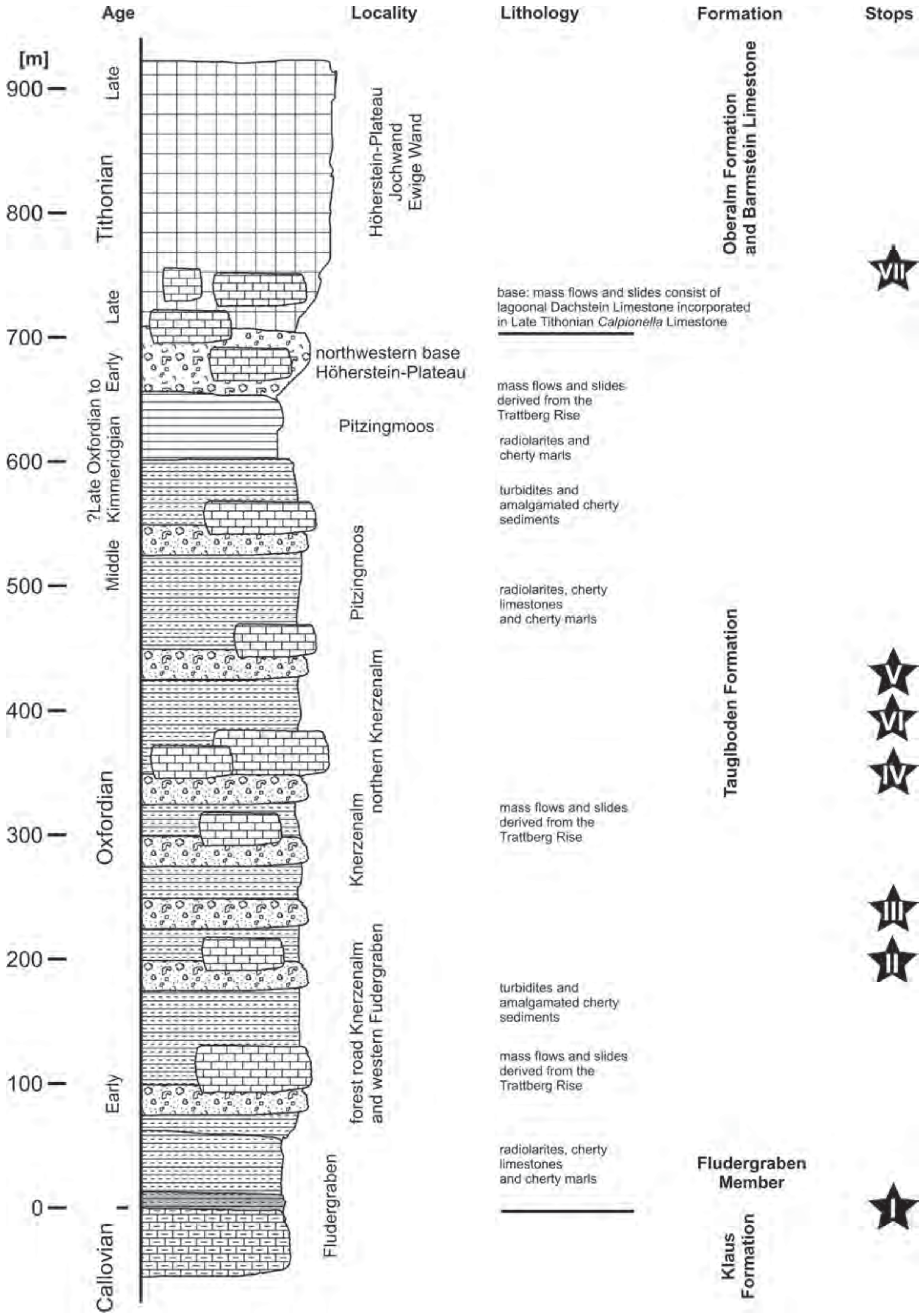

Fig. 50: Schematic illustration of the Tauglboden Basin fill (Tauglboden Formation, Oberalm Formation + Barmstein Limestone) in the region north of the Höherstein plateau and position of the localities visited during this field trip. For the geographic position of the stops see Fig. 11 (map).

Fig. 51: Sedimentary contact between the red limestones of the Klaus Formation (Callovian/Oxfordian boundary) and the bedded red radiolarite; eastern Fludergraben (valley).

800 metres (Fig. 50). The complete section we will visit south of Mt. Höherstein (Fig. 11).

The sedimentary record in the newly formed Tauglboden Basin started sometime in the period Callovian/Oxfordian boundary to Early Oxfordian. The deposition of red radiolarites on top of red nodular limestones (Klaus Formation - Fig. 5) indicated the beginning of rapid subsidence. After the deposition of the red radiolarite first slump deposits occurred, consisting of radiolarite and mass-flow deposits with reworked older material. The colour of the radiolarite changed from red to dark-grey. These dark-grey radiolarites, later also cherty limestones and cherty marls, contain upsection thick mass-flow deposits and 100 m^2 large slides. There is a general coarsening-upward trend of the sequence. The age of the whole sequence was dated roughly as Early to Middle Oxfordian by means of radiolaria (GAWLICK et al. 2007a). In the time span from the latest Oxfordian to earliest Tithonian the Tauglboden Basin was characterized by starved sedimentation. Only few metres of dark-grey cherty limestones to radiolarites were deposited during that time. In Early Tithonian time resedimentation started again, initially with mass-flow deposits containing older material (mainly Late Triassic clasts) and slump deposits. Gradually, progressively more reef debris of the Plassen Carbonate Platform was shed into the Tauglboden Basin. After a period of mixed sedimentation with older clasts, finally the different shallow-water clasts deriving from the Plassen Carbonate Platform *s. str*. (Oberalm Formation + Barmstein Limestone) took completely over. In the area of the Höherstein Plateau the thickness of this coarse-grained reef debris with deep-water calpionellid-bearing limestone intercalations

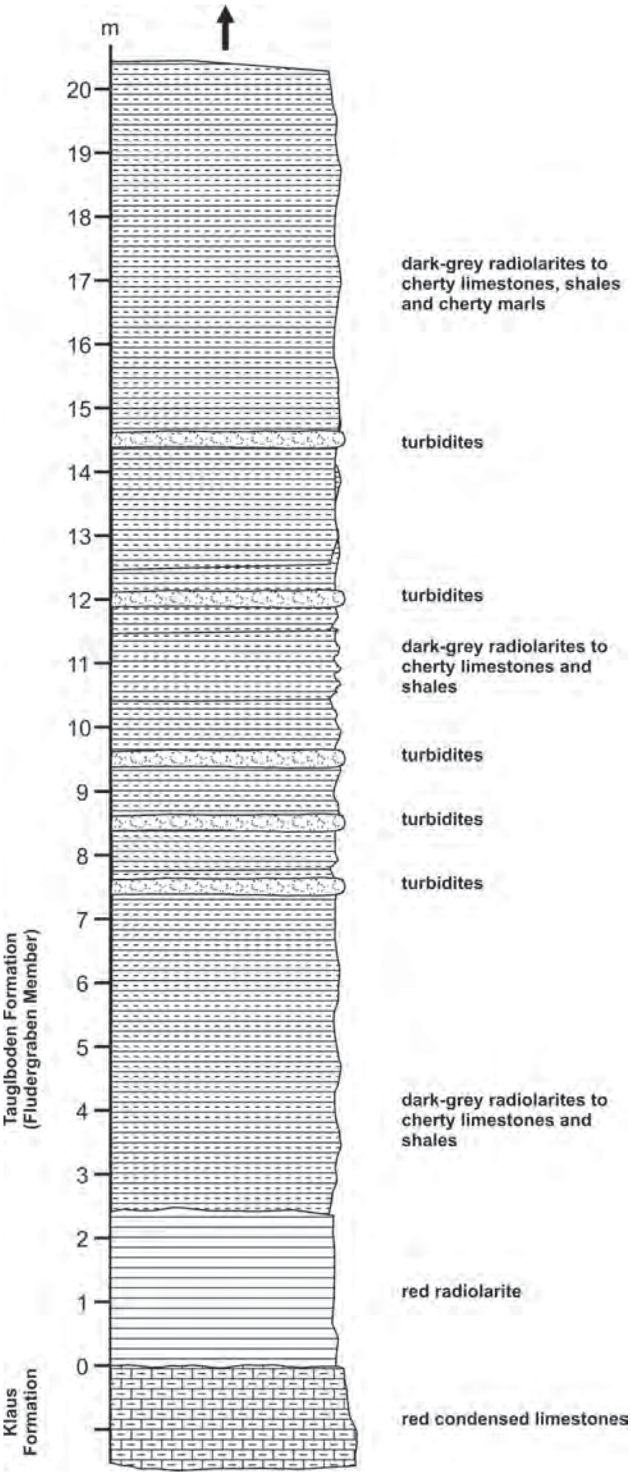

Fig. 52: Detailed lithological section of the succession above the sedimentary contact between the red nodular limestones of the Klaus Formation (Callovian/Oxfordian boundary according to MANDL 1982) and the thin-bedded red radiolarite (Fludergraben Member). The latter are overlain by dark grey laminated radiolarites with the first turbiditic intercalations; eastern Fludergraben (valley).

Fig. 53: Lower part of the succession: thin-bedded grey to violet radiolarites intercalated by carbonate turbidites. These relatively fine-grained carbonate turbidites contain mainly older clasts (Late Triassic to Middle Jurassic). For components compare Fig. 55.

Fig. 54: Lower part of the succession: thin-bedded grey radiolarites with an intercalated mass flow showing an erosive basal contact. The components in this mass-flow deposit are exactly the same as in the turbidites (Fig. 53). For components compare Fig. 55.

exceeds 500 metres. Here, only the Late Tithonian part of this succession is preserved. However, obviously this kind of deposition continued into the Berriasian, as proven in many other sections in the central Northern Calcareous Alps.

A detailed description of the investigation history of this area, including the different interpretations, is given by Mandl (1982) and Gawlick et al. (2007a). Former regional investigations concentrated mainly on the age determination and facies characteristics of the different carbonate slide blocks and the carbonate successions. The radiolarite successions were only dated by means of ammonites occurring in the underlying sedimentary rocks. They were generally attributed to the Oxfordian (e.g., Toll-

Fig. 55: Microfacies of the Klaus Formation from the base of the succession in the Fludergraben valley, the overlying radiolarites (Tauglboden Formation) and the intercalated turbidites with shallow-water debris of the same age; Early Oxfordian (Fludergraben Member) (after Gawlick et al. 2010). Page 240.

1. Topmost bed of the Klaus-Formation: *Bositra* Limestone with some crinoids. Sample D 1051. Width of photo: 1.4 cm. **2**. Magnification of 1. Beside *Bositra* shells and crinoids some reworked hardground clasts occur. Width of photo: 0.5 cm. **3**. Red radiolarite overlying the Klaus Formation. The basal part of the radiolarite is dark-grey to black and contains well preserved radiolaria. Upsection, the radiolarite is red, massive and without lamination. Sample D 1052. Width of photo: 1.4 cm. **4**. Magnification of 3. The most radiolarians of the red radiolarite are recrystallized; only few radiolarians are well preserved. Width of photo: 0.5 cm. **5**. Slightly bioturbated cherty limestone to radiolarite around 6 metres above the top of the Klaus Formation. Radiolaria wackestone with mostly calcitized radiolarians. Sample D 1029. Width of photo: 1.4 cm. **6**. Magnification of 5. Radiolaria wacke- to packstone. Some radiolaria are filled with fine-grained sediment and show good preservation. Width of photo: 0.5 cm. **7**. Calcareous turbidite intercalated in the grey cherty limestones to radiolarites. Beside clasts of the Early and Middle Jurassic Adnet and Klaus Formations, there are clasts from a contemporaneous shallow-water area, a precursor of the Plassen Carbonate Platform. Sample D 1053. Width of photo: 1.4 cm. **8**. Sample D 1053, other view. Crinoids, foraminifera and micrite clasts from the precursor of the Plassen Carbonate Platform occur together with small *Bositra* Limestone components and older radiolarites (Strubberg Formation). Width of photo: 0.5 cm.

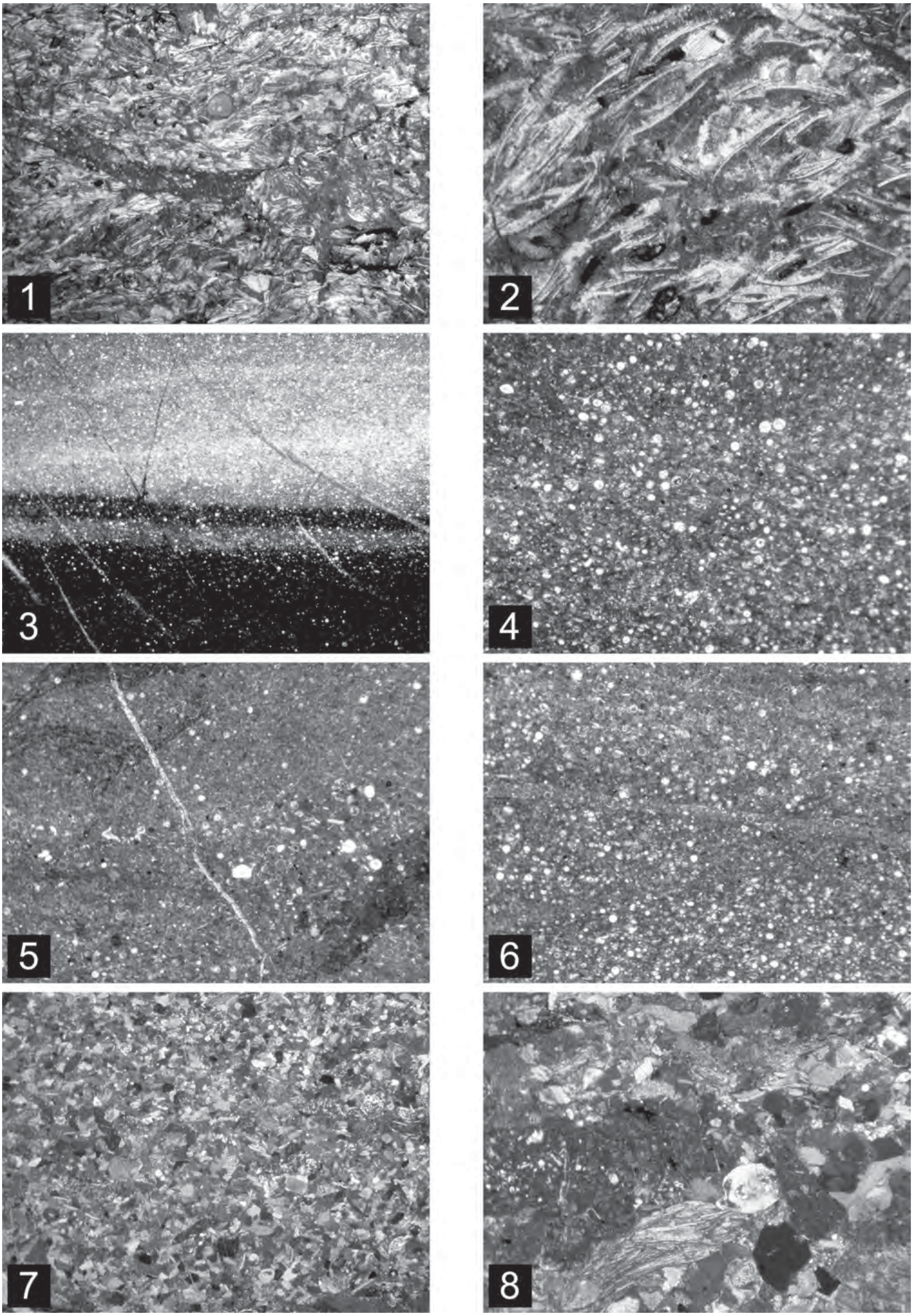
1
2
3
4
5
6
7
8

MANN 1976a, DIERSCHE 1980). Here, in the description of the different stops only the most important references are mentioned.

Stop I in Fig. 11: base of the basin fill, Mt. Brunnkogel - Fludergraben

Early Oxfordian base of the radiolaritic basin fill and its Triassic to Middle Jurassic (Callovian) underlying sedimentary sequence

The Late Triassic to late Middle Jurassic sedimentary sequence below the Tauglboden Basin fill can be described as follows: In the Late Triassic Norian to Rhaetian lagoonal Dachstein Limestone was deposited. In the visited section only the Rhaetian lagoonal Dachstein Limestone is preserved, characterized by thick-bedded grey limestones with different shallow-water organisms, e.g. megalodontidae. In the topmost part of the Dachstein Limestone several corals are preserved, indicating an opening of the depositional area. Around the Triassic/Jurassic boundary shallow-water carbonate production stopped. On top of the Dachstein Limestone red nodular and crinoid-rich limestones were sedimented (Adnet Formation). They represent a drowning sequence most probably of Late Hettangian age, as proven in several sections in the Northern Calcareous Alps (e.g., BÖHM 1992, 2003). In this section, red nodular limestone deposition prevailed, with several stratigraphic gaps (Fig. 5), until the latest Callovian to the Callovian/Oxfordian boundary, as proven by ammonites (MANDL 1982).

The radiolarite section starts almost instantaneously above the red nodular limestones (Fig. 51). The red radiolarite is well-bedded and the beds are massive, partly completely chertified. The microfacies show radiolarian wackestones to packstones. After two to three metres (Fig. 52), the colour of the red radiolarite changes from reddish to grey and upsection grey cherty limestones and cherty shales prevail. Several slumps of reddish radiolarite are intercalated in this lower grey radiolarite part of the section; the grey radiolarites and the reddish radiolarites slumps are all of the same age and contain the same radiolarian fauna (GAWLICK et al. 2010). Upsection, the first fine-grained carbonate turbidites and thin-bedded coarse-grained mass-flow deposits occur (Fig. 52, Fig. 53, Fig. 54). The components in these resediments are mostly older (Late Triassic to Middle Jurassic clasts of the lagoonal Dachstein Limestone facies zone), but occasionally there are also equal-aged carbonate clasts from a (Early

Fig. 56a, b: Polymictic mass-flow deposits of the middle part of the Tauglboden Formation. In this level of the formation, red nodular limestones of the upper part of the Early Jurassic Adnet Group (for ammonite dating see MANDL 1982) occur often beside early Early Jurassic grey cherty limestone clasts and Late Triassic lagoonal Dachstein Limestone clasts (Fig. 57). More upsection Jurassic red limestones and Jurassic clasts generally disappear and the component spectrum exclusively consists of Late Triassic clasts of lagoonal Dachstein Limestone.

Fig. 57: Microfacies of the different components of the mass-flow deposits along the road to the Knerzenalm, just before the entrance to the Knerzenalm area. After Gawlick et al. (2010). Page 242.

1. Component of the Enzesfeld Formation next to a wackestone component. Sample D 3-1. Width of photo: 0.5 cm. **2**. Component of the Scheibelberg Formation (or the Kendlbach Formation) beside a Middle Jurassic radiolaritic component of the Ruhpolding Radiolarite Group. Sample D 3-2. Width of photo: 0.5 cm. **3**. Rhaetian Dachstein Limestone component and red condensed limestone of the Adnet Formation. Sample D 3-4. Width of photo: 1.4 cm. **4**. Different Early and Middle Jurassic clasts beside a Rhaetian Dachstein Limestone component. Sample D 3-5. Width of photo: 1.4 cm. **5**. Small and angular components derived from the late Early Jurassic succession (crinoid-rich higher Adnet Formation) and the Rhaetian Dachstein Limestone. Sample D 4-1. Width of photo: 1.4 cm. **6**. In this mass-flow deposit crinoid-rich clasts of the higher Adnet Formation are dominating. Sample D 4-2. Width of photo: 1.4 cm. **7**. Beside the predominating Rhaetian Dachstein Limestone clasts a late Middle Jurassic radiolarite clast occurs, which shows microfacies characteristic as seen in the distal Strubberg Formation. Sample D 5-1. Width of photo: 1.4 cm. **8**. Clast of Rhaetian Dachstein Limestone. Sample D 5-3. Width of photo: 0.5 cm.

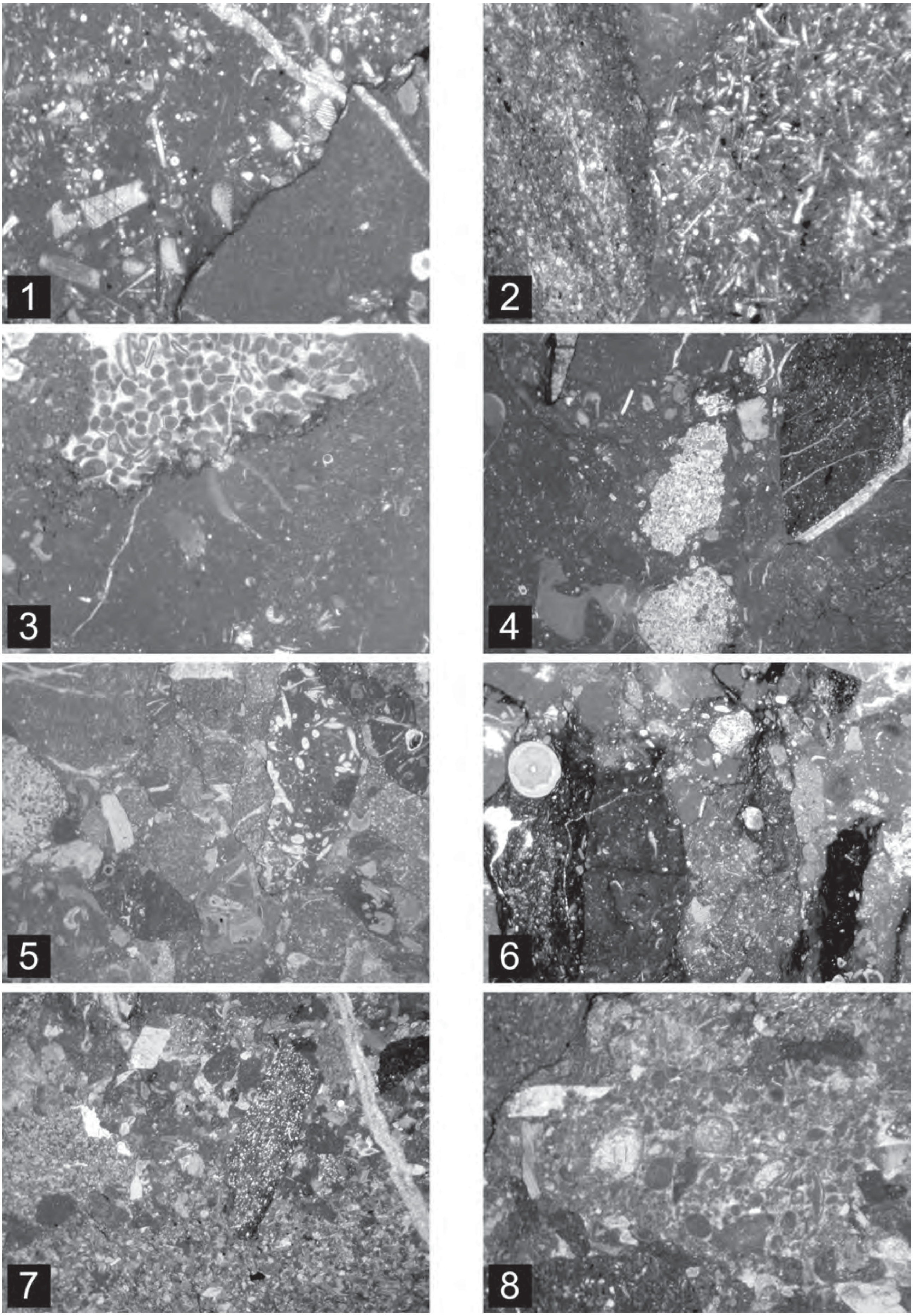
1
2
3
4
5
6
7
8

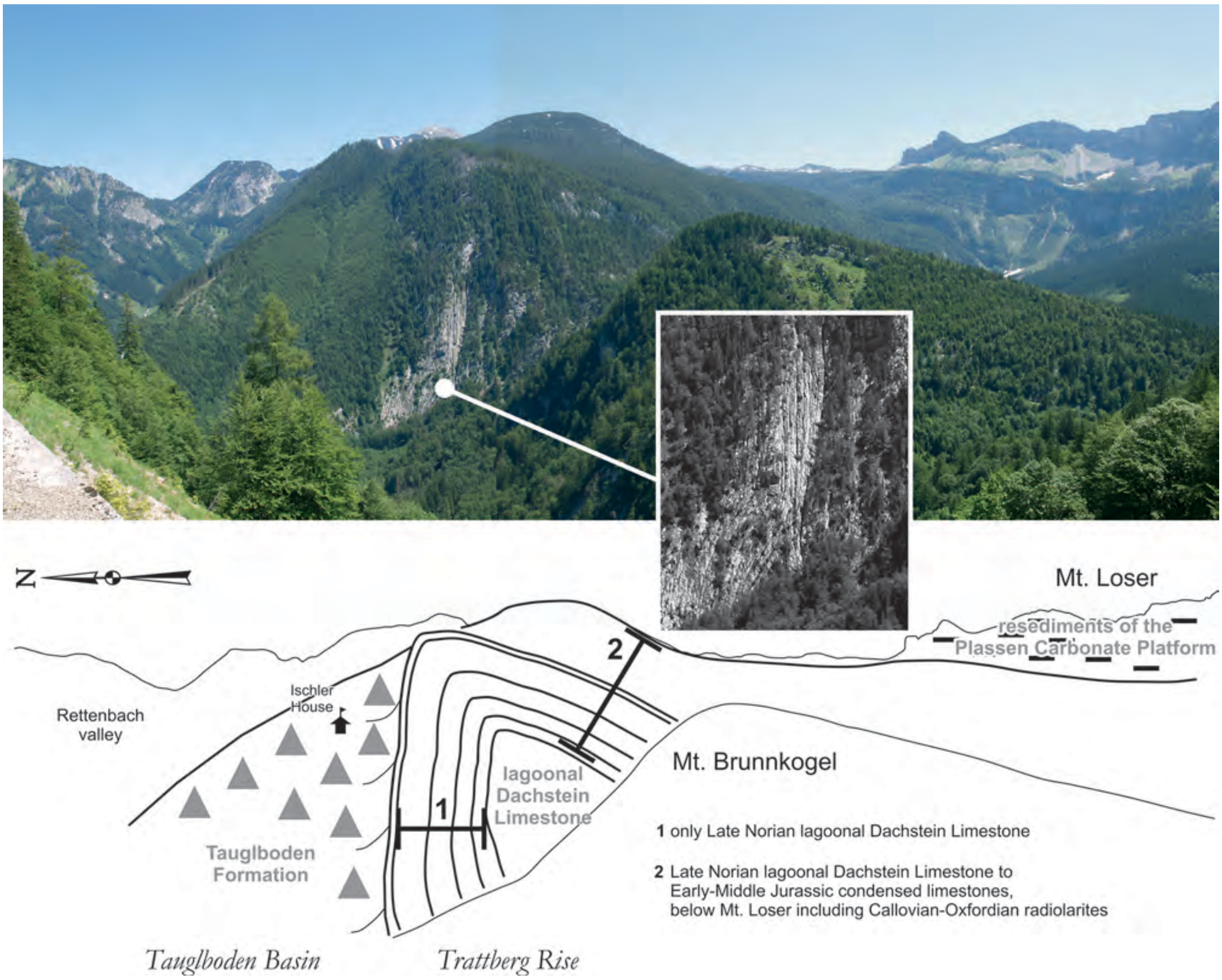

Fig. 58: View towards east on the Trattberg anticline. Tauglboden Formation onlaps on the northern limb of this anticline along an unconformity (after Missoni & Gawlick 2011a).

Oxfordian) precursor of the Plassen Carbonate Platform. At the base of most of the turbidites and mass flows, thin layers of volcanic ashes are preserved. According to radiolarian dating, the whole succession is Early to Middle Oxfordian in age, with an Early Oxfordian age most probable (Gawlick et al. 2007a, 2010).
Upsection, the deep-water sediments become more and more marly or calcareous; in some cases calcareous radiolarites occur. The occurrence of slump deposits increases. There are several mass-flow deposits which consist of older material deriving from the lagoonal Dachstein Limestone facies zone. Also several huge slides of hectometre-size are incorporated in the sedimentary succession.

Middle to upper part of the basin fill, Knerzenalm area - stops II to V in Fig. 11
Early to Middle Oxfordian mass-flow deposits in a radiolaritic/argillaceous matrix

On the way to the Knerzenalm area we cross the fault which separates the Sandlingalm Basin fill in the south from the Tauglboden Basin fill in the north. The age of this fault is unknown, but it must be younger than late Early Cretaceous as proven by the existence of Early Cretaceous sediments to the northwest, which overlie the Tauglboden Basin fill. Along the way there are several outcrops of radiolarites: first violet to grey massive radiolarites, which belong to the Sandlingalm Basin, and later, north of the fault, thin-bedded and laminated radiolarites to cherty limestones, which belong to the Tauglboden Basin fill.

Stop II: Forest road to the Knerzenalm

Along the forest road to the Knerzenalm area, shortly after the fault, several mass-flow deposits intercalated in dark-grey laminated radiolarites occur (Fig. 56). These mass-flow deposits contain a component spectrum of a complete original sedimentary sequence from the Late Triassic to the Middle Jurassic. Beside Rhaetian shallow-water carbonates (Dachstein Limestone), Early Jurassic grey cherty limestones (e.g., Scheibelberg Formation; late

Fig. 59: Contact of a debris-flow deposit with the underlying radiolarites. The component spectrum consists mainly of lagoonal Dachstein Limestone. Jurassic clasts are very seldom.

Fig. 60: Old quarry in the uppermost part of the Tauglboden basin fill. See text for explanation.

Hettangian to late Pliensbachian: GAWLICK et al. 2007a, 2010), late Early Jurassic red nodular limestones (Adnet Formation; late Pliensbachian to Toarcian: MANDL 1982) and, rather seldom, late Middle Jurassic radiolarite components can be observed. Along the forest road a general coarsening-upward trend can be observed in the succession. The biggest blocks occur directly at the entrance area to the Knerzenalm, where many large-scaled slides (up to several hundred metres) exclusively consisting of Rhaetian lagoonal Dachstein Limestone are incorporated into the radiolaritic matrix.

Slightly before the entrance to the Knerzenalm area there is a good view point giving insight into the situation to the east to southeast. The anticline of the Trattberg Rise can be nicely seen (Fig. 58). The Trattberg Rise region acted as derivation area for the mass-flow deposits. The northern, vertical limb of the anticline consists exclusively of Norian lagoonal Dachstein Limestone. All younger sedimentary rocks (latest Triassic to Middle Jurassic) are eroded and occur today only reworked as clasts and slides in the Tauglboden Basin to the north, as visible in the Knerzenalm area. Towards south, the gap in the stratigraphic column becomes successively smaler and in the Mount Loser region a more or less complete Late Triassic to Late Jurassic sequence is preserved.

Stops III, IV and V in Fig. 11: Knerzenalm area

The outcrops in the forest of the Knerzenalm area give an insight of the size of the different slides, which consist mainly of Rhaetian lagoonal Dachstein Limestone. Sometimes the radiolaritic matrix between the different slides is visible.

At a junction of some forest roads (Stop III in Fig. 11), the basal erosive contact of a debris flow on top of laminated cherty limestones to radiolarites can be observed. The components are mainly lagoonal Dachstein Limestone whilst Early Jurassic clasts are rare. Several clasts are rounded.

Along the way to Pitzingmoos (Fig. 11), the upper part of Early to Middle Oxfordian part of the Tauglboden Basin fill is visible in an old quarry (Stop IV in Fig. 11) (Fig. 60). Dark-grey to black radiolarites, cherty limestones and cherty marls are intercalated by carbonate turbidites and fine-grained breccia layers. The component spectrum (Fig. 61) is similar to that in the Knerzenalm area. In addition, several carbonate clasts from a nearby shallow-water area occur, documenting the onset of the Plassen Carbonate Platform. AUER et al. (2009) dated the first onset of the Plassen Carbonate Platform as Late Oxfordian by analysis of reefal debris-flows intercalated in radiolarites; the sequence in this outcrop could represent a more basinal equivalent of similar age.

Some tens of metres upsection (we will not climb) the contact to the Late Tithonian grey cherty limestones with intercalated thick mass flows of reef debris can be seen. The latest Oxfordian to Early Tithonian sequence is strongly condensed in the Tauglboden Basin. This basin starvation is visible also in the central Tauglboden Basin in the southern Salzburg Calcareous Alps. The outcrop situation there is much better than in the Knerzenalm area.

Along the forest road to Pitzingmoos (Fig. 11), different mass-flow deposits intercalations in laminated radiolarites to cherty limestones can be sporadically observed (Stop V in Fig. 11). Although the general outcrop situation is rather poor, the main features are visible. The component spectrum in the different mass-flow deposits is identical to those of the earlier visited mass-flow deposits in the Knerzenalm area.

Stop VI in Fig. 11: Tectonic contact between the Sandlingalm Basin and the Tauglboden Basin (optional)

In the westernmost part of the Fludergraben, the tectonic contact between the black massive radiolarites of the Sandlingalm Basin and the laminated dark-grey radiolarites to cherty limestones of the Tauglboden Basin

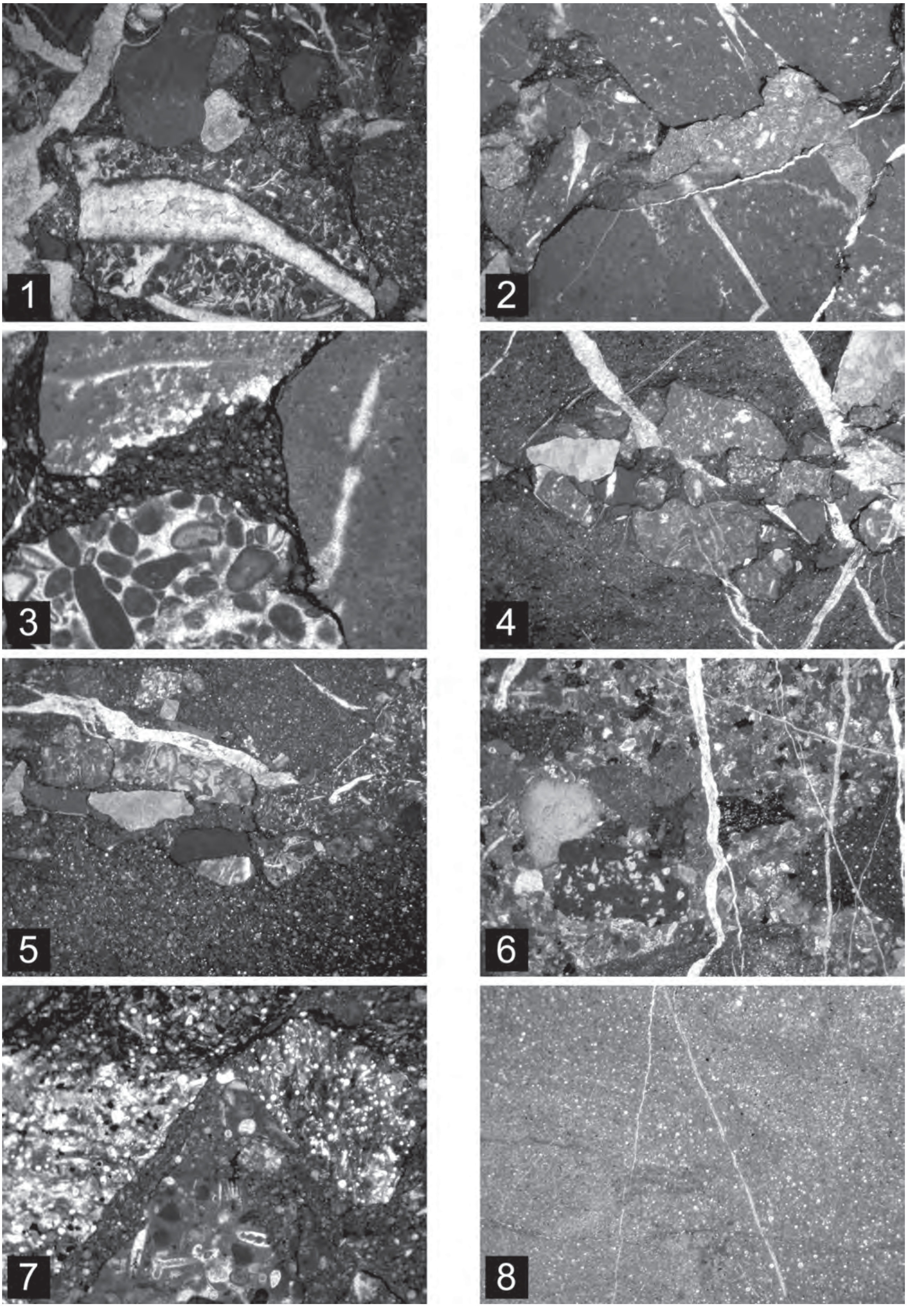
1
2
3
4
5
6
7
8

is exposed. In the furrow, this contact is very sharp and exhibits some evidence for a strike-slip nature of the fault. The mass-flow deposits and slides south of this contact consist exclusively of different Hallstatt Limestone components, whereas the mass flows north of the fault are predominantly made up of lagoonal Dachstein Limestone clasts. Thus not only the different litho- und microfacies of the radiolarites but also the different mass-flows in the series prove this steep, tectonic contact between the both basins fills as a prominent structure.

Radiolarian dating of both types of radiolarites yielded more or less the same age for both successions (Gawlick et al. 2007a),. This is understandable, as we face the middle part of both the Sandlingalm Basin fill and the Tauglboden Basin fill. The radiolarian assemblages of the time span Late Callovian to Middle Oxfordian do not provide an age resolution, which would be necessary for a biostratigraphic differentiation of these two individual successions of the western Fludergraben valley. Clearly visible are the different lithofacies of the radiolarites on both sides of the tectonic contact though.

2.3.2. Central Tauglboden Basin - Salzburg Calcareous Alps; Tauglboden valley

The central part of the Tauglboden Basin is preserved in its type area, the Tauglboden valley in the Salzburg Calcareous Alps (Fig. 7, Fig. 8). In the Tauglboden valley, geographically situated in the central to southern Osterhorn Mountains (Fig. 7), a complete late Early Jurassic to Late Jurassic sedimentary sequence is preserved. This area was intensively investigated since the second half of the 19th century (Suess & Mojsiscovics 1868) (Fig. 62). As almost everywhere in the Northern Calcareous Alps, the carbonate successions, especially the Jurassic ones, were fairly well dated by means of ammonites already since that time (summarized in Böhm 1992). In contrast, the age of the cherty sediments remained generally enigmatic until recently. In the second half of the 20th century the radiolarites were attributed to the Oxfordian, maybe reaching the Kimmeridgian (Diersche 1980, Tollmann 1985). Detailed radiolarian dating since the end of the last century (Gawlick &Suzuki 1999) constrained the biostratigraphic ages of the radiolarite sequences in numerous areas of the Northern Calcareous Alps (for latest review see Gawlick et al. 2009a).

The sedimentology of the Tauglboden sequence and especially the sedimentological features of the different mass movements and breccia intercalations in the type area were investigated in detail by Max and Wolfgang Schlager (summarized in Schlager & Schlager 1969, 1973), and in a more regional context by Diersche (1980). The age of the succession was attributed to the (Late) Oxfordian and Kimmeridgian on the basis of the investigations of Schlager & Schlager (1969) and Huckriede (1971). Huckriede (1971) dated the underlying sediments of the radiolarite by means of aptychi as early Oxfordian. Schlager & Schlager (1969) mentioned the finding of a Kimmeridgian ammonite. Therefore, as elsewhere, the age of radiolarite deposition in the Northern Calcareous Alps was attributed to the Oxfordian (-Kimmeridgian).

Detailed component analyses and direct datings of the radiolaritic matrix sediments of various mass-flow deposits were carried out since the end of the last century (for latest review see Gawlick et al. 2009). The new data resulted in a modified view of the situation of the Tauglboden Basin type-locality.

Stop 1: Base of the basin fill, Urban valley

Where the Urban valley approaches the Taugl valley, the contact between the Early to Middle Jurassic red nodular limestones and the overlying radiolarite sequence is exposed. The age of the red nodular limestones is Late Bathonian to Early Callovian according to Huckriede (1971) and Böhm (1992). On top of the red nodular limestone, a condensed layer contains rhyncholiths of Oxfordian age (Huckriede 1971). On the basis of that,

Fig. 61: Microfacies of components of the coarse-grained turbidites intercalated in cherty sediments. Sample from the old quarry in the area of the western Knerzenalm area (Stop IV in Fig. 11). After Gawlick et al. (2010). Page 245.
1. Different, mostly angular clasts of lagoonal Dachstein Limestone and some micritic clasts of the Kössen Formation. Between the components a dark-grey radiolarian-rich cherty matrix occurs; most radiolarians are recrystallized. Sample D 6-1. Width of photo: 1.4 cm. **2**. Most of the components are Kössen Formation wackestones containing fine-grained biodetritus. Clasts of the Rhaetian lagoonal Dachstein Limestone are rare. Sample D 6-2. Width of photo: 1.4 cm. **3**. A radiolarian-rich matrix fills the space between the components (Rhaetian lagoonal Dachstein Limestone and clasts of the Kössen Formation). The radiolarians are recrystallized and partly deformed. Sample D 6-3. Width of photo: 0.5 cm. **4**. Polymictic breccia with a cherty matrix. The relatively small components mostly consist of Kössen Formation,. Sample D 6-4. Width of photo: 1.4 cm. **5**. Polymictic breccia with relatively small components in a cherty matrix. Beside components of the Kössen Formation, components of the Rhaetian lagoonal Dachstein Limestone are common. The radiolarians are partly well preserved and filled with clay. Sample D 6-5. Width of photo: 1.4 cm. **6**. Polymictic breccia with crinoid-rich Dachstein Limestone components (uppermost part of photo) and radiolarite components. The radiolarite components derive from the underlying radiolarite sequence. They were incorporated in the debris flow before their complete lithification. Sample D 7-3. Width of photo: 1.4 cm. **7**. In addition to the dominating Late Triassic clasts there are rare Early Jurassic clasts. The spicula-rich clasts derive from the Kendlbach or Scheibelberg Formation. The red foraminifera-rich wacke- to packstones derive from the Adnet Formation. Sample D 9-3. Width of photo: 1.4 cm. **8**. Bioturbated dark-grey cherty limestone of the matrix. The radiolarians are partly well preserved and filled with clay. Sample D 12-1. Width of photo: 1.4 cm.

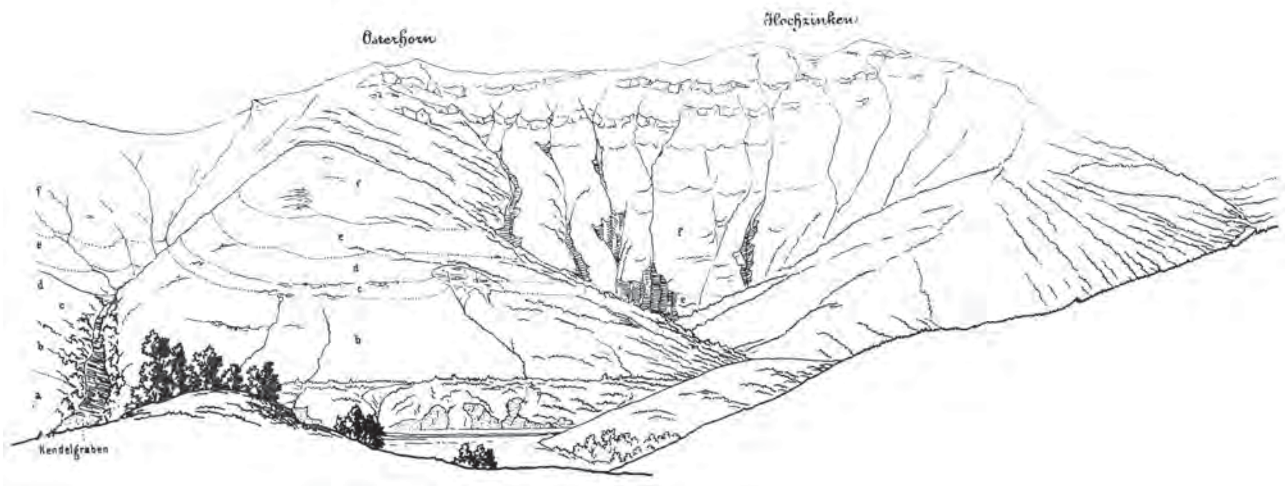

Fig. 62: Original drawing of the central Osterhorn Mountains from Suess & Mojsiscovics (1868). The schematic NW-SE cross-section by and large also applies to the situation of the Tauglboden valley. These authors worked out the main characteristics and the ages of the Late Triassic to Late Jurassic sedimentary succession (see translation of the original legend below).
Legend according to these authors (translated): a - Norian limestones; b - Rhaetian sequence (Kössen Formation and Dachstein Limestone); c - Lower Jurassic and Adnet Limestone (= grey cherty limestones and red nodular limestones); d - bioturbated cherty limestones and marls (“Fleckenmergel“); e - Brown Jurassic (Middle Jurassic); f - White Jurassic (Upper Jurassic). In today´s terms, d and e correspond to the Oxfordian to Early Tithonian Tauglboden Formation, f to the late Early Tithonian to Berriasian Oberalm Formation + Barmstein Limestone.

radiolarite deposition commenced in this section more or less contemporaneously or slightly later than in the Fludergraben valley in the Salzkammergut area. The radiolarian fauna from the overlying red radiolarite is identical with those found in the Fludergraben valley samples.
The microfacies of the upper part of the red nodular limestone correspond to that of the overlying red radiolarite: Radiolarian wacke- to packstones predominate. Therefore this part of the section, where Huckriede (1971) found the rhyncholiths of Oxfordian age, belongs already to the radiolarite succession. The radiolarian fauna of these cherty limestones is identical with the radiolarian fauna of the overlying radiolarite. The latter is well-bedded, of red colour and at maximum 2 metres thick. Radiolarians from these red radiolarites yielded an Early to Middle Oxfordian age (Gawlick 2000a). The radiolarian associations are similar to the radiolarian associations of the grey laminated radiolarites higher in the section. Both the lithology and the colour of the radiolarites change gradually. The radiolarites turn from red over reddish grey and medium grey to finally dark-grey colours. The grey radiolarites are fine laminated. The clay content increases upsection and several few centimetres thick clay layers are intercalated between the radiolarite beds (Fig. 65). The carbonate content increases as well. Similar to the Fludergraben section in the Salzkammergut area, the first resediments occur after the colour change. The overall component spectrum of these fine-grained turbidites is identical to the one described in the Fludergraben section.

Stop 2: Tauglboden road in the Taugl valley
Early Oxfordian mass-flow intercalations in radiolarites

About five metres above the contact between the red nodular limestone and the radiolarite succession, the first coarse-grained mass-flow deposits are intercalated in the radiolarite sequence. The up to 20 cm thick breccia layers overlie the radiolarite beds practically without basal erosion; obviously the breccia layers show the characteristics of channels deposits (Fig. 66A). Below the breccia layers a layer of green volcanic ash is locally preserved (Fig. 66B).
The components in the mass-flow deposit derive exclusively from the lagoonal Dachstein facies zone. Components of the Early Rhaetian Kössen Formation are rare whilst components of Rhaetian lagoonal Dachstein Limestone strongly predominate. Early to Middle Jurassic clasts occur in rock-forming quantities, too. Early Jurassic grey cherty limestones (Scheibelberg Formation), chert nodules and red nodular limestones (Adnet Formation) dominate. In contrast, Middle Jurassic *Bositra* Limestone components are seldom (Fig. 67, Fig. 68).

Stop 3: Outcrops along the forest road Kesselstrasse
Oxfordian mass-flow deposits and radiolarites, Kimmeridgian radiolarites

A strongly variable outcrop situation is met on the walk along the forest road Kesselstrasse. In a small valley beside the forest road and along the forest road there are some good outcrops giving an insight into the early phase of the Tauglboden Basin evolution. The age of the succession

Fig. 63: “Standard profile“ of the Tauglboden Formation in the type area (idealized type section - see SCHLAGER & SCHLAGER 1973 for details), the central Osterhorn Mountains in the Salzburg Calcareous Alps. Unpublished data of M. & W. SCHLAGER. Redrawn and printed with permission of W. SCHLAGER (Amsterdam) in GAWLICK (2000a) and GAWLICK & FRISCH (2003). Ages of the different parts of the section according to HUCKRIEDE (1971), GAWLICK et al. (1999b), GAWLICK & FRISCH (2003), and unpublished data.

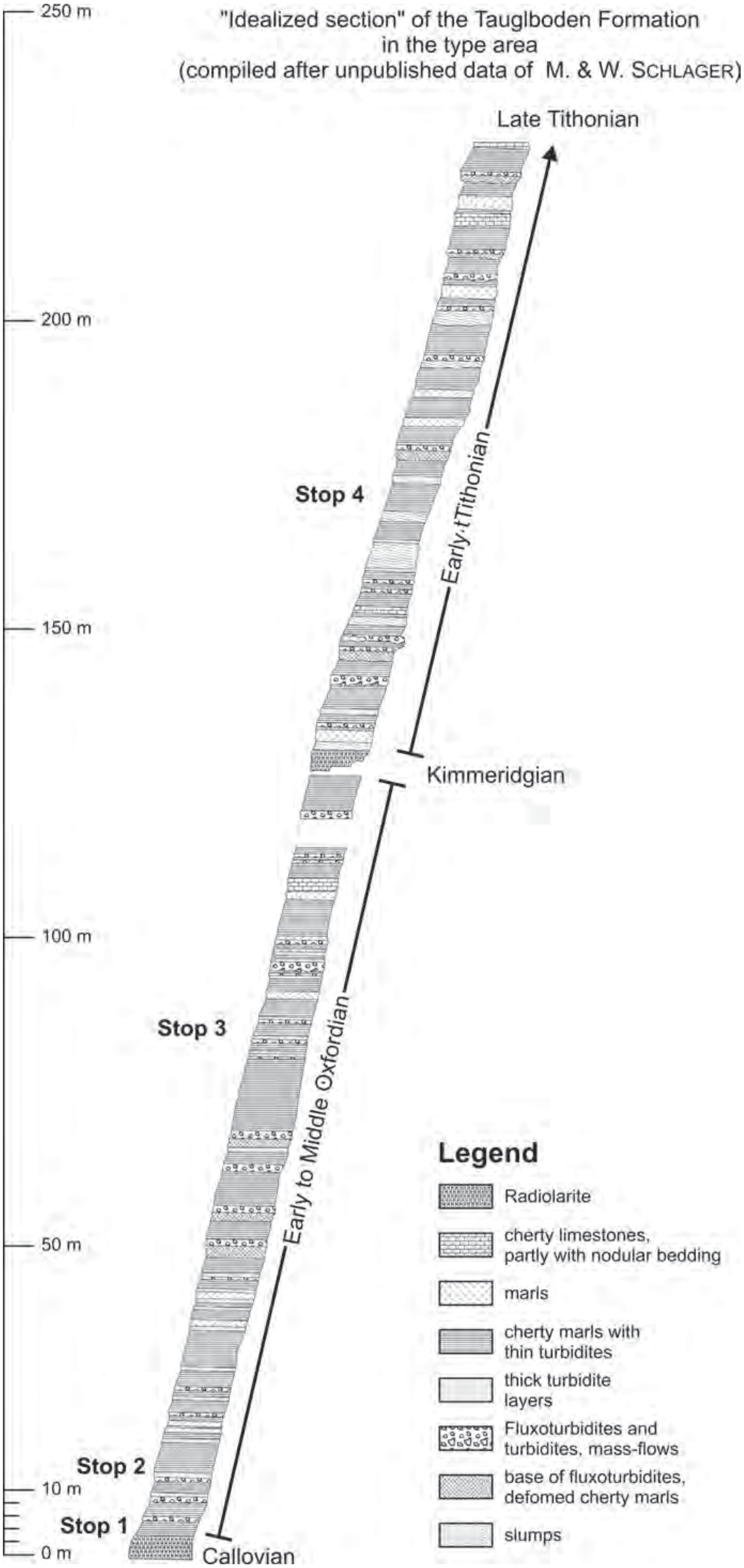

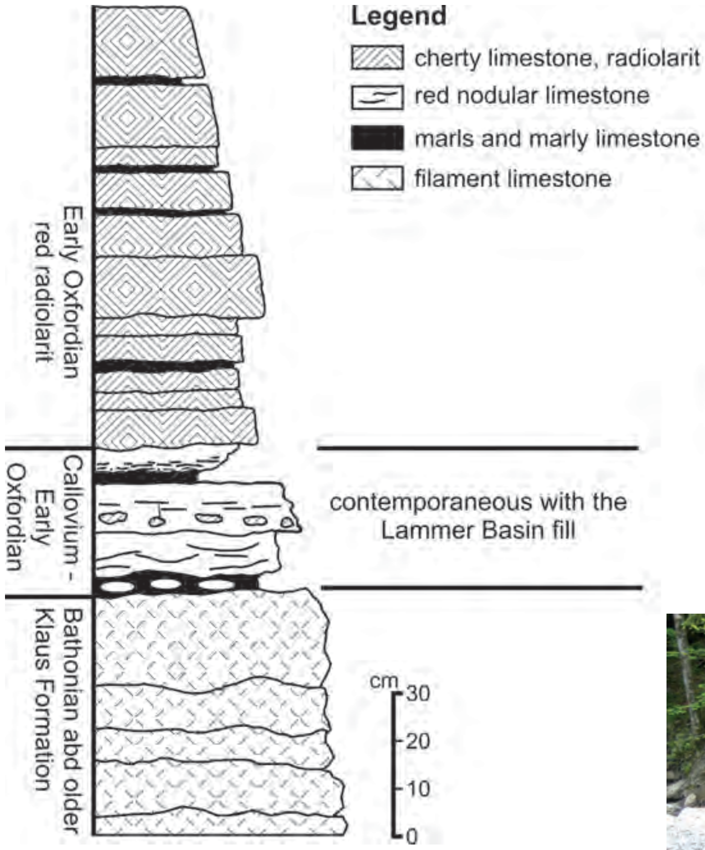

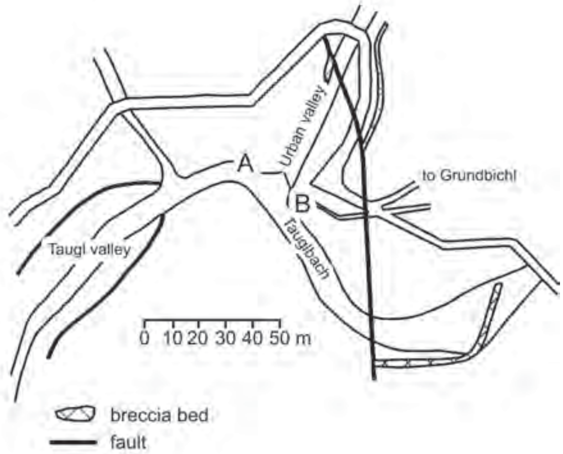

Fig. 64: Area of the Urban creek/Taugl creek in the central Salzburg Calcareous Alps, exposing excellent sections of the succession around the boundary Klaus Formation/ radiolarite (Tauglboden Formation) in the. The drawn detailed section is from west of the Urban valley (A). An equivalent section is seen east of the Urban creek (B). Redrawn after HUCKRIEDE (1971)

along the road is still Early to Middle Oxfordian as proven by radiolarians. Dark grey to black laminated radiolarites with changing clay content, slump deposits and mass flows are the typical sedimentary features of the succession (Fig. 68). The slump deposits consist partly of cherty sediments without older components, large blocks of older components incorporated in the argillaceous matrix, and debris flows. Generally, the older clasts are the same as in the basal breccia layers along the Taugl road, but Jurassic clasts are both smaller in number and older in age. The erosion cut into the Norian lagoonal Dachstein Limestone.

Fig. 65: Reddish-grey massive and laminated Early Oxfordian radiolarite layers with clay intercalations. Taugl valley. Width of the photo: 50 cm.

Stop 4: Forest road to the waterfall Kesselstrasse and waterfall

Tithonian mass-flow deposits in an argillaceous matrix

In the curve before the waterfall, a only few metres thick succession of dark grey to black radiolarites to cherty limestones free of mass flows intercalations occurs on top of the amalgamated sequence. The radiolarites from this amalgamated series below yielded still an Early to Middle Oxfordian age. Thus the whole around 200 metre thick sequence is Early to Middle Oxfordian in age.

Above this radiolarite succession again a thick radiolarite sequence with slumps and mass flows occur along the way. Here, several metres above this mass flow free radiolarites, some layers of volcanic ashes (metabentonites - GAWLICK

Fig. 66: **A**) Up to 20 cm thick breccia layers intercalated in the Early Oxfordian radiolarite sequence. In some cases the breccias cut slightly into the basal series (erosional contact), but more often they overlie the radiolarite sequence concordantly in a parallel manner. **B**) Detail from A. Below the breccia layers a green layer of volcanic ashes is preserved. These fine-grained ashes might have acted as slide horizon for the mass flows.

et al. 1999b) of ten centimetres thickness are intercalated in the sequence. Radiolarians from these volcanic ash layers yielded an Early Tithonian age (Gawlick et al. 1999b). This means, that the time span Latest Oxfordian to Early Tithonian is characterized by a starved sequence. The volume of material shed into the basin decreased rapidly in the Late Oxfordian. In comparison, the Kimmeridgian was characterized by radiolarite deposition.

Fig. 67: Angular to subrounded (rare) components of the Early to Middle Oxfordian mass-flow deposit Taugl road. See text for explanation.

Later, in the Early Tithonian, a new depositional cycle with mobilisation and redeposition of large volumes of rocks started. The series again is characterized by slump deposits, mud and debris flows. Whereas the older components in the different chaotic deposits were still the same as in the Early to Middle Oxfordian sequence, the content of Jurassic clasts was very low. Reworked Norian to Rhaetian clasts are dominating the component spectrum. Radiolarites in this part of the succession are scarce, with cherty marls and cherty limestones being the typical matrix sediment. The preservation quality of the radiolarians in these matrix rocks is generally very bad.

By reaching the waterfall we will see a several tens of metres thick sequence of dark-grey well bedded cherty marls and cherty limestones, intercalated by several slump deposits, mud flows and debris flows. The series is also characterized by the intercalation of semi-consolidated volcanic ash layers.

Stop 5: Forest road above the waterfall Kesselstrasse
Resediments from the Plassen Carbonate Platform

Following the forest road we reach the Late Tithonian sequence. The forest road provides several outcrops where different fine- und coarse-grained turbidites are intercalated in cherty limestones. The components in these turbidites consist of a mixture of older carbonate clasts (Norian to Rhaetian lagoonal Dachstein Limestone and Kössen Formation), like in the series below, and some contemporaneous shallow-water clasts from the Plassen Carbonate Platform to the south. The change from siliceous to calcareous sedimentation cannot be exactly dated, because the radiolarians in the matrix sediments are recrystallized and shallow-water organisms in the mass flows are scarce. The overlying cherty limestones with intercalated slope sediments (Barmstein Limestone: see chapter 2.4) are of Late Tithonian to Early Berriasian age, palaeontologically proven by radiolarians and calpionellids (e.g., Steiger 1981, 1992) as well as shallow-water

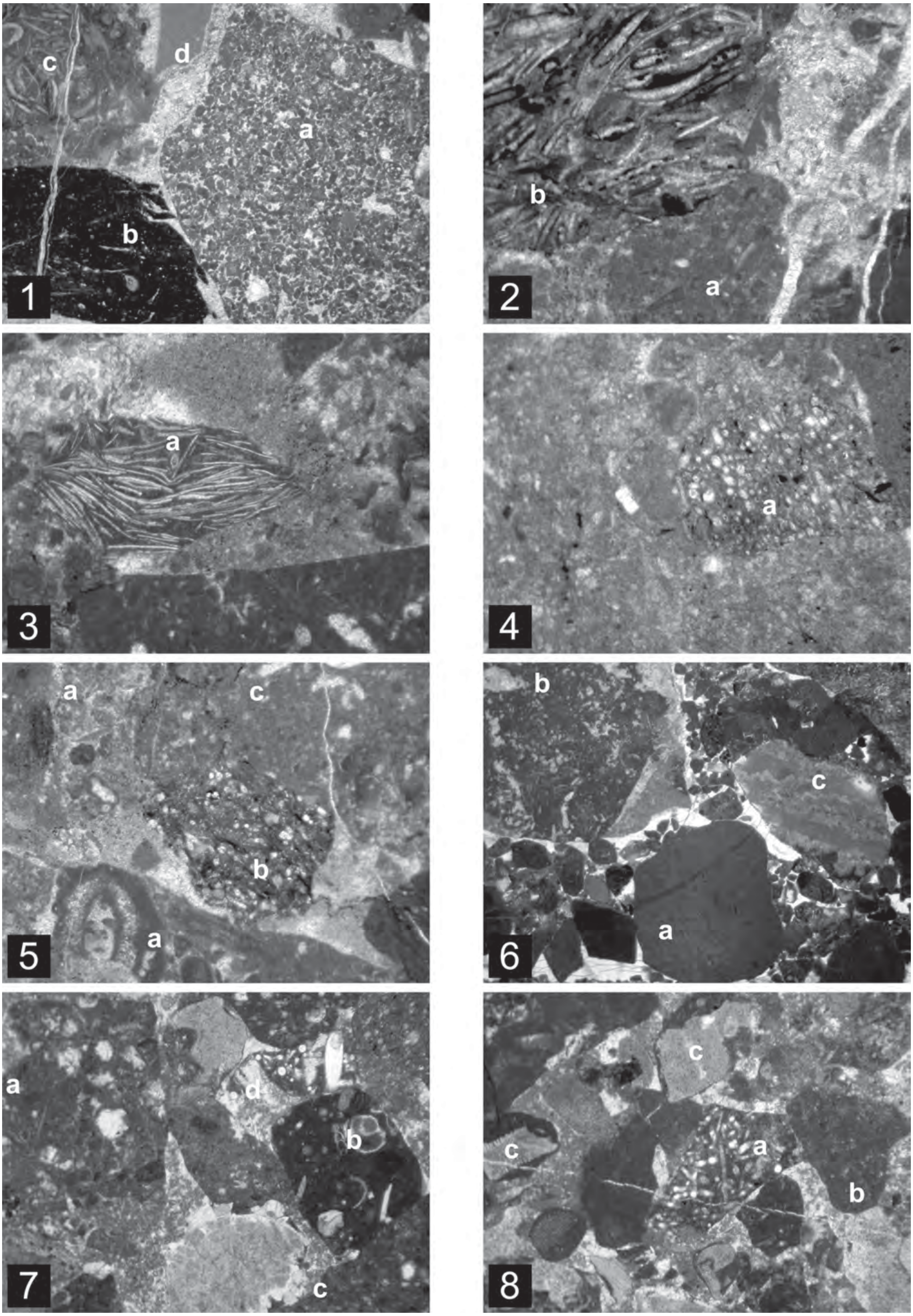
1 a b c d
2 a b
3 a
4 a
5 a b c a
6 a b c
7 a b c d
8 a b c c

Fig. 68: Microfacies of different clasts in the mass-flow deposits along the Tauglboden road in the Taugl valley (lower Tauglboden Formation, Early Oxfordian). After GAWLICK & FRISCH (2003). Page 251.
1. Components from a 60 cm thick mass-flow deposit in the middle part of the section Kesselstrasse. As components occur late Triassic lagoonal Dachstein limestone (a), Early and Middle Jurassic clasts of the Adnet (b) and Klaus Formations (c) and wackestones from the Kössen Formation (d) (sample TB 6/1998). Width of photo: 1.4 cm. **2**. Components from a 60 cm thick mass-flow deposit in the middle part of the section Kesselstrasse. As components occur micritic lagoonal Dachstein limestone (a) and filament rich cherty sediments (b) of the higher parts of the Strubberg Formation (sample TB 6a/1998). Width of photo: 0.5 cm. **3**. Components from a 60 cm thick mass-flow deposit in the middle part of the section Kesselstrasse with a filamentrich clast of Middle Jurassic *Bositra* limestone (a) (sample TBG 2/1998). Width of photo: 0.5 cm. **4**. Components from a 30 cm thick mass-flow deposit in the middle part of the section Kesselstreet. Right side: clast of cherty marl of the distal Strubberg Formation (a) (sample TB 8/1998). Width of photo: 0.5 cm. **5**. Components from a 30 cm thick mass-flow deposit in the middle part of the section Kesselstrasse. Components: lagoonal Dachstein limestone (a), cherty sediments of distal Strubberg Formation (b), Liassic wackestones (c) (sample TBG 3/1998). Width of photo: 0.5 cm. **6**. Components from a 30 cm thick mass-flow deposit in the middle part of the section Kesselstrasse. Components: Kössen beds (a, micrites), Dachstein limestone (b), ?Hauptdolomit or loferitic Dachstein limestone (c) (sample TB 8/1998). Width of photo: 1.4 cm.
7. Components from a 40 cm thick mass-flow deposit from the base of the Tauglboden Formation (Urbangraben). Components: Lagoonal Dachstein Limestone (a), Adnet limestone (b), Kössen beds (c) and radiolarite (d) (sample TBG 3/1997-3). Width of photo: 0.5 cm. **8**. Components from a 40 cm thick mass-flow deposit from the base of the Tauglboden Formation (Urbangraben). Components: radiolarite (a), Kössen beds (b) and encrusted crinoids (c) in the matrix (sample TBG 3/1997-1). Width of photo: 0.5 cm.

organisms (GAWLICK et al. 2005, 2009a for latest reviews). In the area of the Osterhorn Block, the overlying series of cherty limestones with intercalated mass flows (Late Tithonian to earliest Cretaceous Oberalm Formation + Barmstein Limestone; Fig. 5) reaches around 800 metres in thickness (Fig. 74). The Late Tithonian to Berriasian sedimentary succession lies flat above the Tauglboden Basin fill, sealing the older tectonic structures (Fig. 74).

2.3.3. Northern Tauglboden Basin - Salzburg Calcareous Alps

In the northern part of the Tauglboden Basin (Fig. 7B), the thickness of radiolarite deposits does not exceed several tens of metres. Radiolarite deposition followed after a stratigraphic gap on top of red nodular limestones. The basal black massive radiolarites are Callovian in age. A thin-bedded series of red radiolarite of ?Callovian to Early Oxfordian age follows above the black radiolarites,. In this area, these red radiolarites reach thicknesses of 12-15 metres. Upsection, the colour of the massive radiolarite changes from reddish to greyish. The grey coloured radiolarite is fine laminated. First very fine-grained carbonate turbidites are intercalated in the succession. The age of these red radiolarites is still Early to Middle Oxfordian. Higher up, some coarser grained turbidites are intercalated. The component spectrum is identical with the one observed in the central Tauglboden area to the south (see description above). After some tens of metres, the first calcareous resediments from the Plassen Carbo-

Fig. 69: Early to Middle Oxfordian mud flow with large boulders of Late Triassic lagoonal Dachstein Limestone on top of well-bedded grey laminated radiolarites. Kesselstrasse forest road, Taugl valley.

Fig. 70: Components in the Early to Middle Oxfordian mud flow: Subrounded clasts of the Early Rhaetian Kössen Formation and Norian-Rhaetian lagoonal Dachstein Limestone. The matrix consists of marly clays without radiolarians.

Fig. 71: Early Tithonian sedimentary succession with slump deposits, mud flows and debris flows in a matrix of cherty marls and cherty limestones. Waterfall Kesselstrasse, Taugl valley.

Fig. 72: Amalgamated series of cherty marls with breccia layers, overlain by parallel bedded laminated cherty limestones with marl intercalations. Intercalated breccia layers with erosive base. Waterfall Kesselstrasse, Taugl valley.

Fig. 74: Late Tithonian flat lying sedimentary succession of cherty limestones (Oberalm Formation) with intercalations of up to ten metres thick carbonate mass-flow deposits (Barmstein Limestone) consisting of reworked shallow-water material from the Plassen Carbonate Platform. This up to 800 m thick succession overlies the radiolaritic Tauglboden Basin fill (compare Fig. 62).

nate Platform occur, overall reaching several hundred metres thickness in this area.

The evolution of the northernmost part of the Tauglboden Basin was influenced by the establishment of a new nappe front in Late Oxfordian time - the Brunnwinkl Rise (Fig. 7) (GAWLICK et al. 2007b for details). This uplift gave rise to several mass movements affecting the northernmost part of the Tauglboden Basin in a later stadium of the basin evolution. In the Early to Middle Oxfordian, however, only a thin radiolarite succession was deposited (KÜGLER et al. 2003). Contemporaneous to the large-scale mass movements into the southern and central Tauglboden Basin, pure radiolarite sedimentation without any turbidites or mass flows prevailed in the northernmost area.

Fig. 73: Microfacies of the different Late Tithonian calcareous turbidites and coarse-grained mass-flow deposits in the transitional part from the Tauglboden Formation to the Oberalm Formation. Page 254.

1. Graded carbonate turbidite intercalated in cherty limestones with recrystallized radiolarians. Crinoids, micrite clasts and clasts with micritic envelopes characterize the onset of the northern Plassen Carbonate Platform. Older clasts (mainly Late Triassic lagoonal Dachstein Limestone and Early Jurassic clasts) are rare. Sample B 367. Width of photo: 1.4 cm. **2**. Sample B 367, other view. In the lower, coarser-grained part of the turbidite a similar component spectrum is visible. Reef organism and other determable organisms of the Plassen Carbonate Platform are missing. Width of photo: 1.4 cm. **3**. Basal part of a carbonate turbidite above a grey radiolarian-rich cherty limestone. The cherty limestone clast, rich in spicules derive from an Early Jurassic basinal limestone, the shallow-water carbonate clasts are Rhaetian lagoonal Dachstein Limestone clasts. Sample B 371. Width of photo: 1.4 cm. **4**. Coarse-grained carbonate turbidite with several Late Triassic lagoonal Dachstein Limestone clasts and an oncolith from the Plassen Carbonate Platform. Sample B 371-1. Width of photo: 1.4 cm. **5**. Isolated lagoonal Dachstein Limestone clast (Rhaetian) in a radiolarian-rich biomicite. Sample B 376. Width of photo: 1.4 cm. **6**. Coarse-grained carbonate turbidite with several Late Triassic lagoonal Dachstein Limestone clasts, e.g. with Triasina. The radiolarian- and spicules-rich cherty limestone clast is of Early Jurassic age. Sample B 371-3. Width of photo: 1.4 cm. **7**. Finer-grained carbonate turbidite in a matrix of radiolarian packstone. Incrusted shells and micrite clasts are the dominant component. Sample B 373-2. Width of photo: 0.5 cm. **8**. Coarse-grained carbonate tuirbidite with several black pebble clasts, micrite clasts and Dachstein Limestone clasts. Sample B 374. Width of photo: 1.4 cm.

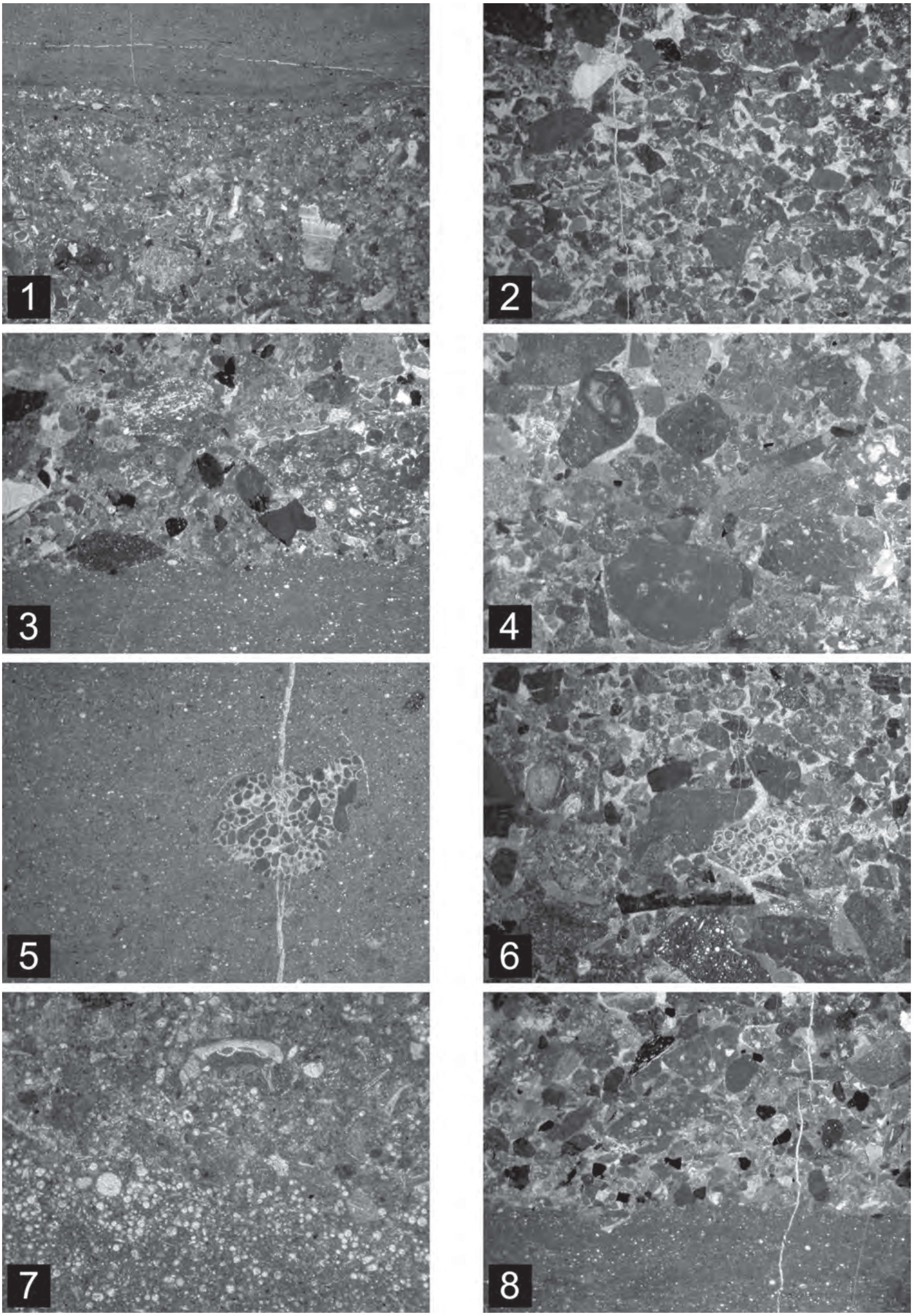
1
2
3
4
5
6
7
8

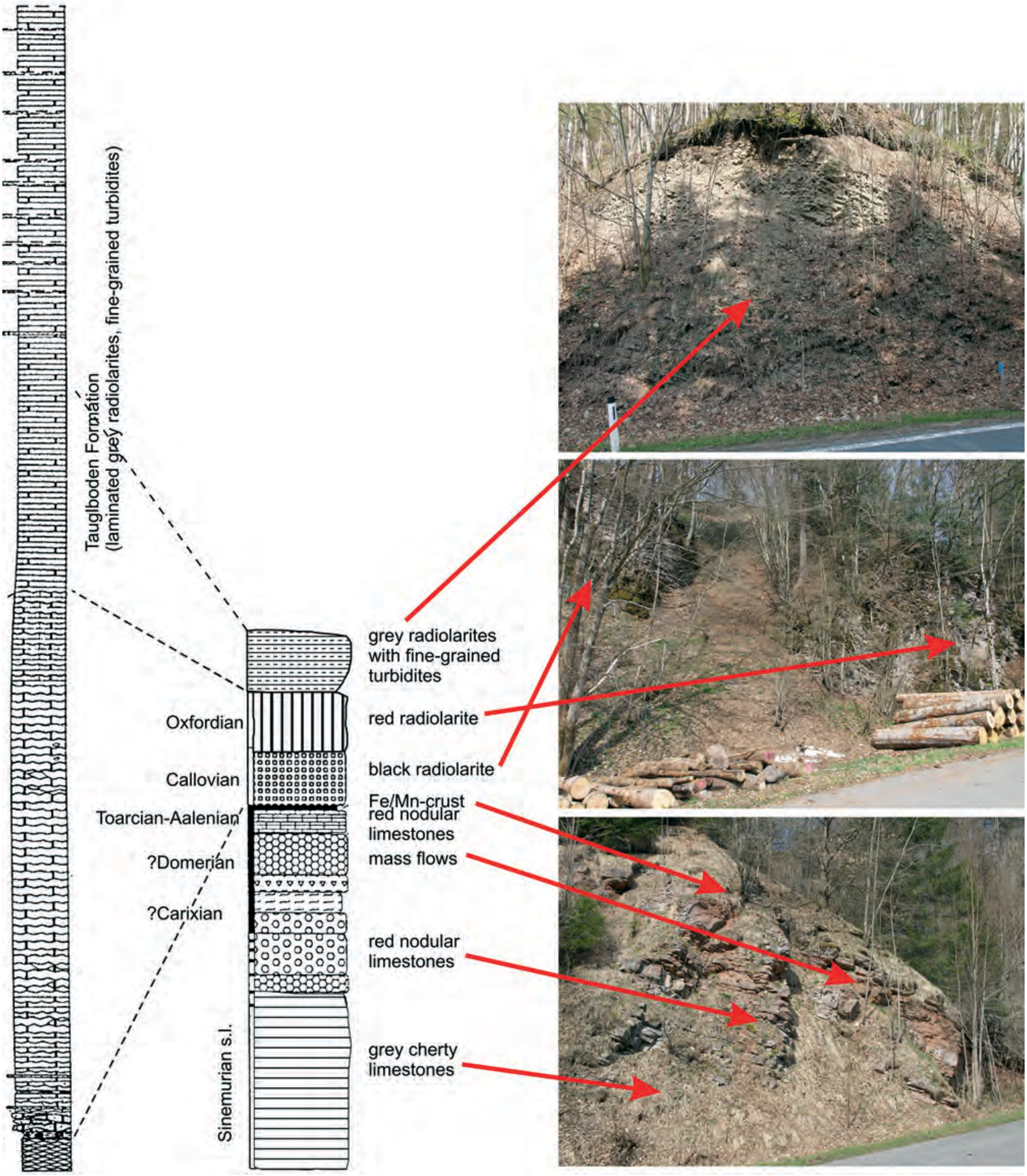

Fig. 75: Stratigraphy and facies of the Early to early Late Jurassic section along the road to the village Krispl in the Mörtlbach valley. Right section with photographs after Böhm (1992), modified and completed for the Callovian-Oxfordian part. Left section from Diersche (1980).

Stop 1: Parking place on the road to Krispl/Mörtlbach valley
Early to Late Jurassic sedimentary sequence, northern Tauglboden Basin

The section starts with grey cherty limestones of Sinemurian to Early Pliensbachian age. The thickness of this sequence does not exceed 5 metres. These grey cherty limestones are overlain by reworked red nodular limestones forming a series of mass-flow deposits. This interval is rich in red marls making up the matrix of the different mass flows. The age of this interval is Late Pliensbachian to Toarcian. The lower Middle Jurassic (Aalenian) is preserved in the form of a very thin layer of *Bositra*-rich marly limestones. On top of these Aalenian sedimentary rocks, a ferro-manganese horizon reflects a long lasting depositional gap (Bajocian to Bathonian). Above, a black massive radiolarite of Callovian age was deposited. The thickness of the black radiolarite is about 1 metre. It changes colour upsection into a reddish radiolarite. The age of the more than 15 metres thick red radiolarite is Late Callovian to Oxfordian, most probably earliest Oxfordian according to radiolarian associations. Still in the Early to Middle Oxfordian the red radiolarite passed into dark-grey radiolarites and cherty limestones. The radiolarites of this part of the section are laminated and contain the first fine-grained turbidites. The clasts are too small to be determined regarding their stratigraphic affiliation. Upsection the turbidites become coarse-grained. The components mainly consist of Late Triassic lagoonal Dachstein Limestone, whilst Early to Middle Jurassic clasts occur only seldom. This component spectrum is identical to that of the Tauglboden valley resediments in the south. So is the age of the radiolarian rich background sediment: Early to Middle Oxfordian. In contrast to the thick succession in the Tauglboden valley, the thickness of the northern Tauglboden Basin succession does not exceed a few tens of metres (details in DIERSCHE 1980) with a maximal thickness of the intercalated mass flows of only 10-20 centimetres.

The components in the different turbiditic layers exclusively derive from the lagoonal Dachstein Limestone facies zone. The component spectrum is identical with the one known from the Taugl valley to the south.

2.4. Sillenkopf Basin: exotic material and resediments from the Plassen Carbonate Platform (optional)

The Sillenkopf Basin was palaeogeographically situated between the Plassen Carbonate Platform *s. str.* to the north and the Lärchberg Carbonate Platform to the south (Fig. 7, Fig. 78). The isolated Sillenkopf Formation outcrops are located in the southern Berchtesgaden Alps and southern Salzburg Calcareous Alps. The underlying radiolaritic sequences either belong to the Sandlingalm or the Lammer Basin fill. The Sillenkopf Basin contains turbidites and mass-flow deposits with various Late Triassic (probably also Middle Triassic) to Late Jurassic lithoclasts as well as siliciclastic-crystalline components (MISSONI et al. 2001a). Important is the occurrence of first detritus of ophiolitic rocks evidenced by detrital chromian spinels (MISSONI & GAWLICK 2011a). Therefore, this component spectrum is significantly different from that of the Tauglboden Basin. The Late Jurassic shallow-water litho- and bioclasts, e.g., the foraminifer *Labyrinthina mirabilis* WEYNSCHENK or the dasycladalean alga *Salpingoporella pygmaea* (GÜMBEL), derive from the Lärchberg Carbonate Platform located south of the Sillenkopf Basin. The age of the Sillenkopf Formation is Kimmeridgian to ?Tithonian as dated by radiolarians and resedimented larger benthic foraminifera and calcareous algae (MISSONI et al. 2001a). The Sillenkopf Formation type-locality is Mts. Sillenköpfe south of Berchtesgaden (Stop 1).

As outstanding characteristic of the Lärchberg Carbonate Platform, in contrast to the Plassen Carbonate Platform *s. str.*, an overall terrigenous input can be stated. This and the occurrence of brackish-water influence in the latest platform stadium, pointing to a final emersion, are assumed as reasons for the discrete inventory of dasycladalean algae including 10 taxa not known from the Plassen Carbonate Platform *s. str.* (SCHLAGINTWEIT 2011b). A characteristic larger benthic foraminifer of the final series exhibiting increasing terrigeneous influx is represented by *Anchispirocyclina lusitanica* (EGGER). This foraminifer was already recognized by HAHN (1910) who described and illustrated the foraminifer as "Hydrocorallinen (?)stöckchen", meaning a stromatoporoid sponge. These strata are referred to as Lofer Beds, originally believed to represent basal, transgressive clastics sediments. In contrast, nowadays this succession is interpreted as deposit of a final coarsening- and shallowing-upward phase that finally led to platform emersion. The facies evolution of the Lärchberg Carbonate Platform, however, is still not known in all details. This is mainly a result of the preservation of only a few, isolated small remnants of the

Fig. 76: Microfacies of the different cherty sediments and some coarse-grained turbiditic intercalations from the northern part of the Tauglboden Basin. Samples are from the section parking place on the road to Krispl/Mörtlbach valley and from the valley in the northwest (compare Fig. 75). Page 257.

1. Microfacies of the not laminated black radiolarite (Callovian). Radiolarian wacke- to packstone. Most radiolarians are recrystallized and occur as quartz. Sample GAI Schwarz. Width of photo: 0.5 cm. **2**. Microfacies of the not laminated red radiolarite (Oxfordian). Radiolarian wacke- to packstone. Most radiolarians are recrystallized and occur as quartz. Few radiolarians are well preserved. Sample GAI rot. Width of photo: 0.5 cm. **3**. Microfacies of the grey-red/violet radiolarite from the transition of the red radiolarite to the grey cherty limestones and radiolarites with intercalated fine-grained turbidites. Sample MOB rot. Width of photo: 0.5 cm. **4**. Microfacies of the grey laminated radiolarite to cherty limestone (base of Tauglboden Formation: Oxfordian). In the limestone layer (lower part of the photograph) the radiolarians are recrystallized to calcite. The radiolarians in the upper part of the photograph occur as quartz. Sample Gu 13a grau. Width of photo: 1.4 cm. **5**. Coarse-grained turbidite from the higher part of the succession. Beside some radiolarians, crinoids and spicules different micrite clasts occur. Sample C 205-1. Width of photo: 0.5 cm. **6**. Sample C 205-1, other view. Larger clast of a Rhaetian lagoonal Dachstein Limestone beside crinoids and micrite clasts. Width of photo: 0.5 cm. **7**. Graded turbidite. Crinoids and micrite clasts are common. Sample C 205-2. Width of photo: 1.4 cm. **8**. Fine-grainend graded carbonate turbidite. Most components cannot be identified any more. Sample C 203-3. Width of photo: 0.5 cm.

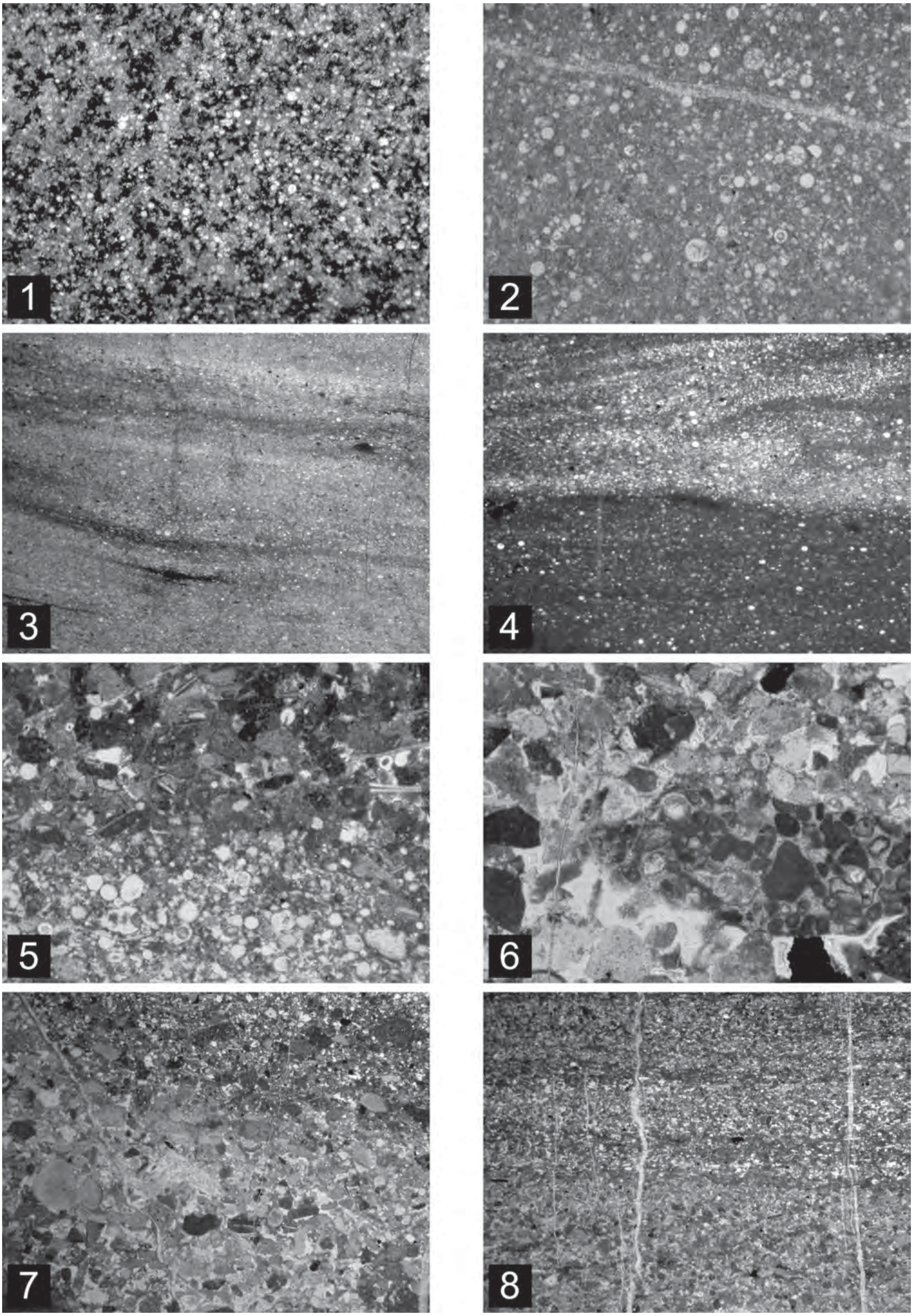
1
2
3
4
5
6
7
8

Lärchberg Platform. For illustrations of the microfacies types of the Lärchberg Carbonate Platform see DARGA & SCHLAGINTWEIT (1991), DYA (1992) and SANDERS et al. (2007).

Stop 1: Mts. Sillenköpfe
Kimmeridgian radiolarite and mass-flow deposits of mixed palaeogeographic derivation

Mts. Sillenköpfe in the southern Berchtesgaden Calcareous represent the type-locality of the Sillenkopf Formation and give an insight into the sedimentary succession of the Sillenkopf Basin. Other sections with generally coarser grained breccias and mass-flow deposits are located more to the south, i.e., nearer to the source area of the exotic clasts. Fig. 77 summarizes the characteristic features of these breccias from the nearby area and not only from the type-locality.
The section Sillenköpfe starts with laminated and well bedded Kimmeridgian radiolarites above clays of the Haselgebirge Mélange. Upsection the first coarse-grained turbidite intercalations quickly occur in the radiolarites. The whole succession shows a coarsening-upwards trend with several mass-flow deposits near the top of the mountain (details in MISSONI et al. 2001a, MISSONI & GAWLICK 2011a).

2.5. Plassen Carbonate Platform

In the Late Jurassic (since Late Oxfordian: AUER et al. 2009), three independent shallow-water carbonate platforms, which belong to the Plassen Carbonate Platform *sensu lato* (SCHLAGINTWEIT & GAWLICK 2007), were formed on rising nappe fronts (details in GAWLICK et al. 2009a) (compare Fig. 78):

a) the Trattberg Rise (Plassen Carbonate Platform *sensu stricto*) (SCHLAGINTWEIT et al. 2005),
b) the Brunnwinkl Rise (Wolfgangsee Carbonate Platform) (GAWLICK et al. 2007b), and
c) an as yet unnamed rise on top of the Hallstatt imbricates to the south (Lärchberg Carbonate Platform) (GAWLICK et al. 2009a). This resulted in a complex basin-and-rise topography with different types of sediments in shallow-water and deep-water areas (GAWLICK & SCHLAGINTWEIT 2006).

Around the Early/Late Tithonian boundary the original topography of the Trattberg Rise with the Plassen Carbonate Platform *s. str.* on top was modified by north-directed normal faulting (compare Fig. 100). The platform became an area of erosion, and a new steep reef rim facing the Tauglboden Basin was formed (GAWLICK & SCHLAGINTWEIT 2009) (compare Fig. 7). From the Late Tithonian onwards, the breakdown of the rises led to shedding of huge amounts of carbonate debris (Barmstein Limestone) and mud into the basins situated to the north (Fig. 78). These Barmstein Limestone redeposits consist of proximal reef debris with allochthonous components (PLÖCHINGER 1976, STEIGER 1981, GAWLICK et al. 2005). They occur as mass flows and turbiditic layers intercalated in a basinal succession (Oberalm Formation). The Barmstein Limestone contains not only components from the adjacent, contemporaneous Plassen Carbonate Platform but also older, reworked material from the Kimmeridgian to Early Tithonian Plassen Carbonate Platform *s. str.* (SCHLAGINTWEIT & GAWLICK 2007). We will visit several sedimentary successions which belong to the Plassen Carbonate Platform in the Salzburg Calcareous Alps and in the Salzkammergut area.

Fig. 77: Characteristic microfacies of different components in the mass-flow deposits of the Sillenkopf Formation in the southern Berchtesgaden Calcareous Alps (Upper Tirolic units, Steinernes Meer). Page 259.
1. Radiolarian wackestone to packstone erosively overlain by a calciturbidite (packstone); most components of these allodapic layers consist of micrite. Sample Ber 105/12, Gotzen(tal)-Alm, Steinernes Meer (Tirolic units, Berchtesgaden Calcareous Alps). Width of photo: 1.4 cm. **2**. Graded calciturbidite with several older clasts of the Pötschen Formation beside clasts from the Lärchberg Carbonate Platform. Sample Ber 31/4b, Sillenköpfe (Tirolic units, Berchtesgaden Calcareous Alps). Width of photo: 1.4 cm. **3**. Well-sorted calciturbidite (packstone). Beside the dominating components of the Lärchberg Carbonate Platform, clasts of the Pötschen Formation and evaporitic clasts, most probably of the Permian Alpine Haselgebirge, occur. Sample Ber 105/1b, Gotzen(tal) Alm, Steinernes Meer (Berchtesgaden Calcareous Alps). Width of photo: 1.4 cm. **4**. Breccia layer with a fine-laminated clast in which float several subangular extraclasts. There are fine-grained siliciclastic clasts and some gypsum clasts most probably from the Permian Alpine Haselgebirge. Sample Ber 105/14b, Gotzen(tal)-Alm, Steinernes Meer (Tirolic units, Berchtesgaden Calcareous Alps). Width of photo: 1.4 cm. **5**. Mass-flow deposit with densely packed litho- and bioclasts, e.g., silicified oncoids and stromatoporoids beside encrusted clasts, most probably derived from the Permian Alpine Haselgebirge. Sample Ber 60/15, Abwärtsgraben section, Steinernes Meer (Tirolic units, Berchtesgaden Calcareous Alps). Width of photo: 1.4 cm. **6**. Mass-flow deposit with *Labyrinthina mirabilis* WEYNSCHENK (L), *Salpingoporella annulata* CAROZZI (S) and *Pinnatiporidium* aff. *untersbergensis* SCHLAGINTWEIT & DRAGASTAN (P) from the Lärchberg Carbonate Platform. Beside these organisms, clasts of Pötschen Dolomite and encrusted evaporites (?Alpine Haselgebirge clasts) occur. Sample Ber 60/10, Abwärtsgraben section, Steinernes Meer (Tirolic units, Berchtesgaden Calcareous Alps). Width of photo: 0.5 cm. **7**. Benthic foraminifer *Labyrinthina mirabilis* WEYNSCHENK with unrolled adult part. Sample A 847, Mount Gerhardstein west of Lofer (Tirolic units, Salzburg Calcareous Alps). Width of photo: 0.5 cm. **8**. Benthic foraminifer *Kilianina*? *rahonensis* FOURY & VINCENT in a mixture of mostly undeterminable clasts of exotic character. Sample Ber 105/6c, Gotzen(tal)-Alm, Steinernes Meer (Tirolic units, Berchtesgaden Calcareous Alps). Width of photo: 0.5 cm.
For more microfacies details see, e.g., MISSONI et al. (2001a) and GAWLICK & FRISCH (2003).

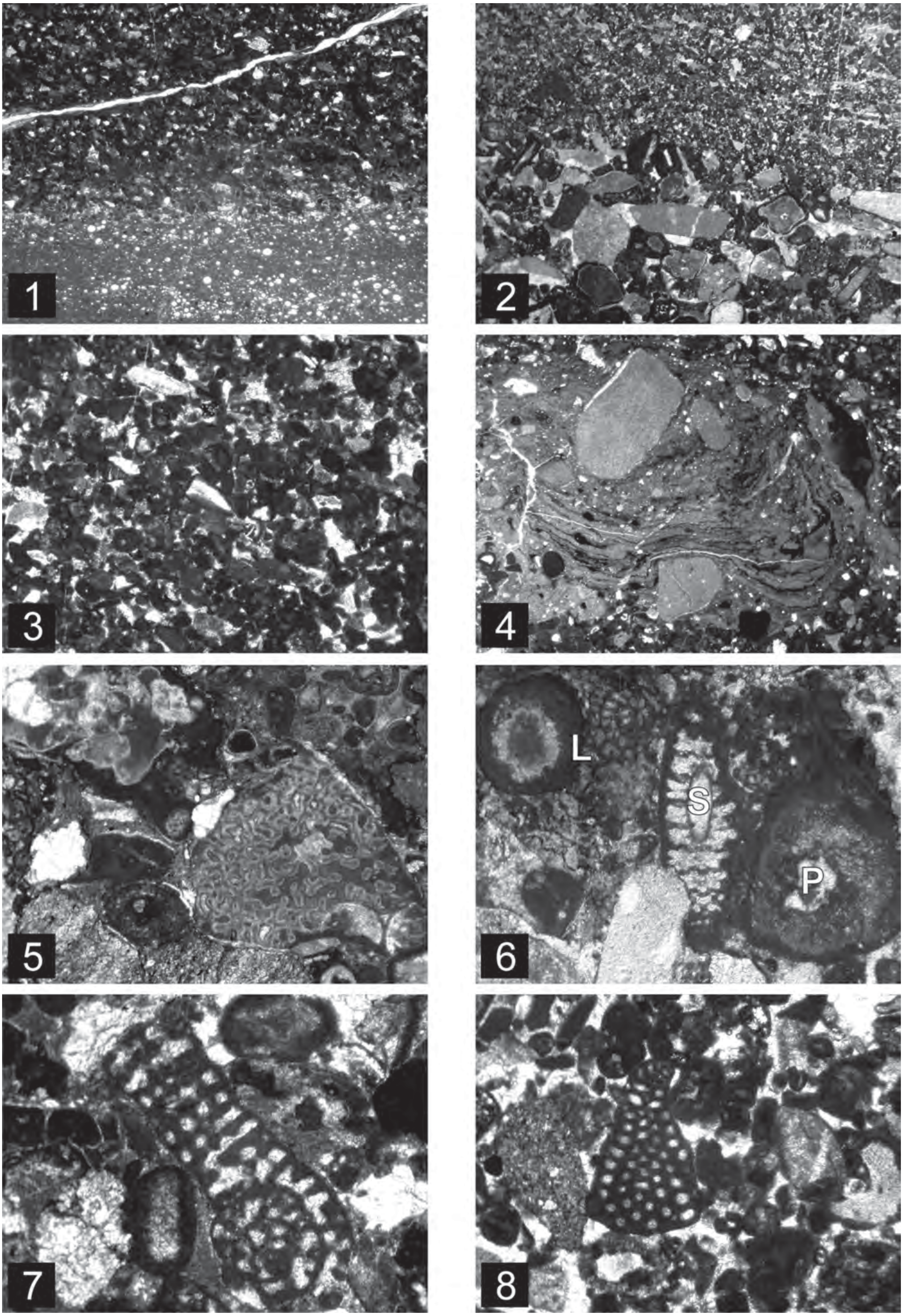
1
2
3
4
5
L
S
P
6
7
8

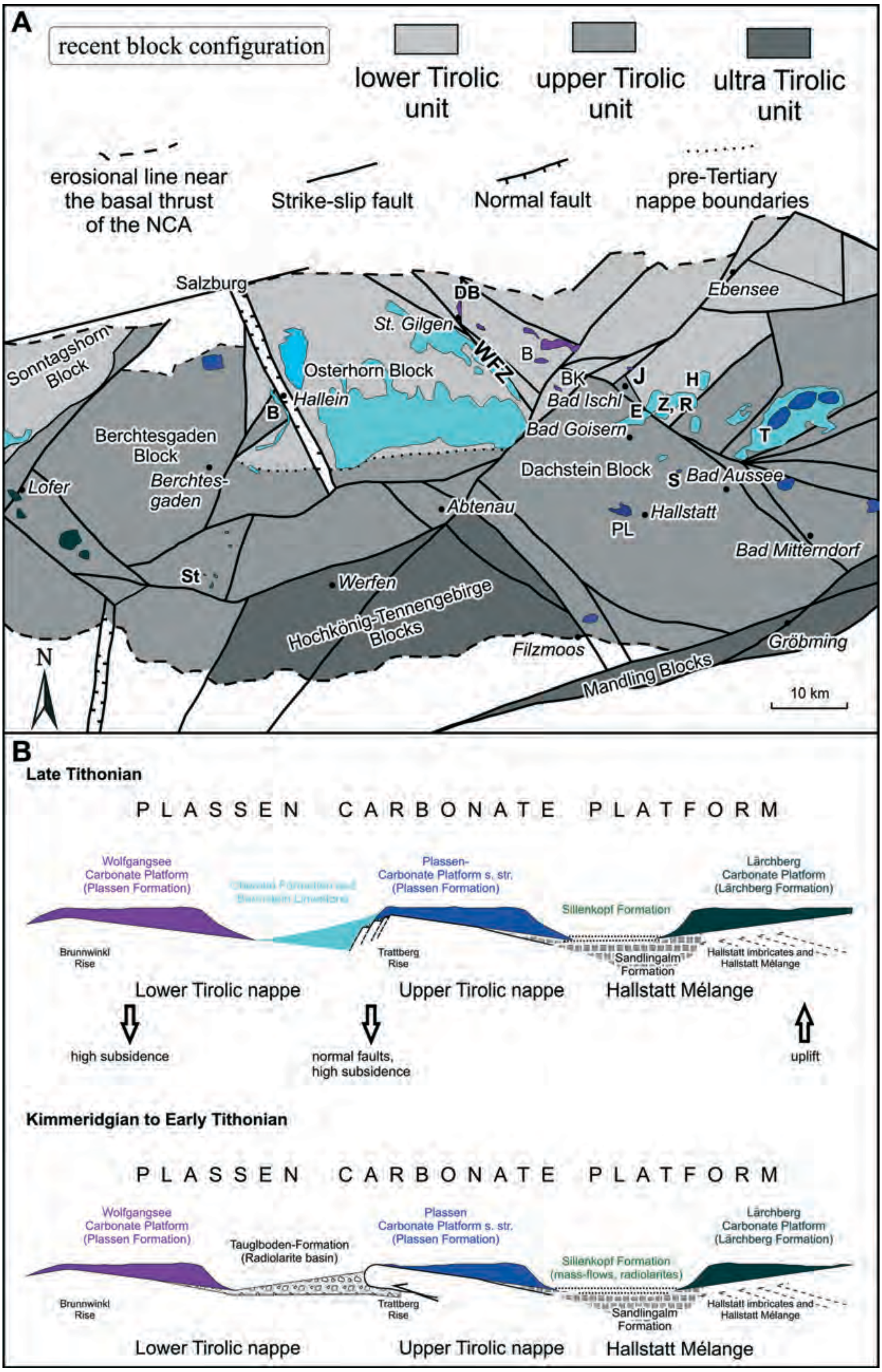

Fig. 78: General evolution and occurrences of the Late Jurassic platform carbonates and their resediments in the central Northern Calcareous Alps (after GAWLICK et al. 2009a). **A**. Occurrences of the platform sediments in the central Northern Calcareous Alps (map base: FRISCH & GAWLICK 2003). **B**. Kimmeridgian to Tithonian general evolution of the Plassen Carbonate Platform *s. l.* In the Late Tithonian the northern platform (Wolfgangsee Carbonate Platform) drowned, the central platform became dissected (Plassen Carbonate Platform *s. str.*) and the southern platform (Lärchberg Carbonate Platform) was uplifted.

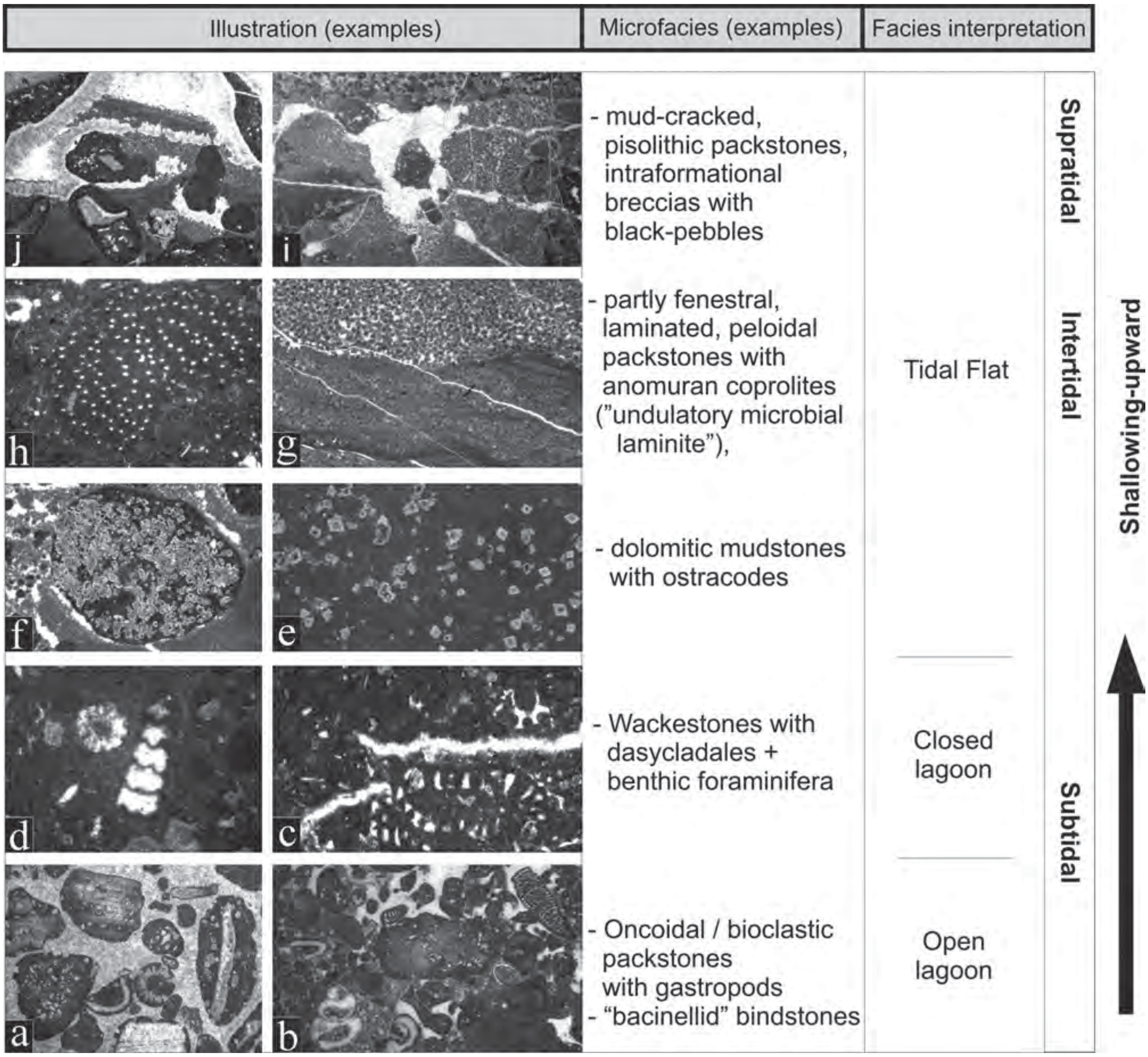

Fig. 79: Microfacies of the transgressive-regressive cycles of subtidal and peritidal carbonates (Late Kimmeridgian to Earliest Tithonian) of the southeastern part of Mount Plassen. The order of the shown examples (a-j; without scale) does not necessarily correlate with the appearance in the lithologic column. See text for explanation.

Fig. 80: Microfacies and facies interpretation of the Plassen Carbonate Platform *s. str.* (Early Kimmeridgian to earliest Tithonian) of Mount Plassen. From Schlagintweit et al. (2003), added. Page 262.

1. Packstone/Wackestone with debris of echinoids, protoglobigerinids (A) and resedimented *Protopeneroplis striata* Weynschenk 1950 (B). Slope facies. Sample Pl 4a-2001, scale bar = 1 mm. **2.** Packstone with remains of echinoids and *Crescentiella morronensis* (Crescenti). Slope facies. Sample A-37, scale bar = 0.5 mm. **3.** Packstone with *Crescentiella morronensis* (Crescenti) (C), echinoid debris, bryozoa (B) and resedimented fragment of *Labyrinthina mirabilis* Weynschenk (L). Slope facies. Sample Pl 6-2001, scale bar = 1 mm. **4.** Rudstone with remains of frame-builders and the benthic foraminifera *Labyrinthina mirabilis* Weynschenk. Platform margin facies. Sample A-41-2, scale bar = 2 mm. **5**. Grainstone with *Labyrinthina mirabilis* Weynschenk ("*Labyrinthina*-Limestone"). Platform margin facies. Sample Pl 9-2001, scale bar = 1 mm. **6.** Bioclastic biosparite with debris of corals, lituolid foraminifera and verticil fragments of *Clypeina jurassica* Favre. Back-reef facies. Sample Pl 10-2001, scale bar = 1 mm. **7.** Bioclastic packstone with gastropods (e.g. nerineids), "Rivulariaceans" (R) and *Labyrinthina mirabilis* Weynschenk (L). Backreef facies. Sample Q 99/2, Hohe Wasserstollen, scale bar = 2 mm. **8.** Algal-Bindstone with "bacinellid" crust and *Thaumatoporella parvovesiculifera* (Raineri). Tidal Flat facies. Sample Pl 63-b-2001, scale bar = 0.5 mm.

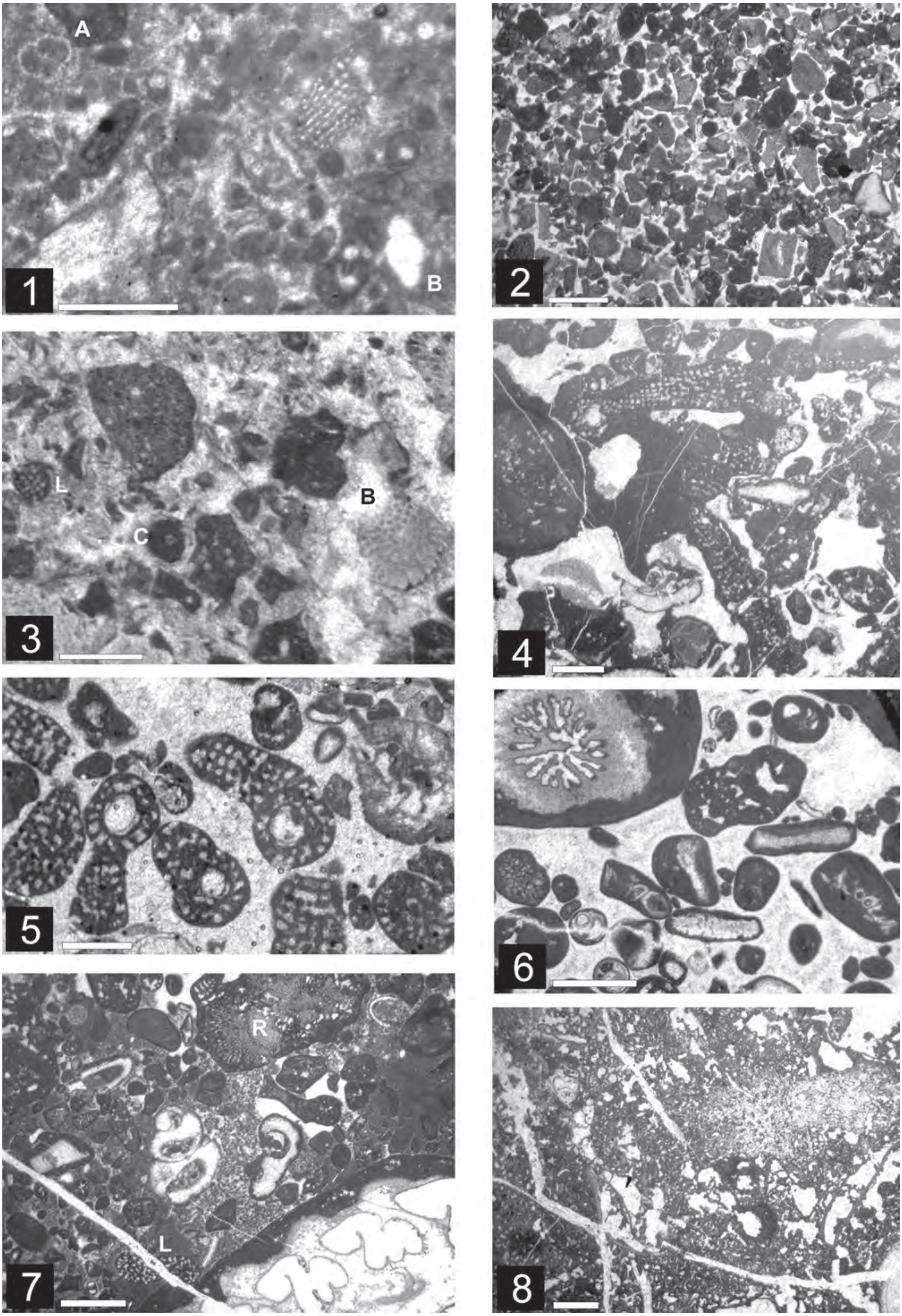
1
A
B
2
3
L
C
B
4
5
6
7
R
L
8

First of all, the three platforms are distinguished by their
(i) stratigraphy,
(ii) general geodynamic and facies evolution,
(iii) partly the occurring microfacies types, and
(iv) the palaeogeographic position and their resediments in the adjacent basins.

The known stratigraphic range of the Wolfgangsee Carbonate Platform is Kimmeridgian (or slightly older?) to early Late Tithonian, of the Plassen Carbonate Platform *s. str.* latest Oxfordian to Early Berriasian and of the Lärchberg Carbonate Platform Kimmeridgian (or slightly older) to Tithonian/Early Berriasian. Concerning the overall platform evolution, all three platforms evolved after a shallowing-upward phase terminating an extended period of regional deep-water sedimentation. The nuclei of these platforms is not preserved due to younger erosional processes. The onset of all platform areas is interpreted to have taken place on top of rising nappe fronts, e.g., the Brunnwinkl Rise - Wolfgangsee Carbonate Platform and Trattberg Rise - Plassen Carbonate Platform *s. str*. During their evolution the platforms prograded towards the basins and started to fill them: this resulted in the preserved sedimentary successions of the platform exhibiting a shallowing-upward evolution. The Wolfgangsee Carbonate platform was drowned in the Late Tithonian (Gawlick & Schlagintweit 2010), the Plassen Carbonate Platform *s. str*. in the Early/Late Berriasian (Gawlick & Schlagintweit 2006). In contrast, the Lärchberg Carbonate Platform emerged most likely during the Berriasian. All these details are not discussed at this point as they are well beyond the scope of this compilation.

In the following, the sedimentological evolution of the Plassen Carbonate Platform on the base of the type-locality succession of Mount Plassen is summarized. Representing the most complete sequence from the installation of the shallow-water platform until its drowning (Schlagintweit et al. 2003, 2005, Gawlick & Schlagintweit 2006), the more or less accidental selection of Mount Plassen as the type-locality more than 150 years ago (Hauer 1850) was in retrospective an excellent choice.

The shallow-water carbonates form the upper part of shallowing-upward sequence. They developed from the deep-water radiolarite succession via a transitional sequence of cherty sediments and protoglobigerinid-bearing limestones This transitional sediments outcrop only on the southeastern side of Mount Plassen. Close to Mount Plassen, the radiolarites were dated approximately to the Oxfordian/Kimmeridgian boundary (Wegerer et al. 2003). The deeper slope facies shows a mixture of pelagic (e.g., protoglobigerinds) and neritic bioclasts. The upper slope deposits contain bryozoans, echinoderms, "tubiphyts" (= *Crescentiella morronensis*) and scattered larger benthic foraminifera such as *Labyrinthina mirabilis* Weynschenk. The platform margin facies is characterized either by bioclastic limestones with corals, sponges ("stromatoporoids") and calcareous algae (e.g., *Nipponophycus ramosus*, *Salpingoporella pygmaea*), or grainstones with abundant larger benthic foraminifera ("*Labyrinthina* shoals"). The back-"reefal" facies consists of various bioclastic grain-, pack- to rudstones with foraminifera, calcareous algae (Dasycladales and "Porostromata") as well as debris of reef-building organisms. Rather quickly, these are followed by oncoidal packstones with abundant porostromate algae, gastropods and wackestones in a repeated manner (transgressive-regressive cycles). Mudstones with idiomorphic dolomites, intraformational breccias, fenestral fabrics and fine-peloidal packstones with anomuran coprolites indicate very shallow-water conditions with presumably short-term emersions (sub- to supratidal tidal flats) (Fig. 79). These are repeated successions (T-R-cycles) of open marine facies passing into Tidal Flats that are commonly capped by emergence horizons with dessication structures, intraformational black pebble breccias and pisolithic limestone facies (Fig. 79i-j). Microfacies include (partly oncoidal) mudstones with ostracods, anomuran coprolites (*Favreina lahngangkogelensis* Schlagintweit, Gawlick & Lein, Fig. 79h, *Agantaxia*? *biserialis* Kristan-Tollmann: for both taxa Mt. Plassen is the type-locality), laminated peloidal grainstones (Fig. 79g) and fenestral limestones (grainstones, mud-/wackestones with vadose silt). Idiomorphic dolomites with indications of early diagenetic origin occur as matrix (mudstones) and in components (oncoids) selective (Fig. 79e-f). The subtidal closed lagoonal facies is represented by wackestones with larger benthic foraminifera, e.g., *Kilianina*? *rahonensis* Foury & Vincent, and dasycladalean algae, e.g., *Salpingoporella annulata* Carozzi (Fig. 79c-d). The back-reefal to open-lagoonal parts of the cycles are composed of sparitic, partly oncoidal limestones (grainstones, rudstones) with gastropods (e.g. nerineids), *Carpathocancer*? *plassenensis*

Fig. 81: Microfacies and facies interpretation of the Plassen Carbonate Platform *s. str.* (latest Kimmeridgian to Early/ Middle Tithonian) of Mount Plassen. From Schlagintweit et al. (2003). Page 264.
1. Mudstone with irregularly distributed dolomite rhombs. Tidal flat facies. Sample Q 70, Hohe Wasserstollen, scale bar = 1 mm. **2.** „Rivulariacean"-biosparite containing *Rivularia piae* (Frollo) (bottom left) and *Hedstroemia* cf. *klausi* Dragastan (central top). Open lagoonal facies. Sample Pl 73d-2001, scale bar = 1 mm. **3.** Intraformational erosion surface. Tidal Flat (? channel deposit). Sample Pl 66-2001, scale bar = 1 mm. **4.** Microconglomerate („mud-pebble conglomerate"), consisting of dark coloured mud pebbles which have been reworked (semiconsolidated plasticlasts). Tidal flat facies (? channel deposit). Sample Pl 7-2000, scale bar = 1 mm. **5.** Peloidal packstone with birdseyes. Tidal flat facies. Sample Pl 75-2001, scale bar = 1 mm. **6.** Wacke- to packstone with birdseyes and geopetal internal sediment (vadose silt) and „caught" air bubbles. Note the thallus fragment of *Clypeina jurassica* Favre in the centre. Tidal flat facies. Sample Pl 3-2000), scale bar = 1 mm. **7.** Packstone with abundant thallus fragments of the dasycladale *Campbelliella striata* (Carozzi). Open lagoonal facies. Sample Pl 42-2001, scale bar = 1 mm. **8.** Grain- to packstone with *Clypeina jurassica* Favre. Open lagoonal facies. Sample Pl 43-2001, scale bar = 0.5 mm.

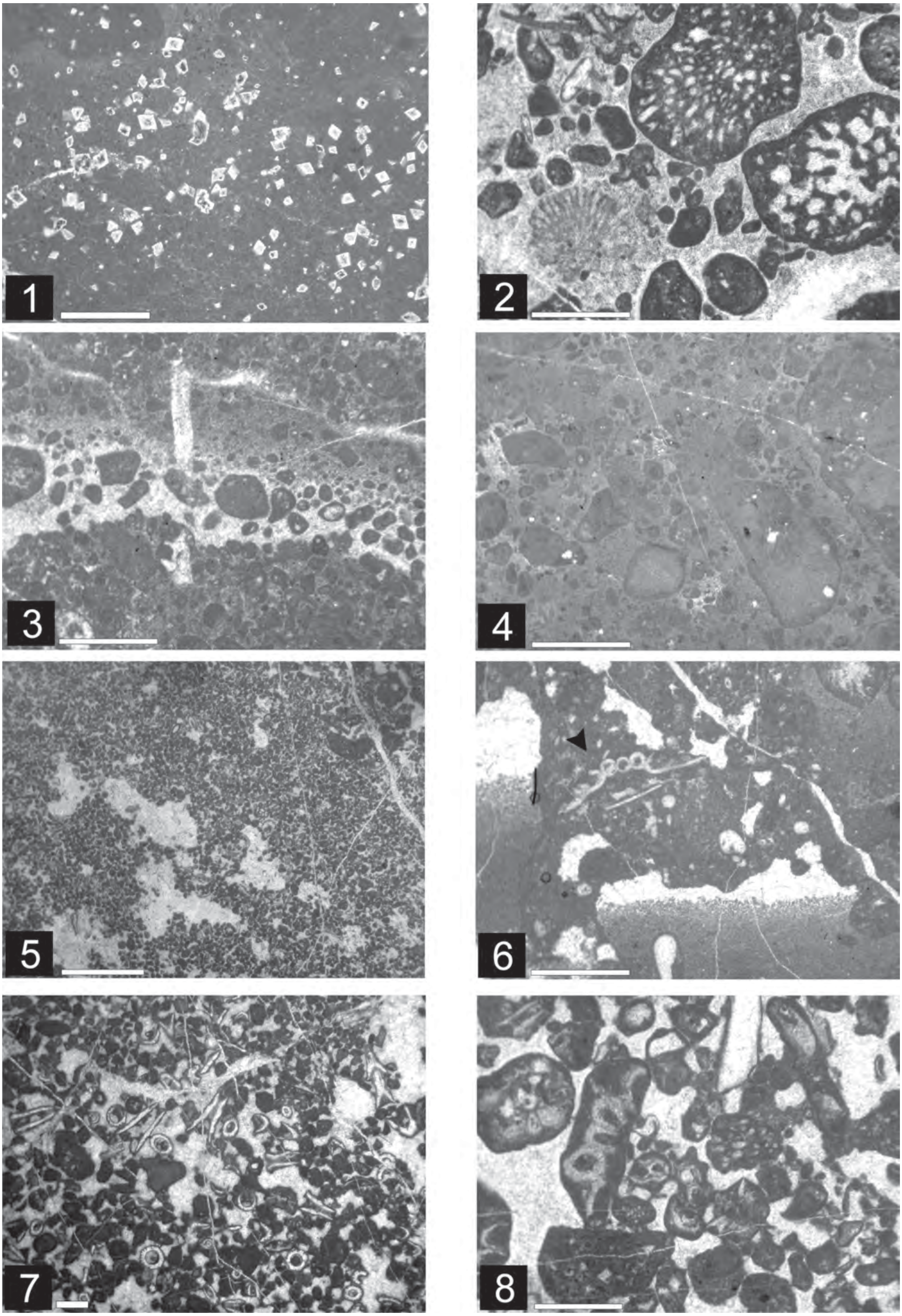
1
2
3
4
5
6
7
8

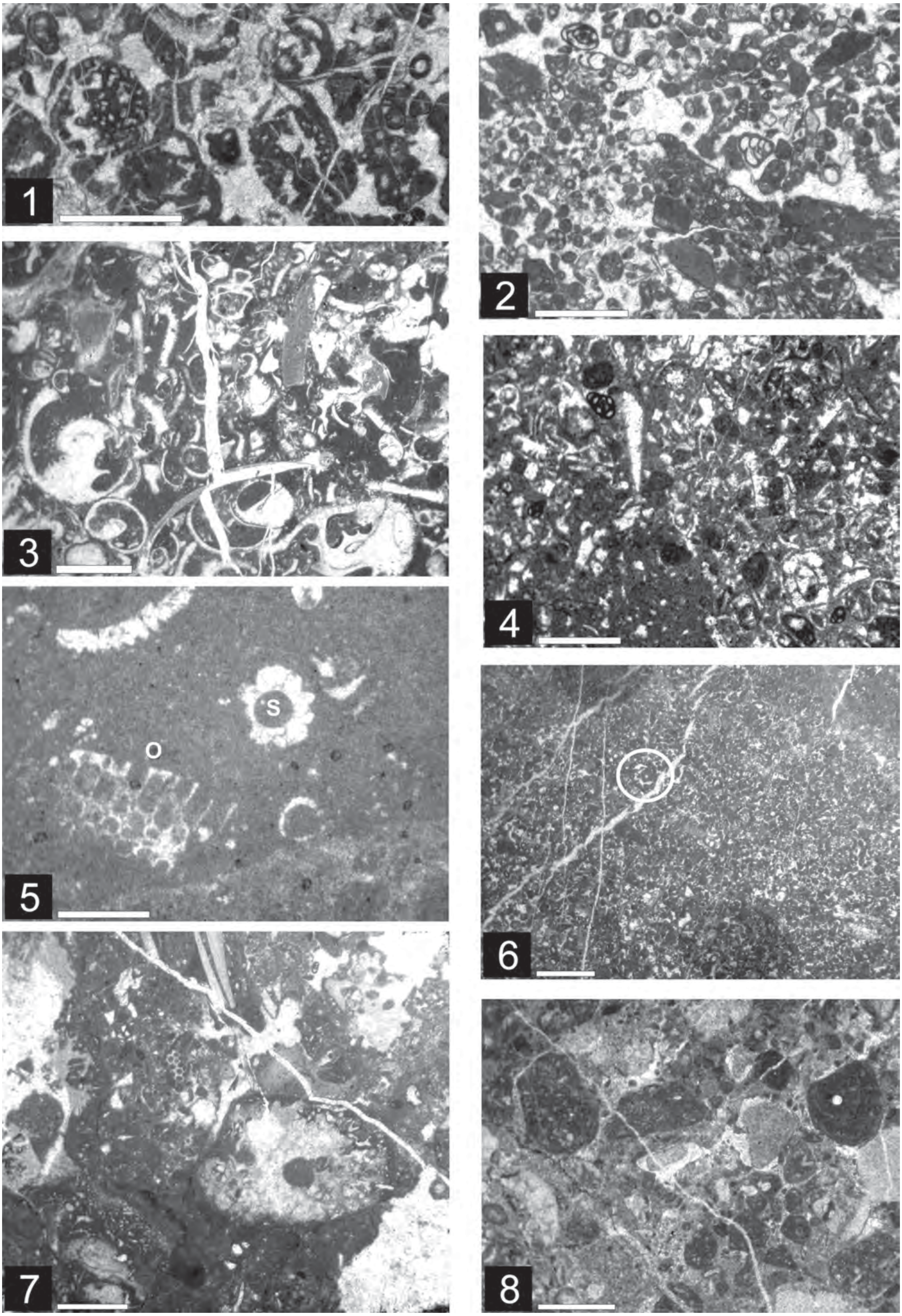
1
2
3
4
s
o
5
6
7
8

Fig. 82: Microfacies and facies interpretation of the Plassen Carbonate Platform *s. str.* (Middle/Late Tithonian-Early Berriasian) of Mount Plassen. From SCHLAGINTWEIT et al. (2003). Page 265.
1. Foraminiferal packstone with several specimens of *Pseudocyclammina* gr. *sphaeroidalis* HOTTINGER. Open lagoonal facies. Sample Pl 38-2001, scale bar = 1 mm. **2.** Foraminiferal packstone with textulariids and miliolids. Open lagoonal facies. Sample Pl 29-2001, scale bar = 1 mm. **3.** Gastropod-biomicrite (lumachelle). Closed lagoonal facies. Sample Pl 21-2001, scale bar = 2 mm. **4.** Dasycladale-wackestone with *Clypeina parasolkani* FARINACCI & RADOICIC, *Salpingoporella annulata* CAROZZI and *Rajkaella* cf. *bartheli* (BERNIER). Closed lagoonal facies. Sample Pl 28d-2001, scale bar = 1 mm. **5.** Wackestone with dasycladales *Salpingoporella annulata* CAROZZI (S) and *Otternstella lemmensis* (BERNIER) (O). Closed lagoonal facies. Sample Pl 17-2001, scale bar = 0.5 mm. **6.** Peloidal packstone with *Pseudocyclammina sphaeroidalis* HOTTINGER (circle). Closed lagoonal facies. Sample Pl 53-2001, scale bar = 2 mm. **7.** Bioclastic packstone with remains of frame-builders encrusted by *Lithocodium aggregatum* ELLIOTT. Reef-debris facies. Sample Pl 58-2001, scale bar = 2 mm. **8.** Packstone with debris of echinoids exhibiting syntaxial rim cements, bryozoa and *Crescentiella morronensis* (CRESCENTI). Slope facies. Sample Pl 54-2001, scale bar = 0.5 mm.

(SCHLAGINTWEIT & GAWLICK) (problematic tube), a diverse association of “rivulariacean“ algae, dasycladales such as *Clypeina jurassica* FAVRE, *Salpingoporella annulata* CAROZZI, *Salpingoporella* gr. *pygmaea* (GÜMBEL) and benthic foraminifera (e.g., trocholinids) (Fig. 79a-b). For a detailed micropalaeontoloigcal inventory see SCHLAGINTWEIT et al. (2005). These lithologies and open lagoonal limestones make up the complete southern part of Mount Plassen.

The transition to the Late Tithonian closed lagoon is marked by grain- to packstones with abundant debris of the dasycladale *Campbelliella striata* (CAROZZI). The former are represented mainly by algal-foraminiferan, partly oncoidal wackestones, gastropod floatstones or stromatoporoid wackestones. The closed lagoonal deposits build up large areas of Mount Plassen (SCHLAGINTWEIT et al. 2005: Fig. 3). This indicates that increasing subsidence in the Late Tithonian was counterbalanced by enhanced carbonate production. Near the summit of Mount Plassen, these lithologies are followed again by back-reefal facies with porostromate algae and debris of reef-builders, e.g., ellipsactinids. In contrast to the Late Kimmeridgian to earliest Tithonian back-“reef“ facies, these Late Tithonian ones are often poorly washed out packstones, indicating sedimentation under less agitated (sheltered) conditions. In older part of the succession, we find the foraminifer *Protopeneroplis striata* WENSCHENK, whereas the younger part contains *Protopeneroplis ultragranulata* (GORBATCHIK). As larger relief-building constructions of *in-situ* reef-building organisms were not observed, the term “reef“ is here used for coral- and stromatoporoid-rich microfacies-types preferentially in a platform marginal setting. The fining-upward succession as observed in the section from the summit towards northwest, indicates deepening (margin > upper > lower slope deposits) and drowning of the platform. These deposits are overlain by Late Berriasian calpionellid wacke- to packstones documenting the onlap of hemipelagic facies onto the platform carbonates (GAWLICK & SCHLAGINTWEIT 2006: *oblonga* zone).

The isolated occurrences of the Plassen Carbonate Platform *s. str*. can lithostratigraphically be correlated with this general facies evolution observed at the type-locality Mount Plassen. The successions at all other occurrences are less complete. Preserved are either only the initial shallowing-upward sequence together with the platform margin deposits or, more rarely, the sediments of the back-reefal to open lagoonal facies as seen, e.g., at Mount Krahstein (GAWLICK et al. 2004).

2.5.1. Salzkammergut area

In the Salzkammergut area several Late Jurassic to earliest Cretaceous shallow-water carbonate platform remains of the Plassen Carbonate Platform are preserved. The most prominent occurrence is Mt. Plassen west of the village Hallstatt. We will not visit Mt. Plassen as it is at high altitude and hard to reach with the relevant sections in quite far distance to each other. Most of the Plassen Carbonate Platform *s. str.* occurrences are remote in steep Alpine terrain though. Therefore it is more suitable to visit the northern representative of the Late Jurassic carbonate platform assemblage, the Wolfgangsee Carbonate Platform (Stop 4), instead, including its drowning sequence . In addition we will study resediments of the Plassen Carbonate Platform in the basinal sequences, which provide an excellent insight into the inventory of platform-building shallow-water organisms and the microfacies types of the Plassen Carbonate Platform.

Stop 1: Mt. Sandling (Stops 6 and 7 in Fig. 11)
Kimmeridgian to Tithonian deep-water sequence and reworked reef material

On top of the Sandlingalm Formation (Hallstatt Mélange *s. str*.) and after the emplacement of the Haselgebirge Mélange the evolution of the Plassen Carbonate Platform *s. l.* started. The nucleus areas of these platforms on the Late Jurassic topographic highs are not observable due to younger erosion. Only the prograding sequences above the earlier basinal areas are preserved. These successions span more or less the complete Kimmeridgian to Early Berriasian.

The Mt. Sandling section starts with Kimmeridgian deep-water cherty limestones, rich in *Saccocoma* and dated by means of radiolarians (GAWLICK et al. 2010). In some areas a polymictic breccia occurs between the Haselgebirge Mélange and the overlying Kimmeridgian deep-water limestones (GAWLICK et al. 2010, MISSONI & GAWLICK

Fig. 83: View of Mt. Sandling from the west. The thin bedded lower part of the succession represents Kimmeridgian to ?Early Tithonian *Saccocoma* Limestone. It is topped by massive mass-flow deposits (Barmstein Limestone) consisting of amalgamated shallow-water material including reef limestones. The salt deposit of the Alpine Haselgebirge Mélange is situated below the *Saccocoma* Limestone and above the Hallstatt Mélange (e.g., location of the viewpoint). In this picture, the contact of the Kimmeridgian to Tithonian succession to the underlying mélange is covered by young rock fall.

2011a). Whereas (today completely chertified) crinoid-rich turbiditic layers occur in the basal part of the sequence, the content of radiolarians decreases upsection. The thickness of this basinal, radiolarian-dated Kimmeridgian to Tithonian sequence (*Saccocoma* Limestone) is around 200 metres (Gawlick et al. 2010). In this *Saccocoma* Limestone shallow-water clasts occur only in the form of very fine-grained debris. Higher in the section, the coarse-grained Tithonian mass-flow deposits consist exclusively of material of the Plassen Carbonate Platform *s. str.*

The floral and faunal content of Tithonian sequence of Mt. Sandling is described in detail in Gawlick et al. (2007a, 2010) and is summarized here in a brief manner. The Barmstein Limestone of Mount Sandling can be compared with other occurrences, e.g., the type-locality Mounts Barmsteine near Hallein in the Salzburg Calcareous Alps (Gawlick et al. 2005). They are characterized by closely-packed lithoclasts exclusively originating from the Plassen Carbonate Platform. They refer to different facies zones, e.g., open and closed lagoon, back-"reefal", "reefal" and fore-"reefal". Therefore, the biogenic content is represented by mixed assemblages from different depositional settings of various water depth and hydrodynamic levels. From the Barmstein Limestone altogether 27 taxa of dasycladalean algae are reported (Schlagintweit 2011b). The most common include *Clypeina jurassica* Favre and *Salpingoporella annulata* Carozzi. Within the Barmstein Limestone of Mount Sandling also comparable large-sized dasycladaleans such as *Petrascula guembeli* Bernier or *Selliporella neocomiensis* (Radoicic) are common. Among the benthic foraminifera, protopeneroplids, *Pseudocyclammina lituus* Yokoyama or trocholinids, e.g., *Andersenolina elongata* (Leupold) are the most common

Fig. 84: Microfacies of the Late Tithonian mass flows of Mount Sandling (from Gawlick et al. 2010). Page 268.
1. Mass flow with bioclasts of corals and poorly rounded lithoclasts of diverse microfacies (packstones, partly bioclastic, wackestones). Sample D 171. Width of photo: 1.4 cm. **2**. Larger clast of the external platform margin; Boundstone with massive crusts and intergrowth of diverse incertae sedis such as *Iberopora bodeuri* Granier & Berthou and *Crescentiella morronensis* (Crescenti). Sample D 176. Width of photo: 0.4 cm. **3**. Mass flow with different clasts and bioclasts; on the left an oblique section of a demosponge (*Sestrostomella*? sp.). Sample D 176. Width of photo: 1.4 cm. **4**. Mass flow with different clasts such as packstones or wackestones of the closed lagoon (A). Sample D 185. Width of photo: 1.4 cm. **5**. Semi-lithified clast of a well washed-out packstone with components surrounded by a thin rim of first generation cement; the remaining pore space consists of microsparite. Note the direct contact of individual components protruding into the surrounding sediment. Sample D 190. Width of photo: 0.46 cm. **6**. Large clast of an oncoidal floatstone. The irregular ovoid oncoids are characterized by comparable dense micritic laminae; lamination is only poorly developed. Sample D 179. Width of photo: 1.4 cm. **7**. Oncoidal packstone showing bimodal grain-size distribution. Besides oncoids, benthic foraminifera and remains of lithocodid-bacinellid fabrics occur. Sample D 194. Width of photo: 1.4 cm. **8**. Larger clast of a dasycladalean wackestone of the closed lagoonal facies of the Plassen Carbonate Platform. Sample D 207. Width of photo: 0.38 cm.

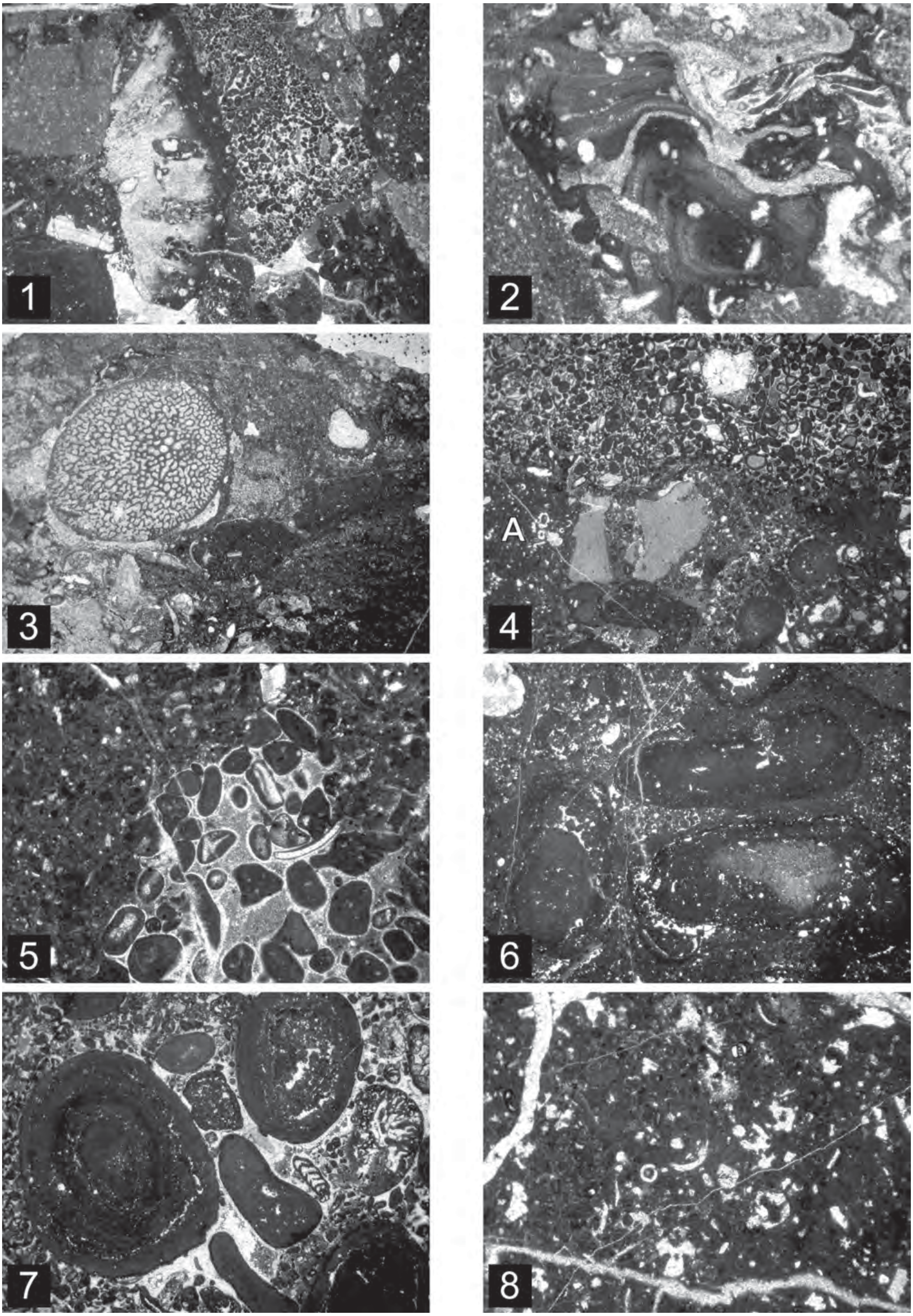
1
2
3
A
4
5
6
7
8

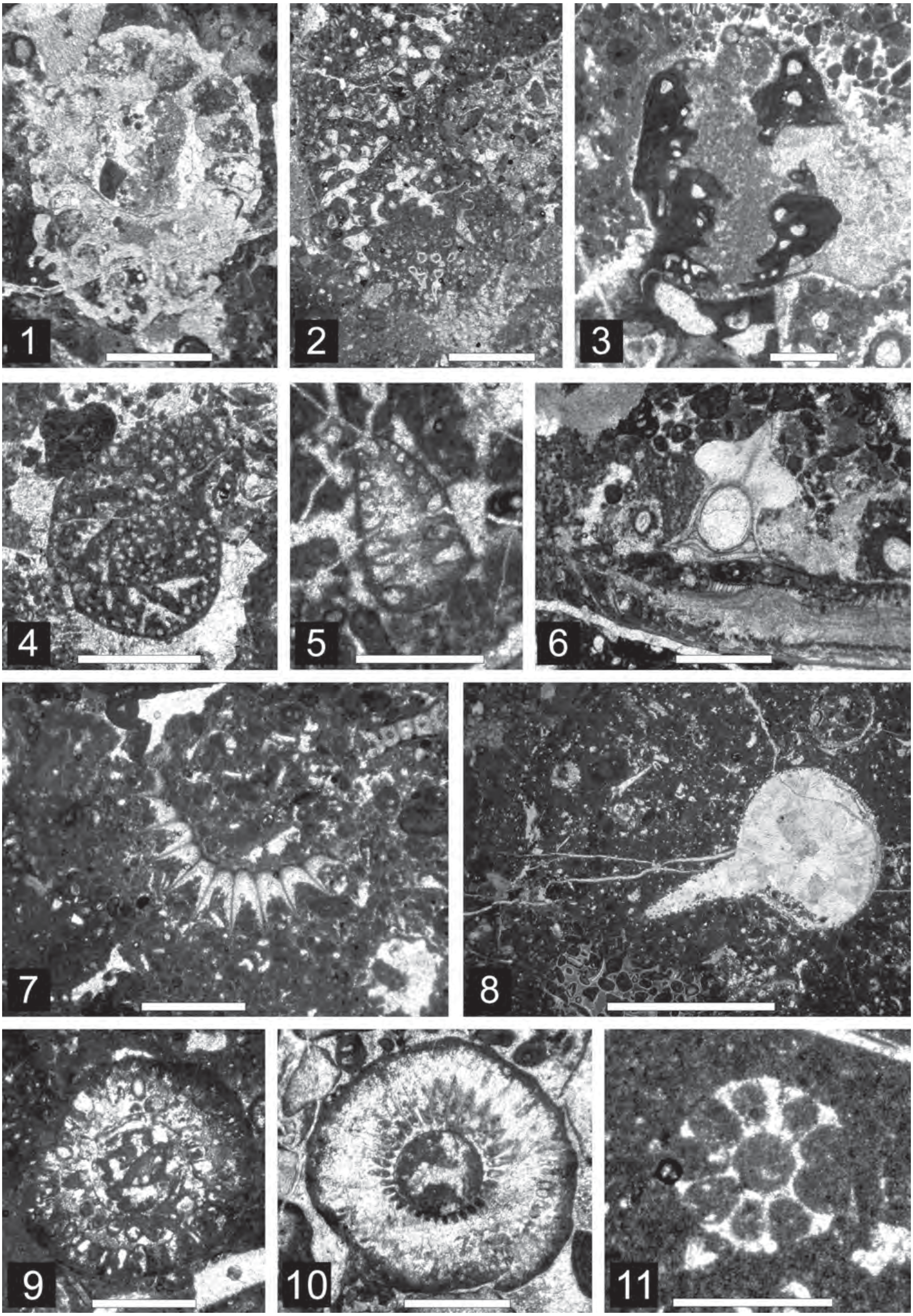
1
2
3
4
5
6
7
8
9
10
11

Fig. 85: Micropalaeontology of the Mount Sandling southwestern slope (1, 3, 10) and summit (2, 4-9, 11). From GAWLICK et al. (2010). Page 269.
1. Sphinctozooid sponge *Thalamopora lusitanica* TERMIER & TERMIER. Sample D 760. Scale bar: 1.0 mm. **2**. Benthic foraminifer *Coscinophragma* aff. *cribrosa* (REUSS). Sample D 176. Scale bar: 1.0 mm. **3**. Incertae sedis *Labes atramentosa* ELIASOVA (= *Tubiphytes*-chimney sensu SCHMID 1996) encrusting an unknown organism (probably a sponge). Sample D 794. Scale bar: 0.5 mm. **4**. Benthic foraminifer *Pseudocyclammina lituus* (YOKOYAMA). Sample D 185. Scale bar: 1.0 mm. **5**. Benthic foraminifer *Andersenolina elongata* (LEUPOLD). Sample D 190. Scale bar: 0.5 cm. **6**. Several serpulid tubes; the specimen in the middle exhibits a pronounced sculpture (keel). Probe D 179. Scale bar: 1.0 mm. **7**. Dasycladale *Clypeina jurassica* FAVRE. Sample D 194. Scale bar: 1.0 mm. **8**. Dasycladale *Petrascula piai* BACHMAYER. Sample D 207. Scale bar: 5.0 mm. **9**. Dasycladale *Selliporella neocomiensis* (RADOIÈIÆ). Sample D 200. Scale bar: 1.0 mm. **10**. Unknown Dasycladale with massive calcification and numerous laterals (w = 32). Sample D 765. Scale bar: 1.0 mm. **11**. Dasycladale *Cylindroporella*/*Otternstella*. Sample D 179. Scale bar: 0.5 mm.

ones. Macroscopically, the Barmstein Limestone of Mt. Sandling is also well-known for its widespread occurrence of "stromatoporoids", e.g., genera *Milleporidium* or *Actinostromaria* (FENNINGER 1969).

Stop 2: Mt. Loser (optional)

Callovian to Tithonian deep-water sequence with reworked shallow-water material (Late Tithonian)

The Middle to Late Jurassic sedimentary succession of Mt. Loser starts with dark-grey bioturbated cherty limestones of Callovian to Oxfordian age as dated by means of radiolarians (unpublished data). The radiolarian fauna is well preserved and contains the typical assemblages as known from similar sequences in the Salzkammergut region (e.g., SUZUKI & GAWLICK 2003). The microfacies of this several tens of metres thick succession is a radiolarian wacke- to packstone. Upsection the succession becomes more and more radiolaritic and is topped by a 2 metres thick level of reddish-greyish radiolarite. In some areas, up to 1 metre thick mass-flow deposits occur intercalated in these radiolarites. Above this interval, the series becomes rapidly more calcareous and light grey in colour. This light-grey cherty limestone succession is rich in *Saccocoma* (*Saccocoma* Limestone: Kimmeridgian to Tithonian) (Fig. 86-1). In the Tithonian the sedimentation rapidly became coarser grained with intercalations of calcareous turbidites made up of shallow-water debris from a near-by shallow-water carbonate platform area (Plassen Carbonate Platform *s. str*.). Soon after the change from pure deep-water limestones to the turbiditic mass-flow deposits consisting of reef-debris, older components of the Plassen Carbonate Platform *s. str.* and the underlying sequence (radiolarites, *Saccocoma* Limestone) occurred. The Kimmeridgian age of the *Saccocoma* Limestone components was determined with the help of ammonites (LUKENEDER et al. 2003).
The mass flows and calciturbidites (Barmstein Limestone) are intercalated in Late Tithonian calpionellid limestones (Oberalm Formation). They contain shallow water bioclasts from the Plassen Carbonate Platform, e.g., skeletons of stromatoporoids (Fig. 86-6), dasycladalean algae such as *Clypeina jurassica* FAVRE, *Salpingoporella annulata* CAROZZI, *Neoteutloporella socialis* PRATURLON (Fig. 86-8) or *Salpingoporella pygmaea* (GÜMBEL) (Fig. 86-4), benthic foraminifera such as *Pseudocyclammina lituus* (YOKOYAMA) (Fig. 86-7), remains of "bacinellid" crusts and incertae sedis *Crescentiella morronensis* (CRESCENTI) (Fig. 86-8).

Stop 3: Mt. Höherstein (optional)

Tithonian cherty limestones with intercalated mass-flow deposits

The succession of the youngest part of the Tauglboden and Oberalm Formations including the intercalated Barmstein Limestone is well exposed at Mt. Höherstein ("Höherstein Plateau") (GAWLICK et al. 2007a, 2010). At the northwestern and southeastern base of the succession, micritic limestones on top of cherty sediments were dated as Late Tithonian by means of calpionellids (*Crassicollaria* Zone). In the cherty sediments, polymictic breccias layers predominated by lagoonal Dachstein Limestone components, e.g., *Triasina* packstones, occur. After a phase of condensed sedimentation in the Tauglboden Basin in Kimmeridgian to Early Tithonian times, resedimentation processes revived around the Early/Late Tithonian boundary. This change is described in detail in chapter 2.3.2 (central Tauglboden Basin). In contrast to the central Tauglboden Basin with its dark-grey cherty limestone to radiolarite with intercalated slump deposits and mass flows succession, contemporaneous deposition in the more proximal part of the Tauglboden Basin was characterized by more calcareous sediments with occurrences of big Late Triassic lagoonal Dachstein Limestone blocks in the Tithonian matrix. In the central Tauglboden Basin, the transition from the dark-grey cherty limestone to radiolarite deposition, and finally to the calcareous sedimentation (Oberalm Formation + Barmstein Limestone) was gradual. The content of shallow-water debris from the Plassen Carbonate Platform *s. str.* increased slowly. In the Höherstein Plateau section, the change from radiolaritic to calcareous sedimentation with coarse-grained reef debris was abrupt (GAWLICK et al. 2007a). This documents clearly a more proximal basin position of the Knerzenalm - Höherstein Plateau area in comparison with the Tauglboden valley (central basin).
The main part of Mt. Höherstein consists of more than 300 metres thick resediments of the Plassen Carbonate Platform. These Barmstein Limestone deposits are either calciturbidites or mass flows. The former are represented by well-washed out packstones to comparably well sorted grainstones with incorporated small slope lithoclasts of the Plassen Carbonate Platform and a variety of individu-

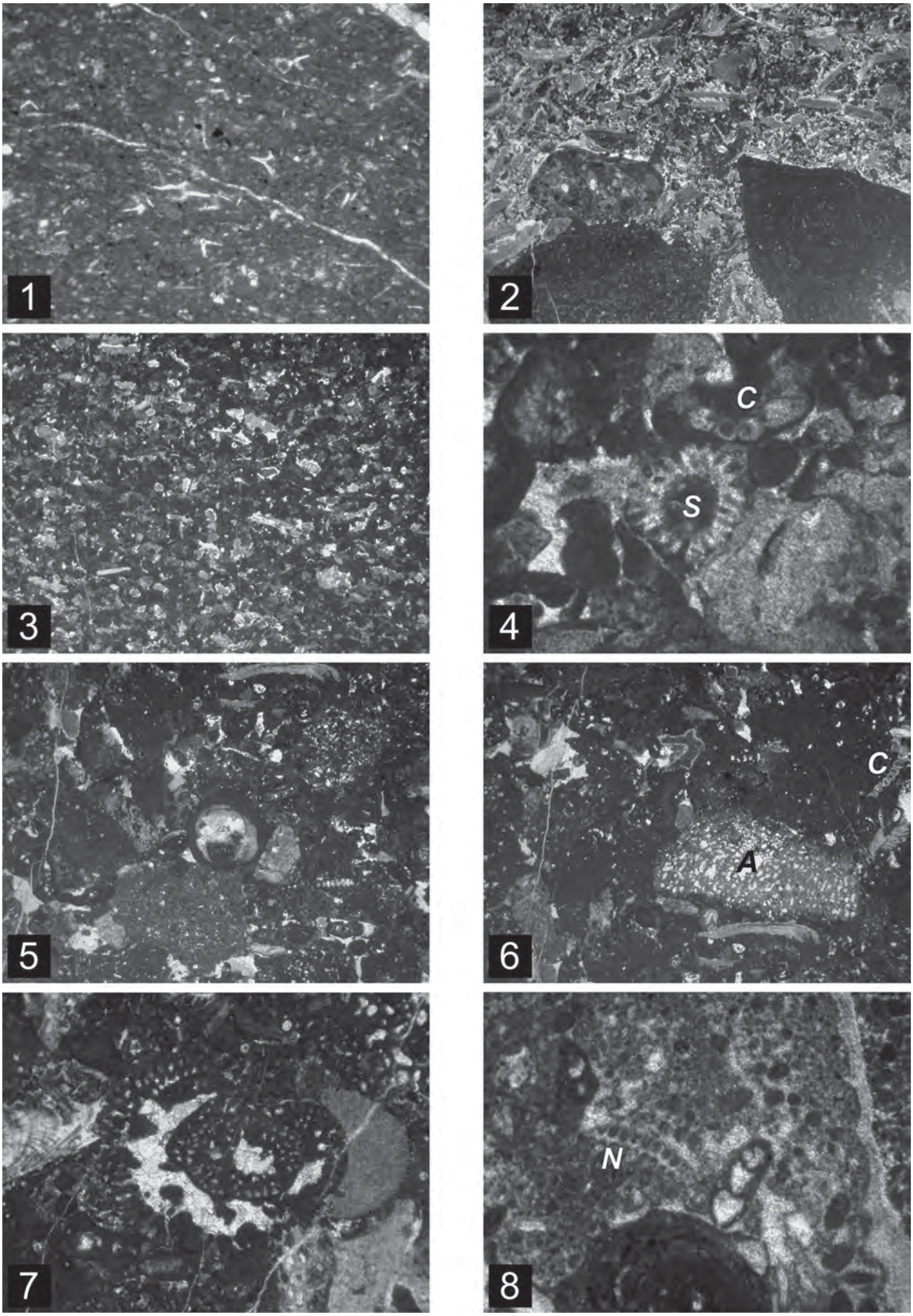
1
2
C
S
3
4
C
A
5
6
N
7
8

Fig. 86: Microfacies of the Late Jurassic succession of Mount Loser (*Saccocoma* limestones, Barmstein Limestone). Page 271.
1. Wackestone with debris of *Saccocoma*. Sample A 3413. Width of photo: 0.5 mm. **2.** Calciturbidite with crinoids and aptychi cutting erosively into basinal sediments. Sample A 3226. Width of photo: 1.4 mm. **3.** Comparably well sorted calciturbidite (packstone) with echinoid remains and debris of shallow-water organisms. Sample A 3230. Width of photo: 0.5 mm. **4.** Detail from a calciturbidite with dasycladalean algae *Salpingoporella pygmaea* (Gümbel) (*S*) and *Clypeina jurassica* Favre (*C*). Sample A 3418. Width of photo 0.25 mm. **5.** Coarse-grained, poorly sorted calciturbidit) with shallow-water litho- and bioclasts of the Plassen Carbonate Platform: "bacinellid" onocoid (b), *Clypeina jurassica* Favre (*C*), *Pseudocyclammina lituus* (Yokoyama) (*P*), *Salpingoporella annulata* Carozzi (*S*). Sample A 3420-2. Width of photo: 1.4 mm. **6.** Same as for **5.** Note the stromatoporoid skeleton (*Actinostromaria-Actinostromina* group, *A*). Sample A 3420-2. Width of photo: 1.4 mm. **7.** Common benthic foraminifer of the Barmstein Limestone: *Pseudocyclammina lituus* (Yokoyama). Sample A 3420-p. Width of photo 0.5 mm. **8.** Detail from Barmstein Limestone: peloidal packstone with small benthic foraminifer and characteristic debris of the Dasycladale *Neoteutloporella socialis* Praturlon (*N*) (see Schlagintweit 2011b); at the bottom, an oblique transverse section of *Crescentiella morronensis* (Crescenti). Sample A 3424-2. Width of photo: 0.5 mm.

al bioclasts, e.g., the benthic foraminifera *Protopeneroplis ultragranulata* (Gorbatchik), *Pseudocyclammina lituus* Yokoyama, *Trocholina* cf. *involuta* Matsurova, *Andersenolina alpina* (Leupold) or *Mohlerina basiliensis* (Mohler). Dasycladales are present with *Clypeina jurassica* Favre, *Selliporella neocomiensis* (Radoicic) and *Salpingoporella pygmaea* (Gümbel). Most of these single bioclasts display micritic coatings.

Stop 4: Mt. Bürgl
Kimmeridgian to Tithonian sequence (reef, fore-reef, drowning)

Mt. Bürgl (or Bürgelstein) is geographically situated in the Salzkammergut area at the southeastern end of lake Wolfgangsee, close to the township Strobl. It represents an east-west extending, isolated forested mountain with a rounded summit (altitude: 745 m. a.s.l.) within a flat landscape. With an east-west extension of about 1.4 km and a maximum north-south stretch of 0.55 km, the Mt. Bürgl Upper Jurassic covers an area of approximately 0.45 km^2. The Late Jurassic shallow-water carbonates belong to the so-called Wolfgangsee Carbonate Platform (Gawlick et al. 2007b). Other, near-by occurrences of this platform include Mounts Drei Brüder, Mount Falkenstein, and Mount Lugberg, all located within an approximately 15 km wide, NW-SE stretching zone along the northern side of Lake Wolfgangsee (Leischner 1961, Plöchinger 1964, 1973, Fenninger & Holzer 1972). Mount Bürgl provides the only complete section from the Early Kimmeridgian onset of the platform evolution to the drowning in the Late Tithonian and is therefore best suited to study the evolution of this platform (Gawlick & Schlagintweit 2010). All other occurrences provide only information on the earlier platform evolution, whilst the younger parts of the succession are eroded (Kügler et al. 2003, Gawlick et al. 2007b). The Late Jurassic shallow-water evolution started with basal ooid-bearing resediments followed by slope sediments often with intercalated breccias; platform margin deposits with corals and stromatoporoids form the topmost parts. At Mount Drei Brüder and Mount Lugberg, the benthic foraminifera *Labyrinthina mirabilis* Weynschenk and "*Kilianina*" *rahonensis* Foury & Vincent were detected in the basal resediments. These taxa are referred mainly to the Kimmeridgian (e.g., Bassoullet 1997). Taking these results into consideration, a Kimmeridgian platform onset is assumed for the Mount Bürgl succession. An older, Late Oxfordian age for the basal resediments cannot be excluded though. The thickness of the whole Late Jurassic shallow-water succession is approximately 200-300 m.
The drowning sequence, exposed at the northwestern side of Mt. Bürgl, abruptly follows platform margin (reefal, fore-reefal) deposits, which show no evidence for emergence/subaerial exposure. The rapid lithological change from shallow-marine carbonates to hemipelagic deeper slope sediments is termed a drowning unconformity in the sense of Schlager (1989). In the platform top to upper slope area, the drowning phase is partly characterized by a microfacies change: reefal rudstones of a platform-near facies belt are substituted by echinoderm dominated grainstones together with recrystallized bioclasts of shallow-marine biota. The investigated drowning sequence starts with a 20 metre thick series of coarse-grained mass flows, in the upper part with intercalated fine-grained calarenites. Both lithologies are made up of reefal material. The sequence after the drowning unconformity was dated by means of calpionellids. The section on top of the drowning unconformity starts with thin bedded biomicritic, partly cherty limestones with some intercalated fine-grained allodapic limestones. Occasionally also some greenish marly intercalations occur. Slump deposits exist especially in the middle part of the section. The first analyzed sample following the drowning disconformity contains calpionellids of the Late Tithonian *intermedia* Subzone. The uppermost part of the exposed section consists of thin bedded, very fine-grained cherty limestones with marly intercalations. Allodapic layers are only thin and very fine-grained. The first sample on the base of this part of the section (E 825) shows the co-occurrence of *Crassicollaria intermedia* (Durand-Delga) and *Calpionella alpina* Lorenz together with several other species.
The drowning event of the Wolfgangsee Carbonate Platform in the northern part of the Northern Calcareous Alps, the onset of N-directed Barmstein Limestone-type resedimentation from the central Plassen Carbonate Platform *s. str.* into the enlarged Tauglboden Basin, the

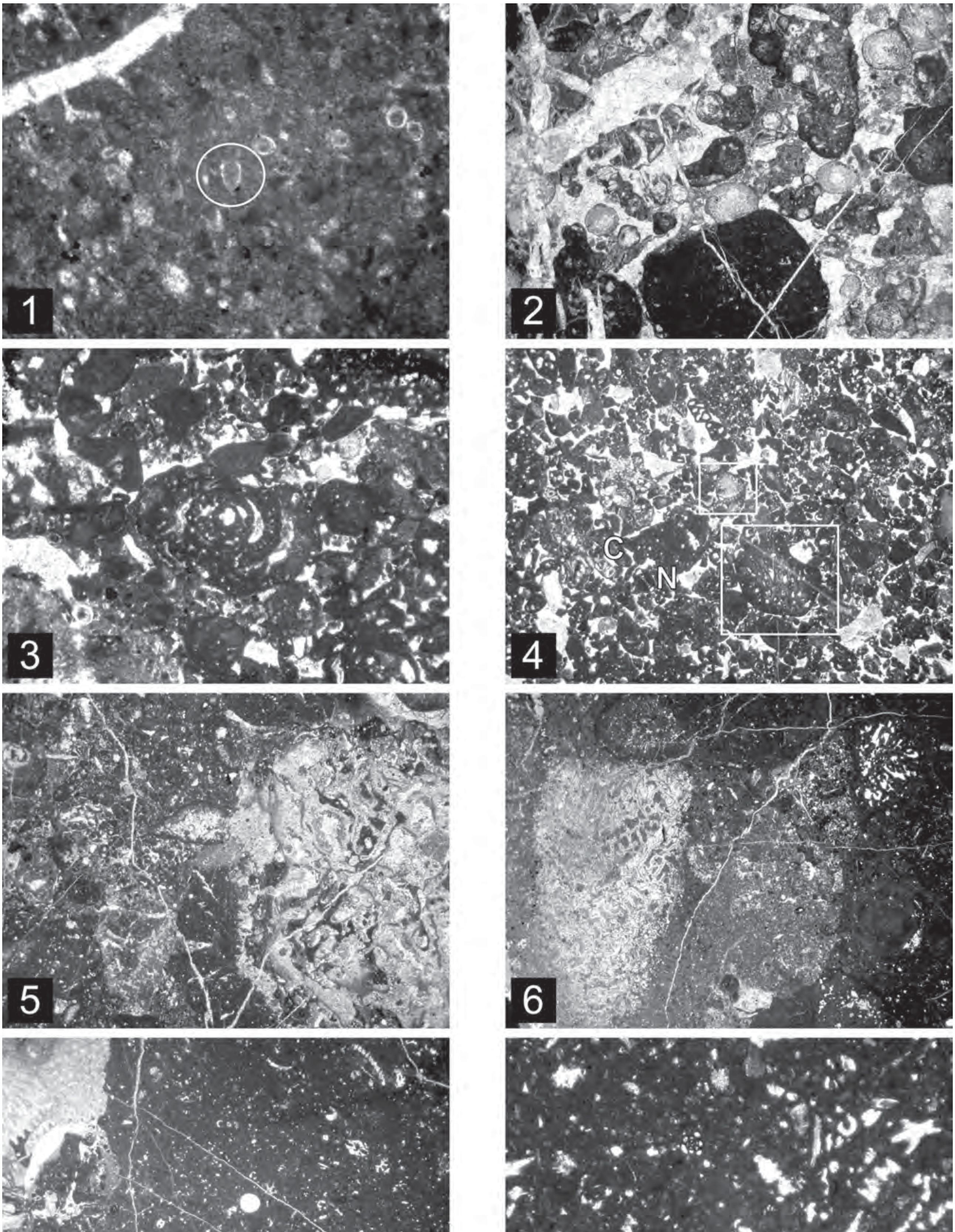
1
2
3
C
N
4
5
6
7
8

Fig. 87: Microfacies of the Late Tithonian succession of the Höherstein Plateau (Oberalm Formation + Barmstein Limestone). Page 273.
1. Calpionellid wacke-/packstone, in the centre *Crassicollaria intermedia* (DURAND-DELGA) (white circle). Sample A-3181. Width of photo: 0.25 cm. **2**. Clast of Late Triassic Dachstein Limestone; bioclastic packstone with numerous specimens of the benthic foraminifer *Triasina hantkeni* MAJZON. Sample D 105. Width of photo: 1.4 cm. **3**. Calciturbidite (packstone) with benthic foraminifer *Pseudocyclammina lituus* (YOKOYAMA). Sample A-3179. Width of photo: 0.5 cm. **4**. Calciturbidite (packstone) with benthic foraminifera, e.g., textulariids, *Nautiloculina oolithica* MOHLER (N), *Andersenolina alpina* (LEUPOLD) (small rectangle, detail see Fig.40/7), *Mohlerina basiliensis* (MOHLER), remains of echinoids and calcareous algae, e.g., *Clypeina jurassica* FAVRE (C) and *Selliporella neocomiensis* (RADOICIC) (large rectangle, detail see Fig. 40, Fig. 12). Sample D 58. Width of photo: 1.4 cm. **5**. Mass flow with clasts from the Plassen Carbonate Platform; on the right a large clast of the platform margin facies with diverse microencrusters. Sample D 67. Width of photo: 1.4 cm. **6**. Mass flow with clasts of the Plassen Carbonate Platform, mostly belonging to the closed lagoon; aside a large stromatoporoid bioclast (*Actinostromaria* cf. *shimizui* YABE & SUGIYAMA). Sample D 100. Width of photo: 1.4 cm. **7**. Clast of the closed lagoonal facies (wackestone with Dasycladales) of the Plassen Carbonate Plattform; on the left stromatoporoid *Milleporidium* sp. Sample D 45. Width of photo: 1.4 cm. **8**. Closed lagoonal facies of the Plassen Carbonate Platform; wackestone with numerous fragments of dasycladalean algae. Sample D 68. Width of photo: 0.5 cm.

creation of a new reef-rim facing the Tauglboden Basin to the north, and the enhanced subsidence with a prominent facies change in the sedimentary succession of the Plassen Carbonate Platform *s. str.* are more or less time-equivalent events (GAWLICK & SCHLAGINTWEIT 2009). This coincidence is due to a general new sedimentological cycle caused by tectonics, which started around the Early/Late Tithonian boundary or in the Late Tithonian.

2.5.2. Salzburg Calcareous Alps

In the Salzburg Calcareous Alps the basinal area between the Wolfgangsee Platform to the north and the Plassen Platform *s. str.* to the south is preserved (Fig. 78). We will visit several outcrops of this basinal sequence. We have visited the transitional part from the underlying radiolarite sediments into the limestone sequence in the Taugl valley (compare chapter 2.3.2). The limestone sequence is of Late Tithonian to earliest Cretaceous age. It consists of deep-water cherty limestones (*Calpionella* Limestone; Oberalm Formation) with upward decreasing radiolarian content. Intercalated mass flows consist of resediments of the Plassen Carbonate Platform *s. str.* (Barmstein Limestone). Beside shallow-water clasts of the contemporaneous Late Tithonian Plassen Carbonate Platform more seldom older (Kimmeridgian to Early Tithonian) clasts from the Plassen Carbonate Platform occur in the Barmstein Limestone also. In addition, clasts from different facies belts of the Tithonian platform were shed as the result of of high-angle normal faults propagating into the interior platform areas, as demonstrated by SCHLAGINTWEIT & GAWLICK (2007). In that manner, characteristic microfacies types, e.g., with specific algal palaeocoenoses, that occur in the Barmstein Limestone, can directly be compared with the Late Tithonian succession of the Plassen Carbonate platform of Mount Plassen. The monotypic *Campbelliella* limestones that characterize the transition from the open to the closed lagoonal depositional area (~ Early to Late Tithonian boundary), however, were obviously not eroded and reworked in the Barmstein Limestone (see Fig. 81/7).

Stop 1: Road cut west of the village Krispl
Late Tithonian cherty limestones and carbonate turbidites (Oberalm Formation): “Maiolica“

The sedimentary succession at the road cut west of the village Krispl consists of a Late Tithonian series of micritic deep-water calpionellid-limestones with intercalated coarse-grained turbiditic layers. This series, defined as Oberalm Formation + Barmstein Limestone represents the Late Tithonian to Berriasian part of the Tauglboden Basin fill and reaches a thickness of around 800 metres in the Osterhorn Mountains (Fig. 74). The deep-water micrites are rich in radiolarians (investigated in detail by STEIGER 1992) and calpionellids. The intercalated carbonate turbidites consist of relatively fine-grained shallow-water debris which derived from the Plassen Carbonate Platform *s. str.* in the south. The shallow-water components and organisms are identical to those in the mass-flow deposits of the Barmstein Limestone (see Stop 2). This outcrop provides the possibility to study different sedimentological features of carbonate turbidites in carbonatic basinal sediments. The intercalated greenish clay material consists exclusively of illite in contrast to the volcanic ashes prevailing in the Early Tithonian sequence. These clay occurrences represent the residual sediment of evaporitic Late Permian Alpine Haselgebirge. Reworked Alpine Haselgebirge occurs as components only in the Late Tithonian sequence of the Oberalm Formation + Barmstein Limestone (e.g., PLÖCHINGER 1974, 1976, GAWLICK et al. 2005). The Alpine Haselgebirge was emplaced around the Oxfordian/Kimmeridgian boundary in the Sandlingalm Basin (see chapter 2.1) and was sealed by the carbonate sediments of the Plassen Carbonate Platform.
Recently this process of resedimentation was interpreted as expression of mountain uplift in the south and the activation of low- and high-angle normal faults (MISSONI & GAWLICK 2011a). These normal faults cut into the older carbonate platform sequences and the underlying evaporites of the Alpine Haselgebirge Mélange. Material from the whole Plassen Carbonate Platform succession and from the evaporitic mélange were mobilized and transported together in the Tauglboden Basin (Fig. 89).

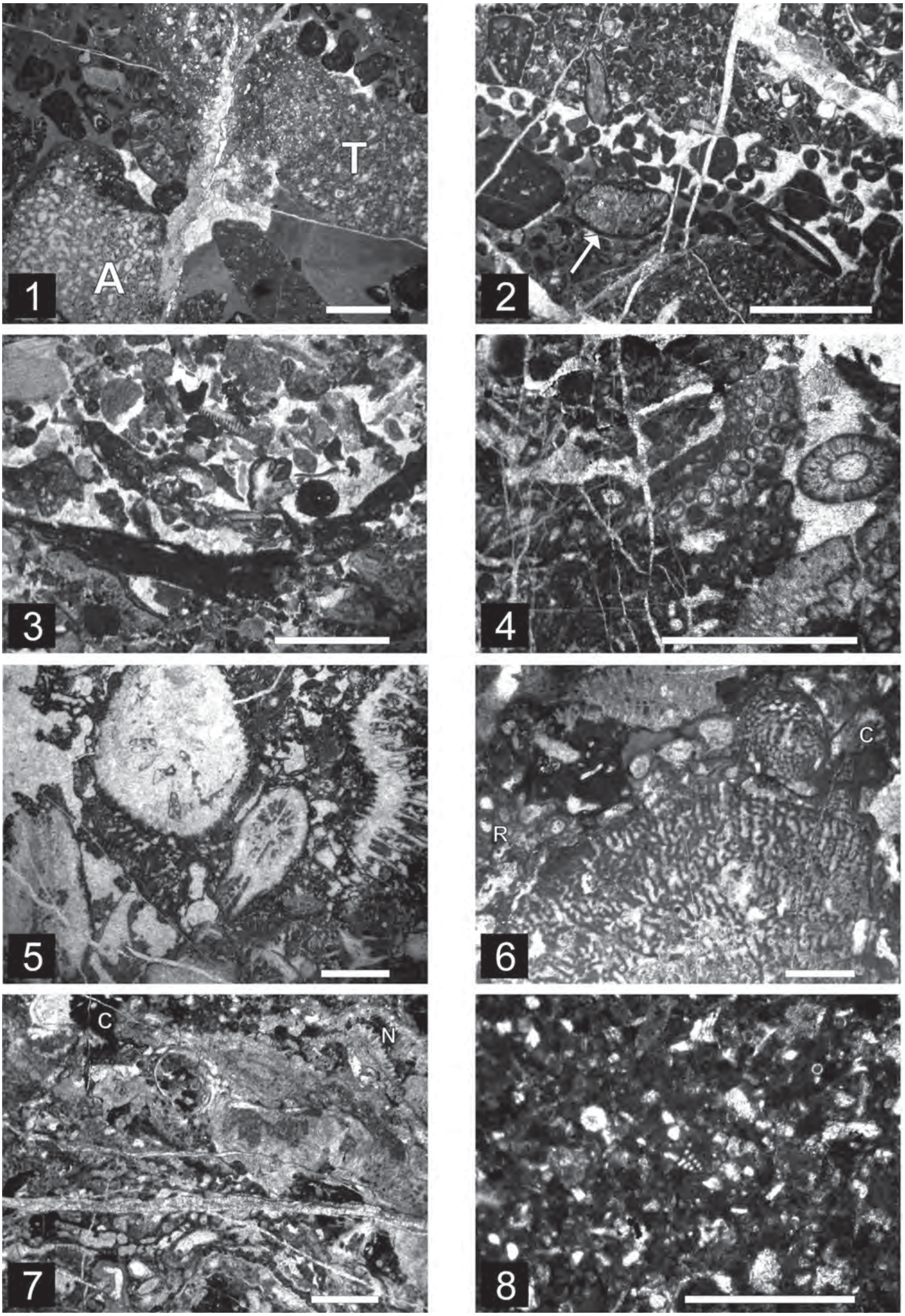
1
A
T
2
3
4
5
6
C
R
7
C
N
8

Fig. 88: Facies evolution of the Wolfgangsee Carbonate Platform of Mount Bürgl. From Gawlick & Schlagintweit (2010). Page 275.
1. Mass flow with Late Triassic extraclasts (T) and Late Jurassic shallow-water clasts and stromatoporoid *Actinostromina grossa* (Germovsek) (A). Sample E 577. Scale bar 2 mm. **2.** Mass flows with extraclasts (? Liassic Klaus Limestone, arrow) and Late Jurassic shallow-water limestones. Sample E 578. Scale bar 2 mm. **3.** Well washed-out packstone with remains of crinoids (C) and microencruster *Crescentiella morronensis* (Crescenti) (CM). Sample E 581. Scale bar 2 mm. **4.** Packstone with dasycladalean algae *Salpingoporella pygmaea* (Gümbel) (right) and a larger unknown taxon (left). Sample E 596. Scale bar 2 mm. **5.** Bioclastic packstone with debris of corals. Sample E 608. Scale bar 2 mm. **6.** Boundstone with "stromatoporoid" sponges, sclerosponges (*Neuropora*, N), microencruster *Crescentiella morronensis* (Crescenti) (C) and *Radiomura cautica* Senowbari-Daryan & Schäfer (R); sample UK 141. Scale bar 2 mm. **7.** Boundstone with microencruster (e.g. *Crescentiella*, C) and sclerosponges (e.g., *Neuropora*, N). Sample E 619. Scale bar 2 mm. **8.** Packstone with radiolarians, calpionellids, sponge spicules, textulariid foraminifera. Sample E 828. Scale bar 1 mm.

Stop 2: Road cut north of the village Adnet, locality Adnet Riedel
Tithonian cherty limestones and mass flows (Barmstein Limestone)

This outcrop is near the old quarry "Adneter Riedel", the type-locality of the Oberalm Formation (compare Schlager 1969). The outcrop provides a series of well-bedded grey deep-water limestones (bed-thickness mostly between 5-10 cm), sometimes with chert layers and nodules (Fig. 90). These deep-water limestones are rich in radiolarians (e.g., Steiger 1992) and calpionellids.
The type-locality of the Barmstein layers (Upper Tithonian–Lower Berriasian), which are intercalated in the Oberalm Formation, is situated northwest of Hallein in the Salzburg Calcareous Alps. The type-locality are the "Kleiner Barmstein" and the "Grosser Barmstein" around the German-Austrian boundary defined by Gümbel (1861) as

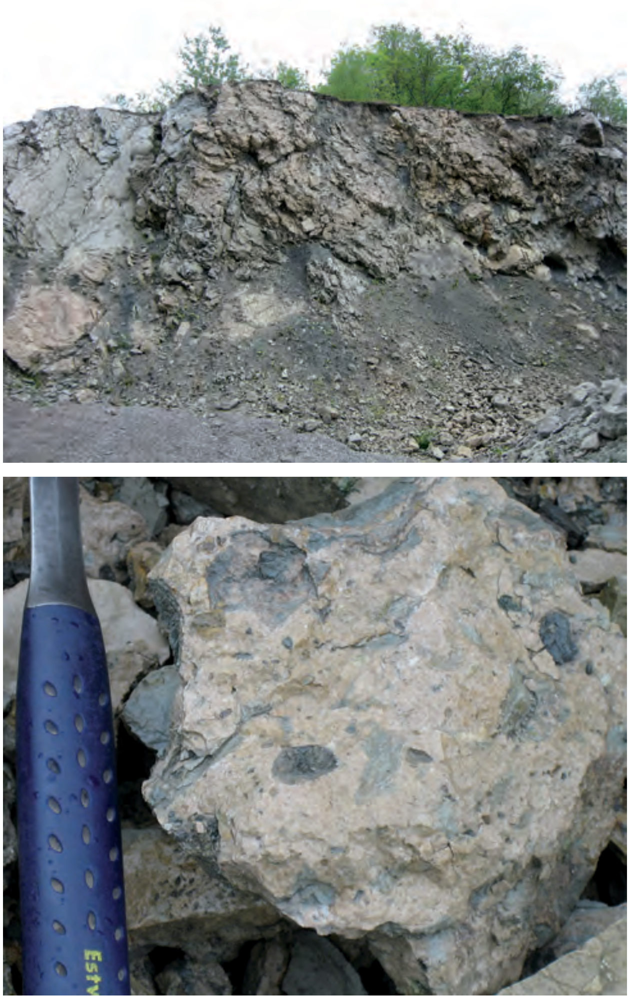

Fig. 89a, b: Special type of Barmstein Limestone with up to metre-sized components of the Permian Alpine Haselgebirge and large blocks of the Plassen Carbonate Platform, intercalated in thin bedded cherty limestones (Oberalm Formation) with Calpionellids. Leube quarry south of Salzburg. See text for explanation.

Fig. 90: Outcrop photo of the Oberalm Formation + Barmstein Limestone on the road cut Adnet Riedel. See text for explanation. The lower part of the succession consists of well bedded grey deep-water limestones with intercalated fine-grained turbiditic carbonate layers. The up to 5 m thick massive bed in the higher part of the succession represents a Barmstein Limestone layer.

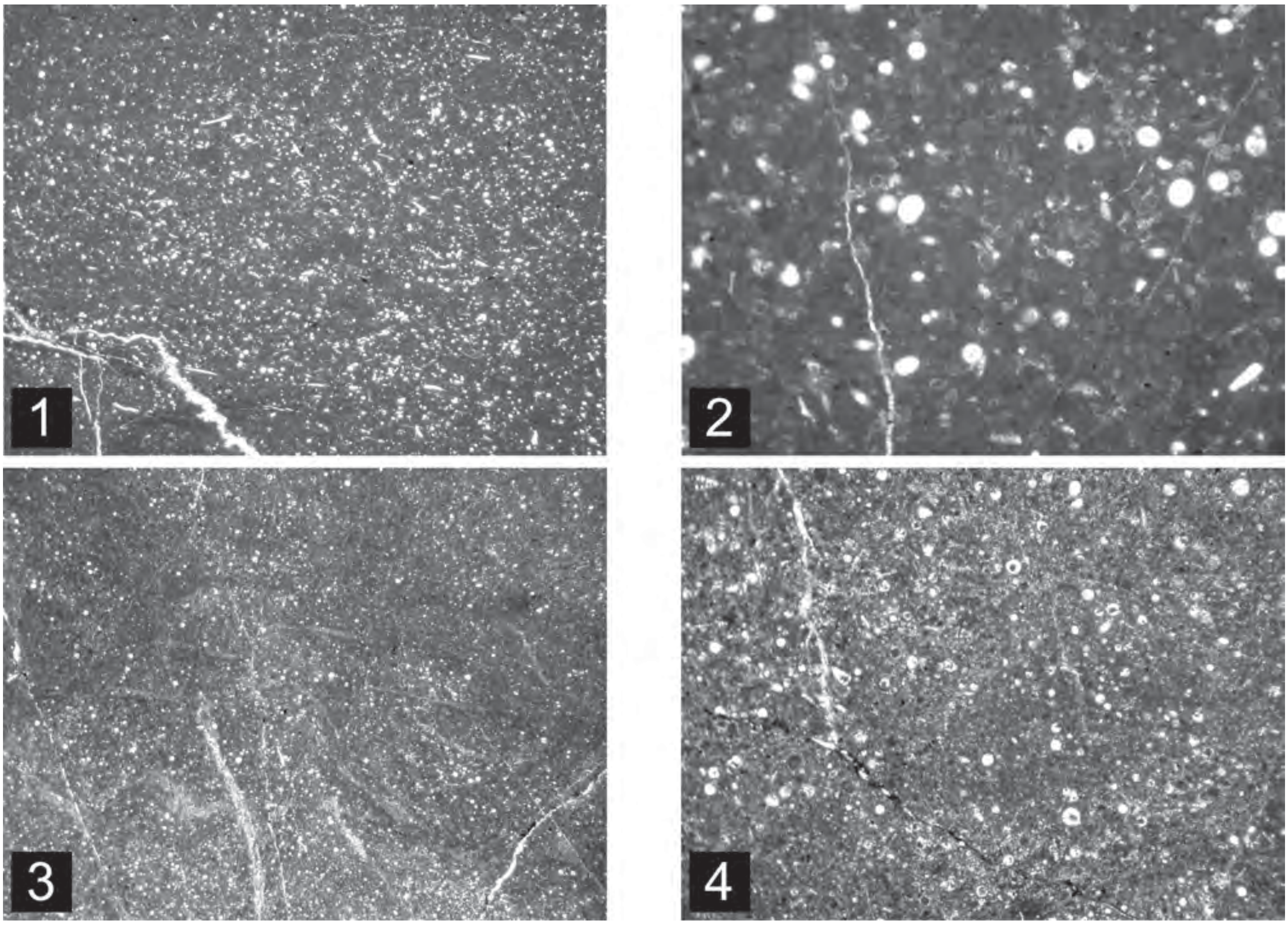

Fig. 91: Microfacies characteristics of the Oberalm Formation (from GAWLICK et al. 2009a).
1. Radiolaria-rich packstone with fine-grained biodetritus, calpionellids and peloids beside some spicula. Most radiolaria and spicula are recrystallized to calcite. Sample D 451, Mount Tressenstein north of the town Bad Aussee (Tirolic units, Salzkammergut area). Width of photo: 1.4 cm. **2**. Magnification of 1. Typical for the Oberalm Formation is the occurrence of calpionellids beside radiolarians. Width of photo: 0.25 cm. **3**. Very fine-grained bioturbated radiolaria wacke- to packstone. All radiolarians are recrystallized. Sample E 52, Mount Ewige Wand northeast of the municipal Bad Goisern (Tirolic units, Salzkammergut area). Width of photo: 1.4 cm. **4**. Magnification of 3. The mostly recrystallized radiolarians occur in a very fine-grained matrix of biodetritus. Width of photo: 0.5 cm.

Fig. 92: Microfacies characteristics of the Barmstein Limestone. In this plate a series of characteristic features of the Barmstein Limestone is figured. The examples mainly stem from the type-locality of the Barmstein Limestone (Mt. Barmstein west of the township Hallein 5 kilometres to the west of the locality Adnet Riedel). Page 278.
1-2. Packstone (component in a mass-flow deposit) with remains of stromatoporoids and reworked clasts of the slope, platform margin and closed lagoonal facies. Samples B 75 and B 82, Mounts Barmsteine west of the town Hallein (Tirolic units, Salzburg Calcareous Alps). Width of photo: 1.4 cm. **3**. Fine-grained calciturbidite (packstone) with debris of echinoids. Sample E 193-1, Mount Jochwand north of the municipal Bad Goisern (Tirolic units, Salzkammergut area). Width of photo: 1.4 cm. **4**. Medium-grained calciturbidite (packstone). Sample E 797, Mount Ewige Wand northeast of the municipal Bad Goisern (Tirolic units, Salzkammergut area). Width of photo: 1.4 cm. **5**. Packstone (mass-flow deposit) with clasts of the Plassen Carbonate Platform from different facies realms (lagoonal areas to reefal areas with slope facies components dominating). Sample E 219-2, Mount Jochwand northwest of the municipal Bad Goisern (Tirolic units, Salzkammergut area). Width of photo: 1.4 cm. **6**. Detail of a mass flow with attaching clasts of high- and low-energetic facies of the Plassen Carbonate Platform. Sample B 84, Mounts Barmsteine west of the town Hallein (Tirolic units, Salzburg Calcareous Alps). Width of photo: 0.5 cm. **7**. Benthic foraminifer *Pseudocyclammina lituus* (YOKOYAMA). Sample E 797, Mount Ewige Wand northeast of the municipal Bad Goisern (Tirolic units, Salzkammergut area). Width of photo: 0.25 cm. **8**. Large dasycladale *Selliporella neocomiensis* (RADOICIC). Sample B 125, Mounts Barmsteine west of the town Hallein (Salzburg Calcareous Alps). Width of photo: 0.5 cm. For details on microfacies see, e.g., FENNINGER & HOLZER (1972), STEIGER (1981, 1992), GAWLICK et al. (2005, 2007b).

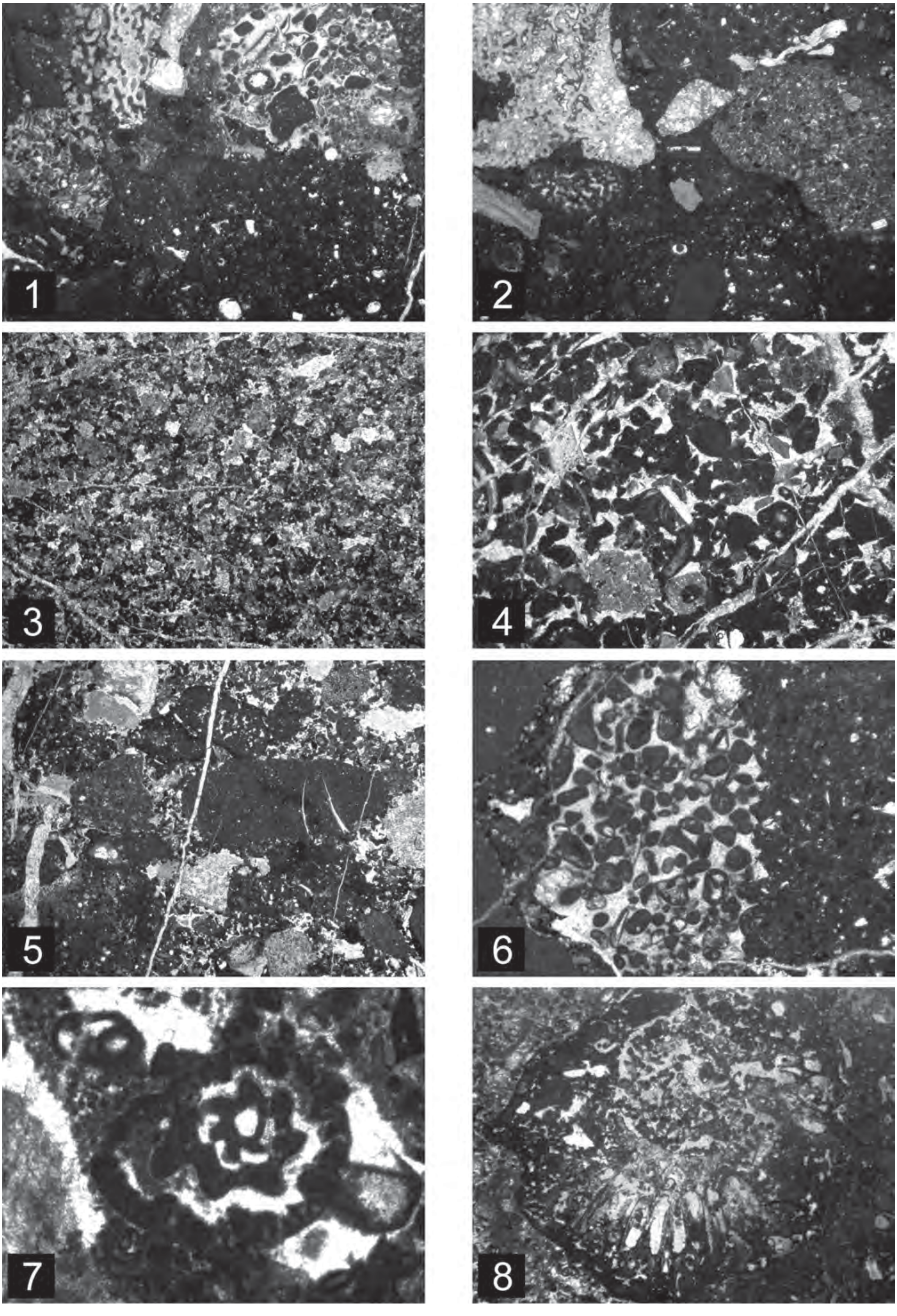
1
2
3
4
5
6
7
8

Barmstein limestone or Barmstein coral limestone. The type section was described in detail by STEIGER (1981, 1992) and GAWLICK et al. (2005). Other important Barmstein Limestone occurrences are for example Mount Höherstein (see GAWLICK et al. 2007), Mount Sandling, Mount Jochwand, Mount Ewige Wand, and Mount Zwerchwand (see GAWLICK et al. 2010). Beside contemporaneous shallow-water material from the newly formed reef rim at the border between the Plassen Carbonate Platform *s. str.* and the Tauglboden Basin, also older components from the Kimmeridgian to Early Tithonian carbonate platform occurred as clasts in the Barmstein Limestone (e.g., SCHLAGINTWEIT & GAWLICK 2007). The dark-grey clay pebbles in the Barmstein Limestone derive from the Late Permian Alpine Haselgebirge Mélange as proven by PLÖCHINGER (1976, 1984).

3. Summary

The Hettangian to Aalenian period was controlled by the following factors:

A) the end-Triassic morphology and biotic crisis,
B) crustal extension in the Penninic realm and in the adjacent Austroalpine domains, resulting in the break-up of the South Penninic Ocean as part of the Alpine Atlantic in the Toarcian, and
C) the onset of inneroceanic thrusting around the Pliensbachian/Toarcian boundary in the Neotethys Ocean.

The Bajocian to Tithonian period was mainly controlled by these circumstances:

A) the Toarcian/Aalenian morphology after the break-up of the Alpine Atlantic Ocean (South Penninic (Piemont) Ocean),
B) the onset of inneroceanic subduction in the Neotethys realm and the formation of a propagating thrust belt, starting in the outer shelf area (Meliata and Hallstatt Zones) in the Bajocian and propagating towards the Tirolic realm in Oxfordian time,
C) the newly formed carbonate platform on top the nappe stack since the Late Oxfordian,
D) the gravitational collapse of this carbonate platform around the Early/Late Tithonian boundary due to uplift in the south and normal faulting in the north.

The Middle to Late Jurassic orogeny resulted in the destruction of the Neotethys-ward Middle Triassic to Early Jurassic passive continental margin (the Triassic south-eastern margin of Europe; Fig. 6) which had experienced crustal extension since Late Permian time. In late Early to Middle Jurassic times the geodynamic regime became convergent and inneroceanic subduction in the Neotethys Ocean commenced. As a consequence, the continental margin become tilted, progressively imbricated with the distal shelf area of the Meliata and Hallstatt Salzberg facies zones involved in stacking first, and obducted by ophiolites. Trench-like basins formed in front of advancing nappes.
As expression of this evolution in the Pliensbachian, sedimentation in the Hallstatt Zone changed from condensed cherty limestones to far more rapidly deposited massive dark-grey, clay-rich siliceous marls and cherty limestones (O´DOGHERTY & GAWLICK 2008). The thickness of the sediments increased accordingly. In Late Toarcian to Aalenian times a thick siliceous marly-sedimentary succession was deposited. This change is interpreted as an effect of tilting and faulting of the distal passive margin due to the onset of thrusting in the Neotethys oceanic realm. Late Early to early Late Jurassic inneroceanic subduction is proven by metamorphic soles in the Dinarides (176-157

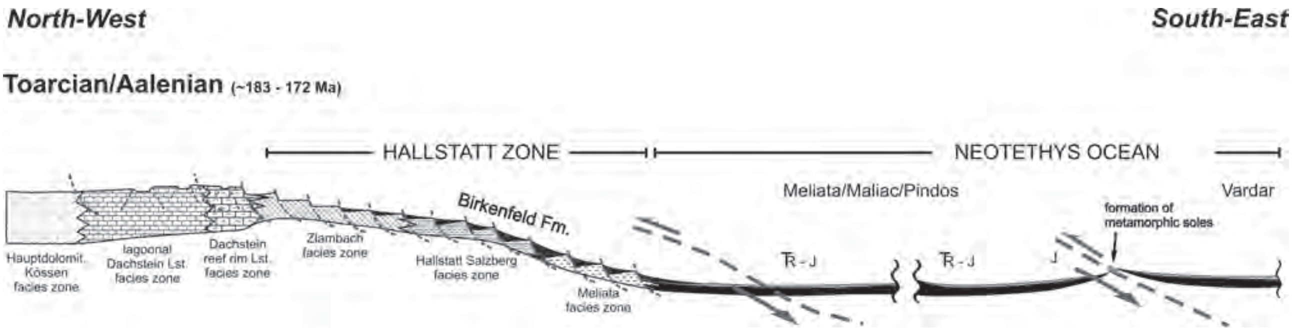

Fig. 93: Reconstruction of the Toarcian/Aalenian to Callovian geodynamic evolution. Absolute ages after GRADSTEIN et al. (2004). See text for further explanation. NW-SE directions refer to Triassic-Jurassic palaeogeographic coordinates. Onset of inneroceanic southeastward subduction in Neotethys Ocean (GAWLICK et al. 2008; for discussion see: KARAMATA 2006). Late Early to early Late Jurassic inneroceanic subduction is proven by metamorphic soles in the Dinarides (176-157 Ma: KARAMATA 2006), Albanides (174-162 Ma: DIMO-LAHITTE et al. 2001), and Hellenides (181-172 Ma: RODDICK et al. 1979, SPRAY & RODDICK 1980). Occurrences of supra-subduction volcanics in the ophiolite belt of Albania reflect an inneroceanic subduction stage (SHALLO & DILEK 2003, KOLLER et al. 2006). Contemporaneously, the first ophiolithic mélanges were formed (BABIC et al. 2002). Slight south-eastward tilt of distal continental margin, formation of half-grabens in the Hallstatt Zone and horst-and-graben structure in Dachstein Limestone facies zone since the Late Pliensbachian (Adnet Scheck event: BERNOULLI & JENKYNS 1974, BÖHM et al. 1995) belong to this event. In the Hallstatt Zone the normal faults cut into the Rhaetian Zlambach marls which probably acted as source area for the clay content in the Birkenfeld Formation beside eroded ophiolites. After MISSONI & GAWLICK (2011a).

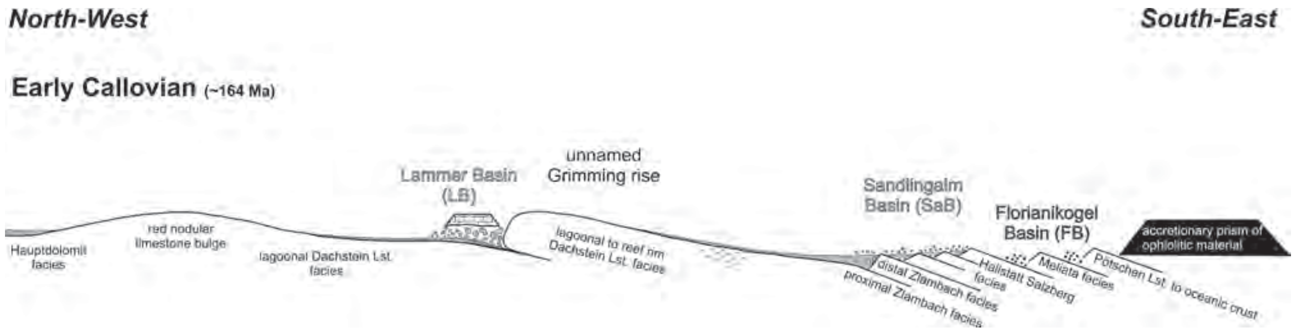

Fig. 94: Reconstruction of the Early Callovian geodynamic evolution. Absolute ages after GRADSTEIN et al. (2004). See text for further explanation. NW-SE directions refer to Triassic-Jurassic palaeogeographic coordinates. The Florianikogel Basin (?Bajocian-Callovian; *FB*) constitutes the oldest radiolaritic trench-like basin in the most oceanward position. In the Early Callovian continentward propagation of thrusting led to the formation of the Sandlingalm Basin (*SaB*) in the Hallstatt Zone and to the formation of the Lammer Basin (*LB*) in the lagoonal Dachstein Limestone facies zone. In this early stage of the Lammer Basin only local material was shed from nearby source regions. Continentward a flexural bulge formed which was characterized by red nodular limestone deposition. This bulge with condensed sedimentation prevailed until the Callovian/Oxfordian boundary (e.g., HUCKRIEDE 1971, MANDL 1982) in the area of the later Tauglboden Basin. After MISSONI & GAWLICK (2011a).

Ma: KARAMATA 2006), the Albanides (174-162 Ma: DIMO-LAHITTE et al. 2001), and the Hellenides (181-172 Ma: RODDICK et al. 1979, SPRAY & RODDICK 1980). As an expression of this change, in the Dachstein Limestone facies zone a forebulge horst-and-graben morphology evolved in Late Pliensbachian to Toarcian times.

Thrusting in the Neotethys Ocean passive margin domain started in Bajocian time, creating the Meliata and distal Hallstatt nappes by imbrication of the outermost part of the former passive continental margin (Fig. 93). The Florianikogel Basin (Meliata Mélange) is the most oceanward preserved relic of a Middle Jurassic trench-like radiolarite basin in the Northern Calcareous Alps (Fig. 94). In the next stage of thrusting the Sandlingalm Basin group established. This comprised material mainly from the Hallstatt Salzberg facies zone. Parts of these older two basin fills became remobilised in the later stages of orogeny and can be found as resediments in the younger basin successions.

Further continuous shortening established the proximal Hallstatt nappes (Fig. 95). Farer to the northwest in front of these nappes, new basins formed in the area of the former Dachstein Limestone lagoon in the Callovian and existed until the Oxfordian (Lammer Basin). Continentwards a flexural buldge with red nodular limestone deposition established and prevailed in the area of the later Tauglboden Basin until the Callovian/Oxfordian boundary. Initially the Lammer Basin received local material from the adjacent nappe front. Later, in the Middle/Late Callovian to Middle Oxfordian, the Zlambach facies zone became imbricated and uplifted. After that, predominantly eroded material from this fazies domain was shed into the Lammer Basin. Further tectonic shortening caused ongoing obduction of ophiolites, as proven in the Dinarides (SCHMID et al. 2008) or the Albanides (GAWLICK et al. 2008), and partial detachment and NW-directed transport of the older, south-eastern basin groups. Around the Callovian/Oxfordian boundary a northwestward shift of the Lammer Basin axis

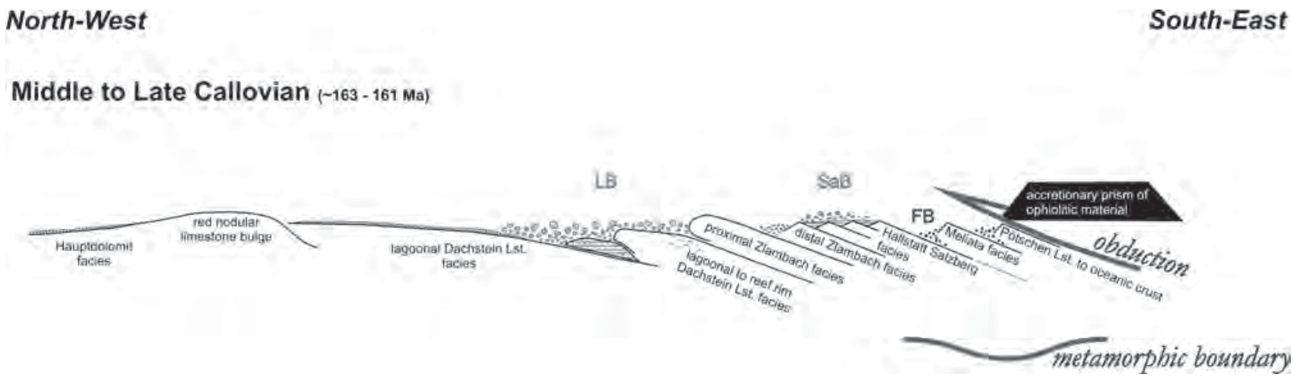

Fig. 95: Reconstruction of the Middle to Late Callovian geodynamic evolution. Absolute ages after GRADSTEIN et al. (2004). See text for further explanation. NW-SE directions refer to Triassic-Jurassic palaeogeographic coordinates. Further tectonic shortening led to the formation of nappe fronts in the Zlambach facies zone. These nappe fronts shed material into the Lammer Basin in Middle Callovian to Middle Oxfordian times. FB: Florianikogel Basin. SaB: Sandlingalm Basin. LB: Lammer Basin. After MISSONI & GAWLICK (2011a).

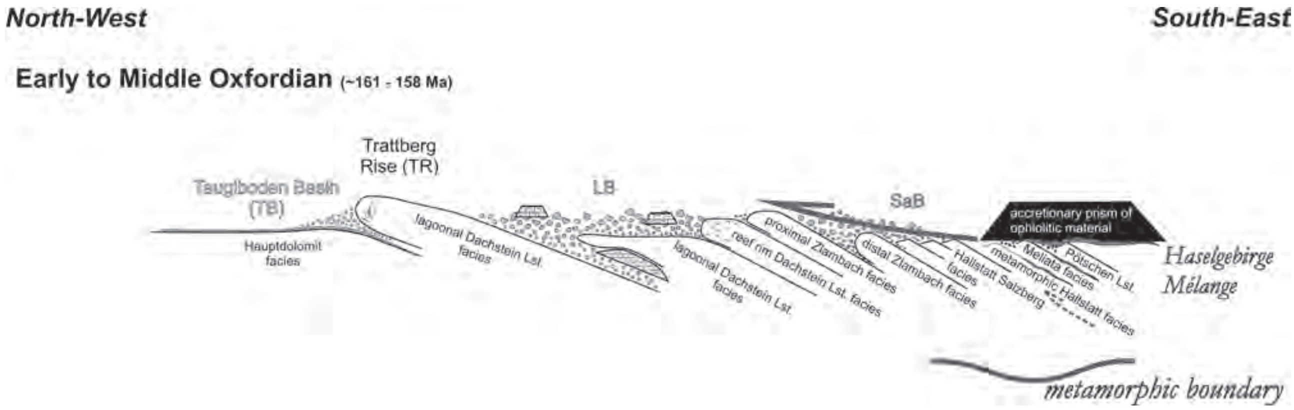

Fig. 96: Reconstruction of the Early to Middle Oxfordian geodynamic evolution. Absolute ages after Gradstein et al. (2004). See text for further explanation. NW-SE directions refer to Triassic-Jurassic palaeogeographic coordinates. Due to further tectonic shortening and ongoing obduction of ophiolites (Dinarides: Schmid et al. 2008, Albanides: Gawlick et al. 2008), the southern basin groups were sheared off and transported towards northwest. Contemporaneously, the basin axis in the Lammer Basin propagated northwestward, too, and the newly formed nappe front in the Dachstein reef rim zone shed its eroded material into this basin. The next nappe front formed in the transitional area of the lagoonal Dachstein Limestone facies zone to the Hauptdolomit facies zone. Eroded material from the uplifted hangingwall (Trattberg Rise) was shed into the newly formed Tauglboden Basin. SaB: Sandlingalm Basin. LB: Lammer Basin. After Missoni & Gawlick (2011a).

can be correlated with the formation of a new nappe front in the Dachstein Limestone reef zone, from which material was shed into this basin. Farther to the southeast, the evaporitic Haselgebirge Mélange (Spötl 1989, Spötl et al. 1998) was formed (Fig. 97). It contains Late Jurassic authigenic feldspars (154-145 Ma: Spötl et al. 1996, 1998), which are interpreted as being related to fluid circulation and mélange formation. The Haselgebirge Mélange carries metamorphosed Hallstatt Limestone, Pötschen Limestone, and Dachstein reefal limestone blocks as well as volcanic rocks, partly with sodic amphiboles (Kirchner 1980a, b), and oceanic basalts, which were metamorphosed under HP/LT conditions (Vozárová et al. 1999) (compare Gawlick & Höpfer 1999, Frank & Schlager 2006).

In the Early Oxfordian, thrust propagation established the upper Tirolic nappe front northwest of the Lammer Basin (Fig. 96) in the area of the Triassic Hauptdolomit lagoon, with the Trattberg Rise as its topographic expression. This rise was an area of intense erosion and the source region for breccias and mass flows in Early to Late Oxfordian times. Continued tectonic shortening led to thrusting over the southeastern margin of the Tauglboden Basin. In ?Middle/Late Oxfordian times, tectonic shortening again propagated northwestwards and the Brunnwinkl Rise was formed (Fig. 96, Fig. 97). This was the northwestern tectonic front of the Jurassic Northern Calcareous Alps

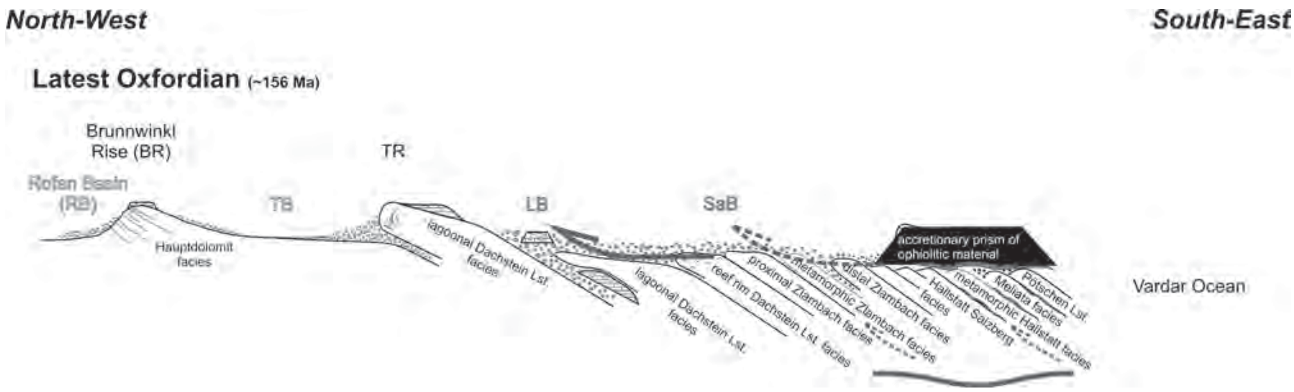

Fig. 97: Reconstruction of the Latest Oxfordian geodynamic evolution. Absolute ages after Gradstein et al. (2004). See text for further explanation. NW-SE directions refer to Triassic-Jurassic palaeogeographic coordinates. Ongoing obduction of the ophiolites, salt flow and tectonically uplifted metamorphosed slices of the Hallstatt Zone resulted in the formation of a chaotic mélange. Northwestward thrusting led to emplacement of a Sandlingalm Basin sheet on top of the Lammer Basin and upramping of the Trattberg Rise (*TR*) onto the south-eastern rim of the Tauglboden Basin. At the northwestern edge, the Brunnwinkl Rise (*BR*) formed as a new nappe front, with the Rofan Basin (*RF*) as trench-like basin in front. The evaporitic Alpine Haselgebirge squeezed out in front of the arriving ophiolite nappes and was emplaced on top of the Sandlingalm Formation until the Early Kimmeridgian. SaB: Sandlingalm Basin. LB: Lammer Basin. After Missoni & Gawlick (2011a).

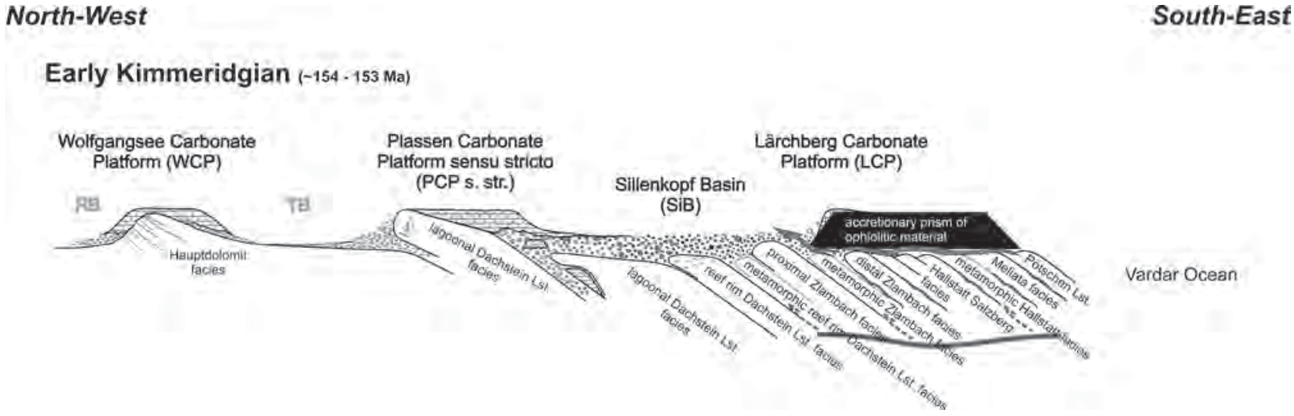

Fig. 98: Reconstruction of the Early Kimmeridgian geodynamic evolution. Absolute ages after GRADSTEIN et al. (2004). See text for further explanation. NW-SE directions refer to Triassic-Jurassic palaeogeographic coordinates. Around the Oxfordian/Kimmeridgian boundary, the formation of shallow-water carbonates on top of the imbricated structures including the obducted ophiolites started. These platforms are summarized as Plassen Carbonate Platform *sensu lato* with the Wolfgangsee Carbonate Platform (*WCP*) in the northwest, the Plassen Carbonate Platform *sensu stricto* (*PCP s. str.*), and the Lärchberg Carbonate Platform (*LCP*) in the southeast. Radiolaritic basins remained as starved basins in between the individual platforms. Delivery of exotic material persisted only into the Sillenkopf Basin (*SiB*). After MISSONI & GAWLICK (2011a).

nappe stack, with the Rofan Basin in its foreland.

In Late Oxfordian time, ongoing ophiolite obduction, salt flow and tectonic uplift of metamorphosed slices of the Hallstatt zone resulted in the creation of a chaotic mélange. The evaporitic Haselgebirge Mélange squeezed out in front of the arriving ophiolite nappes and took position on top of the Sandlingalm Formation around the Oxfordian/Kimmeridgian boundary (Fig. 97). In contrast, in the northwestern part of the preserved nappe stack north of the Hallstatt imbricates, a period of relative tectonic quiescence began. At that time the Plassen Carbonate Platform *sensu lato* started its progradation (Figs. 97, 98). Also the Kimmeridgian to Early Tithonian cherty limestones on top of the mélanges are part of the evolution of the Plassen Carbonate Platform *sensu lato* with the Wolfgangsee Carbonate Platform in the northwest, the Plassen Carbonate Platform *sensu stricto* in central position, and the Lärchberg Carbonate Platform in the southeast. Radiolaritic basins remained as starved basins in between the individual platforms (Fig. 98). At that time only the Sillenkopf Basin received Late Jurassic shallow-water debris, together with exotic clasts. Originating from a southern source area, the latter were transported into the Sillenkopf Basin through channels.

The Kimmeridgian to Early Tithonian time interval was characterized by platform progradation over the adjacent basins. Whereas into the Sillenkopf Basin material was supplied from the platforms on both sides, the Tauglboden

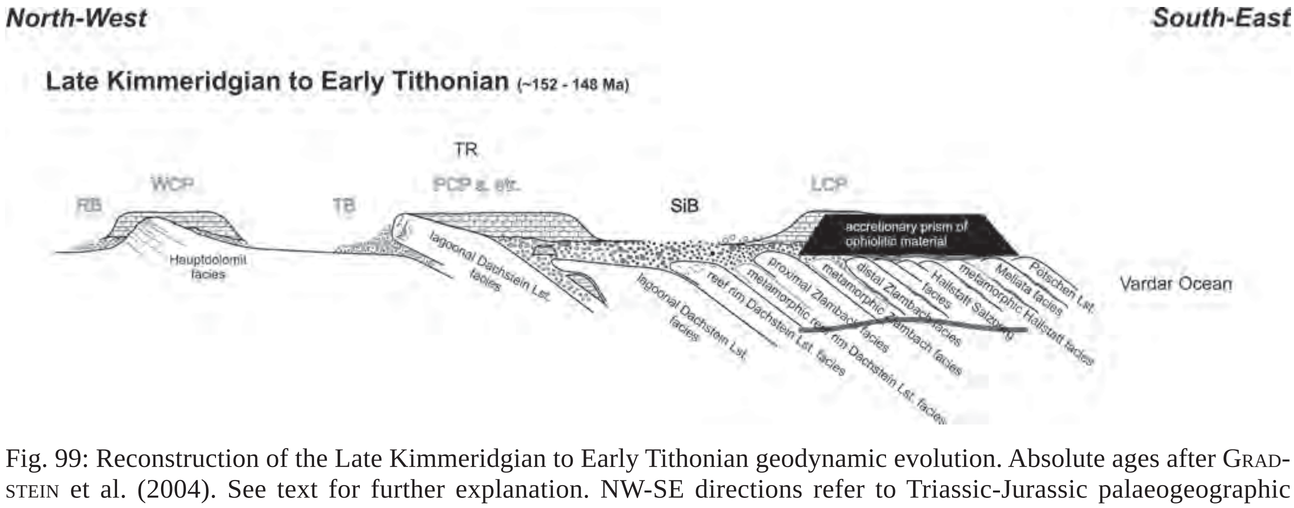

Fig. 99: Reconstruction of the Late Kimmeridgian to Early Tithonian geodynamic evolution. Absolute ages after GRADSTEIN et al. (2004). See text for further explanation. NW-SE directions refer to Triassic-Jurassic palaeogeographic coordinates. This time interval was characterized by platform progradation towards the adjacent basins. Whereas platforms on both sides supplied material into the Sillenkopf Basin, the Tauglboden Basin was shielded to the south by the uplifted Trattberg Rise. In the stacked wedge slight uplift started. WCP: Wolfgangsee Carbonate Platform. TB: Tauglboden Basin. PCP *s. str*.: Plassen Carbonate Platform *sensu stricto*. SiB: Sillenkopf Basin. LCP: Lärchberg Carbonate Platform. After MISSONI & GAWLICK (2011a).

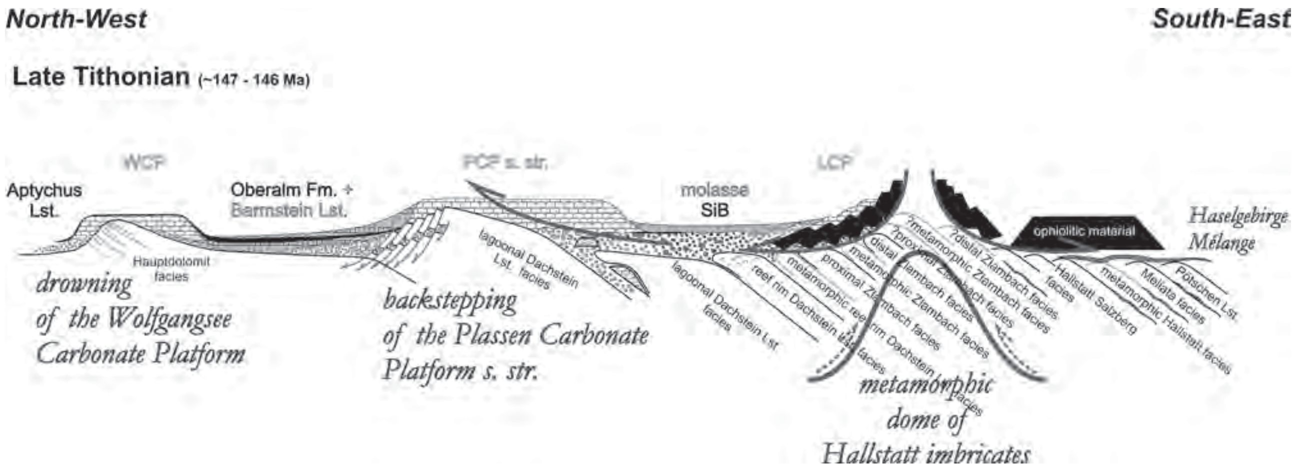

Fig. 100: Reconstruction of the Late Tithonian geodynamic evolution. Absolute ages after Gradstein et al. (2004). See text for further explanation. NW-SE directions refer to Triassic-Jurassic palaeogeographic coordinates. Uplift of the metamorphic dome in the eastern part led to the formation of high- and low-angle normal faults and likely also to strike-slip faults. This led to northwestward transport of several mélange slices and uplift and erosion of parts of the Lärchberg Carbonate Platform (*LCP*). At the northwestern edge, the Trattberg Rise broke down and the Plassen Carbonate Platform *sensu stricto* (*PCP s. str.)* built a new reef rim to the north and shed an enormous amount of carbonate material from there (Oberalm Limestone with intercalated Barmstein Limestone = mass flows consisting mainly of reefal material). Contemporaneously the Wolfgangsee Carbonate Platform (*WCP*) drowned (Gawlick & Schlagintweit 2010). After Missoni & Gawlick (2011a).

Basin was shielded by the uplifted Trattberg Rise in its south (Fig. 99). In the imbricated wedge slight uplift started (Fig. 99).

In the late Early Tithonian, the uplift of the Juvavic nappe pile to the southeast led to northwestward gliding of several mélange blocks along low-angle planes, including the far-travelled „Sandlingalm“ Hallstatt Mélange onto the “Lammer“ Hallstatt Mélange (Figs. 100). Concomitantly, the Plassen Carbonate Platform *sensu stricto* on top of the former Trattberg Rise extensionally collapsed and the Wolfgangsee Carbonate Platform further northwest drowned. The already deeply eroded ramp anticline of the former Trattberg Rise became sealed by hemipelagic sediments with intercalated reef-slope sediments from a newly formed reef rim. In contrast, the southeastern nappe stack with the Lärchberg Carbonate Platform became uplifted around the Jurassic/Cretaceous boundary (Fig. 100). The second metamorphic cycle around 145-135 Ma can most probably be correlated with the increasing heat-flow due to the uplift of the stacked Juvavic (Fig. 100) units in the southeasternmost part of the Northern Calcareous Alps.

The increase of clastic material supply caused the drowning of the Plassen Carbonate Platform *sensu stricto* in Middle to Late Berriasian time and the establishment of a sedimentary succession with increasing siliciclastic input. The Valanginian to Barremian evolution is documented by an increasing supply of siliciclastic and ophiolitic-related detritus into the former Tauglboden/Oberalm Basin area (Rossfeld Molasse - Gawlick et al. 2008). Ongoing uplift of the Juvavic nappe stack in the Early Cretaceous was accompanied by continued erosion and further northwestward gliding of several mélange blocks along low-angle faults in the Valanginian. In the Valanginian and in the Late Barremian, mass-flow deposits with mixed exotic and local material occurred, best explained by regressive cycles at this time (Gradstein et al. 2004). The Rossfeld foreland basin fill and equivalents to the south represents the final stage of the mountain building process along the Neotethys suture (Fig. 3). Around the Barremian/Aptian boundary or in the Early Aptian these basins became filled (Fuchs 1968, Plöchinger 1968, Faupl & Tollmann 1979). This is marked by a facies change to fresh-water conditions with local remnants of coal and amber (Plöchinger 1968).

Acknowledgements

We are thankful for critical discussions on several problems of the Triassic and Jurassic stratigraphy, tectonics and palaeogeography to: e.g., Roman Aubrecht (Bratislava), Matthias Auer (Bissingen/Teck), Daniel Bernoulli (Basel), Florian Böhm (Kiel), Geza Császár (Budapest), Volker Diersche (Sulzfeld/Main), Oskar Ebli (Munich), Nikolaus Froitzheim (Bonn), Bernhard Fügenschuh (Innsbruck), Spela Gorican (Ljubljana), Hans-Jürgen Gursky (Clausthal-Zellerfeld), János Haas (Budapest), Lirim Hoxha (Tirana), Adrian Kosir (Ljubljana), Sándor Kovács (Budapest), Leopold Krystyn (Vienna), Richard Lein (Vienna), Agustin Martin-Algarra (Granada), Csaba Pero (Budapest), Dusan Plasienka (Bratislava), Luis O´Dogherty (Cadiz), Michael Rasser (Stuttgart), Stefan Schmid (Basel), Josip Tisljar (Zagreb), Ivo Velic (Zagreb), Igor Vlahovic (Zagreb), Andreas Wetzel (Basel), Heinrich Zankl (Marburg/Lahn). Thanks to Matthias Auer (Bissingen/Teck) and R. Lein (Vienna) for several thin sections and radiolarian samples.

The results of FWF-projects P 14131 TEC, P 15060 TEC and P 16812-B06 form partly the base of this work. Financial support from a DAAD scholarship (SM), the Aktion Austria-Hungary and a lot of WTZ-projects (HJG, SM) is gratefully acknowledged. Thanks to the Salinen Austria AG for the permission to investigate the salt-mines Bad Dürrnberg, Altaussee, Hallstatt and Bad Ischl. Thanks to the Landratsamt Bad Reichenhall and J. Seidenschwarz (Nationalpark Berchtesgaden) for the permissions to work in the National Park Berchtesgaden. Thanks to the ÖBF in Bad Goisern for permission to use the forest roads in the Salzkammergut area for sample transports by car.

References

AUER, M., GAWLICK, H.-J., SUZUKI, H. & SCHLAGINTWEIT, F. (2009): Spatial and temporal development of siliceous basin and shallow-water carbonate sedimentation in Oxfordian Northern Calcareous Alps. - Facies, **55**: 63-87, (Springer) Berlin Heidelberg.

BABIC, L., HOCHCHULI, P.A. & ZUPANIC, J. (2002): The Jurassic ophiolite mélange in the NE Dinarides: dating, internal structure and geotectonic implications. - Eclogae geologicae Helvetiae, **95**: 263-275, Basel.

BASSOULLET, J.-P. (1997): Les Grands foraminifères. - (In: CARIOU, E. & HANTZPERGUE, P. (coord.), Biostratigraphie du Jurassique ouest-européen et Méditerranéen: zonations paralléles et distribution et microfossiles), Bull. Centres Rech. Explor.-Prod. Elf-Aquitaine, Mém., **17**: 293-304, Pau.

BAUMGARTNER, P.O. (1984): A Middle Jurassic-Early Cretaceous low-latitude radiolarian zonation based on Unitary Associations and age of Tethyan radiolarites. - Eclogae geologicae Helvetiae, **77**: 729-837, Basel.

BAUMGARTNER, P.O. (1987): Age and genesis of Tethyan Jurassic Radiolarites. - Eclogae geologicae Helvetiae, **80**: 831-879, Basel.

BAUMGARTNER, P.O., BARTOLINI, A., CARTER, E.S., CONTI, M., CORTESE, G., DANELIAN, T., DE WEVER, P., DUMITRICA, P., DUMITRICA-JUD, R., GORICAN, S., GUEX, J., HULL, D.M., KITO, N., MARCUCCI, M., MATSUOKA, A., MURCHEY, B., O´DOGHERTY, L., SAVARY, J., VISHNEVSKAYA, V., WIDZ, D. & YAO, A. (1995a): Middle Jurassic to Early Cretaceous Radiolaria Biochronology of Tethys based on Unitary Associations. - (In: BAUMGARTNER, P.O., O´DOGHERTY, L., GORICAN, S., URQUHART, E., PILLEVUIT, A. & DE WEVER, P. (Eds.): Middle Jurassic to Lower Cretaceous Radiolaria of Tethys: Occurrences, Systematics, Biochronology), Memoires de Geologie, **23**: 1013-1048, Lausanne.

BAUMGARTNER, P.O., O´DOGHERTY, L., GORICAN, S., DUMITRICA-JUD, R., DUMITRICA, P., PILLEVUIT, A., URQUHART, E., MATSUOKA, A., DANELIAN, T., BARTOLINI, A., CARTER, E.S., DE WEVER, P., KITO, N., MARCUCCI, M. & STEIGER, T. (1995b): Radiolarian catalogue and systematics of Middle Jurassic to Early Cretaceous Tethyan genera and species. - (In: BAUMGARTNER, P.O., O´DOGHERTY, L., GORICAN, S., URQUHART, E., PILLEVUIT, A. & DE WEVER, P. (Eds.): Middle Jurassic to Lower Cretaceous Radiolaria of Tethys: Occurrences, Systematics, Biochronology), Memoires de Geologie, **23**: 37-685, Lausanne.

BECCARO, P. (2004): Upper Jurassic radiolarians from Inici Mount area (north-western Sicily, Italy): biochronology and calibration by ammonites. - Rivista Italiana Paleontologia Stratigrafia, **110**/1: 289-301, Milano.

BECCARO, P. (2006): Radiolarian correlation of Jurassic siliceous successions of the Rosso Ammonitico Formation in the Southern Alps and Western Sicily (Italy). - Eclogae geologicae Helvetiae, **99** (2006), Supplement 1: S21-S33, Basel.

BECHSTÄDT, TH. & MOSTLER, H. (1974): Mikrofazies und Mikrofauna mitteltriadischer Beckensedimente der Nördlichen Kalkalpen Tirols. - Geologisch Paläontologische Mitteilungen Innsbruck, **4**: 5/6, 1-74, Innsbruck.

BECHSTÄDT, TH. & MOSTLER, H. (1976): Riff-Becken-Entwicklung in der Mitteltrias der westlichen Nördlichen Kalkalpen. - Zeitschrift der Deutschen Geologischen Gesellschaft, **127**: 271-289, München.

BECHTEL, A., GAWLICK, H.-J., GRATZER, R., TOMASELLI, M. & PÜTTMANN, W. (2007): Molecular indicators of palaosalinity and depositional environment of small scale basins within carbonate platforms: The Late Triassic Hauptdolomite section Wiestalstausee near Hallein (Northern Calcareous Alps, Austria). - Organic Geochemistry, **38**: 92-111, Elsevier. doi:10.1016/j.orggeochem.2006.08.016

BERNOULLI, D. & JENKYNS, H.C. (1974): Alpine, Mediterranean, and central Atlantic Mesozoic facies in relation to the early evolution of the Tethys. - SEPM Special Publications, **19**: 129-160, Tulsa.

BERNOULLI, D. & JENKYNS, H. (2009): Ancient oceans and continental margins of the Alpine-Mediterranean Tethys: deciphering clues from Mesozoic pelagic sediments and ophiolites. - Sedimentology, **56**: 149-190, (Blackwell) Oxford.

BÖHM, F. (1992): Mikrofazies und Ablagerungsmilieu des Lias und Dogger der Nordöstlichen Kalkalpen. - Erlanger Geologische Abhandlungen, **121**: 55-217, Erlangen.

BÖHM, F. (2003): Lithostratigraphy of the Adnet Group (Lower to Middle Jurassic, Salzburg, Austria). - (In: PILLER, W.E. (Ed.): Stratigraphia Austriaca. Österreichische Akademie der Wissenschaften), Schriftenreihe der Erdwissenschaftlichen Kommissionen, **16**: 231-268, (Österreichische Akademie Wissenschaften) Wien.

BÖHM, F., DOMMERGUES, J.L. & MEISTER, C. (1995): Breccias of the Adnet Formation: indicators of a Mid-Liassic event in the Northern Calcareous Alps (Salzburg/Austria). - Geologische Rundschau, **84**: 272-286, Berlin Heidelberg.

BOSELLINI, A. & WINTERER, E.L. (1975): Pelagic limestone and radiolarite of the Tethyan Mesozoic. - Geology, **3**: 279-282, Boulder.

BRANDNER, R. (1984): Meeresspiegelschwankungen und Tektonik in der Trias der NW-Tethys. - Jahrbuch der Geologischen Bundesanstalt, **126**: 435-475, Wien.

BRANDNER, R. & RESCH, W. (1981): Reef development in the Middle Triassic (Ladinian and Cordevolian) of the Northern Limestone Alps near Innsbruck, Austria. - SEPM Special Publication, **30**: 203-231, Tulsa.

BRAUN, R. (1998): Die Geologie des Hohen Gölls. Torrener-Joch-Zone/Jenner/Hoher Göll - eine durch Kontinent/Kontinent-Kollision ausgelöste Gleitdecke in den Tauglbodenschichten (mittlerer Oberjura) der Berchtesgadener Alpen. - Nationalpark Berchtesgaden, Forschungsbericht **40**: 1-192, (Plenk) Berchtesgaden.

CHANNELL, J.E.T., BRANDNER, R., SPIELER, A. & SMATHERS, N.P. (1990): Mesozoic paleogeography of the Northern Calcareous Alps - evidence from paleomagnetism and facies analysis. - Geology, **18**: 828-831, Boulder.

CHANNELL, J.E.T., BRANDNER, R., SPIELER, A. & STONER, J.S. (1992): Paleomagnetism and paleogeography of the Northern Calcareous Alps (Austria). - Tectonics, **11**: 792-810, Washington.

CHANNELL J.E.T. & KOZUR H.W. (1997): How many oceans? Meliata, Vardar, and Pindos oceans in the Mesozoic Alpine paleogeography. - Geology, **25**: 183-186, Boulder.

CSONTOS, L. & VÖRÖS, A. (2004): Mesozoic plate tectonic reconstruction of the Carpathian region. - Palaeogeography, Palaeoclimatology, Palaeoecology, **210**: 1-56, Amsterdam.

DAL PIAZ, G.V. (1999): The Austroalpine-Piemont nappe stack and the puzzle of Alpine Tethys. - Memoir Societa Geologia Italiana, **51**: 155-176, Padova.

DARGA, R. & SCHLAGINTWEIT, F. (1991): Mikrofazies, Paläontologie und Stratigraphie der Lerchkogelkalke (Tithon-Berrias) des Dietrichshorns (Salzburger Land, Nördliche Kalkalpen). - Jahrbuch der Geologischen Bundesanstalt, **134**/2: 205-226, Wien.

DECKER, K., PERESSON, H. & FAUPL, P. (1994): Die miozäne Tektonik der östlichen Kalkalpen: Kinematik, Paläospannungen und Deformationsaufteilung während der „lateralen Extrusion" der Zentralalpen. - Jahrbuch der Geologischen Bundesanstalt, **137**: 5-18, Wien.

DERCOURT, J., RICOU, L.E. & VRIELYNCK, B. (1993): Atlas Tethys Palaeoenvironmental Maps. - Gauthier-Villars, Paris.

DERCOURT, J., ZONENSHAIN, L.P., RICOU, L.E., KAZMIN, V.G., LE PICHON, X., KNIPPER, A.L., GRANDJACQUET, C., SBORTSHIKOV, L.M., GEYSSANT, J., LEPVRIER, C., PECHERSKY, D.H., BOULIN, J., SIBUET, J.C., SAVOSTIN, L.A., SOROKHTIN, O., WESTPHAL, M., BAZHENOV, M.I., LAUER, J.P. & BIJU-DUVAL, B. (1986): Geological Evolution of the Tethys Belt from the Atlantic to the Pamirs since the Lias. - Tectonophysics, **123**: 241-315, Amsterdam.

DE WEVER, P., DUMITRICA, P., COULET, J.P., NIGRINI, C. & CARIDOIT, M. (2001): Radiolarians in the Sedimentary Record. - 1-533, (Gordon and Breach Science Publishers) Amsterdam.

DIERSCHE, V. (1978): Upper Jurassic Radiolarites in the Northern Calcareous Alps. - International Union. Commission on Geodynamics, Scientific report, **38**: 113-117, Stuttgart.

DIERSCHE, V. (1980): Die Radiolarite des Oberjura im Mittelabschnitt der Nördlichen Kalkalpen. - Geotektonische Forschungen, **58**: 1-217, Stuttgart.

DIMO-LAHITTE, A., MONIE, P. & VERGELY, P. (2001): Metamorphic soles from the Albanian ophiolites, pertrology, $^{40}Ar/^{39}Ar$ geochronology, and geodynamic evolution. - Tectonics, **20**: 78-96, Washington.

DONOFRIO, D.D., BRANDNER, R. & POLESCHINSKI, W. (2003): Conodonten der Seefeld-Formation: ein Beitrag zur Bio- und Lithostratigraphie der Hauptdolomit-Plattform (Obertrias, westliche Nördliche Kalkalpen, Tirol). - Geologisch-Paläontologische Mitteilungen Innsbruck, **26**: 91-107, Innsbruck.

DULLO, W.C. & LEIN, R. (1982): Facies and environment of the Leckkogel Beds (Carnian; Alps). - Facies, **6**: 5-36, Erlangen.

DYA, M. (1992): Mikropaläontologische und fazielle Untersuchungen im Oberjura zwischen Salzburg und Lofer. - 1-138, PhD-Thesis Technische Universität Berlin, Berlin.

EBERLI, G.P. (1988): The evolution of the southern continental margin of the Jurassic Tethys Ocean as recorded in the Allgäu Formation of the Austroalpine nappes of Graubünden (Switzerland). - Eclogae geologicae Helvetiae, **81**: 175-214, Basel.

EBLI, O. (1997): Sedimentation und Biofazies an passiven Kontinentalrändern: Lias und Dogger des Mittelabschnittes der Nördlichen Kalkalpen und des frühen Atlantik (DSDP site 547B, Marokko). - Münchner Geowissenschaftliche Abhandlungen, Reihe A, **32**: 1-255, München.

FAUPL, P. & TOLLMANN, A. (1979): Die Roßfeldschichten: Ein Beispiel für Sedimentation im Bereich einer tektonisch aktiven Tiefseerinne aus der kalkalpinen Unterkreide. - Geologische Rundschau, **68**: 93-120, Stuttgart.

FAUPL, P. & WAGREICH, M. (2000): Late Jurassic to Eocene palaeogeography and geodynamic evolution of the Eastern Alps. - Mitteilungen der Österreichischen Geologischen Gesellschaft, **92** (1999): 79-94, Wien.

FENNINGER, A. (1969): Die Hydrozoenfauna des Sandling (Kimmeridgium, Nördliche Kalkalpen). - Anzeiger der Österreichischen Akademie der Wissenschaften, mathematisch-naturwissenschaftliche Klasse, **1969**/2: 33-35, Wien.

FENNINGER, A. & HOLZER, H.L. (1972): Fazies und Paläogeographie des oberostalpinen Malms. - Mitteilungen der Geologischen Gesellschaft in Wien, **63** (1970): 52-141, Wien.

FISCHER, A.G. (1965): Eine Lateralverschiebung in den Salzburger Kalkalpen. - Verhandlungen der Geologischen Bundesanstalt, **1965**: 20-33, Wien.

FLÜGEL, E. (1981): Paleoecology and facies of Upper Triassic reefs in the Northern Calcareous Alps. SEPM Special Publication, **30**: 291-359, Tulsa.

FRANK, W. & SCHLAGER, W. (2006): Jurassic strike slip versus subduction in the Eastern Alps. - International Journal of Earth Sciences, **95**: 431-450, Berlin Heidelberg.

FRISCH, W. (1979): Tectonic Progradation on Plate Tectonic Evolution of the Alps. - Tectonophysics, **60**: 121-139, Amsterdam.

FRISCH, W. (1980a): Plate motions in the Alpine region and their correlation to the opening of the Atlantic ocean. - Mitteilungen österreichische Geologische Gesellschaft, **71/72**: 45-48, Wien.

FRISCH, W. (1980b): Plate motions in the Alpine region and their correlation to the opening of the Atlantic ocean. - Geologische Rundschau, **70**: 402-411, Stuttgart.

FRISCH, W. & GAWLICK, H.-J. (2003): The nappe structure of the central Northern Calcareous Alps and its disintegration during Miocene tectonic extrusion - a contribution to understanding the orogenic evolution of the Eastern Alps. - International Journal of Earth Sciences, **92**: 712-727, Berlin Heidelberg.

FROITZHEIM, N., PLASIENKA, D. & SCHUSTER, R. (2008): Alpine tectonics of the Alps and Western Carpathians. - (In: MCCANN, T. (Ed.): The Geology of Central Europe, Volume 2: Mesozoic and Cenozoic), 1141-1232, Geological Society London, London.

FUCHS, W. (1968): Eine bemerkenswerte, tieferes Apt belegende Foraminiferenfauna aus den konglomeratischen Oberen Roßfeldschichten von Grabenwald (Salzburg). - Verhandlungen der Geologischen Bundesanstalt, **1968**: 87-97, Wien.

GALLET, Y., KRYSTYN, L. & BESSE, J. (1998): Upper Anisian to Lower Carnian magnetostratigraphy from the Northern Calcareous Alps (Austria). - Journal Geophysical Research, **103**: 605-621, Washington.

GARRISON, R.E. & FISCHER, A.G. (1969): Deep water Limestones and Radiolarites of the Alpine Jurassic. - SEPM Special Publication, **14**: 20-56, Tulsa.

GAWLICK, H.-J. (1993): Triassische Tiefwasserfazieskomponenten (Kieselkalke, Radiolarite) in der jurassischen Strubbergbrekzie am Tennengebirgsnordrand (Nördliche Kalkalpen, Österreich). - Jahrbuch der Geologischen Bundesanstalt, **136**/2: 347-350, Wien.

GAWLICK, H.-J. (1996): Die früh-oberjurassischen Brekzien der Stubbergschichten im Lammertal - Analyse und tektonische Bedeutung (Nördliche Kalkalpen, Österreich). - Mitteilungen der Gesellschaft Geologie- und Bergbaustudenten in Österreich, **39/40**: 119-186, Wien.

GAWLICK, H.-J. (1998): Obertriassische Brekzienbildung und Schollengleitung im Zlambachfaziesraum (Pötschenschichten) - Stratigraphie, Paläogeographie und diagenetische Überprägung des Lammeregg-Schollenkomplexes (Nördliche Kalkalpen, Salzburg). - Jahrbuch der Geologischen Bundesanstalt, **141**: 147-165, Wien.

GAWLICK, H.-J. (2000a): Paläogeographie der Ober-Trias Karbonatplattform in den Nördlichen Kalkalpen. - Mitteilungen Gesellschaft Geologie- Bergbaustudenten Österreich, **44**: 45-95, Wien.

GAWLICK, H.-J. (2000b): Die Radiolaritbecken in den Nördlichen Kalkalpen (hoher Mittel-Jura, Ober-Jura). - Mitteilungen Gesellschaft Geologie- Bergbaustudenten Österreich, **44**: 97-156, Wien.

GAWLICK, H.-J. & BÖHM, F. (2000): Sequence and isotope stratigraphy of Late Triassic distal periplatform limestones from the Northern Calcareous Alps (Kälberstein Quarry, Berchtesgaden Hallstatt Zone). - International Journal Earth Sciences, **89**: 108-129, Berlin Heidelberg.

GAWLICK, H.-J. & FRISCH, W. (2003): The Middle to Late Jurassic carbonate clastic radiolaritic flysch sediments in the Northern Calcareous Alps: sedimentology, basin evolution and tectonics - an overview. - Neues Jahrbuch Geologie Paläontologie, Abhandlungen, **230**: 163-213, Stuttgart.

GAWLICK, H.-J. & HÖPFER, N. (1999): Stratigraphie, Fazies und Hochdruck-Mitteltemperatur-Metamorphose der Hallstätter

Kalke der Pailwand (Nördliche Kalkalpen, Österreich). - Zeitschrift der Deutschen Geologischen Gesellschaft, **150**: 641-671, Hannover.

GAWLICK, H.-J. & SCHLAGINTWEIT, F. (2006): Berriasian drowning of the Plassen carbonate platform at the type-locality and its bearing on the early Eoalpine orogenic dynamics in the Northern Calcareous Alps (Austria). - International Journal of Earth Sciences, **95**: 451-462, Berlin Heidelberg.

GAWLICK, H.-J. & SCHLAGINTWEIT, F. (2009): Revision of the Tressenstein limestone: reinterpretation of the Late Jurassic to ?Early Cretaceous sedimentary evolution of the Plassen Carbonate Platform (Austria, Northern Calcareous Alps). - Journal Alpine Geology (Mitteilungen Gesellschaft Geologie-Bergbaustudenten Österreich), **51**: 1-30, Wien.

GAWLICK, H.J. & SCHLAGINTWEIT, F. (2010): The drowning sequence of Mount Bürgl in the Salzkammergut area (Northern Calcareous Alps, Austria): Evidence for a diachronous Late Jurassic to Early Cretaceous drowning of the Plassen Carbonate Platform. - Austrian Journal of Earth Sciences, **103** (1): 58-75, Wien.

GAWLICK, H.-J. & SUZUKI, H. (1999): Zur stratigraphischen Stellung der Strubbergschichten in den Nördlichen Kalkalpen (Callovium-Oxfordium). - Neues Jahrbuch Geologie Paläontologie, Abhandlungen, **211**: 233-262, Stuttgart.

GAWLICK, H.-J., FRISCH, W., HOXHA, L., DUMITRICA, P., KRYSTYN, L., LEIN, R., MISSONI, S. & SCHLAGINTWEIT, F. (2008): Mirdita Zone ophiolites and associated sediments in Albania reveal Neotethys Ocean origin. - International Journal of Earth Sciences, **97**: 865-881 (Springer) Berlin Heidelberg.

GAWLICK, H.-J., FRISCH, W., VECSEI, A., STEIGER, T. & BÖHM, F. (1999a): The change from rifting to thrusting in the Northern Calcareous Alps as recorded in Jurassic sediments. - Geologische Rundschau, **87**: 644-657, Berlin Heidelberg.

GAWLICK, H.-J., JANAUSCHEK, W., MISSONI, S., SUZUKI, H., DIERSCHE, V. & ZANKL, H. (2003): Fazies, Alter und Komponentenbestand der jurassischen Kieselsedimente mit polymikten Brekzien (Callovium - Oxfordium) des Büchsenkopfes im Nationalpark Berchtesgaden und deren Bedeutung für die tektonische und paläogeographische Interpretation der Berchtesgadener Kalkalpen (Deutschland). - Neues Jahrbuch Geologie Paläontologie, Abhandlungen, **228**: 275-304, Stuttgart.

GAWLICK, H.-J., MISSONI, S., SCHLAGINTWEIT, F., SUZUKI, H., FRISCH, W., KRYSTYN, L., BLAU, J. & LEIN, R. (2009a): Jurassic Tectonostratigraphy of the Austroalpine domain. - Journal of Alpine Geology, **50**: 1-152, Wien.

GAWLICK, H.-J., MISSONI, S., SCHLAGINTWEIT, F. & SUZUKI, H. (2010): Tiefwasser Beckengenese und Initiierung einer Karbonatplattform im Jura des Salzkammergutes (Nördliche Kalkalpen, Österreich). - Journal of Alpine Geology, **53**: 63-136, Wien.

GAWLICK, H.-J., SCHLAGINTWEIT, F., EBLI, O. & SUZUKI, H. (2004): Die Plassen-Formation (Kimmeridgium) des Krahstein (Steirisches Salzkammergut, Österreich) und ihre Unterlagerung: neue Daten zur Fazies, Biostratigraphie und Sedimentologie. - Zentralblatt Geologie Paläontologie, Teil 1, **2003**, Heft 3/4: 295-334, Stuttgart.

GAWLICK, H.-J., SCHLAGINTWEIT, F. & MISSONI, S. (2005): Die Barmsteinkalke der Typlokalität nordwestlich Hallein (hohes Tithonium bis tieferes Berriasium; Salzburger Kalkalpen) - Sedimentologie, Mikrofazies, Stratigraphie und Mikropaläontologie: neue Aspekte zur Interpretation der Entwicklungsgeschichte der Ober-Jura-Karbonatplattform und der tektonischen Interpretation der Hallstätter Zone von Hallein - Bad Dürrnberg. - Neues Jahrbuch Geologie Paläontologie Abhandlungen, **236**: 351-421, Stuttgart.

GAWLICK, H.-J., SCHLAGINTWEIT, F., MISSONI, S. (2007b): Das Ober-Jura Seichtwasser-Karbonat-Vorkommen der Drei Brüder am Wolfgangsee (Salzkammergut, Österreich): das westlichste Vorkommen der Wolfgangsee-Karbonatplattform südlich der Brunnwinkl-Schwelle am Nordrand des Tauglboden-Beckens. - Journal Alpine Geology (Mitteilungen Gesellschaft Geologie- Bergbaustudenten Österreich), **48**: 83-100, Wien.

GAWLICK, H.-J., SCHLAGINTWEIT, F. & SUZUKI, H. (2007a): Die Ober-Jura bis Unter-Kreide Schichtfolge des Gebietes Sandling-Höherstein (Salzkammergut, Österreich) - Implikationen zur Rekonstruktion des Block-Puzzles der zentralen Nördlichen Kalkalpen, der Gliederung der karbonatklastischen Radiolaritflyschbecken und der Entwicklung der Plassen-Karbonatplattform. - Neues Jahrbuch Geologie Paläontologie, Abhandlungen, **243**/1: 1-70, Stuttgart.

GAWLICK, H.-J., SUDAR, M., SUZUKI, H., DJERIC, N., MISSONI, S., LEIN, R. & JOVANOVIC, D. (2009b): Upper Triassic and Middle Jurassic radiolarians from the ophiolitic mélange of the Dinaridic Ophiolite Belt, SW Serbia. - Neues Jahrbuch Geologisch Paläontologische Abhandlungen, **253**: 293-311, Stuttgart (Schweizerbart).

GAWLICK, H.-J., SUZUKI, H. & MISSONI, S. (2001): Nachweis von unterliassischen Beckensedimenten in Hallstätter Fazies (Dürrnberg-Formation) im Bereich der Hallein - Berchtesgadener Hallstätter Zone und des Lammer Beckens (Hettangium - Sinemurium). - Mitteilungen Gesellschaft Geologie- Bergbaustudenten Österreich, **45**: 39-55, Wien.

GAWLICK, H.-J., SUZUKI, H., VORTISCH, W. & WEGERER, E. (1999b): Zur stratigraphischen Stellung der Tauglbodenschichten an der Typlokalität in der Osterhorngruppe (Nördliche Kalkalpen, Ober-Oxfordium - Unter-Tithonium). - Mitteilungen Gesellschaft Geologie- Bergbaustudenten Österreich, **42**: 1-20, Wien.

GOLEBIOWSKI, R. (1990): The Alpine Kössen Formation, a Key for European Topmost Triassic Correlations. A Sequence- and Ecostratigraphic Contribution to the Norian-Rhaetian Discussion. - Albertiana, **8**: 25-35, Utrecht.

GOLEBIOWSKI, R. (1991): Becken und Riffe der alpinen Obertrias. Lithostratigraphie und Biofazies der Kössener Formation. - (In: NAGEL, D. & RABEDER, G. (Hrsg.): Exkursionen im Jungpaläozoikum und Mesozoikum Österreichs), 79-119, (Österreichische Paläontologische Gesellschaft) Wien.

GOLONKA, J. (2002): Plate-Tectonic Maps of the Phanerozoic. SEPM Special Publications, **72**: 21-75, Tulsa.

GRADSTEIN, F., OGG, J. & SMITH, A. (2004): A Geological Time Scale. - Cambridge University Press, Cambridge

GÜMBEL, C.W. von (1861): Geognostische Beschreibung des Bayrischen Alpengebirges und seines Vorlandes. I-XX. - 1-950, (Justus Perthes) Gotha.

GUEX, J., BARTOLINI, A., ATUDOREL, V. & TAYLOR, D. (2004): High-resolution ammonite and carbon isotope stratigraphy across the Triassic-Jurassic boundary at New York canyon (Nevada). - Earth and Planetary Science Letters, **225**: 29-41 (Elsevier) Amsterdam.

HAAS, J., KOVÁCS, S., KRYSTYN, L. & LEIN, R. (1995): Significance of Late Permian - Triassic facies zones in terrane reconstructions in the Alpine - North Pannonian domain. - Tectonophysics, **242**: 19-40, Amsterdam.

HAAS, J., KOVACS, S., GAWLICK, H.-J., GRADINARU, E., KARAMATA, S., SUDAR, M., PERO, C., MELLO, J., POLAK, M., OGORELIC, B. & BUSER, S. (2011): Jurassic Evolution of the Tectonostratigraphic Units of the Circum-Pannonian Region. - Jahrbuch der Geologischen Bundesanstalt, **151**: 281-354, Wien.

HÄUSLER, H. (1988): Unterostalpine Jurabreccien in Österreich. Versuch einer sedimentologischen und paläogeographischen Analyse nachtriadischer Breccienserien im unterostalpinen Rahmen des Tauernfensters (Salzburg - Tirol). - Jahrbuch der Geologischen Bundesanstalt, **131**: 21-125, Wien.

HAHN, F. (1910): Geologie des oberen Saalachgebietes zwischen Lofer und Diesbachtal. - Jahrbuch der kaiserlich-königlichen Geologischen Reichsanstalt, **63**: 1-76, Wien.

HAHN, F. (1913): Grundzüge des Baues der nördlichen Kalkalpen zwischen Inn und Enns. - Mitteilungen der Geologischen Gesellschaft in Wien, **6**: 238-357 and 374-501, Wien.

HALLAM, A. (1997): Estimates of the amount and rate of sea-level change across the Rhaetian-Hettangian and Pliensbachian-Toarcian boundary (latest Triassic to early Jurassic). - Journal of the Geological Society of London, **154**: 773-779, London.

HAUBOLD, H., SCHOLGER, R., FRISCH, W., SUMMESBERGER, H. & MAURITSCH, H.J. (1999): Reconstruction of the geodynamic evolution of the Northern Calcareous Alps by means of paleomagnetism. - Physics and Chemistry of the Earth, **24**: 697-703, Amsterdam.

HAUER, F. v. (1850): Über die geognostischen Verhältnisse des Nordabhanges der nordöstlichen Alpen zwischen Wien und Salzburg. - Jahrbuch der kaiserlich-königlichen Geologischen Reichsanstalt, **1**: 17-60, Wien.

HAUG, E. (1906): Les nappes de charriage des Alpes calcaires septentrionales. - Bulletin de la Societé Géologique de la France, **6**: 359-422, Paris.

HESSELBO, S.P., ROBINSON, S.A., SURLYK, F. & PIASECKI, S. (2002): Terrestrial and marine mass extinction at the Triassic-Jurassic boundary synchronized with major carbon-cycle perturbation: A link to initiation of massive volcanism? - Geology, **30**: 251-254, Boulder.

HILLEBRANDT, A. von & KRSYTYN, L. (2009): On the oldest Jurassic ammonites of Europe (Northern Calcareous Alps, Austria) and their global significance. - Neues Jahrbuch Geologie Paläontologie, Abhandlungen, **253**: 163-195, Stuttgart.

HÖCK, V. & SCHLAGER, W. (1964): Einsedimentierte Großschollen in den jurassischen Strubbergbrekzien des Tennengebirges (Salzburg). - Anzeiger der Österreichischen Akademie der Wissenschaften. Mathematisch-naturwissenschaftlichen Klasse, **101**: 228-229, (Österreichische Akademie Wissenschaften) Wien.

HOHENEGGER, J. & LEIN, R. (1977): Die Reiflinger Schichten des Schneeberg-Nordostabfalles und ihre Foraminiferenfauna. Teil 1: Geologie, Stratigraphie und Systematik (exklusive Lagenina). - Mitteilungen Gesellschaft Geologie- Bergbaustudenten Österreich, **24**: 203-261, Wien.

HORNUNG, T. (2007): Multistratigraphy of the Draxllehen quarry near Berchtesgaden (Tuvalian - Lacian 2): implications for Hallstatt Limestone-sedimentation and palaeoclimate in the aftermath of the „Carnian Crisis“. - Austrian Journal Earth Sciences, **100**: 82-99, Wien.

HUBBARD, R.N.B.L. & BOUTLER, M.C. (2000): Phytogeography and palaeoecology in Western Europe and Eastern Greenland near the Triassic-Jurassic boundary. - Palaios, **15**: 120-131, Tulsa.

HUCKRIEDE, R. (1971): Rhyncholithen-Anreicherung (Oxfordium) an der Basis des Älteren Radiolarits der Salzburger Kalkalpen. - Geologica et Palaeontologica, **5**: 131-147, Marburg/Lahn.

JENKYNS, H.C. & WINTERER, E.L. (1982): Paleoceanography of Mesozoic ribbon radiolarites. - Earth and Planetary Science Letters, **60**: 351-375, Amsterdam.

KIRCHNER, E.Ch. (1980a): Natriumamphibole und Natriumpyroxene als Mineralneubildungen in Sedimenten und basischen Vulkaniten aus dem Permoskyth der Nördlichen Kalkalpen. - Verhandlungen der Geologischen Bundesanstalt, **1980**(3): 249-279, Wien.

KIRCHNER, E.Ch. (1980b): Vulkanite aus dem Permoskyth der Nördlichen Kalkalpen und ihre Metamorphose. - Mitteilungen österreichische geologische Gesellschaft, **71/72**: 385-396, Wien.

KOBER, L. (1923): Bau und Entstehung der Alpen. - 1-289, (Bornträger) Berlin.

KOLLER, F., HÖCK, V., MEISEL, T., IONESCU, C., ONUZI, K. & GHEGA, D. (2006): Cumulates and gabbros in southern Albanian ophiolites: their bearing on regional tectonic setting. - (In: ROBERTSON, A.H.F., & MOUNTRAKIS, D. (eds.): Tectonic Development of the Eastern Mediterranean Region), Geological Society London Special Publications, **260**, 267-299, London.

KARAMATA, S. (2006): The geological development of the Balkan Peninsula related to the approach, collision and compression of Gondwanan and Eurasian units. - (In: ROBERTSON A.H.F. &, MOUNTRAKIS, D. (Eds.): Tectonic Development of the Eastern Mediterranean Region), Geological Society London Special Publication, **260**: 155-178, London.

KOVACS, S., SUDAR, M., KARAMATA, S., HAAS, J., PERO, C., GRADINARU, E., GAWLICK, H.-J., GAETANI, M., MELLO, J., POLAK, M., ALJINOVIC, D., OGORELIC, B., KOLAR-JURKOVSEK, T., JURKOVSEK, B. & BUSER, S. (2010): Triassic environments in the Circum-Pannonian Region related to the initial Neotethyan rifting stage. - (In: VOZAR, J., EBNER, F., VOZAROVA, A., HAAS, J., KOVACS, S., SUDAR, M., BIELIK, M. & PERO, C. (Eds.): Variscan and Alpine terranes of the Circum-Pannonian Region), 87-156, Geological Institute, SAS, Bratislava.

KOVACS, S., SUDAR, GRADINARU, E., M., GAWLICK, H.-J., KARAMATA, S., HAAS, J., PERO, C., GAETANI, M., MELLO, J., POLAK, M., ALJINOVIC, D., OGORELIC, B., KOLAR-JURKOVSEK, T., JURKOVSEK, B. & BUSER, S. (2011): Triassic Evolution of the Tectonostratigraphic Units of the Circum-Pannonian Region. - Jahrbuch der Geologischen Bundesanstalt, **151**: 199-280, Wien.

KOZUR, H. (1991): The evolution of the Meliata-Hallstatt ocean and its significance for the early evolution of the Eastern Alps and Western Carpathians. - Palaeogeography, Palaeoclimatology, Palaeoecology, **87**: 109-135, Amsterdam.

KOZUR, H. & MOCK, R. (1985): Erster Nachweis von Jura in der Meliata-Einheit der südlichen Westkarpaten. - Geologisch-Paläontologische Mitteilungen, **13**/10: 223-238, Innsbruck.

KOZUR, H. & MOCK, R. (1997): New paleogeographic and tectonic interpretations in the Slovakian Carpathians and their implications for correlations with the Eastern Alps and other parts of the Western Tethys. Part II: Inner Western Carpathians. - Mineralia Slovaca, **29**: 164-209, Bratislava.

KOZUR, H. & MOSTLER, H. (1992): Erster paläontologischer Nachweis von Meliaticum und Süd-Rudabanyaicum in den Nördlichen Kalkalpen (Österreich) und ihre Beziehungen zu den Abfolgen in den Westkarpaten. - Geologisch-Paläontologische Mitteilungen Innsbruck, **18**: 87-129, Innsbruck.

KRAINER, K. (1985): Beitrag zur Mikrofazies, Geochemie und Paläogeographie der Raibler Schichten der östlichen Gailtaler Alpen und des Karwendel. - Archiv für Lagerstättenforschung der Geologischen Bundesanstalt Wien, **6**: 129-142, Wien.

KRAINER, K. & MOSTLER, H. (1997): Die Lias-Beckenentwicklung der Unkener Synklinale (Nördliche Kalkalpen, Salzburg) unter besonderer Berücksichtigung der Scheibelberg Formation. - Geologisch-Paläontologische Mitteilungen Innsbruck, **22**: 1-41, Innsbruck.

KRAINER, K., MOSTLER, H. & HADITSCH J.G. (1994): Jurassische Beckenbildung in den Nördlichen Kalkalpen bei Lofer (Salzburg) unter besonderer Berücksichtigung der Manganerz-Genese. - Abhandlungen der Geologischen Bundesanstalt, **50**: 257-293, Wien.

KRYSTYN, L. (1971): Stratigraphie, Fauna und Fazies der Klaus-Schichten (Aalenium-Oxford) in den östlichen Nordalpen. - Verhandlungen der Geologischen Bundesanstalt, **1971**/3: 486-509, Wien.

KRYSTYN, L. (1972): Die Oberbajocium- und Bathonium-Ammoniten der Klaus-Schichten des Steinbruches Neumühle bei Wien (Österreich). - Annalen des Naturhistorischen Museums in Wien, **76**: 195-310, Wien.

KRYSTYN L. (1980): Triassic Conodont localities in the Salzkammergut Region (Northern Calcareous Alps), mit Beiträgen von B. PLÖCHINGER und H. LOBITZER. - (In: SCHÖNLAUB, H.P. (Ed.): Second European Conodont Symposium - ECOS II, Field-Trip B), Abhandlungen der Geologischen Bundesanstalt, **35**, 61-98, Wien.

KRYSTYN, L. (1987): Zur Rhät-Stratigraphie in den Zlambachschichten (vorläufiger Bericht). - Sitzungsberichte der Österreichischen Akademie der Wissenschaften. Mathematisch-naturwissenschaftliche Klasse: Abteilung 1, **196**: 21-36, (Österreichische Akademie Wissenschaften) Wien.

KRYSTYN, L. (1991): Die Fossillagerstätten der alpinen Trias. - (In: NAGEL, D. & RABEDER, G. (Ed.): Exkursionen im

Jungpaläozoikum und Mesozoikum Österreich), Österreichische Paläontologische Gesellschaft Wien, 24-78, Wien.
KRYSTYN, L. (2008): The Hallstatt pelagics - Norian and Rhaetian Fossillagerstaetten of Hallstatt. - Berichte Geologische Bundesanstalt, **76**: 81-98, Vienna.
KRYSTYN, L. & LEIN, R. (1996): Triassische Becken- und Plattformsedimente der östlichen Kalkalpen. Exkursionsführer Sediment ´96. - Berichte der Geologischen Bundesanstalt Wien, **33**: 1-23, Wien.
KRYSTYN L., LEIN R., MELLO J., RIEDEL P. & PILLER W. (1990): „Tisovec Limestone"- an example of the problems of lithostratigraphic correlation between the Northern Calcareous Alps and the central West Carpathians. - (In: MINARÍKOVÁ D. & LOBITZER H. (Eds.): Thirty years of geological cooperation between Austria and Czechoslovakia), Fed. Geol. Surv.-Geol. Survey, Vienna-Prague, 125-136, Vienna Praha.
KRYSTYN, L. LEIN, R. & GAWLICK, H.-J. (2008): How many Tethyan Triassic Oceans? - (In: KRYSTYN, L. & MANDL, G.W. (Eds.): Upper Triassic Subdivisions, Zonations and Events), Berichte der Geologischen Bundesanstalt, **76**, 12, Wien.
KRYSTYN, L., MANDL, G.W. & SCHAUER, M. (2009): Growth and termination of the Upper Triassic platform margin of the Dachstein area (Northern Calcareous Alps, Austria). - Austrian Journal of Earth Sciences, **102**: 23-33, Wien.
KRYSTYN, L., SCHÄFFER, G. & SCHLAGER, W. (1971): Über die Fossil-Lagerstätten in den triadischen Hallstätter Kalken der Ostalpen. - Neues Jahrbuch für Geologie und Paläontologie Abhandlungen, **137**: 284-304, Stuttgart.
KÜGLER, U., SCHLAGINTWEIT, F., SUZUKI, H. & GAWLICK, H.-J. (2003): Stratigraphie und Fazies des höheren Mittel- bis Ober-Jura im Bereich des Falkensteinzuges am Wolfgangsee, Salzkammergut (Österreich) mit besonderer Berücksichtigung der Plassen-Formation (Kimmeridgium). - Gmundner Geo-Studien **2**: 97-106, Gmunden.
LEBLING, C., HABER, G., HOFFMANN, N., KÜHNEL, J., WIRTH, E. (1935): Geologische Verhältnisse des Gebirges um den Königs-See, **20**. - Abhandlungen Geologische Landesuntersuchung Bayerisches Oberbergamt: 1-46, München.
LEIN, R. (1981): Deckschollen aus Hallstätter Buntkalken in Salzbergfazies in den Mürztaler Alpen südlich von Mariazell (Steiermark). - Mitteilungen Gesellschaft Geologie- Bergbaustudenten Österreich, **27**: 207-235, Wien.
LEIN R. (1982): Paläogeographie und tektonische Deformation des Aflenzer Troges im Bereich der westlichen Mürztaler Alpen südlich Mariazell (Steiermark). - Jahresbericht 1981 Hochschulschwerpkt., S 15, 203-221, Leoben.
LEIN, R. (1985): Das Mesozoikum der Nördlichen Kalkalpen als Beispiel eines gerichteten Sedimentationsverlaufes infolge fortschreitender Krustenausdünnung. - Archiv für Lagerstättenforschung, **6**: 117-128, (Geologische Bundesanstalt) Wien.
LEIN, R. (1987): Zur Verbreitung der Hallstätter Zone beiderseits des Pyhrn-Passes. - Oberösterreichische Geonachrichten, Folge **2**: 21-37, Linz.
LEIN, R. (1987a): Evolution of the Northern Calcareous Alps During Triassic Times. - (In: FLÜGEL, H.W. & FAUPL, P. (Eds.): Geodynamics of the Eastern Alps), 85-102, (Deuticke) Wien.
LEIN, R. (1989): Neufassung des Begriffes Raminger Kalk (Oberladin-Unterkarn) auf mikrofazieller Grundlage. - (In: KRAINER, K. (Ed.): 4. Treffen dtsprach. Sedimentologen, Innsbruck 1989), Zentralblatt Geologie Paläontologie, Teil I, 1989, 9/10, 2 S., Stuttgart.
LEIN, R. (2000): Die Hallstätter Trias der Mürztaler Alpen. - Mitteilungen Gesellschaft Geologie- Bergbaustudenten Österreich, **44**: 289-296, Wien.
LEIN, R. & GAWLICK, H.-J. (1999): Die tektonische Stellung der Hallstätter Schichtfolge des Naßwald-Halbfensters - Neuergebnisse auf der Grundlage von stratigraphischen, faziellen und Conodont Colour Alteration Index (CAI) Untersuchungen (Ober-Trias, Nördliche Kalkalpen). - Kurzfassung Seewalchen, Mitteilungen Gesellschaft Geologie- Bergbaustudenten Österreich, **42**: 197, Wien.
LEIN, R. & GAWLICK, H.-J. (2008): Plattform-Drowning im mittleren Anis - ein überregionaler Event. - Journal of Alpine Geology **49**: 61-62, Wien.
LEIN, R., GAWLICK, H.-J. & KRYSTYN, L. (1997): Paläogeographie und tektonische Herkunft des Drauzuges - Eine Diskussion auf der Basis von Fazies- und Conodont Colour Alteration Index (CAI)-Untersuchungen. - Zbl. Geol. Paläont. **1996** (1/2): 471-483, Stuttgart.
LEIN, R., GAWLICK, H.-J. & KRYSTYN, L. (2010): Die Annaberger Wende: Neudefinition der Annaberg-Formation als Ausdruck der ersten Öffnungsphase der Neotethys im Bereich der Ostalpen. - Journal of Alpine Geology, **52**: 165-166, Wien.
LEISCHNER, W. (1961): Zur Kenntnis der Mikrofauna und -flora der Salzburger Kalkalpen. - Neues Jahrbuch Geologie Paläontologie, Abhandlungen, **112**: 1-47, Stuttgart.
LEMOINE, M. & TRÜMPY, R. (1987): Pre-oceanic rifting in the Alps. - Tectonophysics, **133**: 305-320, Amsterdam.
LOBITZER, H. (1974): Fazielle Untersuchung an norischen Karbonatplattformbecken (Dachsteinkalk-Aflenzer Kalk) im südöstlichen Hochschwabgebiet (Nördliche Kalkalpen, Österreich). - Mitteilungen der Geologischen Gesellschaft Wien, **66/67**: 75-92, Wien.
LUCAS, S.G. & TANNER, L.H. (2007): The nonmarine Triassic-Jurassic boundary in the Newark Supergroup of eastern North America. - Earth-Science Reviews, **84**: 1-20, (Elsevier) Amsterdam.
LUKENEDER, A., KRYSTYN, L., RASSER, M.W. & MÄRZENDORFER, G. (2003): A unique ammonoid fauna from the Upper Jurassic Loser section (Northern Calcareous Alps, Salzkammergut). - (In: PILLER, W.E. (Ed.): Stratigraphia Austriaca. Österreichische Akademie der Wissenschaften). Schriftenreihe der Erdwissenschaftlichen Kommissionen, **16**: 217-229, (Österreichische Akademie Wissenschaften) Wien.
MANDL, G.W. (1982): Jurassische Gleittektonik im Bereich der Hallstätter Zone zwischen Bad Ischl und Bad Aussee (Salzkammergut, Österreich). - Mitteilungen der Gesellschaft Geologie- Bergbaustudenten in Österreich, **28**: 55-76, Wien.
MANDL, G.W. (1984): Zur Trias des Hallstätter Faziesraumes - ein Modell am Beispiel Salzkammergut (Nördliche Kalkalpen, Österreich). - Mitteilungen der Gesellschaft für Geologie und Bergbaustudenten Österreichs, 30/31: 133-176, Wien.
MANDL, G.W. & ONDREJICKOVÁ, A. (1991): Über eine triadische Tiefwasserfazies (Radiolarite, Tonschiefer) in den Nördlichen Kalkalpen - ein Vorbericht. - Jahrbuch der Geologischen Bundesanstalt, **134**: 309-318, Wien.
MANDL, G.W. & ONDREJICKOVA, A. (1993): Radiolarien und Conodonten aus dem Meliatikum im Ostabschitt der Nördlichen Kalkalpen (Österreich). - Jahrbuch der Geologischen Bundesanstalt, **136**: 841-871, Wien.
MARCOUX, J. & BAUD, A. (1996): Late Permian to Late Triassic, Tethyan Paleoenvironments - Three Snapshots: Late Murgabian, Late Anisian, Late Norian. - (In: NAIRN, A.E.M., RICOU, L.-E., VRIELYNCK, B. & DERCOURT, J. (Eds.): The ocean basins and margins. Vol. 8: The Tethys Ocean), 153-190, (Plenum Press) New York.
MARZOLI, A., BERTRAND, H., KNIGHT, K.B., CIRILLI, S., BURATTI, N., VÉRATI, C., NOMADE, S., RENNE, P.R., YOUBI, N., MARTINI, R., ALLENBACH, K., NEUWERTH, R., RAPAILLE, C., ZANINETTI, L. & BELLIENI, G. (2004): Synchrony of the Central Atlantic magmatic province and the Triassic-Jurassic boundary climate and biotic crisis. - Geology, **32**: 973-976, Boulder.
MCELWAIN, J.C., BEERLING, D.J. & WOODWARD, F.I. (1999): Fossil plants and global warming at the Triassic-Jurassic boundary. - Science, **285**: 1386-1390, (HighWirePress) Stanford.
MEDWENITSCH, W (1962): Die Bedeutung der Grubenaufschlüsse des Halleiner Salzberges für die Geologie des Ostrandes der Berchtesgadener Schubmasse. - Zeitschrift der Deutschen Geologischen Gesellschaft, **113**: 463-494, Hannover.
MISSONI, S. (2003): Analyse der mittel- und oberjurassischen

Beckenentwicklung in den Berchtesgadener Kalkalpen - Stratigraphie, Fazies und Paläogeographie. - 1-150, PhD-Thesis Montanuniversität Leoben, Leoben.

MISSONI, S. & GAWLICK, H.-J. (2011a): Jurassic mountain building and Mesozoic-Cenozoic geodynamic evolution of the Northern Calcareous Alps as proven in the Berchtesgaden Alps (Germany). - Facies, **57**: 137-186, (Springer). DOI 10.1007/s10347-010-0225-1

MISSONI, S. & GAWLICK, H.-J. (2011b): Evidence for Jurassic subduction from the Northern Calcareous Alps (Berchtesgaden; Austroalpine, Germany). - International Journal of Earth Sciences **100**: 1605-1631, (Springer). DOI 10.1007/s00531-010-0552-z

MISSONI, S., GAWLICK, H.-J., DUMITRICA, P., KRYSTYN, L. & LEIN, R. (2008): Late Triassic mass-flow deposits in hemipelagic „Slovenian Trough“-like sediments in the Karavank Mountains (Austria) triggered by Late Triassic strike-slip movements. - Journal of Alpine Geology, **49**: 71, Wien.

MISSONI, S. & KUHLEMANN, A. (2001): Geröllpetrographie und Diagenese des karbonatklastischen Radiolaritflysches der Sillenkopf-Formation (Kimmeridgium) in den südlichen Berchtesgadener Alpen. - Schriftenreihe der deutschen geologischen Gesellschaft, **13**: 71, Hannover.

MISSONI, S., GAWLICK, H.-J., SUZUKI, H. & DIERSCHE, V. (2005): Die paläogeographische Stellung des Watzmann Blockes in den Berchtesgadener Kalkalpen - Neuergebnisse auf der Basis der Analyse der Trias- und Jura-Entwicklung. - Journal Alpine Geology (Mitteilungen Gesellschaft Geologie- Bergbaustudenten Österreich), **47**:169-209, Wien.

MISSONI, S., SCHLAGINTWEIT, F., SUZUKI, H. & GAWLICK, H.-J. (2001a): Die oberjurassische Karbonatplattformentwicklung im Bereich der Berchtesgadener Kalkalpen (Deutschland) - eine Rekonstruktion auf der Basis von Untersuchungen polymikter Brekzienkörper in pelagischen Kieselsedimenten (Sillenkopf-Formation). - Zentralblatt Geologie Paläontologie, Teil 1, **2000**: 117-143, Stuttgart.

MISSONI, S., STEIGER, T. & GAWLICK, H.-J. (2001b): Das „Gschirrkopffenster“ in den Berchtesgadener Kalkalpen (Deutschland) und seine Interpretation: Neuergebnisse auf der Basis von stratigraphischen und faziellen Untersuchungen. - Mitteilungen Gesellschaft Geologie- Bergbaustudenten Österreich, **45**: 89-110, Wien.

MOCK, R., SÝKORA, M., AUBRECHT, R., O•VOLDOVÁ, L., KRONOME, B., REICHWALDER, R.P. & JABLONSKÝ, J. (1998): Petrology and stratigraphy of the Meliaticum near the Meliata and Jaklovce villages, Slovakia. - Slovak Geological Magazine, **4**: 223-260, Bratislava.

MOSTLER H. (1978): Ein Beitrag zur Mikrofauna der Pötschenkalke an der Typlokalität unter besonderer Berücksichtigung der Poriferenspiculae. - Geologisch-Paläontolgische Mitteilungen Innsbruck, **7**: 1-128, Innsbruck.

MOSTLER, H. & ROSSNER, R. (1984): Mikrofazies und Palökologie der höheren Werfener Schichten (Untertrias) der Nördlichen Kalkalpen. - Facies, **10**: 87-144, Erlangen.

NEUBAUER, F., GENSER, J. & HANDLER, R. (2000): The Eastern Alps: Result of a two-stage collision process. - Mitteilungen der Österreichischen Geologischen Gesellschaft, **92** (1999):117-134, Wien.

NEUBAUER, F., FRIEDL, G., GENSER, J., HANDLER, R., MADER, D. & SCHNEIDER, D. (2007): Origin and tectonic evolution of the Eastern Alps deduced from dating of detrital white mica: a review. - Austrian Journal Earth Sciences, **100**: 8-23, Wien.

O´DOGHERTY, L. & GAWLICK, H.-J. (2008): Pliensbachian Radiolaria in the Teltschengraben (Northern Calcareous Alps, Salzkammergut area, Austria) and their evidence for the reconstruction of Liassic Tethys. - Stratigraphy, **5**/1: 63-81, New York.

OGG, J.G. (2004a): The Triassic Period. - (In: GRADSTEIN, F., OGG, J. & SMITH, A.: A Geological Time Scale 2004), 271-306, (Cambridge University Press) Cambridge.

OGG, J.G. (2004b): The Jurassic Period. - (In: GRADSTEIN, F., OGG, J. & SMITH, A.: A Geological Time Scale 2004), 307-343, (Cambridge University Press) Cambridge.

ORTNER, H., USTASZEWSKI, M. & RITTNER, M. (2008): Late Jurassic tectonics and sedimentation: breccias in the Unken syncline, central Northern Calcareous Alps. - Swiss Journal Geosciences, Supplement 1, **101**: S55-S71, Basel.

PÁLFY, J. (2008): Triassic-Jurassic boundary. - (In: MCCANN, T. (Ed.): The Geology of Central Europe. Volume 2: Mesozoic and Cenozoic), 826-827, Geological Society (London).

PÁLFY, J., DEMÉNY, A., HAAS, J., HETÉNY, M., ORCHARD, M. & VETÖ, I. (2001): Carbon isotope anomaly and other geochemical changes at the Triassic-Jurassic boundary from a marine section in Hungary. - Geology, **29**: 1047-1050, Boulder.

PILLER, W.E., EGGER, H., ERHART, C.W., GROSS, M., HARZHAUSER, M., HUBMANN, B., VAN HUSEN, D., KRENMAYR, H.G., KRYSTYN, L., LEIN, R., LUKENEDER, A., MANDL, G.W., RÖGL, F., ROETZEL, R., RUPP, C., SCHNABEL, W., SCHÖNLAUB, H.P., SUMMESBERGER, H., WAGREICH, M. & WESSELY, G. (2004): Die stratigraphische Tabelle von Österreich 2004 (sedimentäre Schichtfolgen). - Österreichische Akademie der Wissenschaften und Österreichische Stratigraphische Kommission, Wien.

PLÖCHINGER, B. (1964): Die tektonischen Fenster von St. Gilgen und Strobl am Wolfgangsee (Salzburg, Österreich). - Jahrbuch der Geologischen Bundesanstalt, **107**: 11-64, Wien.

PLÖCHINGER, B. (1968): Die Hallstätter Deckscholle östlich von Kuchl/Salzburg und ihre in das Aptien reichende Roßfeldschichten-Unterlage. - Verhandlungen der Geologischen Bundesanstalt **1968**: 80-87, Wien.

PLÖCHINGER, B. (1973): Erläuterungen zur Geologischen Karte des Wolfgangseegebietes (Salzburg, Oberösterreich). - 1-92, (Geologische Bundesanstalt) Wien.

PLÖCHINGER, B. (1974): Gravitativ transportiertes Haselgebirge in den Oberalmer Schichten (Tithonium, Salzburg). - Verhandlungen der Geologischen Bundesanstalt, **1974**: 71-88, Wien.

PLÖCHINGER, B. (1976): Die Oberalmer Schichten und die Platznahme der Hallstätter Masse in der Zone Hallein-Berchtesgaden, mit Beiträgen von K. BADER und H. HOLZER. - Neues Jahrbuch Geologie Paläontologie, Abhandlungen, **151**: 304-324, Stuttgart.

PLÖCHINGER, B. (1980): Die Nördlichen Kalkalpen. - (In: OBERHAUSER, R. (Ed.): Der geologische Aufbau Österreichs), 217-264, (Springer) Wien New York.

PLÖCHINGER, B. (1984): Zum Nachweis jurassisch-kretazischer Eingleitungen von Hallstätter Gesteinsmassen beiderseits des Salzach-Quertales (Salzburg). - Geologische Rundschau, **73**: 293-306, Stuttgart.

PUEYO, E. L., MAURITSCH, H. J, GAWLICK, H.-J, SCHOLGER, R. & FRISCH, W. (2007): New evidence for block and thrust sheet rotations in the central northern Calcareous Alps deduced from two pervasive remagnetization events. - Tectonics **26**, TC5011, DOI: 10.1029/2006TC001965.

RATSCHBACHER, L., DINGELDEY, C., MILLER, C., HACKER, B.R. & MCWILLIAMS, M.O. (2004): Formation, subduction, and exhumation of Penninic oceanic crust in the Eastern Alps: time constraints from $^{40}Ar/^{39}Ar$ geochronology. - Tectonophysics, **394**: 155- 170, Amsterdam.

RATSCHBACHER, L., FRISCH, W., LINZER, H.G. & MERLE, O. (1991): Lateral extrusion in the Eastern Alps, Part 2: Structural analysis. - Tectonics **10**: 257-271, Washington.

REIJMER, J.J.G. & EVERAAS, S.L. (1991): Carbonate platform facies reflected in carbonate basin facies (Triassic, Northern Calcareous Alps, Austria). - Facies, **25**: 253-278, Erlangen.

ROBERTSON, A.H.F. (2012): Late Palaeozoic-Cenozoic tectonic development of Greece and Albania in the context of alternative reconstructions of Tethey in the Eastern Mediterranean region. – International Geology Review, **54**: 373-454, Taylor & Francis.

RODDICK, J.F., CAMERON, W.E. & SMITH, A.G. (1979): Permo-Triassic and Jurassic Ar-Ar ages from Greek ophiolithes and associated rocks. - Nature, **279**: 788-790, London.

SANDERS, D., LUKESCH, M., RASSER, M. & SKELTON, P. (2007): Shell beds of diceratid rudists ahead of low-energy gravelly beach (Tithonian, Northern Calcareous Alps, Austria): Palaeoecology and Taphonomy. - Austrian Journal Earth Sciences, **100**: 186-199, Wien.

SCHÄFER, P. & SENOWBARI-DARYAN, B. (1981): Facies development and paleoecologic zonation of four upper Triassic patch-reefs, Northern Calcareous Alps near Salzburg, Austria. - SEPM Spec. Publ. **30**: 241-259, Tulsa.

SCHLAGER, M. (1969): Zur Definition der Oberalmer Schichten. - Anzeiger der Österreichischen Akademie der Wissenschaften. Mathematisch-naturwissenschaftliche Klasse, **106**: 85, (Österreichische Akademie Wissenschaften) Wien.

SCHLAGER, M. & SCHLAGER, W. (1969): Über die Sedimentationsbedingungen der jurassischen Tauglbodenschichten (Osterhorngruppe, Salzburg). - Anzeiger der Österreichischen Akademie der Wissenschaften. Mathematisch-naturwissenschaftlichen Klasse, **106**: 178-183, (Österreichische Akademie Wissenschaften) Wien.

SCHLAGER, W. (1989): Drowning unconformities on carbonate platforms. - (In: P.D. CREVELLO, J.L. WILSON, J.F. SARG, & J.F. READ, (eds.): Controls on carbonate platform and basin development), SEPM Special Publication, **44**: 15-25, Tulsa.

SCHLAGER, W. & SCHLAGER, M. (1973): Clastic sediments associated with radiolarites (Tauglbodenschichten, Upper Jurassic, Eastern Alps). - Sedimentology, **20**: 65-89, (Blackwell) Oxford.

SCHLAGER, W. & SCHÖLLNBERGER, W. (1974): Das Prinzip stratigraphischer Wenden in der Schichtfolge der Nördlichen Kalkalpen. - Mitteilungen der geolologischen Gesellschaft Wien, **66/67**: 165-193, Wien.

SCHLAGINTWEIT, F. (2011a): A false aciculariacean alga and its origin: an example from the Upper Jurassic of the Northern Calcareous Alps, Austria. - Facies, **57**: 267-273, Berlin.

SCHLAGINTWEIT, F. (2011b): The dasycladalean algae of the Plassen Carbonate Platform (Kimmeridgian-Early Berriasian): taxonomic inventory and palaeogeographical implications within the platform-basin-system of the Northern Calcareous Alps (Austria, p.p. Germany). - Geologia Croatica, **64** (3): 185-206, Zagreb.

SCHLAGINTWEIT, F. & GAWLICK, H.-J. (2007): Analysis of Late Jurassic to Early Cretaceous algal debris-facies of the Plassen carbonate platform in the Northern Calcareous Alps (Germany, Austria) and in the Kurbnesh area of the Mirdita zone (Albania) - a tool to reconstruct tectonics and paleogeography of eroded platforms. - Facies, **53**: 209-227, Berlin.

SCHLAGINTWEIT, F., GAWLICK, H.-J. & LEIN, R. (2003): Die Plassen-Formation der Typlokalität (Salzkammergut, Österreich) - neue Daten zur Fazies, Sedimentologie und Stratigraphie. - Mitteilungen Gesellschaft Geologie- Bergbaustudenten Österreich, **46**: 1-34, Wien.

SCHLAGINTWEIT, F., GAWLICK, H.-J. & LEIN, R. (2005): Mikropaläontologie und Biostratigraphie der Plassen-Karbonatplattform der Typlokalität (Ober-Jura bis Unter-Kreide, Salzkammergut, Österreich). - Journal of Alpine Geology (Mitteilungen Gesellschaft Geologie- Bergbaustudenten Österreich), **47**: 11-102, Wien.

SCHMID, D.U. (1996): Marine Mikrobolithe und Mikroinkrustierer aus dem Oberjura. - Profil, **9**: 101-251, Stuttgart.

SCHMID, S.M., FÜGENSCHUH, B., KISSLING, E. & SCHUSTER, R. (2004): Tectonic map and overall architecture of the Alpine orogen. - Eclogae geologicae Helvetiae, **97**: 93-117, Basel.

SCHMID, S. M., FÜGENSCHUH, B., MATENCO, L., SCHEFER S., SCHUSTER, R., TISCHLER, M. & USTASZEWSKI, K. (2008): The Alps-Carpathians-Dinarides-connection: a correlation of tectonic units. - Swiss Journal of Geosciences, **101**: 139-183, Basel.

SCHUSTER, R., SCHARBERT, S., ABART, R. & FRANK, W. (2001): Permo-Triassic extension and related HT/LP metamorphism in the Austroalpine - Southalpine realm. - Mitteilungen Gesellschaft Geologie- Bergbaustudenten Österreich, **45**: 111-141, Wien.

SCHUSTER, R. & STÜWE, K. (2008): Permian metamorphic event in the Alps. - Geology, **36**: 603-606, Boulder.

SCHWEIGL, J. & NEUBAUER, F. (1997): Structural evolution of the central Northern Calcareous Alps: Significance for the Jurassic to Tertiary geodynamics in the Alps. - Eclogae geologicae Helvetiae, **90**: 303-323, Basel.

SENGÖR, A.M.C. (1985a): Die Alpiden und die Kimmeriden: die verdoppelte Geschichte der Tethys. - Geologische Rundschau, **74**: 181-213, Stuttgart.

SENGÖR, A.M.C. (1985b): The Story of Tethys: How many Wives Did Okeoanos Have? - Episodes, **8**: 3-12, Beijing.

SEPKOSKI, J.J., JR. (1996): Patterns of Phanerozoic extinction: a perspective from global data bases. - (In: WALLISER, O.H. (Eds.): Global events and Event Stratigraphy in the Phanerozoic), 35-51, (Springer) Berlin Heidelberg.

SHALLO, M. & DILEK, Y. (2003): Development of the ideas on the origin of Albanian ophiolites. - Geological Society of America Special Paper, **373**: 351-363, Washington.

SPENGLER, E. (1951): Die Nördlichen Kalkalpen, die Flyschzone und die Helvetische Zone. - (In: SCHAFFER, F.X. (ed.): Geologie von Österreich). 302-413, (Deuticke) Wien.

SPÖTL, Ch. (1989): The Alpine Haselgebirge Formation, Northern Calcareous Alps (Austria): Permo-Skythian evaporites in an alpine thrust system. - Sedimentary Geology, **65**: 113-125, Amsterdam.

SPÖTL, CH., KRALIK, M. & KUNK, M.J. (1996): Authigenic feldspar as an indicator of paleo-rock/water interactions in Permian carbonates of the Northern Calcareous Alps, Austria. - Journal Sedimentary Research, **A66**: 139-146, Amsterdam.

SPÖTL, C., LONGSTAFFE, F.J., RAMSEYER, K., KUNKS, M.J. & WIESHEU, R. (1998): Fluid-rock reactions in an evaporitic mélange, Permian Haselgebirge, Austrian Alps. - Sedimentology, **45**: 1019-1044, (Blackwell) Oxford.

SPRAY, J.G. & RODDICK, J.C. (1980): Petrology and $^{40}Ar/^{39}Ar$ geochronology of some Hellenic subophiolithic metamorphic rocks. - Contributions to Mineralogy and Petrology, **72**: 4-5, Berlin (Springer).

STAMPFLI, G.M., MOSAR, J., FAURE, PH., PILLEVUIT, A. & VANNAY, J.-C. (2001): Permo-Mesozoic evolution of the Western Tethys realm: the Neo-Tethys East-Mediterranean Basin connection. - (In: ZIEGLER, P.A., CAVAZZA, W., ROBERTSON, A.H.F. & CRASQUIN-SOLEAU, S. (Eds.): Peri-Tethys Memoir 6. Peri-Tethyan rift/wrench basins and passive margins), Mémoire Muséum national d´ Histoire naturelle, **186**, 51-108, Paris.

STAMPFLI G.M. & BOREL, G.D. (2002): A plate tectonic model for the Paleozoic and Mesozoic. - Earth Planetary Science Letters, **196**: 17-33 (Elsevier) Amsterdam.

STAMPFLI, G.M. & KOZUR, H. (2006): Europe from the Variscan to the Alpine cycles. - (In: GEE D.G. & STEPHENSON, R.A. (Eds.): European Lithosphere Dynamics), Geological Society Memoir, **32**: 57-82, London.

STEIGER, T. (1981): Kalkturbidite im Oberjura der Nördlichen Kalkalpen (Barmsteinkalke, Salzburg, Österreich). - Facies, **4**: 215-348, Erlangen.

STEIGER, T. (1992): Systematik, Stratigraphie und Palökologie der Radiolarien des Oberjura-Unterkreide-Grenzbereiches im Osterhorn-Tirolikum (Nördliche Kalkalpen, Salzburg und Bayern). - Zitteliana (Abhandlungen Bayerischen Staatsammlung Paläontologie und historische Geologie), **19**: 1-188, München.

STINGL, V. (1989): Marginal marine sedimentation in the basal alpine Buntsandstein (Skythian) in the western part of the Northern Calcareous Alps (Tyrol/Salzburg, Austria). - Palaeogeography, Palaeoclimatology, Palaeoecology, **72**: 249-262, Amsterdam.

SUESS, E. & MOJSISCOVICS, E. v. (1868): Studien über die Gliederung der Trias- und Jurabildungen in den östlichen Alpen. Nr. II. Die Gebirgsgruppe des Osterhornes. - Jahrbuch der k.k. geologischen Reichsanstalt, **1868**: 167-200, Wien.

SUZUKI, H. & GAWLICK, H.-J. (2003): Die jurassischen Radiolarienzonen der Nördlichen Kalkalpen. - (In: WEIDINGER, J.T., LOBITZER, H. & SPITZBART, I. (Eds.): Beiträge zur Geologie des Salzkammerguts. Gmundner Geo-Studien), **2**: 115-122, Gmunden.

SUZUKI, H. & GAWLICK, H.-J. (2009): Jurassic radiolarians from the base of the Hallstatt salt-mine (Northern Calcareous Alps, Austria). - Neues Jahrbuch Geologie Paläontologie, Abhandlungen, **251**: 155-197, Stuttgart.

THÖNY, W., ORTNER, H. & SCHOLGER, R. (2006): Paleomagnetic evidence for large en-bloc rotations in the Eastern Alps during Neogene orogeny. - Tectonophysics, **414**: 169-189, Amsterdam.

TOLLMANN, A. (1976a): Analyse des klassischen nordalpinen Mesozoikums. Stratigraphie, Fauna und Fazies der Nördlichen Kalkalpen. - 1-580, (Deuticke) Wien.

TOLLMANN, A. (1976b): Der Bau der Nördlichen Kalkalpen. Orogene Stellung und regionale Tektonik. - 1-449, (Deuticke) Wien.

TOLLMANN, A. (1977): Geologie von Österreich, Band **1**: Die Zentralalpen. - 1-766, (Deuticke) Wien.

TOLLMANN, A. (1981): Oberjurassische Gleittektonik als Hauptformungsprozeß der Hallstätter Region und neue Daten zur Gesamttektonik der Nördlichen Kalkalpen in den Ostalpen. - Mitteilungen der Österreichischen Geologischen Gesellschaft, **74/75**: 167-195, Wien.

TOLLMANN, A. (1985): Geologie von Österreich, Band **2**: Außerzentralalpiner Anteil. - 1-710, (Deuticke) Wien.

TOLLMANN, A. (1987): Late Jurassic/Neocomian Gravitational Tectonics in the Northern Calcareous Alps in Austria. - (In: FLÜGEL, H.W. & FAUPL, P. (Eds.): Geodynamics of the Eastern Alps), 112-125, (Deuticke) Wien.

VECSEI, A., FRISCH, W., PIRZER, M. & WETZEL, A. (1989): Origin and tectonic Significance of Radiolarien Chert in the Austroalpine Rifted Continental Margin. - (In: HEIN, J. & OBRADOVIC, J. (Eds.): Siliceous Deposits of the Tethys and Pacific Regions), 65-80, (Springer) Berlin Heidelberg New York.

VLAHOVIC I., TISLJAR J., VELIC I. & MATICEC D. (2005): Evolution of the Adriatic Carbonate Platform: Paleogeography, main events and depositional dynamics. - Palaeogeography, Palaeoclimatology, Palaeoecology, **220**: 333-360, Amsterdam.

VOZÁROVÁ, A., VOZÁR, J. & MAYR, M. (1999): High-pressure metamorphism of basalts in the evaporite sequence of the Haselgebirge: An evidence from Bad Ischl (Austria). - Abhandlungen der Geologischen Bundesanstalt, **56**: 325-330, Wien.

WÄCHTER, J. (1987): Jurassische Massflow- und Internbreccien und ihr sedimentär-tektonisches Umfeld im mittleren Abschnitt der Nördlichen Kalkalpen. - Bochumer geologische geotechnische Arbeiten, **27**: 1-239, Bochum.

WAGREICH, M. & DECKER, K. (2001): Sedimentary tectonics and subsidence modelling on the type Upper Cretaceous Gosau basin (Northern Calcareous Alps, Austria). - International Journal of Earth Sciences, **90**: 714-726, (Springer) Berlin.

WARD, P.D., GARRISON, G.H., HAGGART, J.W., KRING, D.A. & BEATTIE, M.J. (2004): Isotope evidence bearing on Late Triassic extinction events, Queen Charlotte Islands, British Columbia, and implications for the duration and cause of the Triassic/Jurassic mass extinction. - Earth and Planetary Science Letters, **224**: 589-600, (Elsevier) Amsterdam.

WEGERER, E., SUZUKI, H. & GAWLICK, H.-J. (2001): Zur stratigraphischen Einstufung von Kieselsedimenten im Bereich des Sandling (Nördliche Kalkalpen, Callovium-Oxfordium). - Mitteilungen Gesellschaft Geologie- Bergbaustudenten Österreich, **45**: 67-85, Wien.

WEGERER, E., SUZUKI, H. & GAWLICK, H.-J. (2003): Zur stratigraphischen Einstufung von Kieselsedimenten südöstlich des Plassen (Nördliche Kalkalpen, Österreich). - Jahrbuch der Geologischen Bundesanstalt, **143**: 323-335, Wien.

ZACHER, W. & LUPU, M. (1999): Pitfalls on the race for an ultimate Tethys model. - International Journal of Earth Science, **88**: 111-115, Berlin.

ZANKL, H. (1969): Der Hohe Göll. Aufbau und Lebensbild eines Dachsteinkalk-Riffes in der Obertrias der nördlichen Kalkalpen. Abhandlungen der Senckenberg Naturforschenden Gesellschaft, **519**: 1-123, Frankfurt/Main.